INSTITUTO NACIONAL DE PESQUISAS DA AMAZÔNIA – INPA
PROGRAMA DE PÓS-GRADUAÇÃO EM ENTOMOLOGIA – PPG/ENT

SISTEMÁTICA E BIOGEOGRAFIA DE ACHILIXIIDAE MUIR (HEMIPTERA: AUCHENORRHYNCHA: FULGOROIDEA) COM BASE EM CARACTERES MORFOLÓGICOS E MOLECULARES

EDUARDA FERNANDA GOMES VIEGAS

Manaus, Amazonas
Dezembro, 2023

EDUARDA FERNANDA GOMES VIEGAS

SISTEMÁTICA E BIOGEOGRAFIA DE ACHILIXIIDAE MUIR (HEMIPTERA: AUCHENORRHYNCHA: FULGOROIDEA) COM BASE EM CARACTERES MORFOLÓGICOS E MOLECULARES

ORIENTADORA: Dra. Rosaly Ale Rocha (INPA)
COORIENTADORA: Dra. Daniela Maeda Takiya (UFRJ)

Tese apresentada ao Instituto Nacional de Pesquisas da Amazônia, como parte dos requisitos para obtenção do título de Doutor em Ciências Biológicas, área de concentração em Entomologia.

Manaus, Amazonas
Dezembro, 2023

BANCA EXAMINADORA

Dr. José Albertino Rafael

Instituto Nacional de Pesquisas da Amazônia (INPA)

Dra. Jeane Marcelle Cavalcante do Nascimento

Universidade Federal do Pará (UFPA)

Dra. Andressa Paladini

Universidade Federal do Paraná (UFPR)

Dra. Julianna Freires Barbosa

Museu Nacional - Universidade Federal do Rio de Janeiro (UFRJ)

Dr. Bruno Clarkson

Universidade Estadual do Norte Fluminense Darcy Ribeiro (UENF)

Catalogação na Publicação (CIP-Brasil)

V656s Viegas, Eduarda Fernanda Gomes
Sistemática e Biogeografia de Achilixiidae Muir (Hemiptera: Auchenorrhyncha: Fulgoroidea) com base em caracteres morfológicos e moleculares / Eduarda Fernanda Gomes Viegas; orientadora Rosaly Ale Rocha; coorientadora Daniela Maeda Takiya. - Manaus: [s.l.], 2023.

11,2 MB
231p. : il. color.

Tese (Doutorado - Programa de Pós-Graduação em Entomologia) - Coordenação do Programa de Pós-Graduação, INPA, 2024.

1. Auchenorrhyncha. 2. Filogenia. 3. Tempo de Divergência. I. Rocha, Rosaly Ale. II. Takiya, Daniela Maeda. III. Título

CDD 595.7

Sinopse

Foi feito o primeiro estudo filogenético incluindo representantes de ambos os gêneros de Achilixiidae integrando dados morfológicos e moleculares e estimando o tempo de divergência dos clados. Além disso, cinco novas espécies foram adicionadas a *Bebaiotes* Muir, quatro espécies foram redescritas e uma espécie nova foi acrescentada a *Achilixius* Muir. Adicionalmente, diversos caracteres foram estudados de forma sistemática na família pela primeira vez sob a ótica da cladística.

Palavras-chave: *Achilixius*, *Bebaiotes*, Entomologia, Relógio molecular, taxonomia.

Dedicatória

Dedico primeiramente a mim, por todos os sacrifícios aos quais me submeti, perrengues que passei, noites em claro.
À minha irmã Weslla Taina Gomes Viegas, companheira, razão de minha vida e amiga

AGRADECIMENTOS

Agradeço primeiramente a Deus, por iluminar meu caminho, e por me permitir chegar até aqui.

Ao Instituto Nacional de Pesquisas da Amazônia (INPA) e ao Programa de Pós-graduação em Entomologia, por fornecerem condições para a realização do doutorado e aperfeiçoamento profissional.

À Coordenação de Aperfeiçoamento de Pessoal de Nível Superior (CAPES), pela concessão da bolsa de estudos.

À Fundação de Amparo à Pesquisa do Estado do Amazonas (FAPEAM) - POSGRAD pelo apoio Financeiro durante a realização dessa pesquisa.

Ao Laboratório de Entomologia da UFRJ pelo apoio durante ao período que passei fazendo as análises moleculares.

À minha orientadora Dra. Rosaly Ale Rocha, por aceitar o desafio da minha orientação, pelos ensinamentos, confiança, disponibilidade, paciência, incentivo e principalmente por compartilhar parte do seu amor a Taxonomia, sou muito grata pela oportunidade de ter sido sua aluna e por todo suporte durante esses anos de convivência.

À minha coorientadora Dra. Daniela Takiya, que tive a oportunidade de conhecer e pela qual sou extremamente grata por todos os ensinamentos e explicações, especialmente pela paciência demonstrada, pelas conversas descontraídas e não menos importante as tão maravilhosas "coquinhas". Saiba que serei eternamente grata por todo seu investimento em mim.

Aos Doutores Márcio Oliveira (INPA), Orlando Tobias (MPEG), José Albertino Rafael (INPA), Rodney R. Cavichioli (DZUP), Francisco Limeira-de-Oliveira (UEMA), Rodrigo Lopes Ferreira (UFLA), Christopher H. Dietrich, Mick Webb (NHMK) por fornecerem valiosos materiais de estudo para esta tese, seja através do empréstimo de espécimes depositados em coleções científicas, insetos coletados em projetos executados, ou pelo compartilhamento de fotografias de tipos e parátipos. Suas contribuições foram essenciais para o sucesso deste trabalho.

Dentre os doutores citados acima, eu gostaria de destacar minha gratidão a Christopher Dietrich por ter me enviado material de *Achilixius*, que desempenhou um papel fundamental no desenvolvimento desta tese. Também é importante mencionar o Dr. James H. Boone (BPBM) e expressar meu apreço póstumo, pois, apesar de ter falecido durante o período da pandemia,

ele gentilmente já havia me enviado fotos de *Bebaiotes* e de *Bennarella*, que foram de grande valia para a realização deste trabalho. Suas contribuições não serão esquecidas.

A todos os professores que se dedicaram a ministrar uma ampla gama de disciplinas online durante o período desafiador da pandemia de COVID-19. Mesmo diante de todas as dificuldades e mudanças, vocês compartilharam seu valioso conhecimento, tempo e comprometimento. Suas contribuições desempenharam um papel crucial no meu crescimento acadêmico e por isso, sou profundamente grata.

Ao meu amigo André Antunes pela amizade, paciência, hospedagem, comidas deliciosas e por todas as coisas boas que eu aprendi estando em sua companhia durante a minha passagem pelo Laboratório de Entomologia da UFRJ no Rio de Janeiro.

Aos amigos Matheus Bento, Felipe Barbosa, Clayton Gonçalves (Tom), Luana Barros por toda a assistência prestada nos momentos de dúvidas, discussões aleatórias e por dedicarem seu valioso tempo para me ajudar quando mais precisei.

Aos amigos e amigas, que, com sua amizade, atenção e ajuda, tornaram esta jornada possível: Ana Flávia Avelino, Cristiely Maria, Larissa Queiroz, Carla Marques, Daniela Silva, Sandra Duque, Jádila Prando, Victor Quintas, Marcelo Peixoto, Nathalia Hiluy, Maria Rozo, Luiza Hoehne (senhora) e Francisco Xavier (Chico).

A todos os amigos do Laboratório de Entomologia da UFRJ que tive o prazer de conhecer durante minha estadia no LabEnt, fizeram dessa experiência uma época memorável em minha vida, as risadas, cafés, ensinamentos e bons momentos que compartilhamos.

Também não menos importante, gostaria de agradecer a todos os funcionários da limpeza e segurança do INPA pelo empenho e comprometimento, em especial a dona Zelina por sua amizade, dedicação e ajuda.

RESUMO

Apresentamos o primeiro estudo filogenético incluindo representantes de ambos os gêneros de Achilixiidae com base em dados morfológicos e moleculares. Atualmente, a família possui 32 espécies válidas e é dividida em dois gêneros, *Achilixius* com 16 espécies para a região Oriental e *Bebaiotes* com 16 espécies válidas para a Região Neotropical. O estudo foi composto por uma matriz de dados morfológicos que incluiu 44 táxons (35 espécies do grupo interno e nove do grupo externo) e 99 caracteres morfológicos (65 binários e 34 multiestados), além de quatro marcadores moleculares (18S rDNA, 28S rDNA, 16S rRNA e H3). A matriz de dados concatenada foi composta por 67 táxons e 4.379 pares de bases nitrogenadas, sendo que desses 23 espécimes foram sequenciados no presente trabalho, gerando novas sequências que foram depositadas no GenBank, contribuindo para o enriquecimento da base de dados genéticos. As análises foram realizadas sob três critérios filogenéticos: parcimônia (apenas morfologia) no programa TNT; máxima verossimilhança (molecular) no programa IQ-TREE 2.2.0; e inferência Bayesiana (molecular) no programa MrBayes v. 3.2.7a. Em ambas as análises Achilixiidae e *Achilixius* Muir foram recuperados como monofiléticos, entretanto *Bebaiotes* Muir foi recuperado como parafilético na análise de dados moleculares, que consideraram as espécies *Bebaiotes guianesus*, *Bebaiotes bia, Bebaiotes* sp.1, *Bebaiotes banksi* e *Bebaiotes sp. C* como parte do clado, enquanto na análise de dados morfológicos foi recuperado como monofilético. Além disso, foram acrescentadas cinco espécies novas para *Bebaiotes* Muir: *Bebaiotes cavichiolii* **sp. nov.** (Peru), *Bebaiotes clarice* **sp. nov**. (Brasil - Amazonas), *Bebaiotes oiapoquensis* **sp. nov**. (Brasil - Amapá), *Bebaiotes oliveirai* **sp. nov**. (Brasil - Amazonas) e *Bebaiotes specialis* **sp. nov**. (Brasil – Bahia e Alagoas) e uma espécie nova para *Achilixius* Muir, *Achilixius dietrichi* **sp. nov.** (Filipinas). Adicionalmente, é fornecida uma chave de identificação atualizada para as espécies de *Bebaiotes* (machos e fêmeas). A atual estimativa de tempo de divergência sugere que a divergência inicial de Achilixiidae ocorreu em algum momento durante o Triássico até o Jurássico, período marcado pela fragmentação do Gondwana.

Palavras-chaves: *Achilixius*; espécies novas; Filogenia de Achilixiidae; Fulgoromorpha.

ABSTRACT

We provide the first phylogenetic study, including representatives of both genera of Achilixiidae, based on morphological and molecular data. Currently, the family has 32 valid species and is divided into two genera: *Achilixius*, with 16 species in the Oriental Region, and *Bebaiotes*, with 16 species valid for the Neotropical Region. The study was composed of a matrix of morphological data, including 44 taxa (35 species from the ingroup and nine from the outgroup) and 99 morphological characters (65 binary and 34 multistate), in addition to four molecular markers (18S rDNA, 28S rDNA, 16S rRNA, and H3). the concatenated data matrix comprised 67 taxa and 4,379 bp, including twenty-three specimens that were sequenced herein, generating new sequences deposited in GenBank and contributing to the enrichment of the genetic database. Analyses were conducted using three phylogenetic criteria: parsimony (morphology only) in the TNT program, maximum likelihood (molecular) in the IQ-TREE 2.2.0 program, and Bayesian inference (molecular) in the MrBayes v3.2.7a program. In both analyses, Achilixiidae and *Achilixius* Muir were recovered as monophyletic. *Bebaiotes* Muir was found to be paraphyletic in the molecular data analysis, who considered the species *Bebaiotes guianesus*, *Bebaiotes bia*, *Bebaiotes* sp.1, *Bebaiotes banksi* and *Bebaiotes* sp. C, whereas in the morphological data analyses, it was recovered as monophyletic. Additionally, five new species have been added to *Bebaiotes* Muir taxonomy: *Bebaiotes cavichiolii* **sp. nov.** (Peru), *Bebaiotes clarice* **sp. nov**. (Brazil - Amazonas), *Bebaiotes oiapoquensis* **sp. nov**. (Brazil - Amapá), *Bebaiotes oliveirai* **sp. nov**. (Brazil - Amazonas), and *Bebaiotes specialis* **sp. nov**. (Brazil - Bahia and Alagoas) and a new species for *Achilixius* Muir, *Achilixius dietrichi* **sp. nov.** (Filipinas). Additionally, an updated identification key for *Bebaiotes* species (males and females) is provided. The current estimate for the divergence time suggests that the initial divergence of Achilixiidae occurred sometime during the Triassic to Jurassic period, marked by the fragmentation of Gondwana.

Keywords: *Achilixius*; Achilixiidae phylogeny; Fulgoromorpha; new species.

SUMÁRIO

LISTA DE FIGURAS

Introdução

Capitulo 1

Figures 5 A–G. *Bebaiotes cavichiolii* **sp. nov.**, male genitalia, holotype (MUSM): **A.** Pygofer, lateral view; **B**. Genital capsule, posterior view; **C**. Gonostyli, lateral view; **D.** Gonostyli, dorsal view; **E** Periandrium and inner sclerotized plate, lateral view; **F**. Periandrium and inner sclerotized plate, dorsal view; **G**. Anal tube (segment X), dorsal view. Abbreviations: at, anal tube; cp, phallic complex; go, gonostyli; mdp, dorsal margin of periandrium; mvp, ventral margin of periandrium; isp, inner sclerotized plates; pe, periandrium; py, pygofer. Scale bars: A–G = 0.1 mm.

Figures 6 A–E. *Bebaiotes cavichiolii* **sp. nov.**, female genitalia, paratype (MUSM): **A** Pygofer, posterior view; **B**. Gonapophysis VIII, lateral view (first valvula) lateral view; **C**. Gonapophysis IX (second valvula), dorsal view; **D**. Gonoplac (third valvula), lateral view; **E**. Anal tube (segment X), dorsal view. Abbreviations: at, anal tube; bc, bursa copulatrix, py, pygofer; gnp, gonoplac; gnpf IX, gonapophysis IX; gnpf VIII, gonapophysis VIII. Scale bars: A–E = 0.1 mm.

Figures 7 A–E. *Bebaiotes clarice* **sp. nov.**, male holotype (INPA): **A, C-F**. male holotype. **A**. Male habitus, lateral view; **B**. Female, habitus, lateral view; **C**. Male head, anterior view; **D.** Female head and thorax, lateral view; **E.** Male head and thorax, dorsal view; **F**. Male abdominal process, lateral view. Scale bars: A = 1 mm; B = 2 mm; C, E = 0.4 mm; D = 0.5 mm; F = 0.2 mm.

Figures 8 A–G. *Bebaiotes clarice* **sp. nov.**, male genitalia, holotype (INPA): **A.** Pygofer, lateral view; **B**. Genital capsule, posterior view; **C**. Gonostyli, lateral view; **D.** Gonostyli, dorsal view; **E** Periandrium and inner sclerotized plate, lateral view; **F**. Periandrium and inner sclerotized plate, dorsal view; **G**. Anal tube (segment X) dorsal view. Scale bars: A–G = 0.1 mm.

Figures 9 A–E. *Bebaiotes clarice* **sp. nov.**, female genitalia, paratype (INPA): **A**. Pygofer posterior view; **B**. Gonapophysis VIII, lateral view (first valvula) lateral view; **C**. Gonapophysis IX (second valvula), dorsal view; **D**. Gonoplac (third valvula), lateral view; **E**. Anal tube (segment X), dorsal view. Abbreviations: at, anal tube; bc, bursa copulatrix, dmp, dorsal margin projections, gnp, gonoplac; gnpf IX, gonapophysis IX; gnpf VIII, gonapophysis VIII, lmp, lateroapical margin projections, py, pygofer. Scale bars: A–E = 0.1 mm.

Figures 10 A–D. *Bebaiotes nigrigaster* Muir, 1924, female paratype (NHM): **A.** Female habitus, lateral view; **B**. Female head, anterior view; **C**. Female head, thorax, wings, dorsal view; **D.** Information tags. Fotos: Webb (2019).

Figures 11 A–F. *Bebaiotes nivosa* Fennah, 1947, female holotype (NHM): **A.** Female habitus, lateral view; **B**. Female head, anterior view; **C**. Female head, thorax, wings, dorsal view; **D.** Labels and abdomen and terminalia mounted slide. Fotos: Webb (2019).

Figures 12 A–E. *Bebaiotes oiapoquensis* **sp. nov.**, male holotype (INPA): **A**. Male habitus, lateral view; **B**. Male head, anterior view; **C.** Male head and thorax, lateral view; **D.** Male head and thorax, dorsal view; **E**. Male abdominal process, lateral view. Scale bars: A = 1 mm; B–D = 0.5 mm; E = 0.2 mm.

Figures 13 A–G. *Bebaiotes oiapoquensis* **sp. nov.**, male genitalia, holotype (INPA): **A.** Pygofer, lateral view; **B**. Genital capsule, posterior view; **C**. Gonostyli, lateral view; **D.** Gonostyli, dorsal view; **E** Periandrium and inner sclerotized plate, lateral view; **F**. Periandrium and inner sclerotized plate, dorsal view; **G**. Anal tube (segment X), dorsal view. Scale bars: A–G = 0.1 mm.

Figures 14 A–E. *Bebaiotes oliveirai* **sp. nov.**, female holotype (INPA): **A**. Male habitus, lateral view; **B**. Male head, anterior view; **C**. Male head and thorax, lateral view; **D.** Male head and thorax, dorsal view; **E**. Male abdominal process, lateral view. Scale bars: A = 1mm; B–D = 0.4 mm; E = 0.3 mm.

Figures 15 A–G. *Bebaiotes oliveirai* **sp. nov.**, male genitalia, paratype (INPA): **A.** Pygofer, lateral view; **B**. Genital capsule, posterior view; **C**. Gonostyli, lateral view; **D.** Gonostyli, dorsal view; **E** Periandrium and inner sclerotized plate, lateral view; **F**. Periandrium and inner sclerotized plate, dorsal view; **G**. Anal tube (segment X), dorsal view. Scale bars: A–G = 0.1 mm.

Figures 16 A–E. *Bebaiotes oliveirai* **sp. nov.**, female genitalia, holotype (INPA): **A**. Pygofer posterior view; **B**. Gonapophysis VIII, lateral view (first valvula) lateral view; **C**. Gonapophysis IX (second valvula), dorsal view; **D**. Gonoplac (third valvula), lateral view; **E**. Anal tube (segment X), dorsal view. Scale bars: A–E = 0.1 mm.

Figures 17 A–D. *Bebaiotes pallidinervis* Muir, 1934, male paratype (NHM): **A.** Male habitus, lateral view; **B**. Male head, anterior view; **C**. Male head, thorax, wings, dorsal view; **D.** Information tags. Fotos: Webb (2019).

Figures 18 A–E. *Bebaiotes specialis* **sp. nov.**, female holotype (DZRJ): **A**. Female habitus, lateral view; **B**. Female head, anterior view; **C**. Female head and thorax, lateral view **D.** Female head and thorax, dorsal view; **E**. Male abdominal process, lateral view. Scale bars: A = 1 mm; B, C = 0.4 mm; D, E = 0.3 mm.

Figures 19 A–E. *Bebaiotes specialis* **sp. nov.**, female genitalia, paratype (DZRJ): **A**. Pygofer posterior view; **B**. Gonapophysis VIII, lateral view (first valvula) lateral view; **C**. Gonapophysis IX (second valvula), dorsal view; **D**. Gonoplac (third valvula), lateral view; **E**. Anal tube (segment X), dorsal view. Scale bars: A-E = 0.1 mm.

Figures 20 A–F. Wings of *Achilixius* and *Bebaiotes* species. **A.** *Achilixius dietrichi* **sp. nov.**, forewing; **B.** *Achilixius dietrichi* **sp. nov.**, hind wing, **C.** *Bebaiotes cavichiolii* **sp. nov.**, female forewing; **D.** *Bebaiotes cavichiolii* **sp. nov.**, female hind wing; **E.** *Bebaiotes clarice* **sp. nov.**, forewing; **F.** *Bebaiotes clarice* **sp. nov.**, hind wing; Abbreviations: Forewing: A1, first anal vein; C4, cell C4; C5, cell C5; CuA1, first cubitus anterior branch; CuA2, second cubitus anterior branch; CuP, cubitus posterior; icu cross-vein, cubital area; icua cross-vein, anterior cubital area; m-cu, m-cu2 cross-vein; median cell; MP1, first media posterior branch; MP2, second media posterior branch; MP3, third media posterior branch; MP4, fourth media posterior branch; Pcu, postcubitus; Pcu+A1, postcubitus+first anal vein; radial cell; r-m1, r-m2 cross-vein; RA, radius anterior branch; RP, radius posterior branch. Hind wing: AA, anterior Anal; AP, posterior Anal; CuA, anterior cubitus; CuP, posterior cubitus; m-cu, cross-vein; MP, posterior media. Scale bars: A–F = 1 mm.

Figures 21 A–F. Wings of *Bebaiotes* species. **A.** *Bebaiotes oiapoquensis* **sp. nov.**, **B.** *Bebaiotes oiapoquenis* **sp. nov.**; **C.** *Bebaiotes oliveirai* **sp. nov.**, forewing; **D.** *Bebaiotes oliveirai* **sp. nov.**, hind wing; **E**. *Bebaiotes specialis* **sp. nov.**, female forewing; **F**. *Bebaiotes specialis* **sp. nov.**, female hind wing. Scale bars: A–F = 1 mm.

Figure 22. Geographical distribution of *Achilixius*. Previous known distribution of *Achilixius* Muir in black circles and of *Achilixius dietrichi* **sp. nov.** in red circles.

Figure 23. Geographical distribution of *Bebaiotes*. Previous known distribution of *Bebaiotes* Muir in black circles. See legend for symbols referring to the distribution of the new species: *Bebaiotes cavichiolii* **sp. nov.**; *Bebaiotes clarice* **sp. nov.**; *Bebaiotes oiapoquensis* **sp. nov.**; *Bebaiotes oliveirai* **sp. nov.** and *Bebaiotes specialis* **sp. nov.**

Capitulo 2

Fig. 1. Maximum likelihood tree of Achilixiidae and outgroups based on 4,379 bp of 16S, 18S, 28S, and H3 (-lnL= 40210.5464). Thickened branches are those also recovered in the Bayesian inference analysis. Values above branches are likelihood SH-aLRT / ultrafast bootstrap and below are Bayesian posterior probabilities (in percentages). We only show support values PP > 0.90, SH-aLRT ≥ 80 and UFBoot ≥ 95.

Fig. 2. Dated phylogenetic tree of Achilixiidae (yellow *Achilixius* and red *Bebaiotes*) and other planthoppers. Chronogram based on the same concatenated dataset (67 taxa; 4 gene regions: 16S, 18S, 28S, and H3), using unlinked substitution models (GTR+I+G), uncorrelated lognormal relaxed clock, and five fossil calibration points (black asterisks at nodes). Horizontal bars correspond to the 95% highest posterior density (HPD) of each node age.

Supplementary Figure S1. Maximum likelihood tree of Achilixiidae and outgroups based on 465 bp of 16S rDNA. Values above branches are likelihood SH-aLRT ≥ 80 / ultrafast bootstrap ≥ 95.

Supplementary Figure S2. Maximum likelihood tree of Achilixiidae and outgroups based on 1301 bp of 18S rDNA. Values above branches are likelihood SH-aLRT ≥ 80 / ultrafast bootstrap ≥ 95.

Supplementary Figure S3. Maximum likelihood tree of Achilixiidae and outgroups based on 2278 bp of 28S rDNA. Values above branches are likelihood SH-aLRT ≥ 80 / ultrafast bootstrap ≥ 95.

Supplementary Figure S4. Maximum likelihood tree of Achilixiidae and outgroups based on 339 bp of histone H3. Values above branches are likelihood SH-aLRT ≥ 80 / ultrafast bootstrap ≥ 95.

Capitulo 3

Figures 1 A–D. Head, transition frons to vertex. **A**, *Pintalia* sp. 1, anterior view. **B**, *Pintalia* sp. 1, lateral view. **C**, *Achilixius dietrichi*, anterior view. **D**, *Achilixius dietrichi*, lateral view. Scale bars: A, D = 0.4 mm; B, C = 0.3 mm. Arrow highlighting the presence of the transverse carina (char. 1, state 0).

Figures 2 A–D. Head, frons, anterior view. **A**, *Synecdoche* sp. 2. **B**, *Achilixius dietrichi*. **C**, *Persis* (*Persis*). **D**, *Bebaiotes tigrina*. Scale bars: A, B = 0.3 mm; C = 0.5 mm; D = 0.4 mm. Arrow highlighting the presence of the median longitudinal carina (char. 2, state 0).

Figures 3 A–D. Head, frons, anterior view. **A**, *Bebaiotes cavichiolii*. **B**, *Bennarella bicoloripennis*. **C**, *Catonia* sp. 2. **D**, *Bebaiotes amazonica*. Scale bars: A–D= 0.4 mm. White arrows highlighting direction of lateral longitudinal carinae (char. 3): A, *Bebaiotes cavichiolii* (state 0) and C, *Catonia* sp. 2 (state 1). Red arrows highlighting the direction of the apex of lateral longitudinal carinae (char. 4): B, *Bennarella bicoloripennis* (state 0) and D, *Bebaiotes amazonica* (state 1).

Figures 4 A–D. Head. **A**, **C**, **D**. Head, frons, anterior view. **A**, *Sevia* sp. A. **C**, *Bebaiotes clarice.* **D**, *Melanoliarius* sp. 1. **B**. Head, vertex, dorsal view. **B**, *Sevia* sp. A. Scale bars: A, B = 0.6 mm; C = 0.4 mm; D = 0.5 mm. White arrows highlighting the median width of the frons in relation to maximum width of the vertex (char. 5): A, B *Sevia* sp. A (state 0), *C*, *Bebaiotes clarice* (state 1) and D, *Melanoliarius* sp. 1 (state 2). Red arrows highlighting the extension of lateral margins at median region of the frons (char. 6): C, *Bebaiotes clarice* (state 0) and D,

Melanoliarius sp. 1 (state 1). Blue arrow highlighting the presence of the median ocellus (char. 7, state 1). Abbreviation: v, vertex.

Figures 5 A–D. Head, lateral view. **A**, *Synecdoche* sp. 2. **B**, *Melanoliarius* sp. 1. **C**, *Bebaiotes tigrina*. **D**, *Bebaiotes clarice*. Scale bars: A, C = 0.4 mm; B, D = 0.5 mm. Black arrows highlighting the lateral ocellus insertion (char. 8): A, *Synecdoche* sp. 2. (state 0) and D, *Bebaiotes clarice* (state 1). Red arrows highlighting the compound eye shape (char. 9): B, *Melanoliarius* sp. 1 (state 0) and D, *Bebaiotes clarice* (state 1).

Figures 6 A–B. Head, frons, anterior view. **A**, *Bebaiotes dichromata*. **B**, *Bennarella bicoloripennis*. Scale bars: A= 0.5 mm; B= 0.4 mm. Arrow highlighting the pedicel (char. 10, state 0).

Figures 7 A–C. Head, lateral view. **A**, *Achilixius dietrichi*. **B**, *Bebaiotes specialis*. **C**, *Synecdoche* sp. 2. Scale bars: A–C= 0.4 mm. Red arrow highlighting antennal insertion (char. 11): *Achilixius dietrichi* (state 0) and C, *Synecdoche* sp. 2 (state 1). Black arrow highlighting the presence of the subantenal carina (char. 11, state 1).

Figures 8 A–C. Head, frons, epistomal suture, anterior view. **A**, *Synecdoche* sp. 2. **B**, *Achilixius dietrichi*. **C**, *Bothriocera* sp. 1. Scale bars: A, B= 0.3 mm; C = 0.4 mm. Red arrow highlighting epistomal suture (char. 13): A, *Synecdoche* sp. 2. (state 0), B, *Achilixius dietrichi* (state 1), and C, *Bothriocera* sp. 1 (state 2).

Figures 9 A–B. Head, lateral view. **A**, *Melanoliarius* sp. 1. **B**, *Bebaiotes specialis*. Scale bars: A= 0.4 mm; B= 0.5 mm. White arrows highlighting the lora (char. 14): A, *Melanoliarius* sp. 1. (state 0) and B, *Bebaiotes specialis* (state 1).

Figures 10 A–C. Head, frons, anterior view. **A**, *Sevia* sp. A. **B**, *Bebaiotes macroptera*. **C**, *Bebaiotes dorsivittata*. Scale bars: A= 0.6 mm; B= 0.3 mm; C = 0.5 mm. White arrow highlighting the absence of the median carina of the clypeus (char. 15, state 1). Red arrows highlighting the extension of the median carina of the clypeus (char. 16): B, *Bebaiotes macroptera* (state 0) and C, *Bebaiotes dorsivittata* (state 1).

Figures 11 A–C. Clypeus and labium, ventral view. **A**, *Synecdoche* sp. 2. **B**, *Bebaiotes oiapoquensis*. **C**, *Anotia* sp. 2. Scale bars: A, B= 0.5 mm; C = 1 mm. White arrows highlighting the extension of the clypeus (char. 17): A, *Synecdoche* sp. 2 (state 0), B, *Bebaiotes oiapoquensis* (state 1), and C, *Anotia* sp. 2 (state 2). Red arrows highlighting the apex of the second labial segment (char. 18): A, *Synecdoche* sp. 2 (state 0) and C, *Anotia* sp. 2 (state 2).

Figures 12 A–D. Thorax, dorsal view. **A**, *Bennarella bicoloripennis*. **B**, *Achilixius dietrichi*. **C**, *Bebaiotes specialis*. **D**, *Bebaiotes pulla*. Scale bars: A= 0.4 mm; ; B, C = 0.3 mm, D = 0.4 mm. Black arrows highlighting the pronotum and mesonotum (char. 19): A, *Bennarella*

bicoloripennis (state 0) and B*, Achilixius dietrichi* (state 1). Red arrows highlighting the anterior pronotum pronotum (char. 20): A, *Bennarella bicoloripennis* (state 0), C, *Bebaiotes specialis* (state 2), and C, *Bebaiotes pulla* (state 1). Blue circle highlighting the presence of pustules on the posterior margin of the pronotum (char. 21, state 1).

Figures 13 A–D. Thorax, pronotum, dorsal view. **A**, *Anotia* sp. 2. **B**, *Bebaiotes pulla*. **C**, *Bennarella bicoloripennis*. **D**, *Achilixius dietrichi*. Scale bars: A = 0.6 mm; B = 0.5 mm; C = 0.4 mm; D = 0.3 mm. Black arrow highlighting the lateral longitudinal carinae on the posterior margin (char. 22, state 0). Red arrows highlighting the direction of lateral longitudinal carinae on the posterior margin (char. 23): B, *Bebaiotes pulla* (state 0) and D, *Achilixius dietrichi* (state 1). Blue arrows highlighting the direction of posterior half of lateral longitudinal carinae (char. 24): C, *Bennarella bicoloripennis* (state 1) and D, *Achilixius dietrichi* (state 2).

Figures 14 A–B. Thorax, dorsal view. **A**, *Synecdoche* sp. 2. **B**, *Bothriocera* sp. 1. Scale bars: A–B= 0.4 mm. Black arrows highlighting the posterior margin of the pronotum (char. 25): A, *Synecdoche* sp. 2 (state 1) and B, *Bothriocera* sp. 1. (state 0). Blue arrows highlighting the apex of the scutellum (char. 26): A, *Synecdoche* sp. 2 (state 0) and B, *Bothriocera* sp. 1. (state 1).

Figures 15 A–C. Forewing. **A**, *Sevia* sp. A. **B**, *Melanoliarus* sp. 1. **C**, *Bebaiotes dichromata*. Scale bars: A–C= 1 mm. Red arrows highlighting the position of the ScP+RP branching (char. 27): A, *Sevia* sp. A (state 0) and B, *Melanoliarus* sp. 1 (state 1). Blue arrow highlighting the RP vein (char. 28): B, *Melanoliarus* sp. 1and C (state 0), *Bebaiotes dichromata* (state 1). Abbreviations: CuA, anterior cubitus; RP, radial posterior; ScP, posterior subcosta.

Figures 16 A–C. Forewing. **A**, *Anotia* sp. 2. **B**, *Bebaiotes parallela*. **C**, *Bebaiotes clarice*. Scale bars: A–C= 1 mm. Blach arrow highlighting the MP1 vein (char. 29): A, *Anotia* sp. 2 (state 0) and B, *Bebaiotes parallela* (state 1). Blue arrows highlighting the MP2 vein (char. 30): C, *Bebaiotes clarice* (state 0) and B, *Bebaiotes parallela* (state 1). Abbreviations: MP1, first media posterior branch; MP2, second media posterior branch.

Figures 17 A–C. Forewing. **A**, *Catonia* sp. 2. **B,** *Achilixius dietrichi.* **C,** *Sevia* sp. A. Scale bars: A–*B*= 1 mm. Red arrow highlighting MP3+MP4 vein fused (char. 31, state 0). Blue arrows highlighting MP4 vein (char. 33): B, *Achilixius dietrichi* (state 1) and C, *Sevia* sp. A (state 0). Abbreviations: MP3+4, third media + fourth media posterior branches; MP3, third media posterior branch; MP4, fourth media posterior branch. Abbreviations: MP3+4, third media + fourth media posterior branches; MP3, third media posterior branch; MP4, fourth media posterior branch.

Figures 18 A–C. Forewing. **A**, *Bothriocera* sp. 1. **B**, *Bebaiotes pulla.* **C**, *Achilixius dietrichi*. Scale bars: A–C= 1 mm. Black arrows highlighting the radial cell in relation to median cell

(char. 35): A, *Bothriocera* sp. 1 (state 0) and B, *Bebaiotes pulla* (state 1). Blue arrows highlighting the r-m crossvein. Red arrows highlighting the position MP1+2 and MP3+4 branching (char. 36): A, *Bothriocera* sp. 1 (state 2), B, *Bebaiotes pulla* (state 1), C, *Achilixius dietrichi* (state 0). Abbreviations: mc, median cell; MP1+2, first media + second media posterior branches MP3+4, third media + fourth media posterior branches; rc, radial cell; r-m, radio-medial crossvein.

Figures 19 A–C. Forewing. **A**, *Melanoliarus* sp. 1. **B**, *Bebaiotes wilsoni*. **C**, *Achilixius dietrichi*. Scale bars: A–C= 1 mm. Black arrows highlighting the position m-cua crossvein (char. 38): A, *Melanoliarus* sp. 1 (state 0), B, *Bebaiotes wilsoni* (state 1) and C, *Achilixius dietrichi* (state 2). Red arrows highlighting the presence and absence of the m-cua2 crossvein (char. 39): B, *Bebaiotes wilsoni* (state 0) and C, *Achilixius dietrichi* (state 1). Abbreviations: CuA, cubitus anterior; MP, posterior media; m-cua1, first mediocubital crossvein; m-cua2, second mediocubital crossvein; icua, intercubital crossvein.

Figures 20 A–C. Forewing. **A**, *Bebaiotes oiapoquensis*. **B**, *Pintalia* sp. 2. **C**, *Bebaiotes parallela*. Scale bars: A–C= 1 mm. Red arrow*s* highlighting the position of the m-cu2 crossvein in relation to icua crossvein (char. 40, state 0). Blue arrow*s* highlighting the length of C4 cell in relation to C5 cell (char. 41): A, *Bebaiotes oiapoquensis* (state 2) and C, *Bebaiotes parallela* (state 0). Black arrow*s* highlighting the apex of the CuP vein (char. 42): B, *Pintalia* sp. 02 (state 0), C, *Bebaiotes parallela* (state 1). Abbreviations:C4, cell C4; C5, cell C5; CuP, cubitus posterior; icua, intercubital crossvein; m-cua2, second mediocubital crossvein.

Figures 21 A–C. Forewing. **A**, *Synecdoche* sp. 2. **B**, *Pintalia* sp. 2. **C**, *Bebaiotes dorsivittata*. Scale bars: A–C= 1 mm. Black arrows highlighting the position apex position of the forewings (char. 44): A, *Synecdoche* sp. 2 (state 0), B, *Pintalia* sp. 2 (state 0), and C, *Bebaiotes dorsivittata* (state 0).

Figures 22 A–B. Forewings. **A**, *Achilixius dietrichi*. **B**, *Melanoliarus* sp. 01. Scale bars: A–B= 1 mm. Red arrows highlighting the apex of the Pcu vein (char. 45): A, *Achilixius dietrichi* (state 0) and B, *Melanoliarus* sp. 01 (state 1). Blue arrows highlighting the postclaval margin (char. 46): A, *Achilixius dietrichi* (state 1) and B, *Melanoliarus* sp. 01 (state 0). Abbreviations: Pcu, postcubitus.

Figures 23 A–C. Hindwings **A**, *Bebaiotes wilsoni*. **B**, *Achilixius dietrichi*. **C**, *Bebaiotes tigrina*. Scale bars: A–C= 1 mm. Black arrows highlighting the MP1+2 and MP3+4 branch (char. 47): B, *Achilixius dietrichi* (state 1) and C, *Bebaiotes tigrina* (state 2). Abbreviations: MP1+2, first media + second media posterior branches MP3+4, third media + fourth media posterior branches; m-cu, mediocubital crossvein.

Figures 24 A–B. Profemur, anterior face. **A**, *Bebaiotes amazonica*. 1. **B**, *Sevia* sp. A. Scale bars: A, B= 0.2 mm. Black arrows highlighting the seta (char. 48): A, *Bebaiotes amazonica* (state 1) and B, *Sevia* sp. A (state 0).

Figures 25 A–C. Abdomen, sternite III. **A**, *Catonia* sp. 2. **B**, *Bebaiotes clarice.* **C**, *Achilixius dietrichi*. Scale bars: A, C= 0.5 mm; B = 1 mm. Red arrow highlighting the shape of the abdomen (char. 53, state 1). Blue arrow highlighting the sternite III (char. 54, state 1). Abbreviations: st III, sternite III.

Figures 26 A–B. Abdomen, sternite III. **A**, *Achilixius dietrichi*. **B**, *Bebaiotes macroptera*. Scale bars: A = 0.2 mm; B = 0.3 mm. Abbreviations: st III, sternite III.

Figures 27 A–B. Abdomen, sternite III, ventral view. **A**, *Pintalia* sp. 2. **B**, *Bebaiotes specialis*. Scale bars: A–B = 0.5 mm. Black arrows highlighting the median longitudinal region of the sternite III (char. 56): A, *Pintalia* sp. 2 (state 0) and B, *Bebaiotes specialis* (state 1). Abbreviations: st III, sternite III.

Figures 28 A–B. Abdomen, sternite IV, lateral view. **A**, *Melanoliarus* sp. 2. **B**, *Bennarella bicoloripennis*. Scale bars: A, B = 0.5 mm. Red arrow highlighting the sternite IV (char. 57, state 1). Abbreviations: st IV, sternite IV.

Figures 29 A–C. Abdomen, sternites IV and V, lateral view. **A**, *Synecdoche* sp. 2. **B**, *Bennarella bicoloripennis*. **C**, *Achilixius dietrichi.* Scale bars: A–C = 0.5 mm. Black arrow highlighting the connection of sternites IV (char. 58, state 0). Abbreviations: st IV, sternite IV; st V, sternite V.

Figures 30 A–C. Abdomen, sternite IV, ventral view. **A**, *Sevia* sp. A. **B**, *Pintalia* sp. 2. **C**, *Bebaiotes clarice*. Scale bars: A= 1 mm; B, C = 0.5 mm. Black arrows highlighting the median longitudinal region of the sternite IV (char. 59): A, *Sevia* sp. A (state 0), B, *Pintalia* sp. 2 (state 1) and C, *Bebaiotes clarice* (state 1). Abbreviations: st IV, sternite IV.

Figures 31 A–C. Abdomen, sternite IV, ventral view. **A**, Sevia sp. A. **B**, *Achilixius dietrichi*. **C**, *Bennarella bicoloripennis*. Scale bars: A= 1 mm; B, C = 0.2 mm. Blue arrows highlighting the number of pits in sternite V (char. 61): B, *Achilixius dietrichi* (state 0), C, *Bennarella bicoloripennis* (state 1). Abbreviations: st V, sternite V.

Figures 32 A–B. Abdomen, sternites VII and VIII, ventral view. **A**, *Catonia* sp. 2. **B**, *Pintalia* sp. 2. Scale bars: A= 1 mm; A, B = 0.5 mm. Abbreviations: st VII, sternite VII; st VIII, sternite VIII.

Figures 33 A–C. Pygofer, lateral view. **A**, *Achilixius dietrichi.* **B**, *Pintalia* sp. 2. **C**, *Catonia* sp. 2. Scale bars: A, C= 0.1 mm; B= 0.2 mm. Red arrow*s* highlighting the absence (A) or presence (B) of the medioventral process. Blue arrow*s* highlighting the posterior margin of pygofer (char.

65): A, *Achilixius dietrichi* (state 0) and B, *Pintalia* sp. 2 (state 1). Abbreviations: lmp, length medioventral process; lp, length pygofer.

Figures 34 A–C. Gonostylus, lateral view. **A**, *Pintalia* sp. 02. **B**, *Achilixius dietrichi.* **C**, *Persis* (*Persis*). Scale bars: A, B= 0.1 mm; C= 0.2 mm. Blue arrow*s* highlighting the apex of gonostylus (char. 67): A, *Pintalia* sp. 2 (state 0) and B, *Achilixius dietrichi* (state 1). Red arrow highlighting the projection on the outer margin (char. 69, state 1). Abbreviations: ha, length apex; hb, length base.

Figures 35 A–F. Phallic complex. **A**, *Melanoliarus* sp. 1, left lateral view, lateral view. 02. **B**, *Achilixius dietrichi,* dorsal view. **C**, *Achilixius dietrichi*, left lateral view, lateral view. **D**, *Bennarella bicoloripennis,* left lateral view, lateral view. **E**, *Bebaiotes bia*, left lateral view, lateral view. **F**, *Bebaiotes bia*, dorsal view. Scale bars: A= 0.3 mm; B–F = 0.1 mm; C= 0.2 mm. Black arrow*s* highlighting the phallic complex (char. 70): A, *Melanoliarus* sp. 1 (state 0) and B, C *Achilixius dietrichi* (state 1).

Figures 36 A–D. Periandrium, dorsal margin apex, dorsal view. **A**, *Bebaiotes amazonica*. **B**, *Bebaiotes dorsivittata*. **C**, *Bebaiotes macroptera*. **D**, *Bebaiotes clarice.* Scale bars: A–D = 0.1 mm. Red arrows highlighting the dorsal margin apex (char. 71): A, *Bebaiotes amazonica* (state 0), B, *Bebaiotes dorsivittata* (state 1), C, *Bebaiotes macroptera* (state 2), and D, *Bebaiotes clarice* (state 3).

Figures 37 A–D. Phallic complex, shape. **A**, *Achilixius dietrichi*, left lateral view, lateral view. **B**, *Achilixius dietrichi*, dorsal view. **C**, *Bebaiotes clarice*, left lateral view, lateral view. **D**, *Bebaiotes clarice*, dorsal view. Scale bars: A–D = 0.1 mm.

Figures 38 A–B. Phallic complex, articulation. **A**, *Persis* (*Persis*), left lateral view, lateral view. **B**, *Bebaiotes clarice*, left lateral view, lateral view. Scale bars: A= 0.2 mm; B= 0.1 mm. Red arrow highlighting the articulation of the phallic complex (char. 73, state 0).

74. Phallic complex, inner sclerotized plates: (0) absent; (1) present. [CI=1.0; RI=1.0]. Figures 39 A–C.

Figures 39 A–C. Inner sclerotized plates, dorsal view. **A**, *Achilixius dietrichi*, dorsal view. **B**, *Bebaiotes oiapoquensis*. **C**, *Bebaiotes clarice*. Scale bars: A–C = 0.1 mm. Black arrow highlighting the inner sclerotized plates (char. 74, state 1). Blue arrows highlighting the direction of the inner sclerotized plates (char. 75): B, *Bebaiotes oiapoquensis* (state 0) and C, *Bebaiotes clarice* (state 1). Abbreviation: ps, inner sclerotized plates.

Figures 40 A–C. Periandrium, dorsal margin apex, dorsal view. **A**, *Bebaiotes banksi*. **B**, *Bebaiotes amazonica*. **C**, *Bebaiotes parallela*. Scale bars: A–C = 0.1 mm. Red arrows

highlighting the concavity of the apex of the dorsal margin (char. 77): A, *Bebaiotes banksi* (state 0), B, *Bebaiotes amazonica* (state 1) and C, *Bebaiotes parallela* (state 2).

78. Periandrium, dorsal margin, apex, dorsal view, aspect: (0) smooth; (1) serrate. [CI=0.5; RI=0.5]. Figures 41 A–B.

Figures 41 A–B. Periandrium, dorsal margin apex, dorsal view. **A**, *Bebaiotes cavichiolii*. **B**, *Bebaiotes bia*. Scale bars: A, B= 0.1 mm. Red arrows highlighting the aspect of the apex of the dorsal margin (char. 78): A, *Bebaiotes cavichiolii* (state 0) and B, *Bebaiotes bia* (state 1).

Figures 42 A–D. Periandrium, ventral margin apex, dorsal view. **A**, *Bebaiotes banksi*. **B**, *Bebaiotes tigrina*. **C**, *Bebaiotes pulla*. **D**, *Bebaiotes oliveirai*. Scale bars: A–D = 0.1 mm. Red arrows highlighting the ventral margin apex (char. 79): A, *Bebaiotes banksi* (state 1), B, *Bebaiotes tigrina* (state 0), C, *Bebaiotes pulla* (state 2) and D, *Bebaiotes oliveirai* (state 3).

Figures 43 A–C. Periandrium, ventral margin apex, dorsal view. **A**, *Bebaiotes pennyi*. **B**, *Bebaiotes guianesus*. **C**, *Bebaiotes macroptera*. Scale bars: A–C = 0.1 mm. Red arrow*s* highlighting the concavity of the apex of the ventral margin (char. 80): A, *Bebaiotes pennyi* (state 0), B, *Bebaiotes guianesus* (state 1) and C, *Bebaiotes macroptera* (state 2).

Figures 44 A–D. *Anal tube (segment X)*, apex, shape, dorsal view. **A**, Bebaiotes clarice. **B**, Bennarella bicoloripennis. **C**, Achilixius dietrichi. **D**, Persis (Persis). Scale bars: A–C = 0.1 mm; D= 0.2 mm.

Figures 45 A–D. Anal tube (segment X), shape, dorsal view. **A**, *Bebaiotes clarice*. **B**, *Bothriocera* sp. 1. **C**, *Persis* (*Persis*). ***D***, *Synecdoche* sp. 2. Scale bars: A, B, D = 0.1 mm; C= 0.2 mm.

Figures 46 A–C. Anal tube (segment X), lateral view. **A**, *Bebaiotes clarice.* **B**, *Achilixius dietrichi* **C**, *Persis* (*Persis*). Scale bars: A, B = 0.1 mm; C= 0.2 mm. Red arrow highlighting the length of dorsal margin in relation to ventral margin of Anal tube (segment X) (char. 83, state 0). Abbreviations: md, dorsal margin; mv, ventral margin.

Figures 47 A–D. Ovipositor. **A**, *Bothriocera* sp. 1, lateral view. 1. **B**, *Bothriocera* sp. 1, posterior view. **C**, *Bebaiotes pulla*, lateral view. **D**, *Bebaiotes pulla*, posterior view. Scale bars: A, B = 0.4 mm; C, D= 0.3 mm.

Figures 48 A–C. Gonapophysis VIII (first valvula), lateral view. **A**, *Bennarella bicoloripennis*. 1. **B**, *Bebaiotes clarice.* **C**, *Synecdoche* sp. 2. Scale bars: A–C = 0.1 mm. Black arrows highlighting the dorsoapical margin (char. 85): A, *Bennarella bicoloripennis* (state 0) and B, *Bebaiotes clarice* (state 1). Blue arrows highlighting the lateroapical margin (char. 86): B, *Bebaiotes clarice* (state 1) and C, *Synecdoche* sp. 2 (state 0).

Figures 49 A–D. Gonapophysis VIII (first valvula), lateral view. **A**, *Bebaiotes cavichiolii*. **B**, *Bebaiotes pulla*. **C**, *Bebaiotes amazonica*. **D**, *Bebaiotes banksi*. Scale bars: A–D = 0.1 mm. Blue arrows highlighting the number of projections on the apical side margin (char. 87): A, *Bebaiotes cavichiolii* (state 0), B, *Bebaiotes pulla* (state 1), C, *Bebaiotes amazonica* (state 2) and D, *Bebaiotes banksi* (state 3). Red arrows highlighting the aspect of the latero-apical margin (char. 88): C, *Bebaiotes amazonica* (state 1), D, *Bebaiotes banksi* (state 0).

Figures 50 A–D. Gonapophysis VIII (first valvula), lateral view. **A**, *Bennarella bicoloripennis*. 1. **B**, *Bebaiotes wilsoni*. **C**, *Bebaiotes amazonica*. **D**, *Bebaiotes guianesus*. Scale bars: A–D = 0.1 mm. Red arrows highlighting the apex of the bursa copulatrix (char. 90): B, *Bebaiotes wilsoni* (state 0), C, *Bebaiotes amazonica* (state 1) and D, *Bebaiotes guianesus* (state 2).

Figures 51 A–D. Gonapophysis IX (second valvula), dorsal view. **A**, *Bothriocera* sp. 1. **B**, *Anotia* sp. 2. **C**, *Bebaiotes cavichiolii***. D**, *Bebaiotes pennyi*. Scale bars: A–D = 0.1 mm. Red arrow highlighting maximum width in relation to total length of Gonapophysis IX (second valvula) (char. 91, state 1). Black arrows highlighting central region (char. 92): A, *Bothriocera* sp. 1 (sate 0) and B, *Anotia* sp. 2 (state 1). Blue arrows highlighting the apexes of lobes (char. 93): B, *Anotia* sp. 2 (state 0) and C, *Bebaiotes cavichiolii* (state 1). Abbreviations: mv, maximum width; tl, total length.

Figures 52 A–D. Gonapophysis IX (second valvula), dorsal view. **A**, *Persis* (*Persis*). **B**, *Bebaiotes clarice.* **C**, *Synecdoche* sp. 2. **D**, *Bebaiotes amazonica*. Scale bars: A–D = 0.1 mm. Black arrows highlighting the direction of the apexes of lobes (char. 94): A, *Persis* (*Persis*) (state 0), B, *Bebaiotes clarice* (state 1), C, *Synecdoche* sp. 2 (state 2). Red arrows highlighting the curvature of the apexes of lobes (char. 96): B, *Bebaiotes clarice* (state 0) and D, *Bebaiotes amazonica* (state 1).

Figures 53 A–D. Gonapophysis IX (second valvula), dorsal view. **A**, *Catonia* sp. 2. **B**, *Bebaiotes cavichiolii*. **C**, *Bebaiotes oliveirai*. **D**, *Bebaiotes macroptera*. Scale bars: A–D = 0.1 mm. Black arrows highlighting the inner margin of the apexes of lobes (char. 97): A, *Catonia* sp. 2 (state 1), B, *Bebaiotes cavichiolii* (state 0), and D, *Bebaiotes macroptera* (state 2). Abbreviations: lb, length of base; ll, length of lobes.

Figures 54 A–C. Gonoplac, lateral view. **A**, *Bothriocera* sp. 1. **B**, *Anotia* sp. 2. **C**, *Bebaiotes clarice*. Scale bars: A–C = 0.1 mm. Black arrow highlighting gonoplac division (char. 99, state 1).

Figure 55. Strict consensus of 640 most parsimonious trees (L=338, IC=0.42 e IR =0.71) resulting from the analysis of 99 morphological characters of Achilixiidae. Numbers above

branches are bootstrap values > 80 (in percentage). Numbers below branches are Bremer support. Red clades indicate genera of Achilixiidae.

Figure 56. Strict consensus of 640 most parsimonious trees ((L=338, IC=0.42 and IR =0.71) resulting from the analysis of 99 morphological characters of Achilixiidae. Unambiguous ancestral characters optimized with parsimony are plotted over branches, with cyan squares referring to homoplastic and black to non-homoplastic synapomorphies. Numbers above rectangles refer to character number and below to state number.

LISTA DE TABELAS

Introdução

Capítulo 2

Capitulo 3

LISTA DE ABREVIATURAS

et.al. – et alii (e outros);
Fig. – Figura;
mm – milímetros;
sp. – espécie;
spp. – espécies;
sp. nov. – espécie nova;

PREFÁCIO

A presente tese é parte dos requisitos para obtenção do título de Doutor no Programa de Pós-Graduação em Entomologia, e, como tal, não é considerada uma publicação válida para fins de nomenclatura zoológica, de acordo com os requisitos do Código Internacional de Nomenclatura Zoológica (edição 1999), capítulo três, artigos 8.2 e 8.3.

1. INTRODUÇÃO

1.1. Hemiptera

Os hemípteros ocupam a primeira posição dentre os maiores grupos em diversidade de insetos não-holometábolos (Grazia *et al*., 2012). Há registro desses insetos em todos os continentes, exceto na Antártica (Gallo *et al*., 2002). Atualmente, a ordem está dividida em quatro subordens: Auchenorrhyncha Duméril, 1806, Coleorrhyncha Myers & China, 1929 Heteroptera Linnaeus, 1758 e Sternorrhyncha Amyot & Serville, 1843 (Grazia *et al*., 2012).

Os representantes de Hemiptera possuem hábitos alimentares distintos, podendo ser fitófagos, zoófagos e hematófagos (Triplehorn e Jonnson, 2011). Em virtude desses hábitos, muitas espécies são pragas importantes de diversos cultivos, pois se alimentam do xilema, floema ou conteúdo celular de plantas. Essas interações podem ser observadas, por exemplo, em culturas como o milho, cana-de-açúcar e citros, causando danos diretos com o hábito da fitofagia ou sendo vetores de fitopatógenos, como vírus e bactérias, em decorrência disso, é possível observar sintomas como o amarelecimento das folhas e uma redução no crescimento das plantas (Oliveira *et al*., 2007; Bellman, 2009; Ravaneli *et al*., 2011; Azevedo e Lima, 2015). Além de seu impacto nas culturas, alguns hemípteros são vetores importantes de patógenos que podem causar graves problemas à saúde do ser humano, um exemplo é o *Triatoma infestans* (Klug, 1834) (Reduviidae), vetor do protozoário *Trypanosoma cruzi* Chagas, 1909, responsável pela transmissão da doença de Chagas (Almeida *et al*., 2008; Kawaguchi *et al*., 2019). Além disso, algumas espécies desempenham um papel importante no manejo de pragas, sendo utilizados como controle biológico de outros insetos indesejados (Pereira *et al*., 2014), como por exemplo *Podisus nigrispinus* (Dallas, 1851) (Pentatomidae) que vem sendo estudado para predação de *Diatrae asaccharalis* (Fabricius, 1794) (Lepidoptera: Crambidae (Vacari *et al*., 2007).

Sternorrhyncha é considerada o grupo irmão de todas as outras subordens de hemípteros. Essa relação é corroborada por vários estudos que utilizaram análises filogenômicas, dados morfológicos e moleculares, e afirmam que o grupo Hemiptera Linnaeus, 1758 é monofilético (Johnson *et al*., 2018), assim como suas subordens (Campbell *et al*., 1995; Cryan e Urban, 2012; Li *et al*., 2017; Johnson *et al*., 2018).

Sternorrhyncha é subdividida em quatro superfamílias: Aleyrodoidea Westwood, 1840, Aphidoidea Geoffroy, 1762, Coccoidea Handlirsch, 1903 e Psylloidea Latreille, 1807, abrangendo 67 famílias. Esta subordem inclui uma variedade de insetos sugadores de seiva de

plantas que são considerados pragas importantes na agricultura, e conhecidos popularmente como os pulgões, cochonilhas e moscas-brancas (Grazia *et al*., 2012).

Coleorrhyncha é considerada a menor subordem de Hemiptera, composta pela família Peloridiidae Breddin, 1897 e duas famílias extintas: †Progonocimicidae Handlirsch, 1906 e †Karabasiidae Popov, 1985 (Szwedo, 2011; Jiang e Huang, 2017), atualmente ocorre na Região Australiana e no Sul da América do Sul, não ocorrendo para o Brasil (Grazia *et al*., 2012).

Heteroptera é a maior subordem e a mais diversa, composta por aproximadamente 42.000 espécies descritas, dividida em sete infraordens: Enicocephalomorpha Stichel, 1955, Dipsocoromorpha Miyamoto, 1961, Gerromorpha Popov, 1971, Nepomorpha Popov, 1971, Leptopodomorpha Popov, 1971, Cimicomorpha Leston *et al.*, 1954 e Pentatomomorpha Leston, Pendergrast & Southwood, 1954, abrangendo 89 famílias (Henry, 2009). Alguns grupos dentro dessa subordem são conhecidos popularmente como percevejos, maria-fedida e barbeiros (Ribeiro *et al.*, 2014).

Por fim, Auchenorrhyncha é dividida em quatro superfamílias, Cercopoidea Westwood, 1838, Cicadoidea Latreille, 1802, Membracoidea Rafinesque 1815 e Fulgoroidea Latreille, 1807, e composta por 33 famílias. São conhecidos popularmente como cigarras, cigarrinhas e soldadinhos (Grazia *et al.*, 2012).

Historicamente Auchenorrhyncha é composta por duas infraordens, Cicadomorpha Evans, 1946, que engloba as superfamílias Cercopoidea, Cicadoidea e Membracoidea, e Fulgoromorpha Evans, 1946 (Grimaldi e Engel, 2005; Gallo *et al*., 2002; Grazia *et al*., 2012). Durante muito tempo, com base em caracteres morfológicos e moleculares a filogenia de Auchenorrhyncha foi alvo de grandes discussões, sendo a subordem considerada parafilético (Goodchild, 1966; Hamilton, 1981; Li *et al*., 2017). Contrariamente, há estudos que recuperaram o clado Auchenorrhyncha como um grupo monofilético, com base em caracteres morfológicos e moleculares (Cryan e Urban, 2012), e recentemente seu monofiletismo foi corroborado com base em análises filogenômicas (Johnson *et al*., 2018). Neste estudo, o grupo alvo da pesquisa foi Achilixiidae Muir, que está inserido em Fulgoroidea.

1.2. Fulgoroidea Latreille, 1807

Os Fulgoroidea são cosmopolitas e incluem aproximadamente 14.000 espécies descritas, divididas em 19 famílias viventes (Boucher et al., 2023), e sua maior diversidade está concentrada nos trópicos (Mifsud *et al.*, 2010; Grazia *et al*., 2012; Bourgoin, 2023). O monofiletismo de Fulgoroidea tem sido corroborado em análises filogenéticas baseadas em

dados morfológicos, moleculares e filogenômicos (Asche, 1987; Urban e Cryan, 2007; Li *et al*., 2017; Johnson *et al*., 2018). Os fósseis mais antigos de Fulgoromorpha datam do período Permiano, com registros que remontam cerca de 258 milhões de anos (Bourgoin, 2023).

Os fulgoroideos são diversos em forma, possuem ampla variedade de cores, tamanho e características distintas em diferentes grupos, podendo ser identificados por meio de um conjunto de características: cabeça consideravelmente grande; antenas com pedicelo dilatado e alongado, localizadas abaixo dos olhos compostos; asas anteriores com veias anais formando um "Y" na região do clavo e tégula geralmente presente (Gallo *et al*., 2002; Grazia *et al*., 2012).

A relação entre as famílias de Fulgoroidea ainda é motivo de discussão, além do posicionamento de algumas famílias ser considerado incerto, como ocorre com Achilixiidae, objeto deste estudo.

1.2.1. Achilixiidae Muir, 1923

Achilixiidae é uma das famílias menos diversa dentro de Fulgoroidea, contando com apenas 24 espécies conhecidas, as quais estão inseridas em dois gêneros: *Achilixius* Muir, 1923 (Oriental) e *Bebaiotes* Muir, 1924 (Neotropical) (Wilson, 1989) (Figura 1). Com o trabalho de Viegas e Ale-Rocha (2023, submetido), mais 8 espécies foram descritas para *Bebaiotes*, totalizando agora 32 espécies conhecidas para a família (Tabela 1).

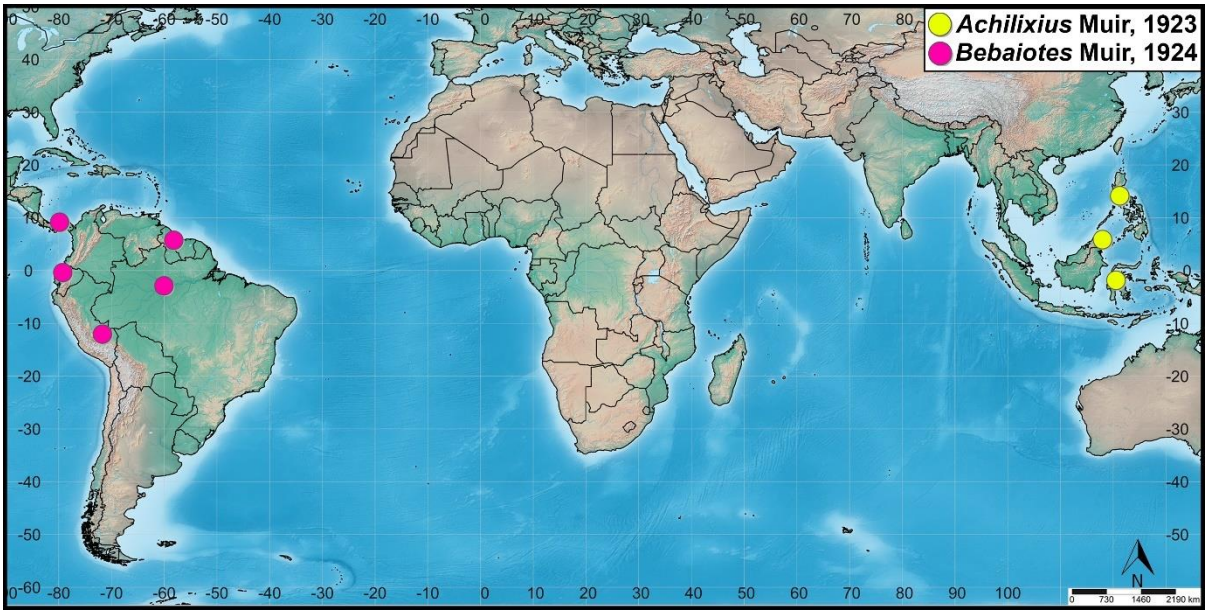

Figura 1. Mapa de distribuição de Achilixiidae. Distribuição conhecida de *Achilixius* Muir em círculos amarelos. Distribuição conhecida de *Bebaiotes* Muir em círculos rosa. Disponível em: http://www.simplemappr.net/

Tabela 1. Lista de gêneros e espécies de Achilixiidae, com respectivos dados de distribuição e depósito do holótipo.

Gêneros	Espécies	Distribuição	Dep. holótipo
***Achilixius* Muir**			
	A. bakeri Wilson	Filipinas (Laguna)	NHM
	A. danaumoati Wilson	Indonésia (Celebes do Norte)	NHM
	A. davaoensis Muir	Filipinas (Davao); Indonésia (Celebes do Norte)	BPBM
	A. fasciata Wilson	Indonésia (Celebes do Norte)	NHM
	A. fennahi Wilson	Malásia (Sabah)	BPBM
	A. irigae Wilson	Filipinas (Luzon)	BPPM
	A. kofintangi Wilson	Indonésia (Celebes do Norte)	IRSNB
	A. mayoyae Wilson	Filipinas (Mayoyao)	BPMN
	A. minahassae Wilson	Indonésia (Celebes do Norte)	NHM
	A. morowali Wilson	Indonésia (Celebes Central)	NHM
	A. muiri Wilson	Malásia (Sabah)	BPBM
	A. muujati Wilson	Indonésia (Celebes do Norte)	NHM
	A. sandakanensis Muir	Malásia (Sabah)	BPBM
	A. singularis Muir	Filipinas (Baguio)	BPBM
	A. torautensis Wilson	Indonésia (Celebes do Norte)	NHM
	A. tubulifer (Melichar)	Filipinas (Luzon)	NHM
***Bebaiotes* Muir**			
	B. amazonica Viegas & Ale-Rocha	Brasil (Amazonas, Pará, Rondônia e Roraima)	INPA
	B. banksi (Metcalf)	Brasil (Pará), Panamá (Barro Colorado)	Perdido
	B. bia Viegas & Ale-Rocha	Brasil (Acre)	INPA
	B. bucayensis Muir	Equador (Bucay)	BPBM
	B. dichromata Viegas & Ale-Rocha	Brasil (Amazonas)	INPA
	B. dorsivittata Fennah	Brasil, Equador, Peru	NHM
	*B. guianesus (*Fennah)	Brasil (Amazonas), Guiana (New River)	NHM
	B. macroptera Viegas & Ale-Rocha	Brasil (Amazonas e Amapá)	INPA
	B. nigrigaster Muir	Equador (Bucay)	BPBM
	B. nivosa Fennah	Guiana	NHM
	B. parallela Viegas & Ale-Rocha	Brasil (Amazonas)	INPA
	B. pallidinervis Muir	Equador (Napo)	BPBM
	B. pennyi Viegas & Ale-Rocha	Brasil (Amazonas e Maranhão)	INPA
	B. pulla Muir	Brasil (Acre e Amazonas); Equador (Felton)	BPBM
	B. tigrina Viegas & Ale-Rocha	Brasil (Amazonas)	INPA
	B. wilsoni Viegas & Ale-Rocha	Brasil (Amazonas)	INPA

NHM: Natural History Museum, U.K.; BPBM: Bernice P. Bishop Museum, Honolulu, Hawaii, U.S.A.; MA: Manfred Asche collection, Marburg, West Germany; USNM: United States National Museum, Washington, U.S.A.; IRSNB: Institut Royal des Sciences Naturelles de Belgique, Brussels, Belgium; INPA: Instituto Nacional de Pesquisas da Amazônia.

A família Achilixiidae foi estabelecida por Muir (1923) ao verificar que *Syntames tubulifer* Melichar, 1914, inicialmente alocada em Derbidae, possuía diversas diferenças em relação aos membros da família, como por exemplo, o comprimento do articulo apical do rostro, mais longo do que largo. Ao tentar realocar esta espécie em outra família, Muir observou que *S. tubulifer* compartilhava algumas características com alguns representantes de Cixiidae e Achilidae, embora possuísse particularidades que a excluíam de ambas as famílias.

As semelhanças de *S. tubulifer* com os representantes de Cixiidae da tribo Bennini observadas por Muir (1923) consistia nos processos laterais no abdômen, assim como a disposição das asas de maneira tectiforme (formando um "telhado") quando em repouso sobre o corpo. Entretanto, o autor observou algumas diferenças significativas de *S. tubulifer* em relação aos representantes de Bennini que o fez excluir esse gênero de Cixiidae, como a ausência do ocelo mediano, asa anterior com veia anal tocando a veia cubital posterior, o posicionamento e o formato dos processos laterais do abdômen, e diferenças na terminália masculina, incluindo variações no pigóforo e complexo fálico (Penny, 1980; Wilson, 1989).

Por outro lado, *S. tubulifer* também possuía semelhanças com os Achilidae devido ao arranjo das veias da asa anterior (Muir, op. cit.). No entanto, é importante ressaltar que a posição do ápice das asas anteriores, quando em repouso, não apresenta sobreposição em *S. tubulifer*, característica comum nos representantes de Achilidae. Além disso, a terminália masculina era destoante do padrão encontrado em Achilidae, especificamente a forma do pigóforo, tubo anal segmento X.

Assim, Muir (1923), propôs a família Achilixiidae para alocar as espécies que exibiam essas características distintivas, incluindo inicialmente as espécies do gênero-tipo *Achilixius* Muir, espécie-tipo *Achilixius singularis* Muir, 1923 das Filipinas. Nesse trabalho o autor também descreveu *Achilixius sandakanensis* Muir, 1923, *Achilixius davaoensis* Muir, 1923 e transferiu *S. tubulifer* Melichar, 1914 de Derbidae para sua nova família [*Achilixius tubulifer (*Melichar, 1914)], todas ocorrentes na região Oriental. As características estabelecidas por Muir (1923) para a identificação dos representantes dessa família são: 1) vértice e fronte, em perfil, convexo; 2) ausência de ocelo mediano; 3) carena mediana e laterais da fronte completas (Figura 2 C); 4) asas anteriores não se sobrepondo quando recolhidas, mantendo-se de maneira tectiforme, e; 5) abdômen com dois pares de processos laterais, localizados no esternitos III e V respectivamente (Figura 2 E).

Muir (1924) descreveu um segundo gênero, *Bebaiotes*, com base em duas espécies, *Bebaiotes bucayensis* Muir (espécie-tipo) e *Bebaiotes nigrigaster* Muir, ambas do Equador, registrando pela primeira vez a família para a região Neotropical. Posteriormente, Muir (1934)

incluiu mais duas espécies no gênero: *Bebaiotes pallidinervis* Muir, 1934 e *Bebaiotes pulla* Muir, 1934, também do Equador.

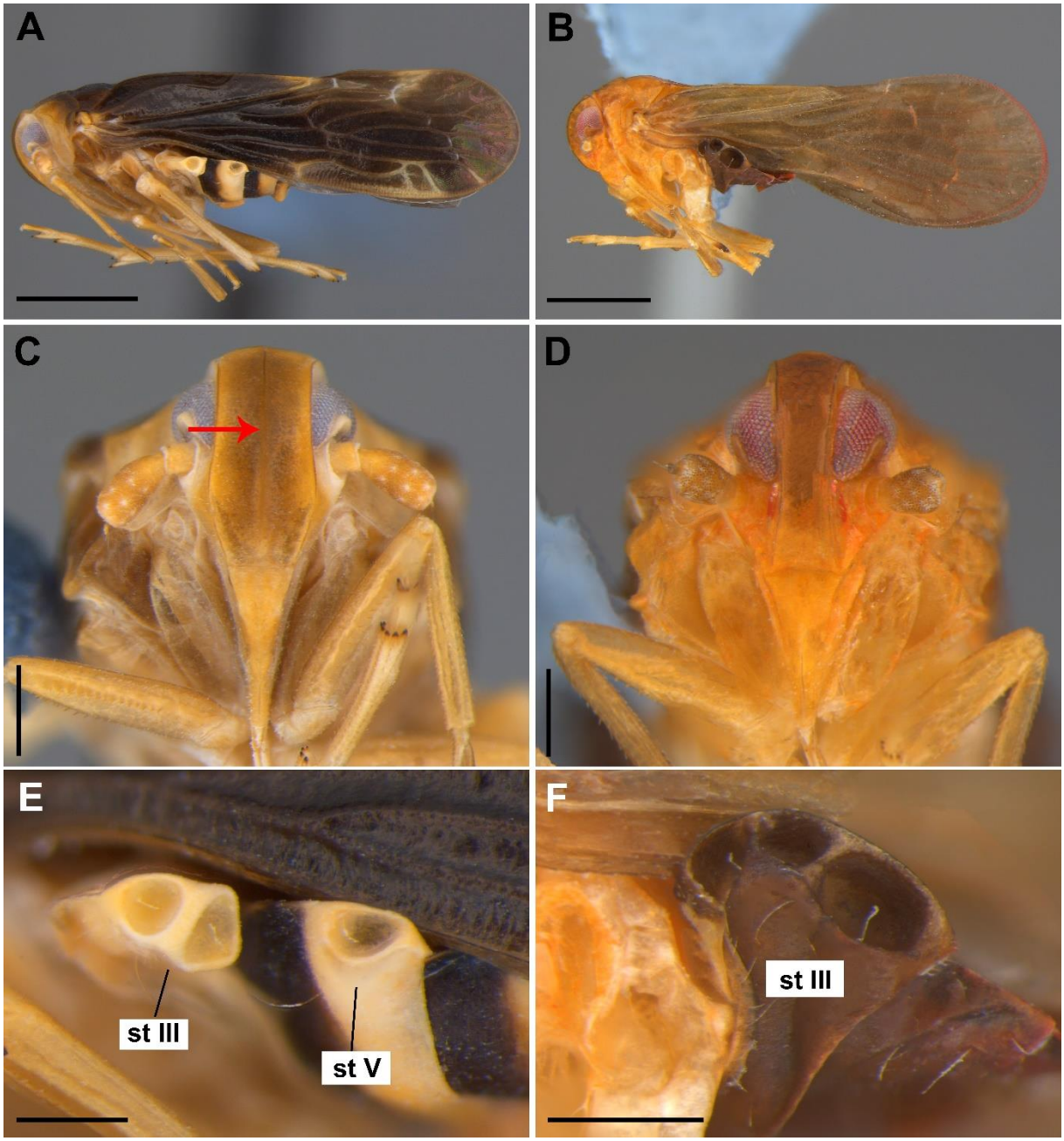

Figura 2 A–F. Espécies de Achilixiidae: **A, C, E,** *Achilixius* sp. **A**, vista lateral; **C,** cabeça, vista anterior; **E,** processos abdominais vista lateral; **B, D, F,** *Bebaiotes macroptera* Viegas & Ale-Rocha, 2023. **B**, vista lateral; **D**, cabeça, vista anterior; **F**, processos abdominais vista lateral. Escalas: A, D: 1 mm; B, E: 0.3 mm; C: 0.2 mm; F: 0.3 mm. Seta vermelha destacando a carena longitudinal mediana da fronte. Abreviações: st III, esternito III; st V, esternito V.

O terceiro gênero da família foi proposto por Metcalf (1938), *Muirilixius*, espécie-tipo *Muirilixius banksi* Metcalf, coletado no Panamá.

Fennah (1947) realizou um estudo sobre os Achilixiidae do Novo Mundo, onde foram descritas duas espécies para *Bebaiotes*: *Bebaiotes dorsivittata* Fennah, 1947 do Equador e *Bebaiotes nivosa* Fennah, 1947 da Guiana. Além dessas, foi descrita uma espécie para *Muirilixius*, *M. guianesus* Fennah, 1947 coletada na Guiana, e *B. nigrigaster* Muir, 1924 foi transferida para *Muirilixius.* Nesse trabalho, foi proposta uma chave de identificação onde constam todas as espécies de *Bebaiotes* descritas até então.

Uma sinopse sobre Achilixiidae foi feita por Wilson (1989), com base em dados morfológicos, incluindo a revisão de *Achilixius*, uma análise morfológica dos gêneros, assim como a sinonimização de *Muirilixius* com *Bebaiotes*. Nesse trabalho foram redescritas as quatros espécies de *Achilixus* conhecidas até o momento, e foram descritas mais 12 espécies para o gênero: *A. danaurnoati* Wilson, 1989, *A. fasciuta* Wilson, 1989, *A. kofintangi* Wilson, 1989, *A. rninahassae* Wilson, 1989, *A. morowali* Wilson, 1989, *A. muujati* Wilson, 1989 e *A. torautensis* Wilson, 1989, da Indonésia; *A. fennahi* Wilson, 1989 e *A. muiri* Wilson, 1989, ambas da Malásia; *A. bakeri* Wilson, 1989, *A. irigae* Wilson, 1989 e *A. mayoyae* Wilson, 1989, das Filipinas.

Viegas e Ale-Rocha (2023, submetido) realizaram um estudo taxonômico de Achilixiidae para o Brasil, onde quatro espécies de *Bebaiotes* foram revisadas e suas distribuições foram ampliadas: *B. banksi* (Metcalf, 1938), *B. dorsivittata* Fennah, 1947, *B. guianesus* (Fennah, 1947) e *B. pulla* Muir, 1934; e foram descritas mais oito espécies para o gênero (Tabela 1).

Em resumo, atualmente a família inclui os gêneros *Achilixius* e *Bebaiote*s (Figuras 2 A, B), e é caracterizada pela transição do vértice com a fronte sem carena transversal, presença de processos abdominais (Figuras 2 C, F) e pelo complexo fálico tubular e simples (Figuras 4 A–D). Seus gêneros são facilmente diferenciados: *Achilixius*, com uma carena mediana distinta na fronte (Figura 2 C), asa anterior com a veia radial posterior ramificada e veia transversal intercubital (icua) ausente (Figura 3 A), abdômen com dois pares de processos localizados nos esternitos III e V (Figura 2 E) e complexo fálico sem placas esclerosadas interna (Figuras 4 A, B); *Bebaiotes*, com a fronte sem carena mediana (Figura 2 D), veia radial posterior da asa anterior sem ramificação e veia transversal intercubital (icua) presente (Figura 3 B), abdômen com um par de processos formado por três fossas localizado na lateral do esternito III (Figura 2 F), complexo fálico com um par de placas esclerosadas internas (Figuras 4 C, D).

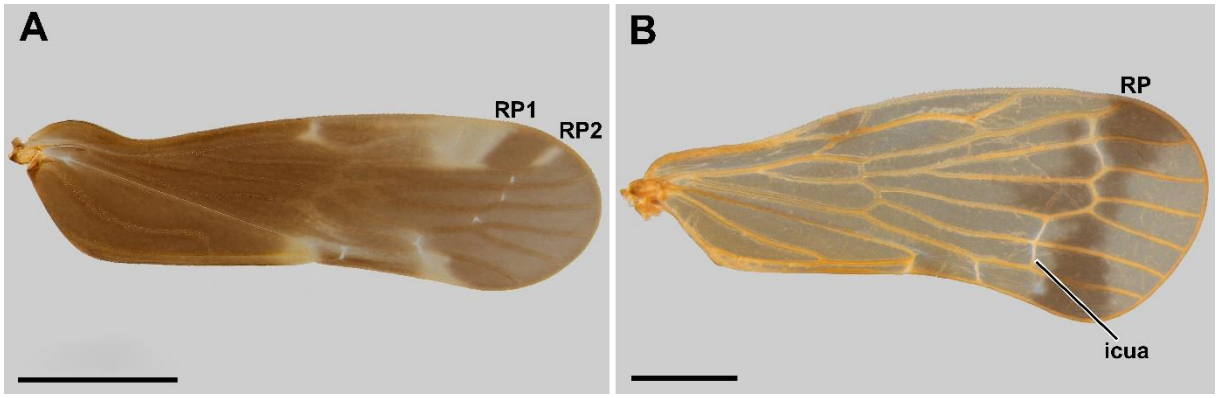

Figura 3 A–B. Achilixiidae, asa anterior direita. **A**, *Achilixius* sp. **B**. *Bebaiotes* sp. Escalas: A–B = 1 mm. Abreviações: RP, ramo posterior da veia radial; RP1; primeiro ramo da veia radial posterior; RP2, segundo ramo da veia radial posterior; icua, veia transversal intercubital.

Figura 4 A–D. Achilixiidae, Complexo fálico. **A–B**, *Achilixius* sp. **A**, vista lateral esquerda. **B**, vista dorsal. **C–D**, *Bebaiotes* sp. **C**, vista lateral esquerda. **D**, vista dorsal. Escalas: A–D = 0.1 mm. Abreviação: ps, placas esclerosadas internas.

1.2.2. Filogenia de Achilixiidae

Até o momento, não há estudos filogenéticos focados em Achilixiidae. Apenas um representante de *Bebaiotes* fêmea, não identificado, tem sido incluído em estudos mais abrangentes de Fulgoroidea baseados em análises moleculares (Urban e Cryan, 2007; Song e Liang, 2013; Bucher *et al*., 2023). Devido a presença dos processos abdominais laterais nos representantes de Achilixiidae, assim como em alguns cixídeos (Bennini e Bennarellini), questionamentos foram levantados por Metcalf (1945) e Hoch (1987) sobre o status de família dos Achilixiidae, mas sem se aprofundar na questão. Fennah (1947) também questionou a presença desses processos em ambas as famílias, mas considerou essa característica de pouca significância para a reconstrução do relacionamento entre as espécies, interpretando que o surgimento desses processos se deu provavelmente por paralelismo.

Posteriormente, surgiram algumas propostas filogenéticas para a classificação de Achilixiidae, como, por exemplo, Asche (1987), que com base em caracteres morfológicos, incluindo terminália do macho e da fêmea, propôs uma filogenia preliminar das famílias de Fulgoromorpha. Nessa análise, Achilixiidae foi considerada monofilética com base nos processos abdominais e próxima de Achilidae devido às características do ovipositor, que nessas famílias desempenha a função de escavar.

Wilson (1989), com base em um estudo morfológico dos gêneros de Achilixiidae, levantou a hipótese de que os processos abdominais dos gêneros não seriam homólogos, pois em *Achilixius* ocorrem dois pares de processos e em *Bebaiotes* apenas um par, sugerindo que novos estudos são necessários para definir as relações entre os gêneros.

Emeljanov (1990) optou por uma abordagem que colocou Achilixiidae dentro de Achilidae, e Chen e Yang (1995) posicionaram Achilixiidae dentro de Cixiidae.

Emeljanov (1991), com base em estudos da morfologia externa e da terminália do macho, não considerou Achilixiidae uma família, e propôs as subfamílias Bebaiotinae e Achilixiinae em Achilidae.

Contrariamente, Liang (2001), com base no estudo da morfologia das sensilas antenais de *Achilixius sandakanensis* Muir, considerou o processo flagelar como uma sinapomorfia de Achilixiidae e Cixiidae, sugerindo a transferência das subfamílias Bebaiotinae e Achilixiinae de Achilidae para Cixiidae.

Urban e Cryan (2007), por meio de dados moleculares (18S rDNA, 28S rDNA, H3-Histone subunit 3 e Wg-Wingless) concluíram que Achilixiidae não tem relação com Cixiidae. No cladograma resultante da análise de parcimônia deste trabalho, *Bebaiotes* foi recuperado como grupo-irmão de um clado formado por várias famílias de Fulgoromorpha, incluindo em

parte representantes de Achilidae. Porém na árvore resultante da análise de inferência Bayesiana, *Bebaiotes* foi recuperado como grupo-irmão de um clado formado em parte por "Achilidae" e Derbidae.

Song e Liang (2013), acrescentaram mais marcadores moleculares ao trabalho de Urban e Cryan (2007) resultando em um conjunto com sequências nucleares (18S e 28S rDNA) e sequências mitocondriais (16S rDNA e cytb) e o resultado obtido corrobora com a hipótese de que Achilixiidae e Cixiidae não sejam proximamente relacionados. No cladograma resultante da análise de máxima verossimilhança, *Bebaiotes* foi recuperado como grupo-irmão de um clado formado em parte por "Nogodinidae" e Derbidae. Porém na árvore resultante da análise de inferência Bayesiana, *Bebaiotes* foi recuperado como grupo-irmão de *Deferunda acuminata* Chou & Wang, 1985 e *Magadha flavisigna* (Walker, 1851), ambas de Achilidae.

Por fim, no estudo de Bucher *et al* (2023) sobre filogenia de Fulgoromorpha com base em dados moleculares (18S, 28S D3-D5, 28S D6-D10, Wg, COI, Cytb), o cladograma gerado pela análise da máxima verossimilhança recuperou *Bebaiotes* dentro do clado formado por espécies de Achilidae como grupo-irmão do gênero *Spino* sp.

Nesse contexto, este estudo propõe a primeira análise filogenética de Achilixiidae com amostragem de todos os gêneros. Essa família tem distintos caracteres morfológicos e nada se sabe ao certo as relações entre esses gêneros. Outro ponto importante sobre essa família são os processos abdominais, importante caráter diagnóstico da família, cuja homologia permanece questionável. O estudo da sistemática da família deve incrementar o conhecimento sobre as relações da mesma com outras famílias de Fulgoroidea ao testar as hipóteses anteriormente propostas sobre os relacionamentos entre as espécies. Por fim, o presente estudo representa o primeiro a abordar o tempo de divergência dos táxons dentro de sua linhagem. Desta forma, a realização desse trabalho, aliado a um estudo filogenético com base em caracteres morfológicos e moleculares, deve ajudar na elucidação dos questionamentos presentes na família.

1.3. Organização da presente tese

A tese foi estruturada na forma de artigos, abrangendo três capítulos distintos, cada um focado em aspectos específicos. O primeiro capítulo, intitulado "Taxonomy study of Achilixiidae Muir, 1923 (Hemiptera: Auchenorrhyncha: Fulgoroidea): description of five new species of *Bebaiotes* Muir from South America and description of a new species of *Achilixius* Muir from Philippines" teve como objetivo descrever, ilustrar e propor novos táxons que foram encontradas durante o desenvolvimento do trabalho como um todo. Foram descritas cinco

espécies novas para *Bebaiotes* e uma espécie nova para *Achilixius*. Adicionalmente, é fornecida uma chave de identificação atualizada para as espécies de *Bebaiotes* (machos e fêmeas).

O segundo capítulo intitulado "Evolution of the disjunct Neotropical and Oriental Achilixiidae (Hemiptera: Fulgoromorpha) during the gondwanan breakup" teve como objetivo propor uma hipótese filogenética com base em dados moleculares (18S rDNA, 28S rDNA, 16S rRNA e H3). Adicionalmente, este estudo fornece, pela primeira vez, informações sobre tempo de divergência das principais linhagens dentro de Achilixiidae. A matriz de dados concatenada foi composta por 67 táxons, 4.379 pares de bases nitrogenadas e 23 espécies foram sequenciadas, gerando novas sequências que foram depositadas no GenBank, contribuindo para o enriquecimento da base de dados genômicos.

Por fim, o terceiro capítulo intitulado "Morphology-based phylogeny of Achilixiidae (Hemiptera: Fulgoromorpha) with emphasis on the internal relationships of *Bebaiotes* Muir, 1924", teve como objetivo propor uma hipótese filogenética com base em dados morfológicos. A matriz de dados foi composta por 44 táxons (35 espécies do grupo interno e nove do grupo externo) e 99 caracteres morfológicos (65 binários e 34 multiestados). Devido à maior representatividade de *Bebaiotes*, as relações internas deste grupo tiveram uma melhor resolução.

Ao final, é apresentada uma síntese dos resultados, visando estabelecer a relação entre ambos os capítulos desta tese.

Cada capítulo foi formatado de acordo com as revistas científicas de interesse.

2. OBJETIVOS

2.1. Geral

Propor hipóteses de relacionamento filogenético entre as espécies de Achilixiidae com base em dados morfológicos e moleculares, a fim de compreender as suas histórias evolutivas e biogeográficas.

2.2. Específicos

- Testar o monofiletismo de Achilixiidae, *Achilixius* e *Bebaiotes* por meio de análises filogenéticas com base em caracteres morfológicos e de marcadores moleculares;
- Delimitar e diagnosticar os gêneros;
- Estimar o tempo de divergência das principais linhagens de Achilixiidae para compreender os processos históricos que moldaram a distribuição atual da família, seus gêneros e espécies;
- Atualizar a chave dicotômica para a identificação das espécies dos gêneros;
- Descrever as espécies novas já detectadas no material examinado para o desenvolvimento da tese.
- Elaborar mapas de distribuição para as espécies de Achilixiidae.

3. MATERIAL E MÉTODOS

3.1. Origem do material

Grande parte do material utilizado neste trabalho é proveniente do acervo da Coleção de Invertebrados do Instituto Nacional de Pesquisas da Amazônia - INPA. Coletas mais recentes são oriundas dos projetos "Biodiversidade de Insecta na Amazônia– rede BIA" (MCTI, CNPq e FNDCT) e "Entomologia na Amazônia: Diversidade de Insetos (MCTI), ambos coordenados pelo Dr. José Albertino Rafael. Além disso, recebemos empréstimos da Coleção Entomológica Professor Padre Jesus Santiago Moure, Universidade Federal do Paraná, Curitiba (DZUP); Museu Paraense Emílio Goeldi, Belém (MPEG); Coleção Zoológica do Maranhão, Universidade Estadual do Maranhão, Caxias (CZMA); Centro de Estudos em Biologia Subterrânea, Universidade Federal de Lavras, Lavras (CEBS); Coleção Entomológica José Alfredo Pinheiro Dutra, Rio de Janeiro, Universidade Federal do Rio de Janeiro (DZRJ) e Illinois Natural History Survey, University of Illinois, Champaign (INHS). Fotografias de material-tipo armazenado no Museu Bernice Pauhai Bishop, Honolulu (BPBM) e no Museu de História Natural, Londres (NHM) também foram analisadas.

Todo o material obtido por empréstimo encontra-se provisoriamente depositado no Laboratório de Sistemática de Diptera (LabDip) do INPA e, posteriormente, será devolvido às suas respectivas instituições, devidamente identificado e etiquetado. Os espécimes-tipo dos novos táxons serão depositados nas instituições de origem. As sequências geradas foram depositadas no GenBank®.

3.2. Identificação, Terminologia, preparação das genitálias e asas

O material foi identificado por meio dos trabalhos de Muir (1924, 1934), Metcalf (1938), Fennah (1947), Wilson (1989) e Viegas e Ale-Rocha (2023, submetido), e pela comparação com material-tipo em laboratório ou por meio de fotografias e material identificado, quando disponíveis.

A terminologia adotada para a morfologia externa seguiu O'Brien e Wilson (1985), exceto para a venação das asas anteriores que seguiu a terminologia de Bourgoin *et al*. (2015), das asas posteriores que seguiu Dworakowska (1988), das antenas que seguiu Liang (2001), da terminália do macho que seguiu Bourgoin (1988) e Bourgoin e Huang (1990), e da terminália da fêmea que seguiu Bourgoin (1993).

Para análise das estruturas genitais, o abdome foi separado do tórax, macerado em ácido lático 85% quente, estudado em um estereomicroscópio Leica® M165C e imerso em gel de glicerina. Depois, a genitália foi acondicionada em microtubos plásticos preenchidos com glicerina e montado em alfinete juntamente com o espécime. As asas anterior e posterior de um espécime foram destacadas, limpas por um banho curto de xilol e montadas entre lamínulas com Euparal. Após a secagem, o conjunto foi colado a um pequeno pedaço de papel e montado em alfinete no mesmo alfinete do espécime.

3.3. Fotografias

O material utilizado nesse trabalho foi fotografado com auxílio de microscópio estereomicroscópio binocular Leica® M205C com câmera digital acoplada, com uso do software Auto-Montage®. Foram feitas fotografias do hábito em vista dorsal e frontal, antena, tórax, asa anterior e posterior e outras estruturas de importância taxonômica. As imagens foram editadas e montadas em pranchas no programa Adobe Photoshop®.

4. CAPÍTULO I

Viegas, E. F.G.; Takiya, D. M. & Ale-Rocha, R. Taxonomy study of Achilixiidae Muir, 1923 (Hemiptera: Auchenorrhyncha: Fulgoroidea): description of five new species of Bebaiotes Muir from South America and description of a new species of Achilixius Muir from Philippines

Manuscrito formatado para *European Journal of Taxonomy*[1]

[1]Fator de impacto:1.2; Qualis biodiversidade: A4

Taxonomic study of the Achilixiidae Muir, 1923 (Hemiptera: Auchenorrhyncha: Fulgoromorpha): description of five new species of *Bebaiotes* Muir from South America and a new species of *Achilixius* Muir from the Philippines

Eduarda Fernanda Gomes Viegas[1*], Daniela Maeda Takiya[2], Rosaly Ale-Rocha[3]

[1*] Postgraduate Program in Entomology (PPG-Ent), Instituto Nacional de Pesquisas da Amazônia, Caixa Postal 2223, CEP 69080-971, Manaus, Amazonas, Brazil. Corresponding author: edwviegasgomes@gmail.com, ORCID: https://orcid.org/0000-0003-3349-5639

[2] Laboratório de Entomologia, Departamento de Zoologia, Instituto de Biologia, Universidade Federal do Rio de Janeiro, Rio de Janeiro, 21941-902, Rio de Janeiro, Brazil. Email: takiya@gmail.com, ORCID: https://orcid.org/0000-0002-6233-3615

[3] Coordenação de Biodiversidade, Instituto Nacional de Pesquisas da Amazônia, Caixa Postal 2223, CEP 69080-971, Manaus, Amazonas, Brasil. Email: alerocha@inpa.gov.br, ORCID: https://orcid.org/0000-0001-9874-9770

Running title: Taxonomy of Achilixiidae (Hemiptera: Fulgoromorpha)

The present paper has not been submitted to another journal, nor will it be in the 6 months after initial submission to *EJT*. All co-authors are aware of the present submission.

4.1. Abstract

Five new species of *Bebaiotes* Muir are described and illustrated from South America: *Bebaiotes cavichiolii* **sp. nov**. from Cusco Department, Peru; *Bebaiotes clarice* **sp. nov**. from Amazonas States, Brazil; *Bebaiotes oiapoquensis* **sp. nov**. from Amapá State, Brazil; *Bebaiotes oliveirai* **sp. nov**. from Amazonas State, Brazil, and *Bebaiotes specialis* **sp. nov**. from Alagoas and Bahia States, Brazil. In addition, a new species of *Achilixius* Muir, *Achilixius dietrichi* **sp. nov.** from Bukidnon Province, Philippines, is described and illustrated. Finally, an updated identification key to species of *Bebaiotes* (males and females) is provided.

Keywords. Abdominal appendages, Neotropical Region, Oriental Region, planthopper.

4.2. Introduction

Achilixiidae Muir is a small family of planthoppers with two genera and 32 described species (Wilson, 1989; Viegas & Ale-Rocha, 2023). This family has a disjunct distribution, with records for the Oriental (*Achilixius* Muir) and Neotropical (*Bebaiotes* Muir) regions (Wilson, 1989). The Achilixiidae are characterized by absence of a transverse carina separating the frons and vertex, forewings arranged in a tectiform manner, lora subtriangular, abdominal appendages present, and periandrium simple, as a symmetrical tube, and aedeagus not distinct (Viegas & Ale-Rocha, 2023).

The presence of abdominal processes is not exclusive to Achilixiidae, but are also present in Bennini Metcalf and Bennarellini Emeljanov (Cixiidae). However, the morphology and location of these abdominal appendages are distinct from that of Bennarellini and Bennini (Hoch et al. 2014; Viegas & Ale-Rocha, 2022). Within the genera of Achilixiidae the location of these abdominal appendages varies, in *Achilixius* they originate from the third and fifth abdominal segments, while in *Bebaiotes* it

originates from the third abdominal segment only (Wilson, 1989; Viegas & Ale-Rocha, 2022).

Currently, there is little information about the biology of this family, however, according to the information on labels of specimens, *Achilixius* can be found on the understory of lowland rain forest (200-500 m) and volcanic areas (at 1100 m). Besides that, specimens are known to be collected by different types of light trap, Malaise trap, yellow trap, and by sweeping vegetation (Wilson, 1989). According to Wilson (1989), *Achilixius* nymphs may feed on rotten or decaying vegetation, similar to the behavior of nymphs belonging to the Derbidae and Achilidae families, while adults can feed on plant tissues. On the other hand, *Bebaiotes* can be found on the understory and canopy of trees of tropical rainforests. Besides that, specimens are known to be collected by different types of light traps, Malaise trap, and by sweeping vegetation (Wilson, 1989; Viegas & Ale-Rocha, 2023). In addition, there is record of *Bebaiotes* spp. in caves in Brazil, in Tocantins and Pará states by Santos et al. (2022).

Bebaiotes was studied by Viegas & Ale-Rocha (2023), who revised four species found in Brazil, described eight new species, presented a key to species, illustrations, and distribution maps. *Achilixius* was reviewed by Wilson (1989), who revised the previously known species, described new species, and proposed a key to species. No subsequent information has been published on *Achilixius* until now.

In the present manuscript, we describe five new species of the *Bebaiotes* being four species from Brazil and one from Peru, and a new species of *Achilixius* from Philippines. Additionally, an updated identification key to males and females of *Bebaiotes* is provided. The distribution of the *Bebaiotes* in Brazil was expanded to the states of Bahia and Alagoas.

4.3. Material and methods

Terminology of the head mostly follows O'Brien & Wilson (1985), forewing venation follows Bourgoin et al. (2015), hind wing venation follows Dworakowska (1988), and antennae follows Liang (2001). We have adopted the terminology of Bourgoin (1993) for female genitalia and Bourgoin (1988) and Bourgoin & Huang (1990) for male terminalia.

For analysis of genital structures, abdomen was detached from the thorax, macerated with hot 85% lactic acid, and illustrated immersed in glycerin. Afterwards, genitalia were kept in plastic microvials filled with glycerin and pinned together with the specimen. Forewing of a specimen was detached, cleaned by a short xylol bath, and mounted between cover glasses with Euparal. After drying, sides of cover slides were glued to a small piece of cardboard and pinned with the specimen. Digital photographs were taken with a Leica MC 170 HD camera attached on a Leica M165C stereomicroscope and combined into expanded focus images by Leica Application Suite software.

Measurements taken in this study: body length (tip of head to tip of anal tube) and body length including wings (from tip of head to tip of wing). Measurements are taken in lateral view.

The distribution map was created with SimpleMappr (Shorthouse 2010), using geographical coordinates from specimen labels. Square brackets were used to complement label information of the material examined.

Specimens studied are deposited in the following institutions:

DZRJ = Coleção Entomológica Professor José Alfredo Pinheiro Dutra, Universidade Federal do Rio de Janeiro, Rio de Janeiro, Brazil

INHS = Illinois Natural History Survey, University of Illinois, Champaign, USA

INPA = Coleção de Invertebrados do Instituto Nacional de Pesquisas da Amazônia, Manaus, Brazil

MUSM = Museo de Historia Natural de la Universidade Mayor de San Marcos, Lima, Peru

4.4. Results

Taxonomy

Class Insecta Linnaeus, 1758

Order Hemiptera Linnaeus, 1758

Suborder Fulgoromorpha Evans, 1946

Family Achilixiidae Muir, 1923

Genus ***Achilixius*** Muir, 1923

Figs 1, 2, 20 A, B

Achilixius Muir, 1923: 33-34, fig.1 a-b (tegmen and genitalia); Metcalf, 1945: 215-217 (citation, world catalogue); Wilson, 1989: 487-505, figs 1-3, 5, 6, 12-107 (head, thorax, tegmen, antenna, sternites III and V, habitus of adult, male genitalia, female genitalia) (illustrations, description, key); Emeljanov, 1991: 54-58, figs 1-3, 8, 9 (head, thorax, forewing, and hind wing) (status of family, key to the subfamilies).

Type-species

Achilixius singularis Muir, 1923; by original designation.

Updated description. Medium sized: body length 2.3–4.3 mm in males. Frons approximately 2.0 times longer than wide; median carina of the frons present; gena without subantennal carina (Fig. 1 C); epistomal suture straight (Fig. 1 A). Pronotum with lateral carinae divergent laterally; posterior margin roundly concave. Mesonotum

with three longitudinal carinae. Forewings. branched RP vein, sub-rectangular Radial cell, MP vein with four branches, icua cross-vein absent, and apex of clavus with straight angle (Fig. 20 A). Abdominal pleura with two lateral pairs of modified abdominal processes, being one originating from the third sternite with two deep sensory pits and another originating from the fifth sternite with one deep sensory pit, each sensory pit with a single seta (Fig. 1 E). Male terminalia: pygofer symmetrical; medioventral process absent or present; gonostyli claviform, in posterior view, symmetrical, external margin with short projection, internal margin with several microsetae. Phallic complex: periandrium simple, symmetrical tube; inner sclerotized plates absent, aedeagus not distinguished (Figs 2 E-G). Anal tube (segment X) with variable shape. Female terminalia: Pygofer bilobed symmetrical, with abundant microsetae. Gonapophysis VIII with three spiniform projections of unequal sizes, curved to the external face, and variable projections on the lateroapical margin. Bursa copulatrix filamentous apically, bristles present laterally, on apical half. Gonapophysis IX (second valvula) sclerotized, bifid, lobes with pointed apex, wider at base and narrowing towards apex, apex curved latero-ventrally in dorsal view, bristles present laterally and inner margin of the lobes, on apical half. Gonoplac (third valvula) as long as wide, in lateral view, numerous setae apically. Anal tube (segment X) short; rounded in dorsal view; apex truncated in dorsal view, with many sparse setae.

Distribution. Oriental: Philippines, Indonesia, and Malaysia (Fig. 22).

Remarks. This genus may be easily distinguished from *Bebaiotes* by the following set of characters: median carina of frons present; lateral carinae of pronotum strongly diverging towards the tegula; two lateral pairs of modified abdominal processes (Figs 1 A, C, D).

Until now, little is known about the distribution of the *Achilixius*, with records of the genus only from the Malay Archipelago: Philippines, Sulawesi, and Sabah. There is no information on the biology of *Achilixius*, however, according to the information of labels of specimens, they can be found on the understory of tropical forests, in lowland rain forest, volcanic area, and collected in all months of the year. Besides that, based on information from labels of specimens studied, and on the literature, collecting methods used were sweep nets, Malaise, light traps, and yellow pan trap (Wilson, 1989).

Achilixius dietrichi Viegas, Takiya & Ale-Rocha sp. nov.

Figs 1 A–E, 2 A–H, 20 A, B, 22

Diagnosis. Frons predominantly yellow (Fig. 1 C). Pygofer without medioventral process (Figs 1 A, B). Basal width of gonostyli subequal to apical width in lateral view (Fig. 2 D).

Type material

Holotype

PHILIPPINES • ♂; [Mindanao] Bukidnon Province, Musuan Municipality, Maramag Barangay, slopes of Mt Musuan; 19-21 Apr. 2011; Malaise trap, base of forest, T. Catanach leg. (TAC2012-014), 6 m; INHS (Holotype condition: glued on paper triangle; right forewing and right hind wing mounted between coverslips).

Paratypes

PHILIPPINES • 1 ♂; Camiguim Island; 27 Jun. 2010; sweeping; J. Jones leg (ENT6102); INHS • 1 ♂; same collection data as for preceding, except sweeping Junk, just above sea level; DZRJ.

Measurements. Body length: male 2.3-2.5 mm (4.1-4.2 mm including wings) (N=2).

Description. Coloration. General body color yellowish brown (Figs 1 A, B). Frons predominantly yellow. Forewing predominantly dark brown, with translucid apex and yellow regions: narrow yellow stripes covering c-sc cross-vein; apex of vein RP2 yellow; C1a cell predominantly yellow; small yellow spot at apex of clavus; C5 cell with a horizontal narrow yellow stripe; Cubital cell with a horizontal, wide, yellow strip, a short, yellow, diffuse band at apical portion covering m-c1 cross-vein extending to the CuA2 vein; white r- m2, m1-m2, m2-m3, icua, and icu cross-veins; apex of clavus white (Fig. 20 A). Hind wing hyaline, light brown (Fig. 20 B). Legs yellow, except apex of spines of metatibiae and metatarsi black. Abdomen yellow, except sternites IV and VI brown (Fig. 1 A).

Head: frons wide, distance between lateral carinae of frons, at median portion, subequal to the maximum width of vertex (Figs 1 C, D). Clypeus approximately 2 times longer than maximum width; median carina strongly marked, present at distal two-fourths, but not reaching epistomal suture, (Fig. 1 C). Scape as long as wide (Fig. 1 C). Pedicel oblong, approximately 2 times longer than scape (Fig. 1 C).

Thorax: Pronotum anterior margin truncated; median longitudinal carina present; lateral carinae strongly diverging towards the tegula in dorsal view; posterior margin slightly concave; without pustules on posterior margin. Mesonotum with median and lateral longitudinal carinae present, strongly marked (Fig.1 D). Forewing: RA and RP1 veins with apexes strongly curved anteriorly; r-m cross-vein subequal to length of r-m2 cross-vein; ir cross-vein distant from r-m2 cross-vein; MP vein with four branches with uncurved apex; MP1, MP2, MP3, MP4 vein unbranching; MP1+2 and MP3+4 branching arising basad to r-m cross-vein; m-cu cross-vein present; m-cu approximately 2 times longer than m-cu2 cross-vein; CuA vein bifurcation arising before to r-m cross-vein; CuP vein approximately three times longer than Pcu + A1 vein; apex of clavus

197 forming straight angle (Fig. 20 A). Hind wing: first bifurcation of MP vein arising before
198 to m-cu cross-vein (Fig. 20 B). Legs: metatibia with 7 apical spines; metatarsus with 6+6
199 apical spines.

200 Male terminalia (Figs 2 A–H): Pygofer subtriangular in lateral view, without
201 medioventral process; posterior margin with short triangular protuberance; many sparse
202 setae ventrally (Figs 2 A, B). Gonostyli symmetrical; outer margin with short lobe near
203 apex, inner margins with several setae; basal width of gonostyli subequal to apical width
204 in lateral view; apex truncated in lateral view, claviform (Figs 2 C, D). Phallic complex
205 (Figs 2 E–G): periandrium subrectangular in lateral view, laterally compressed; dorsal
206 margin with indentation at the apex in dorsal view. Inner sclerotized plates absent. Anal
207 tube (segment X) short; subrectangular in dorsal view; apex truncated in dorsal view, with
208 many sparse setae (Figs 2 A, B, H).

209 **Etymology.** The species is named in honor of Dr. Christopher H. Dietrich from the
210 Illinois Natural History Survey for his immense contribution to the knowledge of the
211 Auchenorrhyncha fauna, and for lending specimens used in this work.

212 **Distribution**. Philippines (Camiguim and Mindanao islands) (Fig. 22).

213 **Taxonomic notes.** *Achilixius dietrichi* **sp. nov.** and *A. minahassae* Wilson, 1989 are very
214 similar species based on the coloration of the body, wings, anterior margin of the
215 pronotum truncated, and MP vein with four branches, however, *A. dietrichi* **sp. nov.** can
216 be promptly distinguished from *A. minahassae* Wilson, 1989 by, lora and body coloration
217 yellow, pygofer without medioventral process, anal tube (segment X) with rounded distal
218 corners in dorsal view, and gonostyli with short projection on the outer margin near apex
219 and apex curved posteriorly. *Achilixius minahassae* has lora and body coloration
220 yellowish brown, pygofer with a medioventral process, and anal tube (segment X) with
221 tapered distal corners in dorsal view.

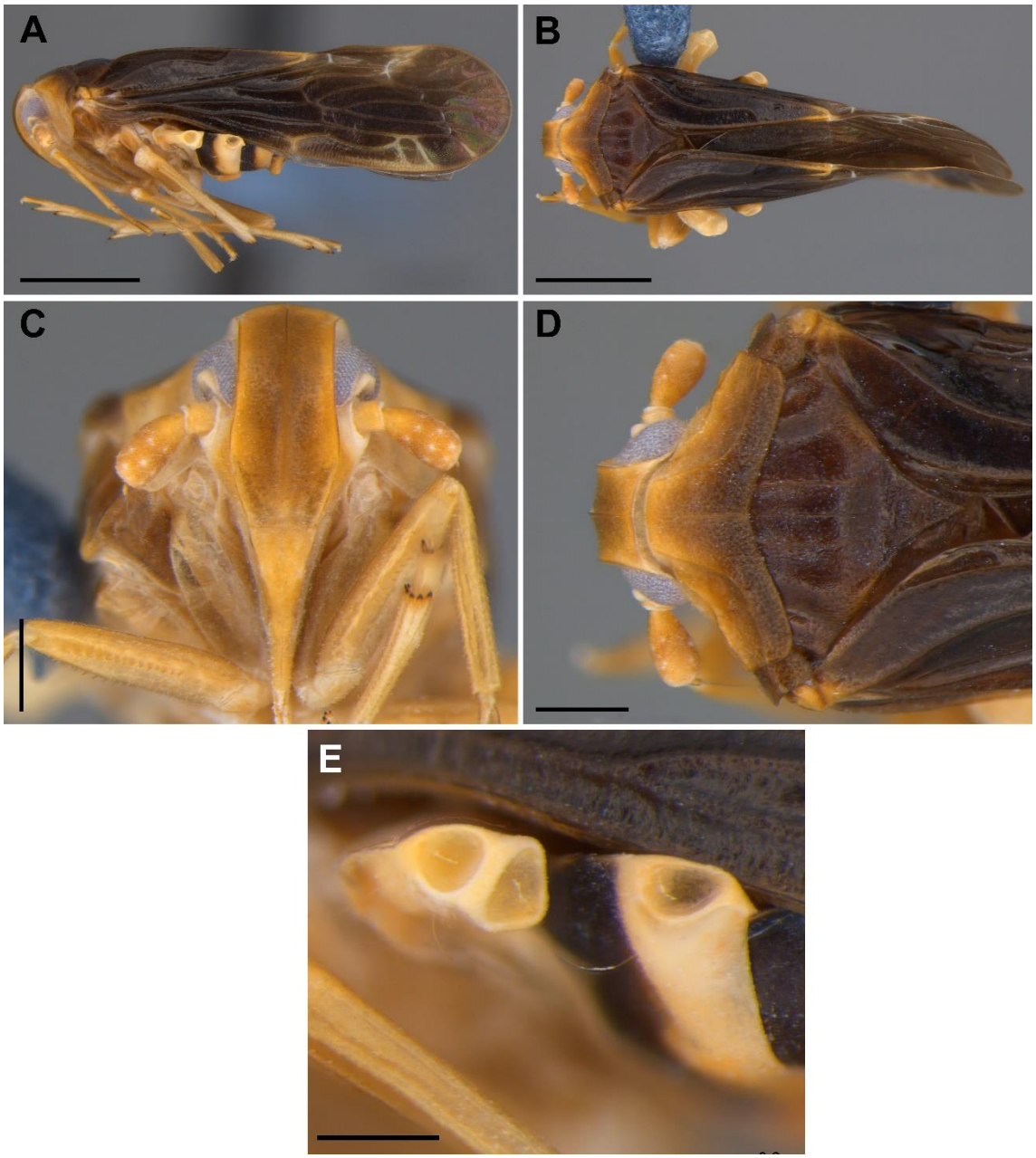

Figures 1 A–E. *Achilixius dietrichi* **sp. nov.**, male holotype (INHS): **A**. Lateral habitus; **B**. Dorsal habitus; **C**. Head, anterior view; **D.** Head and thorax, dorsal view; **E**. Abdominal process, lateral view. Scale bars: A, B = 1 mm; C, D = 0.3 mm; E = 0.2 mm.

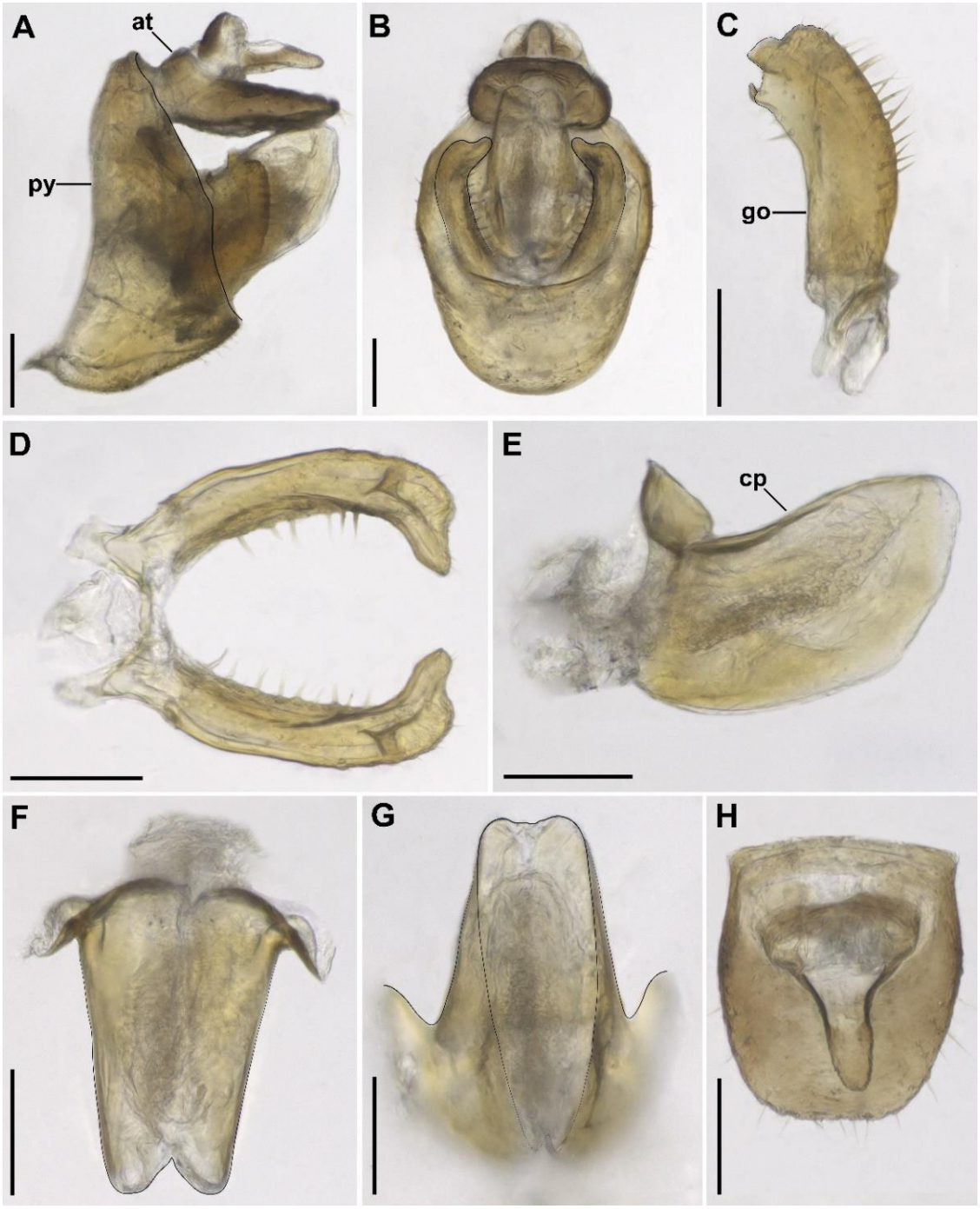

Figures 2 A–H. *Achilixius dietrichi* **sp. nov.**, male genitalia, paratype (INHS): **A.** Genital capsule, lateral view; **B.** Genital capsule, posterior view; **C**. Gonostyli, lateral view; **D.** Gonostyli, dorsal view.; **E**. Periandrium, lateral view; **F**. Periandrium, dorsal view; **G**. Periandrium, posterior view; **H**. Anal tube (segment X), dorsal view. Abbreviations: at, anal tube; cp, phallic complex; go, gonostyli; pe, periandrium; py, pygofer. Scale bars: A–G = 0.1 mm.

Genus ***Bebaiotes*** Muir, 1924

Figs 3-19, 20 C-F, 21, 23

Bebaiotes Muir, 1924:33-34, fig.1 a-b (tegmen and genitalia); Metcalf, 1945: 217 (world catalogue); Fennah, 1947:185, 186, 188, 189,190, figs. 1 a-b, 2 a-g; 3a-b (head, tegmen, thorax, sternite III, male and female terminalia) (description, illustrations, and key); O'Brien & Wilson, 1985: 90 (habitus, male and female terminalia) (citation illustrations); Wilson, 1989: 487-492, figs. 4, 7, 8, 9, 10,11 (head, tegmen, thorax, sternite III) (citation, illustrations, synonymy); Emeljanov, 1991: 54, 56, 58, figs. 4-7 (head, sternite III), 10-11 (tegmen) (citation, illustrations); Viegas & Ale-Rocha, 2023 (head, tegmen, thorax, sternite III, male and female terminalia) (description, illustrations, key, and distribution maps).

Type species: *Bebaiotes bucayensis* Muir, 1924; by original designation.

Updated description. Medium sized: body length 2.1–8.0 mm in males, 2.2–7.6 mm in females. Frons large or narrow; median carina of the frons absent (Figs 3 C, 4 B); gena with subantennal carina (Figs 18 B, C); epistomal suture curved upwards or almost straight. Antenna with scape short or long; pedicel globose or oblong (Figs 4 C, 7 C). Pronotum with lateral carinae gently diverging towards tegulae (Fig. 12 D) or subparallel to each other directed towards posterior margin. Forewings**.** unbranched RP vein, icua cross-vein present (Fig. 17 B). Male terminalia. pygofer symmetrical; medioventral process absent or present; gonostyli claviform, symmetrical, external margin with short and pointed projection apically, basal width subequal to apical width in lateral view (Figs 13 D, 15 D). Phallic complex: periandrium as simple tube, symmetrical; compressed dorsoventrally (Figs 5 G, 8 G); with a pair of internal sclerotized elongate plates, aedeagus not distinguished. Female. Similar to male, except by the shorter length. Female terminalia. pygofer bilobed with several setae and small spiniform projections near

ventral region in posterior view (Figs 6 A, 9 A, 16 A, 19 A). Gonapophysis VIII with three spiniform projections curved to the external face, of unequal sizes; variable projections on the lateroapical margin (Figs 6 B, 9 B, 16 B). Bursa copulatrix filamentous apically; bristles present laterally on apical half (Figs 6 B, 19 B). Gonapophysis IX (second valvula) sclerotized; bifid; lobes with pointed apex, wider at base and narrowing towards apex; apex curved latero-ventrally in dorsal view (Figs 16 C, 19 C). Gonoplac (third valvula) with variable shape, in lateral view, enlarged and bearing numerous setae apically (Figs 6 D, 9 D).

Distribution. Brazil (Acre, Alagoas [**new record**], Amapá, Amazonas, Bahia [**new record**], Maranhão, Pará, Rondônia, Roraima); Ecuador (Feltons); Guiana (New River); Panama (Barro Colorado); and Peru (Cusco, Madre de Dios) (Fig. 23).

Remarks. This genus can be easily distinguished from *Achilixius* by the following set of characters: median carina of frons absent; RP vein of the forewing unbranched; one lateral pair of modified abdominal processes; phallic complex with a pair of internal sclerotized plates (Figs 3 A, 7 A)**.**

Key to male and female specimens of *Bebaiotes* Muir species (updated from Viegas & Ale-Rocha, 2023)

1 Frons wide (distance between lateral carinae of frons, at median portion, half of or longer than the maximum vertex width measurement) in frontal view (Fig. 3 C) ... 2

- Frons narrow (distance between lateral carinae of frons, at median portion, approximately twice shorter than maximum width of vertex) in frontal view (Figs 4 C, 10 C) ... 11

2(1) Pronotum with pustules near posterior margin (Figs 3 A, 17 A) … 3

- Pronotum without pustules on posterior margin (Figs 18 C, D) … 4

3(2) Median region of frons without lozenge-shaped spots (Fig. 17 C);Forewing with MP vein with four branches (Fig. 17 A) and m-cu cross-vein absent (Fig. 17 A); anterior margin of the pronotum tapering (Fig. 17 B) ... *B. pallidinervis* Muir, 1934

- Median region of frons with lozenge-shaped spots (Fig. 3 C); forewing with MP vein with five branches (Fig. 3 A) and m-cu cross-vein present (Fig. 3 A); anterior margin of the pronotum rounded (Fig. 3 B) ... *B. bucayensis* Muir, 1924

4(2) Forewing MP vein with four branches (Fig. 21 E); median carina covering distal two or three-fourths of clypeus and extending to a distance far from epistomal suture (Fig. 18 B) ... 5

- Forewing MP vein with six or seven branches (Fig. A); median carina covering almost completely the clypeus and extending to very close to epistomal suture ... *B. dorsivittata* Fennah, 1947

5(4) Body coloration varying from light brown to dark brown; wings varying from light brown to dark brown; projections of lateroapical margin of the gonapophysis VIII with dorsal margin serrate … 6

- Body coloration whitish yellow (Figs 11 A, C); wings white (Fig. 11 B); projections of lateroapical margin of the gonapophysis VIII with dorsal margin smooth (Fennah, 1947: Fig. 5 E) … *B. nivosa* Fennah, 1947

6(5) Pedicel globose; anterior margin of the pronotum truncated or tapering; Gonapophysis VIII (first valvula) with three projections on lateroapical margin … 7

- Pedicel oblong (Fig. 18 B); anterior margin of the pronotum rounded (Fig. 18 D); Gonapophysis VIII (first valvula) with one projection on lateroapical margin (Fig.19 B) … *B. specialis* **sp. nov**.

7(6) Anterior margin of the pronotum truncated; periandrium with apex of dorsal margin indented; extensions of the gonapophysis IX (second valvula) with apices not bifid ... 8

- Anterior margin of the pronotum tapering; periandrium with apex of dorsal margin without indentation; extensions of the gonapophysis IX (second valvula) with apices bifid ... *B. macroptera* Viegas & Ale-Rocha, 2023

8(7) Median region of pronotum brown; tegula brown ... 9

- Median region of pronotum whitish yellow; tegula whitish yellow ... 10

9(8). Body coloration light brown; forewing CA vein light brown at medial area; hind tibia with 8 apical spines; periandrium with short indentation on dorsal margin ... *B. amazonica* Viegas & Ale-Rocha, 2023

- Body coloration dark brown; forewing CA vein red at medial area; hind tibia with 9 apical spines; periandrium with long indentation on dorsal margin ... *B. parallela* Viegas & Ale-Rocha, 2023

10(8) Clypeus without brown band; m-cu cross-vein of the forewing present; periandrium with apex of dorsal margin with long indentation; bursa copulatrix densely filamentous apically ... *B. dichromata* Viegas & Ale-Rocha, 2023

- Clypeus with two brown longitudinal bands; m-cu cross-vein of the forewing absent; periandrium with apex of dorsal margin with short indentation; bursa copulatrix sparsely filamentous apically ... *B. tigrina* Viegas & Ale-Rocha, 2023

11(1). Pustules present near posterior margin of pronotum (Fig. 12 D) ... 12

- Pustules absent near posterior margin of pronotum (Fig. 7 D) ... 14

12(11). Pustules of the pronotum brown; posterior margin of pronotum with angled indentation; apex of ventral margin of periandrium with indentation … 13

- Pustules of the pronotum pale yellow; posterior margin of pronotum almost straight; apex of ventral margin of periandrium without indentation … *B. pulla* Muir, 1934

13(12). General body coloration light brown; lateral carinae of pronotum subparallel to each other directed towards the posterior margin; outer margin of the gonostyli with pointed projection near to apex; dorsal margin of the periandrium without short indentation at apex … *B. pennyi* Viegas & Ale-Rocha, 2023

- General body coloration dark brown; lateral carinae of pronotum gently diverging towards the tegula (Fig. 9D); outer margin of the gonostyli with rounded projection near to apex (Fig. 10 C); dorsal margin of the periandrium with short indentation at apex (Fig. 10 F) … *B. oiapoquensis* **sp. nov**.

14(11). General body coloration yellow (Figs 3 A, 11 A) … 15

- General body coloration brown (Figs 6 A) … 18

15(14). Abdomen predominantly yellow (Figs 3 A, 11 A) … 16

- Abdomen predominantly dark brown (Figs10 A–C) … *B. nigrigaster* Muir, 1924

16(15). Body length, including wings, around 6.3 mm (Fig.11 A); pedicel oblong (Fig. 11 B); ventral margin of periandrium without indentation at apex (Fig. 8 F); gonapophysis VIII (first valvula) with four projections on lateroapical margin (Fig. 16 B) ... 17

- Body length, including wings, around 4.8 mm (Fig. 3 A); pedicel globose (Fig. 3 C, 11 A); ventral margin of periandrium with short indentation at apex (Fig. 4 F); gonapophysis VIII (first valvula) with one projection on lateroapical margin (Fig. 5 B) … *B. cavichiolii* **sp. nov**.

17(16). Median longitudinal carina of pronotum strongly marked (Fig. 14 D); apex of the margin of the periandrium truncated (Fig. 14 F); gonapophysis VIII (first valvula) with projections on the lateroapical margin with irregular teeth (Fig. 15 B) … *B. oliveirai* **sp. nov**.

- Median longitudinal carina of pronotum weakly marked; apex of the margin of the periandrium rounded; gonapophysis VIII (first valvula) with projections on the lateroapical margin with smooth dorsal margin ... *B. banksi* (Metcalf, 1938)

18(14). Median region of the pronotum brown; tegula brown; periandrium with apex of dorsal and ventral margins variable (Fig. 8 F) ... 19

- Median region of the pronotum white; tegula white; periandrium with apex of dorsal margin serrated and ventral margin with short indentation ... *B. guianesus* (Fennah, 1947)

19(18). Gena and lora brown; forewing with m-cu2 cross-vein aligned with icua cross-vein and MP vein with four branches; dorsal margin of periandrium with rounded apex; projections of lateroapical margin of gonapophysis VIII (first valvula) with dorsal margin variable... 20

- Gena and lora light yellow (Figs 6 C, D); forewing with m-cu2 cross-vein not aligned with icua cross-vein (Fig. 17 A) and MP vein with five branches (Fig. 17 A); dorsal margin of periandrium with triangular apex (Fig. 8 F); projections of lateroapical margin of gonapophysis VIII (first valvula) with dentate dorsal margin (Fig. 9 B) ... *B. clarice* **sp. nov**.

20(19). Forewing without broad transverse dark brown band at apical third; periandrium with apex of dorsal margin serrated; gonapophysis VIII (first valvula) with four projections at lateroapical margin ... *B. bia* Viegas & Ale-Rocha, 2023

- Forewing with broad transverse dark brown band at apical third; periandrium with apex of dorsal margin smooth; gonapophysis VIII (first valvula) with three projections at lateroapical margin ... *B. wilsoni* Viegas & Ale-Rocha, 2023

Bebaiotes bucayensis Muir, 1924

Figs 3 A–D

Bebaiotes bucayensis Muir, 1924: 34: fig.1 a-b (tegmen and genitalia) (description); Metcalf, 1945: 217 (world catalogue) Wilson, 1989: 491-492, 488, figs 9, 10 (head, tegmen) (citation, illustrations); Emeljanov, 1991: 54, 56, 58, figs. 4-7 (head, sternite III), 10-11 (tegmen) (citation, illustrations).

Diagnosis. Frons large (Fig. 3 C). Median region of frons with lozenge-shaped spots (Fig. 3 C). Forewing with MP3 branched (Fig. 3 A).

Type material

Holotype

ECUADOR • ♂; Bucay, 1000 feet elevation, 10.x.1922, F. X. Williams, nº 1097; BPBM.

Paratype

ECUADOR • ♂; Bucay, 1000 feet elevation, 10.x.1922, F. X. Williams, 013585361; NHM (Paratype condition: glued on paper triangle; right antenna broken and lost, left flagellum broken and lost; left proleg broken and lost).

Redescription. Coloration. General body color light brown (Figs 3 A, B). Median region of frons with lozenge-shaped spots brown (Fig. 3 C); scape, median and lateral longitudinal carinae of pronotum and mesonotum, pustules, long narrow stripe at lateral region of mesonotum, epimeron, and episternum, yellow. Forewing semihyaline, yellowish brown, with yellow regions mainly along veins: narrow stripe covering c-sc cross-vein, ir cross-vein, RA vein, and RP vein; medial region of CA vein red basal region of postcostalcell with wide light yellow horizontal band; basal region of MP vein yellow; large yellow stripe extending from r-m1 cross-vein, band passing through the m-cu cross-vein and covering half of CuA vein, and extending through the CuA1 and CuA2 vein narrow yellow stripe extending from r-m2 cross-vein to MP5 vein base; yellow X-

shaped spot covering m-cu2 cross-vein, middle region of the CuA1 vein, and the icua cross-vein; yellow oval spot at apical portion of CuA1 and CuA2 veins; narrow yellow stripe covering A1 vein; postclaval margin yellow (Fig. 3 B). Abdomen yellowish brown, except, sternite II light yellow.

Head: Frons large (Fig. 3 C); median carina of clypeus strongly marked, present on distal three-fourths, not extending to epistomal suture (Fig. 3 C). Scape as long as wide (Fig. 3 C). Pedicel oblong (Fig. 3 C). Thorax: Pronotum anterior margin rounded; median longitudinal carina present, weakly marked; lateral carinae gently diverging towards tegulae in dorsal view; posterior margin concave with shallow median notch in dorsal view; with pustules on posterior margin; mesonotum with median and lateral longitudinal carinae present, weakly marked (Fig. 3 B). Forewing: RA vein with apex gently curved anteriorly; RP vein with strongly curved anteriorly; r-m cross-vein approximately half length than r-m2 cross-vein; ir cross-vein distant from r-m2 cross-vein; MP vein with five branches with gently curved anteriorly; MP1, MP2, MP4 veins unbranched and MP3 branched; MP1+2 and MP3+4 branching arising distad to r-m cross-vein; m-cu cross-vein present; m-cu cross-vein approximately three times shorter than m-cu2; m-cu2 cross-vein aligned with icua cross-vein; CuA vein bifurcation before to r-m cross-vein; apex of clavus forming acute angle (Fig. 3 A).

Male terminalia not examined.

Distribution. Ecuador (Bucay).

Taxonomic notes. *B. bucayensis* Muir, 1924 is most similar to *B. pallidinervis* Muir, 1934 because they forewing yellowish brown and with yellow regions mainly along veins but can be promptly distinguished from the latter by, pronotum with pustules on posterior margin, pronotum with anterior margin rounded, MP vein of forewing with five branches, and m-cu cross-vein present.

Figures 3 A–D. *Bebaiotes bucayensis* Muir, 1924, male paratype (NHM): **A.** Lateral habitus; **B**. Head, anterior view; **C**. Head, thorax, wings, dorsal view; **D.** Specimen labels. Fotos: Webb (2019).

***Bebaiotes cavichiolii* Viegas, Takiya & Ale-Rocha sp. nov.**

Figs 4 A–F, 5 A–G, 6 A–E, 20 C, D, 23

Diagnosis. Body coloration yellow (Figs 4 A, B). Anterior margin of pronotum tapering (Fig. 4 D). Median longitudinal carina of pronotum strongly marked (Fig. 4 D). Dorsal margin of periandrium entire and ventral margin of periandrium with short indentation (Fig. 5 F).

Type material.

Holotype

PERU • ♂; **Cusco**, Quincemil; 13˚13'03.4"S, 70˚43'40"W; 633 m; 23–31 Aug. 2012; Sweep; J.A. Rafael, R.R. Cavichioli, D.M.Takiya leg.; MUSM (Holotype condition: glued on paper triangle; right and left flagellum broken and lost. Right and left forewing

torn at apex of clavus; right proleg broken and stored in a microtube and left proleg broken and lost; abdomen removed and stored in a microtube; genitalia dissected and stored in a microtube).

Paratypes

PERU • 1 ♀; **Cusco**, Quincemil; 31˚08'27"S, 70˚23'14"W; 350 m; 01 Set. 2012; Sweep; J.A. Rafael, R.R. Cavichioli leg.; MUSM (ENT6270).

Measurements. Body length: male 2.4 mm (4.8 mm including wings) (n=1) holotype; female: 2.7 mm (4.7 mm including wings) (n=1).

Description. Coloration. General body color yellow (Figs 4 A, B). Forewing semihyaline, yellow with white regions: white r-m2, m1-m2, m-cu2, icua, and icu cross-veins (Fig. 20 C). Hind wing hyaline, with light yellow spots (Fig. 20 D). Legs yellow, except black apices of spines of metatibiae and metatarsus.

Head: frons narrow, distance between lateral carinae of frons, at median portion, approximately twice smaller than maximum width of vertex (Fig. 4 C). Clypeus approximately 2.5 times longer than maximum width; median carina weakly marked, not extending to epistomal suture, present at distal three-fourths (Fig. 4 C). Scape wider than long (Fig. 4 C). Pedicel globose, approximately twice longer than scape (Fig. 4 C).

Thorax: Pronotum with anterior margin tapering; median longitudinal carina present, strongly marked; lateral carinae moderately diverging towards tegulae; posterior margin with angled indentation in dorsal view; without pustules on posterior margin. Mesonotum with longitudinal carina present, strongly marked; lateral longitudinal carinae absent (Fig. 4 D). Forewing: RA vein with apex strongly curved anteriorly; RP vein with apex gently curved anteriorly; r-m cross-vein approximately three times shorter than r-m2 cross-vein; ir cross-vein close to r-m2 cross-vein, not aligned; MP vein with four branches with straight apex; MP1, MP2, MP3, MP4 veins unbranched; MP1+2 and

MP3+4 branching arising distad to r-m cross-vein; m-cu cross-vein present; m-cu cross-vein subequal in length to m-cu2 cross-vein; m-cu2 cross-vein aligned with icua cross-vein; CuA vein bifurcation basad to r-m cross-vein; CuP vein approximately six times longer than the Pcu + A1 vein; apex of clavus forming acute angle (Fig. 20 C). Hind wing: first bifurcation of MP vein arising distad to m-cu cross-vein (Fig. 20 D). Legs: metatibia with 9 apical spines; metatarsus with 6+6 apical spines. Female. Similar to male, except the general body color dark yellow (Fig. 4 B)**.**

Male terminalia (Figs 5 A–G): Pygofer subtriangular in lateral view, posterior margin without projections and almost straight (Fig. 5 A). Gonostyli symmetrical; outer margin with short, rounded and posteriorly directed lobe near apex; inner margin slightly arched, convergent distally in dorsal and posterior views; apex truncated in lateral view, claviform (Figs 5 B–D). Phallic complex: periandrium semi-rounded in dorsal view, compressed dorsoventrally; dorsal margin of periandrium without apical indentation and ventral margin with short indentation at apex in dorsal view (Figs 5 E, F). Inner sclerotized plates slender in dorsal view, with serrated margin (Figs 5 E, F). Anal tube (segment X), short; rounded in dorsal view; apex truncated in dorsal view (Fig. 5 G).

Female terminalia (Figs 6 A–E): Gonapophysis VIII (first valvula) broad, with sparse setae at median region; small spiniform projections at basal half in lateral view; one lateroapical projection with irregular teeth at dorsal margin in lateral view (Fig. 6 B). Bursa copulatrix densely filamentous apically, acute apex, covered by setae laterally in the apical half (Fig. 6 B). Gonapophysis IX (second valvula) robust; bifid at apical half; lobes with pointed, strongly curved latero-ventrally apex, hook-like in dorsal view; and membranous prolongations at ventral region near apex (Fig. 6 C). Gonoplac (third valvula) broad, subtrapezoidal; apex truncated with numerous apical and laterally setae

(Fig. 6 D). Anal tube (segment X) short and rounded in dorsal view; apex rounded in dorsal view (Fig. 6 E).

Etymology. The species is named in honor of Dr. Rodney Ramiro Cavichioli from the Universidade Federal do Paraná, Curitiba, Brazil, for his immense contribution to the knowledge to the Auchenorrhyncha fauna, and for being one of the collectors of the holotype of the species described herein.

Distribution. Peru (Cusco) (Fig. 23).

Taxonomic notes. *B. cavichiolii* **sp. nov**. can be promptly distinguished from other species of *Bebaiotes* with narrow frons by its general coloration of body yellow, male body length about 2.4 mm, and female genitalia with gonapophysis VIII (first valvula) with one projection on lateroapical margin.

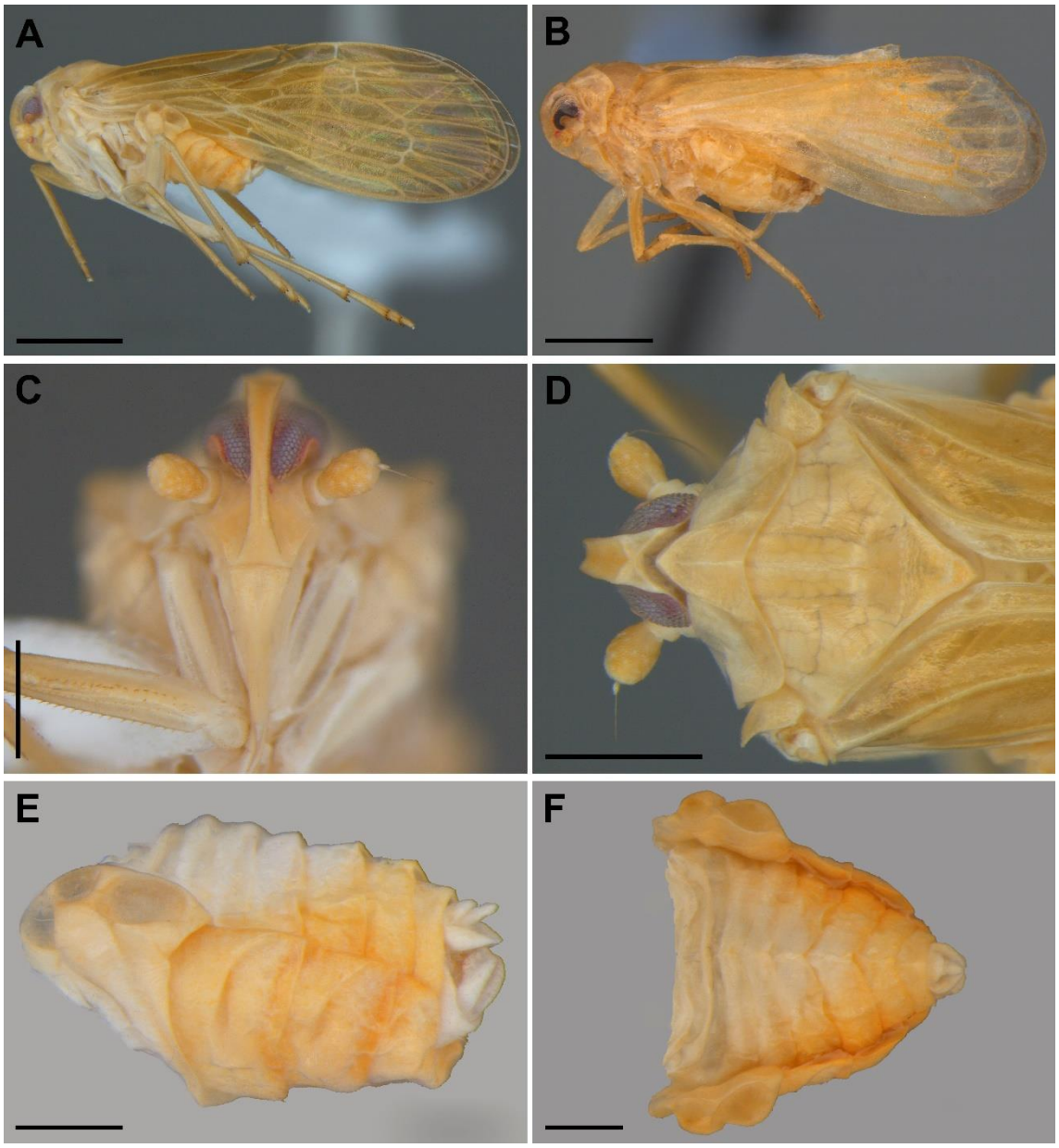

Figures 4 A–F. *Bebaiotes cavichiolii* **sp. nov.**: **A, C-F**. male holotype (MUSM). **A**. Lateral habitus; **B**. Lateral habitus, female paratype (MUSM); **C**. Head, anterior view; **D.** Head and thorax, dorsal view; **E**. Abdomen, lateral view; **F**. Abdomen, dorsal view. Scale bars: A, B = 1mm; C = 0.4 mm; D = 0.5 mm; E, F = 0.3mm.

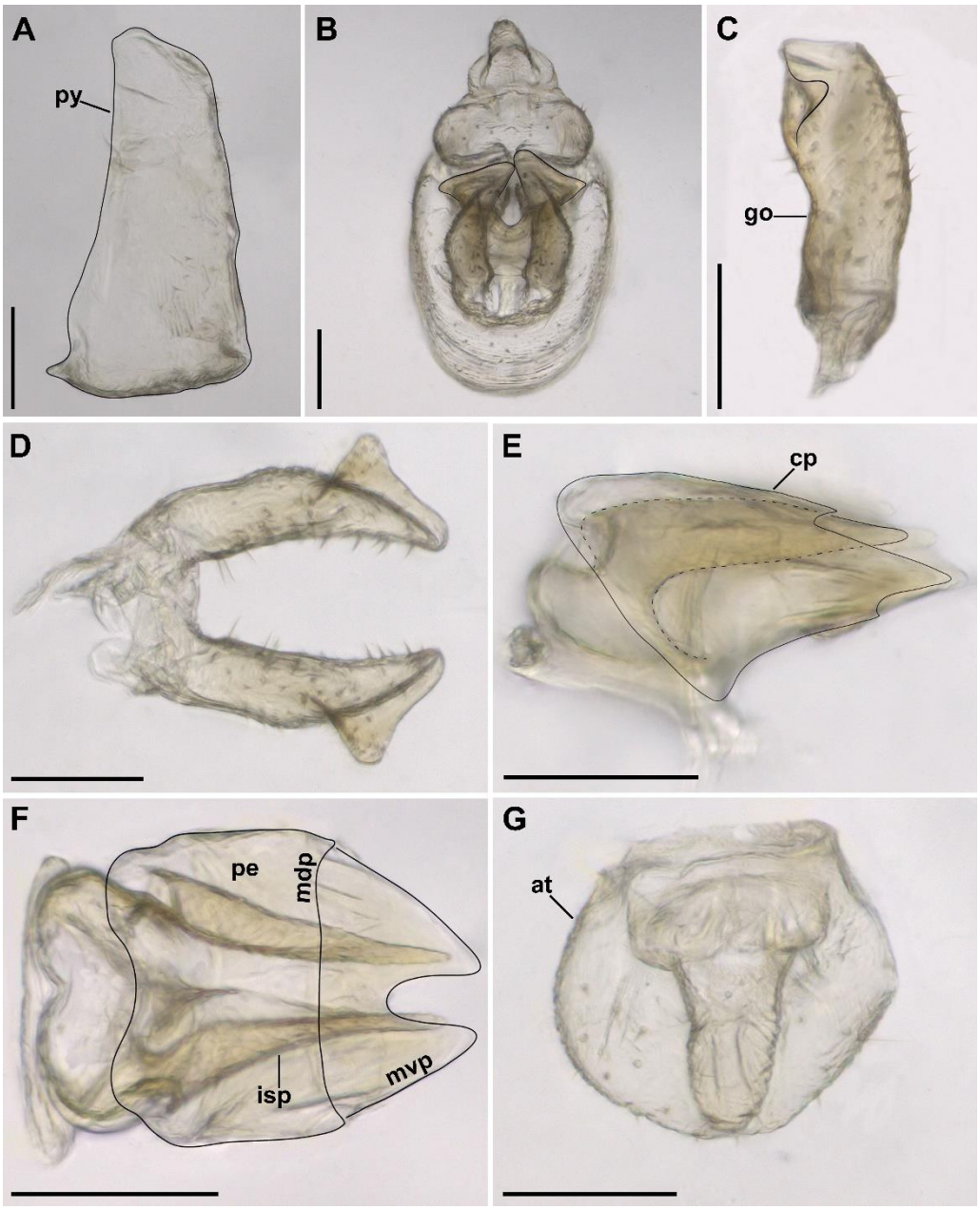

Figures 5 A–G. *Bebaiotes cavichiolii* **sp. nov.**, male genitalia, holotype (MUSM): **A.** Pygofer, lateral view; **B**. Genital capsule, posterior view; **C**. Gonostyli, lateral view; **D.** Gonostyli, dorsal view; **E** Periandrium and inner sclerotized plate, lateral view; **F**. Periandrium and inner sclerotized plate, dorsal view; **G**. Anal tube (segment X), dorsal view. Abbreviations: at, anal tube; cp, phallic complex; go, gonostyli; mdp, dorsal margin of periandrium; mvp, ventral margin of periandrium; isp, inner sclerotized plates; pe, periandrium; py, pygofer. Scale bars: A–G = 0.1 mm.

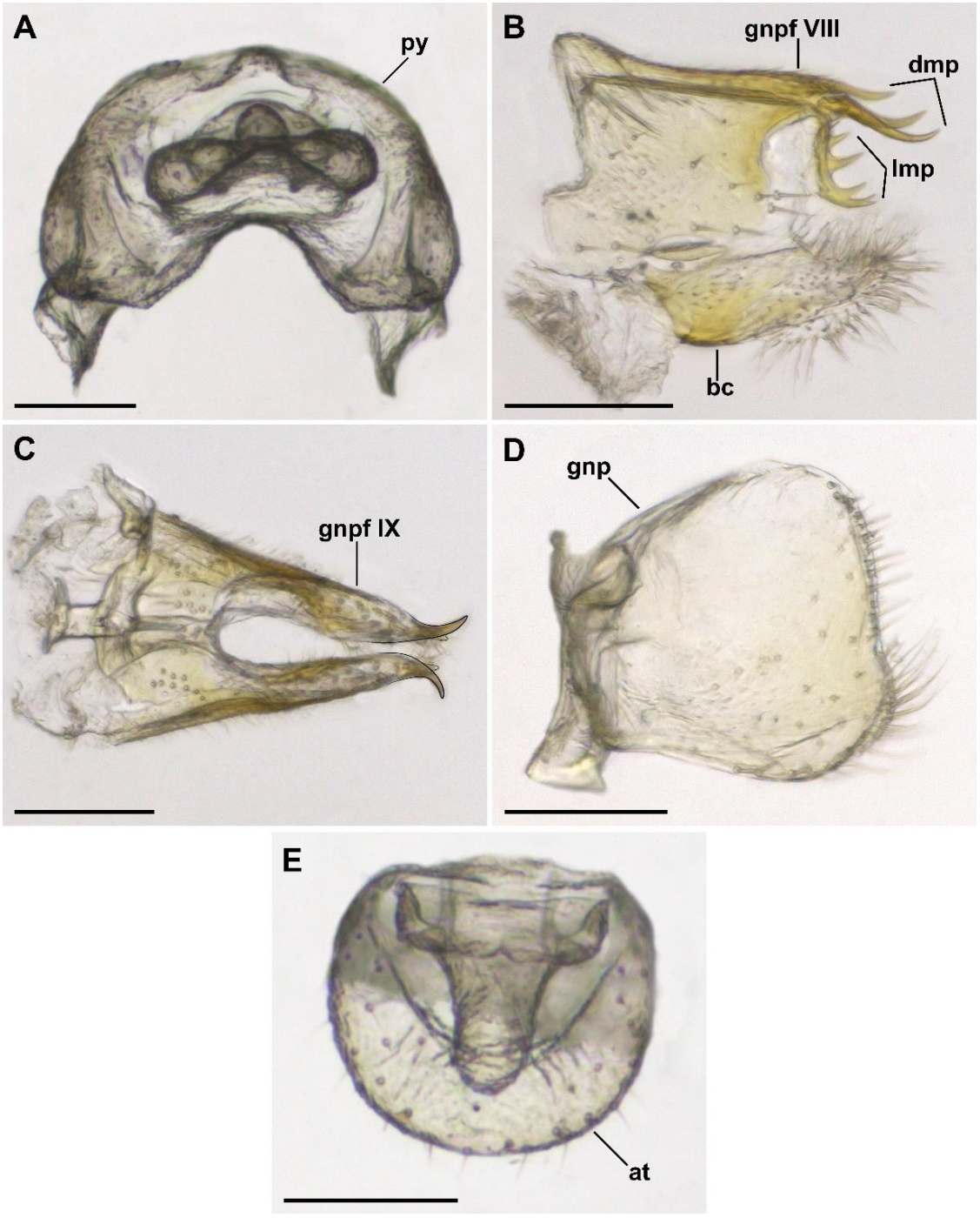

519
520 **Figures 6 A–E.** *Bebaiotes cavichiolii* **sp. nov.**, female genitalia, paratype (MUSM): **A**
521 Pygofer, posterior view; **B**. Gonapophysis VIII, lateral view (first valvula) lateral view;
522 **C**. Gonapophysis IX (second valvula), dorsal view; **D**. Gonoplac (third valvula), lateral
523 view; **E**. Anal tube (segment X), dorsal view. Abbreviations: at, anal tube; bc, bursa
524 copulatrix, py, pygofer; gnp, gonoplac; gnpf IX, gonapophysis IX; gnpf VIII,
525 gonapophysis VIII. Scale bars: A–E = 0.1 mm.

526 ***Bebaiotes clarice* Viegas, Takiya & Ale-Rocha sp. nov.**

527 Figs 7 A–F, 8 A–G, 9 A–E, 20 E, F, 23

528 **Diagnosis.** Gena, lora, upper half of maxillary lobe, and lateral margin of pronotum light
529 yellow (Fig. 7 D). Posterior margin of the pronotum without pustules (Fig. 7 A). Posterior
530 margin of pygofer with a dorsal triangular protuberance on each side (Fig. 8 A).

531 **Type material**

532 **Holotype**

533 BRAZIL • ♂; **Amazonas**, Tabatinga, Zoológico; 4˚14'39"S, 69˚56'17"W; 16–31 May
534 2019; "Malaise grande" [large Malaise]; M.L. Oliveira, S.P. Lima leg.; INPA (Holotype
535 condition: glued on paper triangle; left flagellum broken and lost; left tegula broken and
536 lost; right forewing and hind wing mounted between coverslips; abdomen removed and
537 stored in a microtube; genitalia dissected and stored in a microtube).

538 **Paratypes**

539 BRAZIL • 1 ♀; same data as for holotype; INPA • 2 ♀♀; same data as for holotype; 16–
540 30 Jun. 2019; INPA; • 1♀; same data as for holotype; 16–30 Jun. 2019 (ENT6123); INPA.

541 **Measurements**. Body length: male 4.8 mm (6.4 mm including wings) (n=1)
542 holotype; female: 4.0-4.3 mm (6.5-6.9 mm including wings) (n=3).

543 **Description.** Coloration. General body color dark brown (Figs 7 A, B). Lateral
544 regions of frons, gena, lora, upper half of maxillary lobe, lateral margins of pronotum,
545 epimeron, and episternum, light yellow (Figs 7 C, D). Mesonotum with pair of
546 subtriangular yellow areas near posterolateral margin (Fig. 7 E). Forewing semihyaline,
547 dark brown with yellow regions mainly along veins: narrow yellow stripes covering c-sc
548 cross-vein, ir cross-vein, and RA vein; median region of cell C2 with wide yellow
549 transverse band; basal region of MP vein yellow; large yellow stripe extending from r-
550 m1 cross-vein to m-cu cross-vein; narrow yellow band covering half of CuA vein and

extending through the CuA1 vein passing through the m-cu cross-vein; narrow yellow stripe extending from r-m2 cross-vein to MP5 vein base; yellow X-shaped spot covering m-cu2 cross-vein, middle region of the CuA1 vein, and the icua cross-vein; yellow oval spot at apical portion of CuA1 and CuA2 veins; narrow yellow stripe covering CuP and Pcu veins; postclaval margin yellow (Fig. 20 E). Hind wing semihyaline, dark brown with white regions (Fig. 20 F). Legs dark brown, except mesocoxae, mesotrochanters, mesotibiae, metacoxae, metatrochanters, metatibiae, and metatarsi, yellowish brown. Abdomen dark brown, except, tergite VIII yellowish brown; sternite II, first sensory pit of the sternite III, posterior half of sternite III, posterior margin of sternites V, VI, and VII, light yellow (Figs 7 A, F).

Head: frons narrow, distance between lateral carinae of frons at median portion, approximately twice smaller than maximum width of vertex (Fig. 7 C). Clypeus approximately 2.5 times longer than maximum width; median carina strongly marked, almost extending to epistomal suture (Fig. 7 C). Scape as long as wide (Fig. 7 C). Pedicel oblong, approximately three times longer than scape (Fig. 7 C).

Thorax: pronotum anterior margin tapering; median longitudinal carina present, strongly marked; lateral carinae moderately diverging towards tegula; posterior margin with angled indentation in dorsal view; without pustules on posterior margin. Mesonotum with median and lateral longitudinal carinae present, strongly marked (Fig.7 D). Forewing: RA vein with apex gently curved anteriorly; RP vein with apex strongly curved anteriorly; r-m cross-vein approximately three times smaller than r-m2 cross-vein; ir cross-vein distant from r-m2 cross-vein; MP vein with five branches with straight apex; MP1, MP3, and MP4 veins unbranched and MP2 branched; MP1+2 and MP3+4 branching arising near r-m cross-vein; m-cu cross-vein present; m-cu cross-vein about three times shorter than m-cu2 cross-vein; m-cu2 cross-vein near icua cross-vein, not

aligned; CuA vein bifurcation basad to r-m cross-vein; CuP vein approximately three times longer than Pcu + A1 vein; apex of clavus forming acute angle (Fig. 20 E). Hind wing: first bifurcation of MP vein to m-cu cross-vein (Fig. 20 F). Legs: metatibia with 8 apical spines; metatarsus with 7+6 apical spines. Female. Similar to male, except sternite VII and lateral region of pygofer yellow (Fig. 7 B).

Male terminalia (Figs 8 A–G): Pygofer subtriangular in lateral view; posterior margin with a dorsal triangular protuberance, few long setae on dorsal half; ventral margin with a few long setae on posterior half (Fig. 8 A). Gonostyli symmetrical; outer margin with short and pointed lobe next to apex; inner margin with a few setae; apex truncated in lateral view, claviform (Figs 8 B–D). Phallic complex: periandrium approximately 2.5 times as long as broad in lateral view; dorsal margin with triangular apex; ventral margin with rounded apex (Figs 8 E, F). Inner sclerotized plates narrowing towards apex; with serrated margin; surface with small spiniform projections (Figs 8 F, G). Anal tube (segment X) short rounded; apex rounded in dorsal view (Fig. 8 G)**.**

Female terminalia (Figs 9 A–E): Gonapophysis VIII (first valvula) broad; with sparse setae at median region; small spiniform projections at basal half in lateral view; three lateroapical projections with irregular teeth on dorsal margin in lateral view (Fig 9 B). Bursa copulatrix densely filamentous apically; covered by setae laterally at apical half; apex obtuse (Fig. 9 B). Gonapophysis IX (second valvula) robust; bifid at apical half; lobes with pointed, strongly curved latero-ventrally apex, hook-like in dorsal view (Fig. 9 C). Gonoplac (third valvula) subtrapezoidal; apex truncated with many apical setae and sparse setae laterally (Fig. 9 D). Anal tube (segment X) short and rounded in dorsal view; apex truncated in dorsal view (Fig. 9 E).

Etymology. The species is named in honor of Me. Clarice Guilherme Barreto from the Instituto Federal de Educação, Ciência e Tecnologia do Rio Grande do Norte, Campus

601 Natal Central, Brazil, for her contribution to the academic education of the first author,
602 as an excellent teacher, friend, and researcher. The species epithet is treated as a noun in
603 apposition.

604 **Distribution**. Brazil (Amazonas) (Fig. 23).

605 **Taxonomic notes**. *B. clarice* **sp nov.** is most similar to *B. pulla* Muir, 1934 because they
606 share lateral region of frons yellow, median carina of clypeus almost extending to
607 epistomal suture, forewing dark brown and with yellow regions mainly along veins. But
608 can be promptly distinguished from the latter by its pronotum without pustules on
609 posterior margin; gena, lora, and lateral margin of pronotum light yellow; lateral carinae
610 of pronotum gently diverging towards tegulae, and ventral margin of periandrium with
611 rounded apex.

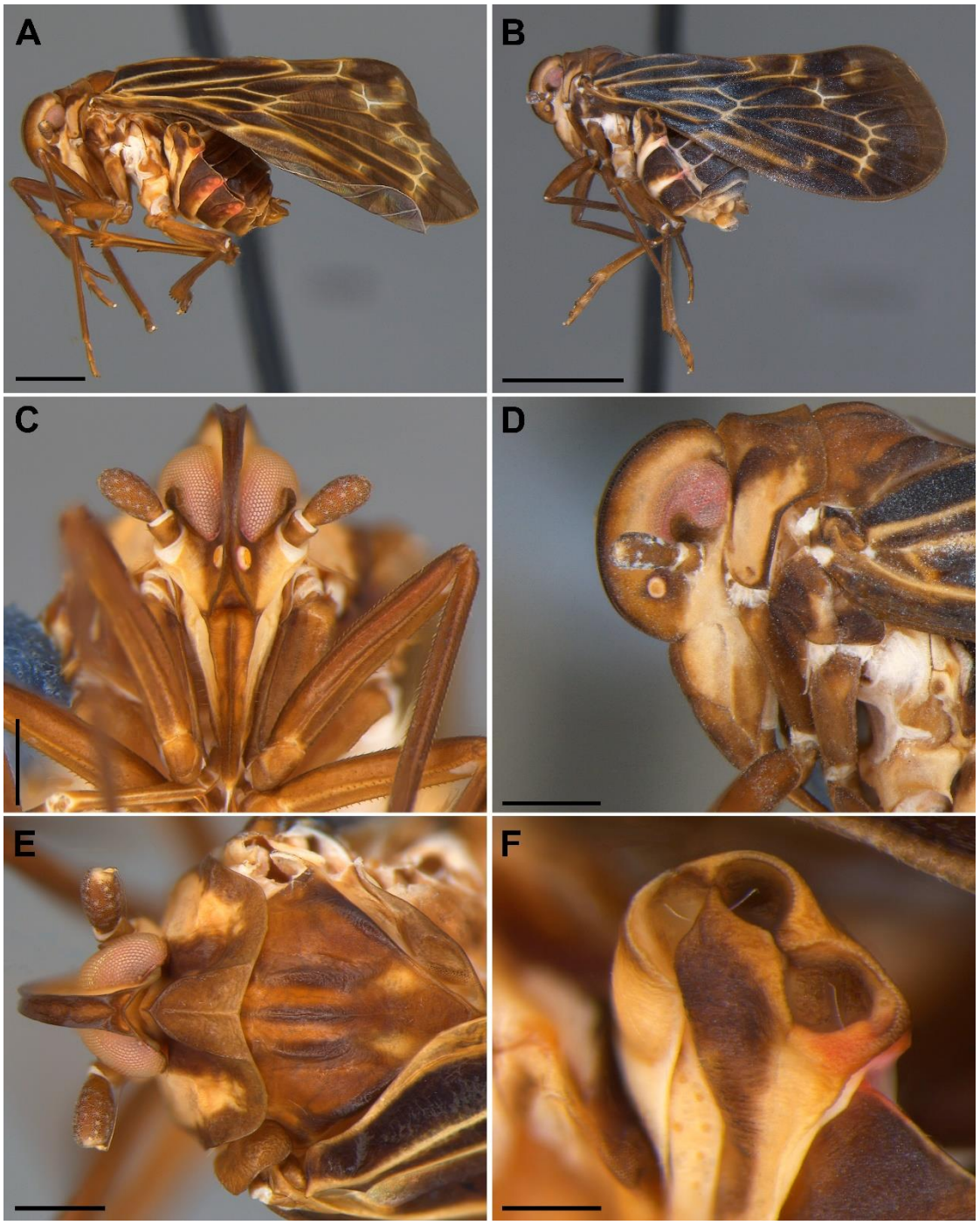

Figures 7 A–E. *Bebaiotes clarice* **sp. nov.**, male holotype (INPA): **A, C-F**. male holotype. **A**. Male habitus, lateral view; **B**. Female, habitus, lateral view; **C**. Male head, anterior view; **D.** Female head and thorax, lateral view; **E.** Male head and thorax, dorsal view; **F**. Male abdominal process, lateral view. Scale bars: A = 1 mm; B = 2 mm; C, E = 0.4 mm; D = 0.5 mm; F = 0.2 mm.

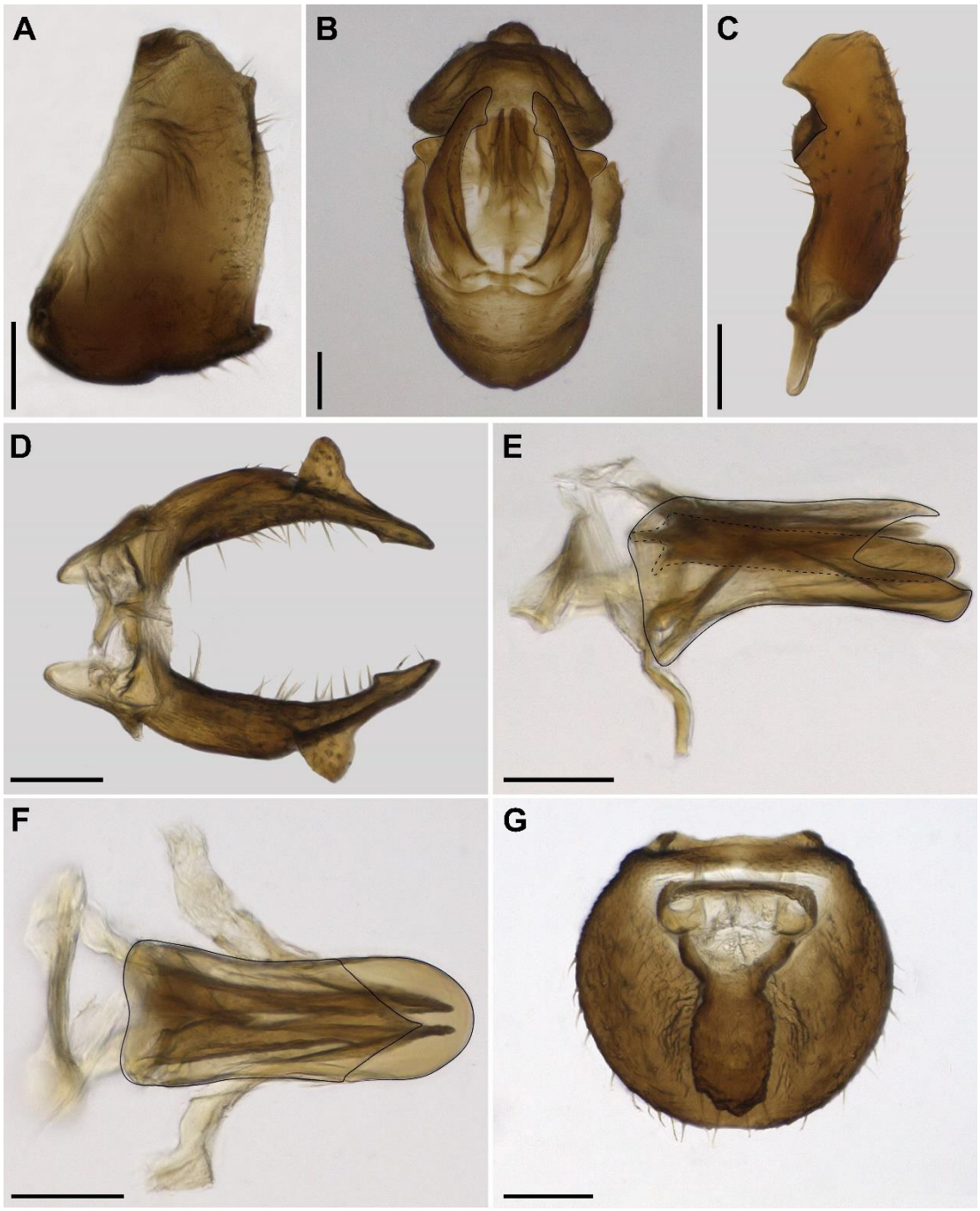

Figures 8 A–G. *Bebaiotes clarice* **sp. nov.**, male genitalia, holotype (INPA): **A.** Pygofer, lateral view; **B**. Genital capsule, posterior view; **C**. Gonostyli, lateral view; **D.** Gonostyli, dorsal view; **E** Periandrium and inner sclerotized plate, lateral view; **F**. Periandrium and inner sclerotized plate, dorsal view; **G**. Anal tube (segment X) dorsal view. Scale bars: A–G = 0.1 mm.

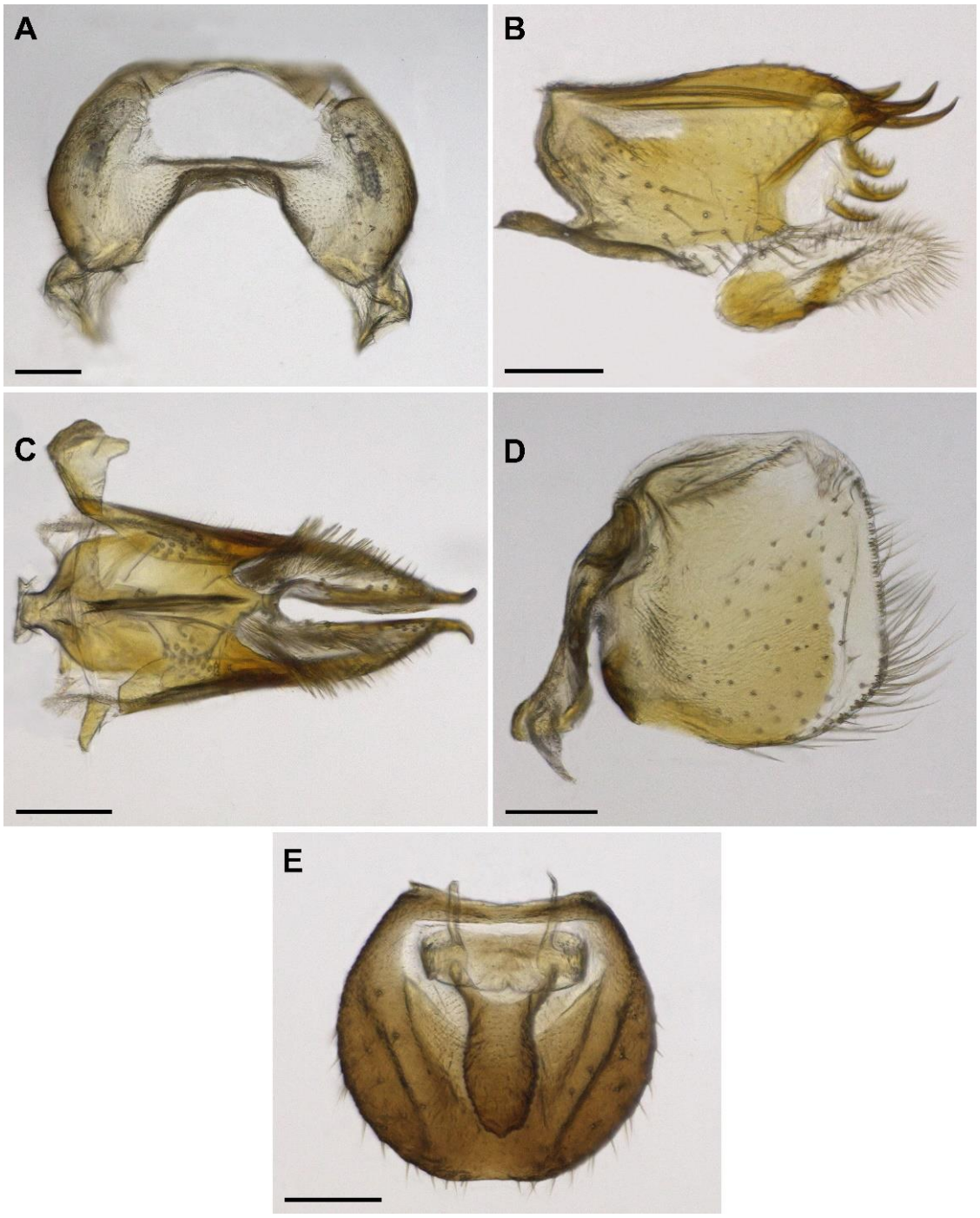

Figures 9 A–E. *Bebaiotes clarice* **sp. nov.**, female genitalia, paratype (INPA): **A**. Pygofer posterior view; **B**. Gonapophysis VIII, lateral view (first valvula) lateral view; **C**. Gonapophysis IX (second valvula), dorsal view; **D**. Gonoplac (third valvula), lateral view; **E**. Anal tube (segment X), dorsal view. Abbreviations: at, anal tube; bc, bursa copulatrix, dmp, dorsal margin projections, gnp, gonoplac; gnpf IX, gonapophysis IX; gnpf VIII, gonapophysis VIII, lmp, lateroapical margin projections, py, pygofer. Scale bars: A–E = 0.1 mm.

Bebaiotes nigrigaster Muir, 1924

Figs 10 A–D

Bebaiotes nigrigaster Muir, 1924: 34; Metcalf, 1945: 217 (world catalogue)

Muirilixius nigrigaster (Muir, 1924) Fennah, 1947: 186, 188 (taxonomy, key)

Bebaiotes nigrigaster Muir, 1924: Wilson, 1989: 487, 488, 491, 492, fig 11 (tegmen) (citation, illustration).

Diagnosis. frons narrow (Fig. 10 C). Abdomen predominantly black (Fig. 10 A). MP vein of the forewing with four branches (Fig. 10 C).

Type material

Holotype

ECUADOR • ♂; Bucay, 1000 feet elevation, 07.x.1922, F. X. Williams, nº 1098; BPBM

Paratype

ECUADOR • ♀; Bucay, 1000 feet elevation, 07.x.1922, F. X. Williams, 013585590; NHM (Paratype condition: glued on paper triangle; right antenna broken and lost, left flagellum broken and lost; left proleg broken and lost).

Redescription. Coloration. Body coloration dark yellow (Figs 10 A, B). Forewing yellow with a "T"-shape black mark, present in the basal two-third (Figs 10 A). Abdomen predominantly black, except sternite II and upper half of sternite III yellow.

Head: frons narrow (Fig. 10 C). median carina of clypeus weakly marked, present on distal three-fourths, not extending to epistomal suture (Fig. 10 C). Scape as long as wide (Fig. 10 C). Pedicel oblong (Fig. 10 C). Thorax: Pronotum anterior margin tapering; median longitudinal carina present, weakly marked; lateral carinae moderately diverging towards tegulae; posterior margin concave with shallow median notch in dorsal view; without pustules at posterior margin; median and lateral longitudinal carinae of mesonotum absent (Figs 10 B, C). Forewing: RA and RP vein with apex gently curved

anteriorly; ir cross-vein distant from r-m2 cross-vein; MP vein with four branches; MP1, MP2, MP3 MP4 veins unbranched; MP1+2 and MP3+4 branching arising based to r-m cross-vein; m-cu cross-vein present; m-cu2 cross-vein aligned with icua cross-vein; CuA vein bifurcation based to r-m cross-vein; apex of clavus forming acute angle (Fig. 10 E).

Female terminalia not examined.

Distribution. Ecuador (Bucay).

Taxonomic notes. *B. nigrigaster* Muir, 1924 is most similar to *B. banksi* (Metcalf, 1938) because they share the frons narrow and anterior margin of pronotum tapering. But it can be promptly distinguished from *B. banksi* by mesonotum with median and lateral longitudinal carinae absent and abdomen predominantly black.

Figures 10 A–D. *Bebaiotes nigrigaster* Muir, 1924, female paratype (NHM): **A.** Female habitus, lateral view; **B**. Female head, anterior view; **C**. Female head, thorax, wings, dorsal view; **D.** Information tags. Fotos: Webb (2019).

Bebaiotes nivosa Fennah, 1947

Figs 11 A–D

Bebaiotes nivosa Fennah, 1947: 190: fig.5 a-g (tegmen and genitalia); Wilson, 1989: 491 (citation).

Diagnosis. Head and thorax yellow (Figs 11 A, B). Mesonotum with median and lateral longitudinal carinae absent (Fig 11 B). Forewing white with small brown spot at apex of clavus (Figs 11 A, B). Projections of lateroapical margin of the gonapophysis VIII with dorsal margin smooth (Fennah, 1947: Fig. 5 E).

Type material.

Holotype

BRITISH GUIANA • ♀; Kutari Sources, i-ii.1936, G. A. Hudson, 013585539; NHM (Holotype condition: glued on paper triangle; abdomen removed and mounted slide; genitalia dissected).

Redescription. Coloration. Body coloration yellow (Figs 11 A, B). Tegula, metafemur and metatibia light yellow. Forewing white with small brown spot at apex of clavus (Figs 11 A, B).

Head: Frons large (Fig. 11 C). Pedicel globose (Fig. 11 C). Thorax: Pronotum anterior margin truncated; median longitudinal carina present, weakly marked; lateral carinae moderately diverging towards tegulae; posterior margin concave with shallow median notch in dorsal view; without pustules at posterior margin; Mesonotum with median and lateral longitudinal carinae absent (Figs 11 B, C). Forewing: RA and RP vein with apex gently curved anteriorly; ir cross-vein distant from r-m2 cross-vein; MP vein with four branches; MP1, MP2, MP3 MP4 veins unbranched; m-cu cross-vein present; m-cu2 cross-vein aligned with icua cross-vein (Fennah, 1947: Fig. 5 A). Female terminalia: Gonapophysis VIII (first valvula) with three lateroapical projections of

subequal sizes with smooth dorsal margin in lateral view (Fennah, 1947: Fig. 5 E). Anal tube (segment X) short and rounded in dorsal view; apex with smooth indentation in dorsal view (Fennah, 1947: Fig. 5 G)

Distribution. Guiana.

Taxonomic notes. *Bebaiotes nivosa* Fennah, 1947 can be promptly distinguished from other species of *Bebaiotes* with large frons by its general coloration of body yellow, forewing white, and female genitalia with gonapophysis VIII (first valvula) with three lateroapical projections with smooth dorsal margin in lateral view.

Figures 11 A–F. *Bebaiotes nivosa* Fennah, 1947, female holotype (NHM): **A.** Female habitus, lateral view; **B**. Female head, anterior view; **C**. Female head, thorax, wings, dorsal view; **D.** Labels and abdomen and terminalia mounted slide. Fotos: Webb (2019).

712 ***Bebaiotes oiapoquensis* Viegas, Takiya & Ale-Rocha sp. nov.**

713 Figs 12 A–E, 13 A–G, 14 A, B, 21 A, B, 23

714 **Diagnosis.** Lateral region of frons dark brown (Fig. 12 C). Lateral carinae of pronotum
715 gently diverging towards tegulae (Fig. 12 D). Forewing m-cu2 cross-vein aligned with
716 icua cross-vein (Fig. 21 A).

717

718 **Type material**

719 **Holotype**

720 BRASIL • ♂; **Amapá**, Oiapoque, BR 156, Km 25; 3˚39'35"N, 51˚46'17"W; iii-vii.2020;
721 Malaise, "Floresta" [Forest]; J.A. Rafael, S.P. Lima & F.F. Xavier leg; INPA (Holotype
722 condition: right and left antennal flagellum lost; forewings and hind wings mounted
723 between coverslips; abdomen removed and stored in a microtube; genitalia dissected and
724 stored in a microtube).

725 **Measurements:** Body length: male 5.0 mm (6.1 mm including wings) (N=1).

726 **Description.** Coloration. Body coloration dark brown (Figs 12 A–D). Lateral
727 carinae of frons above compound eye, lateral longitudinal carinae of pronotum, median
728 longitudinal carina of mesonotum, diffuse spot at anterolateral region of mesonotum,
729 epimeron, and episternum, yellow. Forewing semihyaline, dark brown with basal half of
730 postcostal cell, narrow stripe covering almost all of RA vein, and most of radial cell,
731 yellow; narrow white stripe covering c-sc and ir cross-veins; narrow yellow stripe
732 extending from median region of radial vein to CuA1 vein base; narrow yellow stripe
733 extending from r-m2 cross-vein to MP4 vein base; narrow yellow stripe covering
734 approximately 2/3 of the MP1+2 vein; narrow yellow stripe covering approximately 1/3
735 of the MP3+4 vein; narrow yellow stripe extending from half of CuA2 vein to icu cross-
736 vein; yellow X-shaped region covering m-cu2 cross-vein, median region of CuA1 vein,

and icua cross-vein; narrow yellow stripe covering approximately two-thirds of CuP vein; narrow yellow stripe covering Pcu vein; apex of clavus yellow (Fig. 21 A). Hind wing semihyaline; dark brown with hyaline regions (Fig. 21 B). Legs dark brown, except metathoracic legs yellowish brown (Fig. 12 A).

Head: frons narrow, distance between lateral carinae of frons at median portion approximately twice smaller than maximum width of vertex (Fig. 12 B). Clypeus approximately 2.5 times longer than maximum width; median carina strongly marked, present on distal three-fourths, not extended to epistomal suture (Fig. 12 B). Scape as long as wide (Fig. 12 B). Pedicel oblong, approximately three times longer than scape (Fig. 12 B).

Thorax: pronotum anterior margin tapering; median longitudinal carina present, strongly marked; lateral carinae gently diverging towards tegulae; posterior margin with angled indentation; with pustules on posterior margin. Mesonotum with median longitudinal carina present, strongly marked (Figs 12 C, D). Forewing. RA and RP veins with apices strongly curved anteriorly; r-m cross-vein approximately three times shorter than r-m2 cross-vein; ir cross-vein distant from r-m2 cross-vein; MP vein with five branches with gently curved apex; MP1, MP3, and MP4 veins unbranched and MP2 vein branched; MP1+2 and MP3+4 branching arising near r-m cross-vein; m-cu cross-vein present; m-cu cross-vein subequal to m-cu2 cross-vein; m-cu2 cross-vein aligned with icua cross-vein; CuA vein bifurcation aligned with r-m cross-vein. CuP vein approximately three times longer than Pcu + A1 vein; apex of clavus forming straight angle (Fig. 21 A). Hind wing: first bifurcation of MP vein distad to m-cu cross-vein (Fig. 21 B). Legs: metatibia with 7 apical spines; metatarsus with 6+5 apical spines.

Male terminalia (Figs 13 A–G): Pygofer subrectangular in lateral view; posterior margin without projections and sinuous, with a few long setae on dorsal half (Figs 13 A,

B). Gonostyli symmetrical; outer margin with short and rounded lobe near apex, inner margin with a few setae; apex truncated in lateral view, claviform (Figs 13 B–D). Phallic complex: periandrium with rounded base and subtrapezoidal towards apex; dorsal and ventral margins with short indentation at apex in dorsal view; surface with small spiniform projections (Figs 13 E, F). Inner sclerotized plates narrowing towards apex; serrated margin; surface with small spiniform projections (Figs 13 E, F). Anal tube (segment X) short and rounded in dorsal view; apex with smooth indentation in dorsal view (Fig. 13 G).

Etymology. The species is named in reference to the municipality of Oiapoque, where it was collected.

Distribution. Brazil (Amapá) (Fig. 23).

Taxonomic notes. *B. oiapoquensis* **sp nov.** is most similar to *B. pennyi* Viegas & Ale-Rocha, 2023 because they share median carina strongly marked, present on distal three-fourths, not extended to epistomal suture, anterior margin of pronotum with tapered apex, and lateral longitudinal carinae converging subparallel to each other towards posterior margin. But it can be promptly distinguished from the latter by the coloration of body dark brown; lateral carinae of pronotum gently diverging towards tegulae; hind wing MP1+2 vein arising distad of m-cu cross-vein; dorsal and ventral margins of periandrium with short indentation at apex.

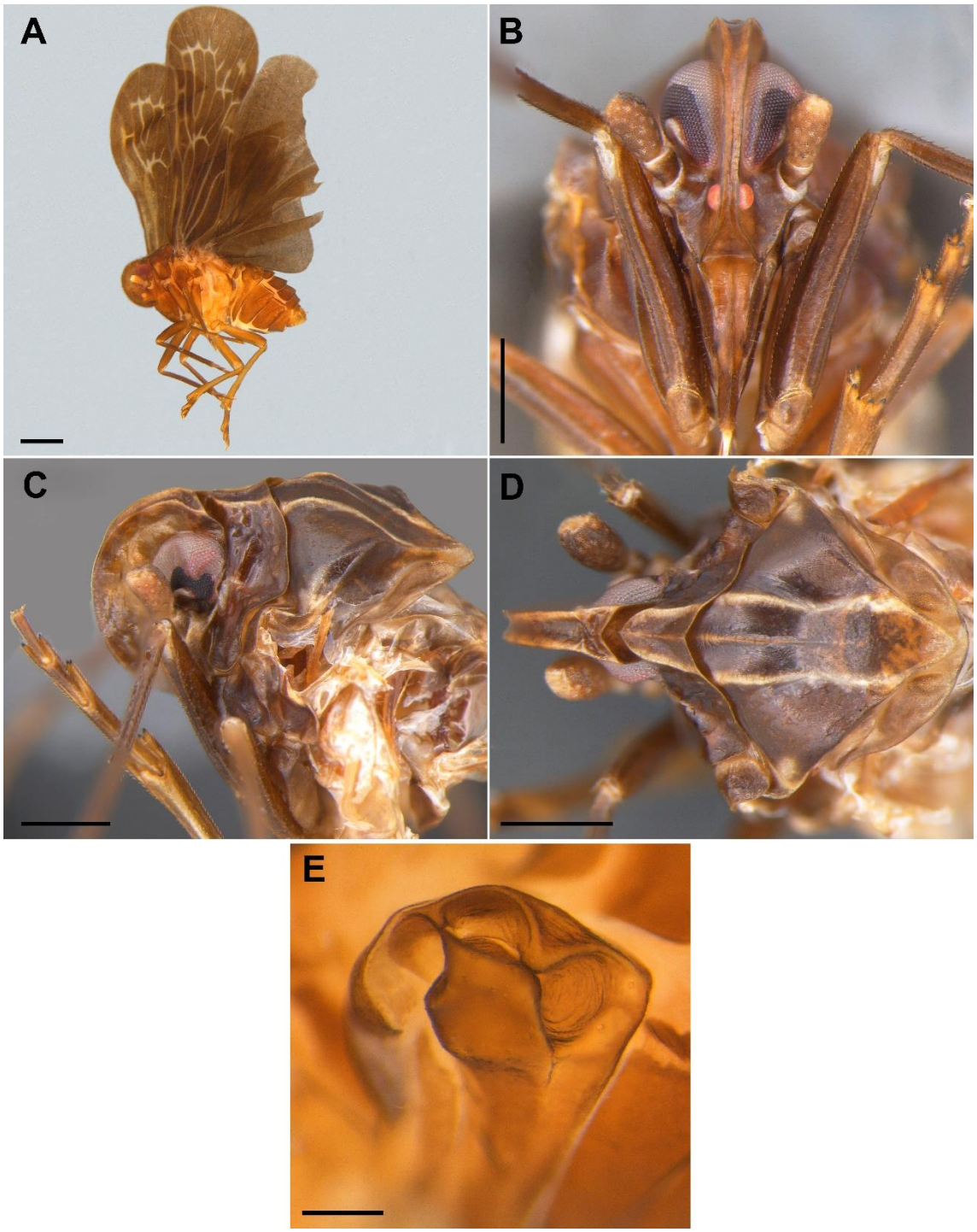

781
782 **Figures 12 A–E.** *Bebaiotes oiapoquensis* **sp. nov.**, male holotype (INPA): **A**. Male
783 habitus, lateral view; **B**. Male head, anterior view; **C.** Male head and thorax, lateral view;
784 **D.** Male head and thorax, dorsal view; **E**. Male abdominal process, lateral view. Scale
785 bars: A = 1 mm; B–D = 0.5 mm; E = 0.2 mm.

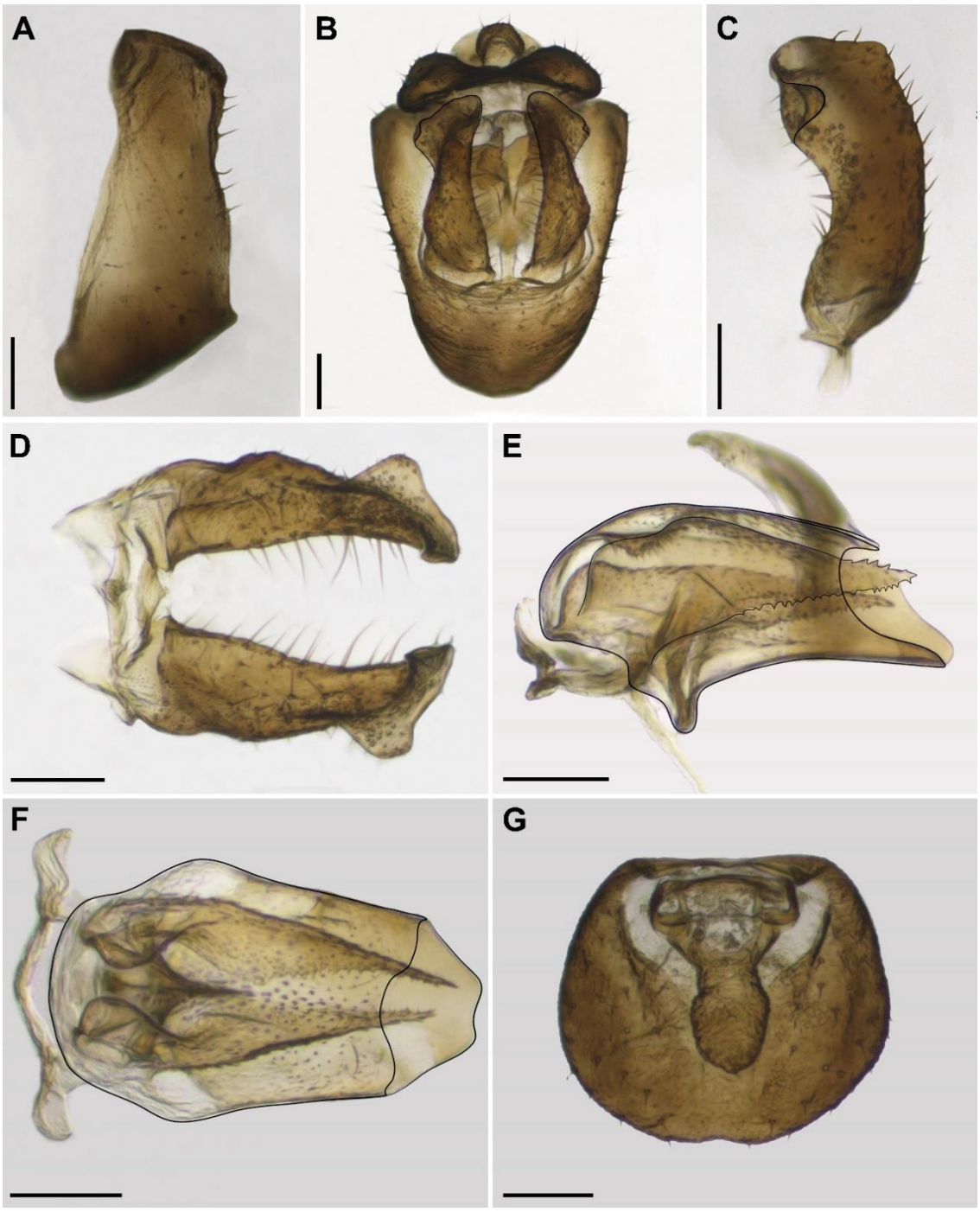

Figures 13 A–G. *Bebaiotes oiapoquensis* **sp. nov.**, male genitalia, holotype (INPA): **A.** Pygofer, lateral view; **B**. Genital capsule, posterior view; **C**. Gonostyli, lateral view; **D.** Gonostyli, dorsal view; **E** Periandrium and inner sclerotized plate, lateral view; **F**. Periandrium and inner sclerotized plate, dorsal view; **G**. Anal tube (segment X), dorsal view. Scale bars: A–G = 0.1 mm.

Bebaiotes oliveirai Viegas, Takiya & Ale-Rocha sp. nov.

Figs 14 A–E, 15 A–G, 16 A–E, 21 C, D, 23

Diagnosis. General body color yellow (Fig. 14 A). Apical article of rostrum dark brown (Fig. 14 A). Forewing with long, wide, brown transverse band at apical region (Fig. 21 C). Median longitudinal carina of pronotum strongly marked (Fig. 14 D).

Type material

Holotype

BRASIL • ♀; **Amazonas**, Benjamim Constant, BR 307, Km-05; 4˚23'35"S, 70˚01'59"W; 16–31 Jul. vii.2019; **"**Malaise grande" [large Malaise]; M. Oliveira & S.P. Lima leg.; INPA (Holotype condition: apical half of the left antennal flagellum broken and lost; right forewing and hind wing mounted between coverslips; left hind wing torn near apex; right mesotarsus lost; abdomen removed and stored in a microtube; genitalia dissected and stored in a microtube).

Paratypes

BRASIL • 1 ♂; same data as the holotype; 1–15 Sep. 2019 (ENT6168); INPA (material in alcohol).

Measurements. Body length: male 3.9 mm (6.3 mm including wings) (n=1) (holotype); female: 3.8 mm (6.2 mm including wings) (n=1).

Description. Coloration. General body color yellow (Fig. 14 A). Apical article of rostrum dark brown. Forewing semihyaline, yellow with white regions: narrow white band covering r- m2, m1-m2, m-cu2, icua, and icu cross-veins; long, wide, and brown transverse band at apical region extending from apex of radial vein to apex of cubital cell (Fig. 21 C). Hind wing semihyaline, yellowish brown with hyaline regions (Fig. 21 D).

Head: frons narrow, distance between lateral carinae of frons, at median portion, approximately four times smaller than maximum width of vertex (Fig. 14 B). Clypeus approximately 3.5 times longer than maximum width; median carina strongly marked, present on distal three-fourths, not extending to epistomal suture (Fig. 14 B). Scape as long as wide (Fig. 14 B). Pedicel oblong, approximately 1.5 times longer than scape (Fig. 14 B).

Thorax: pronotum anterior margin tapering; median longitudinal carina present, strongly marked; lateral carinae gently diverging towards tegulae; posterior margin with angled indentation; without pustules on posterior margin. Mesonotum with median longitudinal carinae present, strongly marked (Fig. 14 D). Forewing: RA and RP veins with apex gently curved anteriorly; r-m cross-vein about half the length of r-m2 cross-vein; ir cross-vein distant from r-m2 cross-vein; MP vein with four branches with uncurved apex; MP1, MP2, MP3, and MP4 vein unbranched; MP1+2 and MP3+4 branching arising basad to r-m cross-vein; m-cu cross-vein present; m-cu cross-vein approximately three times shorter than m-cu2 cross-vein; m-cu2 cross-vein aligned with icua cross-vein; CuA vein bifurcating basad to r-m cross-vein; CuP vein approximately three times longer than the Pcu + A1 vein; apex of clavus forming acute angle (Fig. 21 C). Hind wing: first bifurcation of MP vein arising basad to m-cu cross-vein (Fig. 21 D). Legs: metatibia with 9 apical spines; metatarsus with 7+6 apical spines.

Male terminalia (Figs 15 A–G): Pygofer subtriangular in lateral view; posterior margin without projections, almost straight, and with few setae (Figs 15 A, B). Gonostyli symmetrical; outer margin with short and rounded lobe near to apex, inner margin with some setae; apex truncated in lateral view, claviform (Figs 15 B–D). Phallic complex: periandrium with sinuous lateral margin; dorsal margin crenate at apex; ventral margin with apex truncated (Fig. 15 F). Inner sclerotized plates slender; with serrated margin;

surface with small spiniform projections (Figs 15 E, F). Anal tube (segment X) short rounded in dorsal view; apex rounded in dorsal view (Fig. 15 G).

Female terminalia (Figs 16 A–E): Gonapophysis VIII (first valvula) with sparse setae at basal and median regions; with small spiniform projections in lateral view; four lateroapical projections with irregular teeth on dorsal margin in lateral view (Fig. 16 B). Bursa copulatrix densely filamentous apically; covered by setae laterally at apical half; apex acute (Fig. 16 B). Gonapophysis IX (second valvula) robust; bifid at apical half; lobes with pointed, strongly curved latero-ventrally apex, hook-like in dorsal view (Fig. 16 C). Gonoplac (third valvula) subtrapezoidal; apex almost straight with several apical setae and sparse laterally setae (Fig. 16 D). Anal tube (segment X) short and rounded in dorsal view; apex truncated in dorsal view (Fig. 16 E).

Etymology. The species is named in honor of Dr. Marcio Luiz de Oliveira from the National Institute of Amazonian Research - INPA, Manaus, Brazil, for his important contribution to the knowledge of the Amazonian entomofauna, and for collecting several specimens used in this work, including the holotype of this species.

Distribution. Brazil (Amazonas) (Fig. 23).

Taxonomic notes. *B. oliveirai* **sp nov.** is most similar to *B. banksi* (Metcalf, 1938) because they share frons narrow and general coloration of body yellow, but can be promptly distinguished from the latter by its median longitudinal carina of pronotum strongly marked, apex of ventral margin of periandrium truncated, and gonapophysis VIII (first valvula) with irregular teeth at dorsal margin of lateroapical projection.

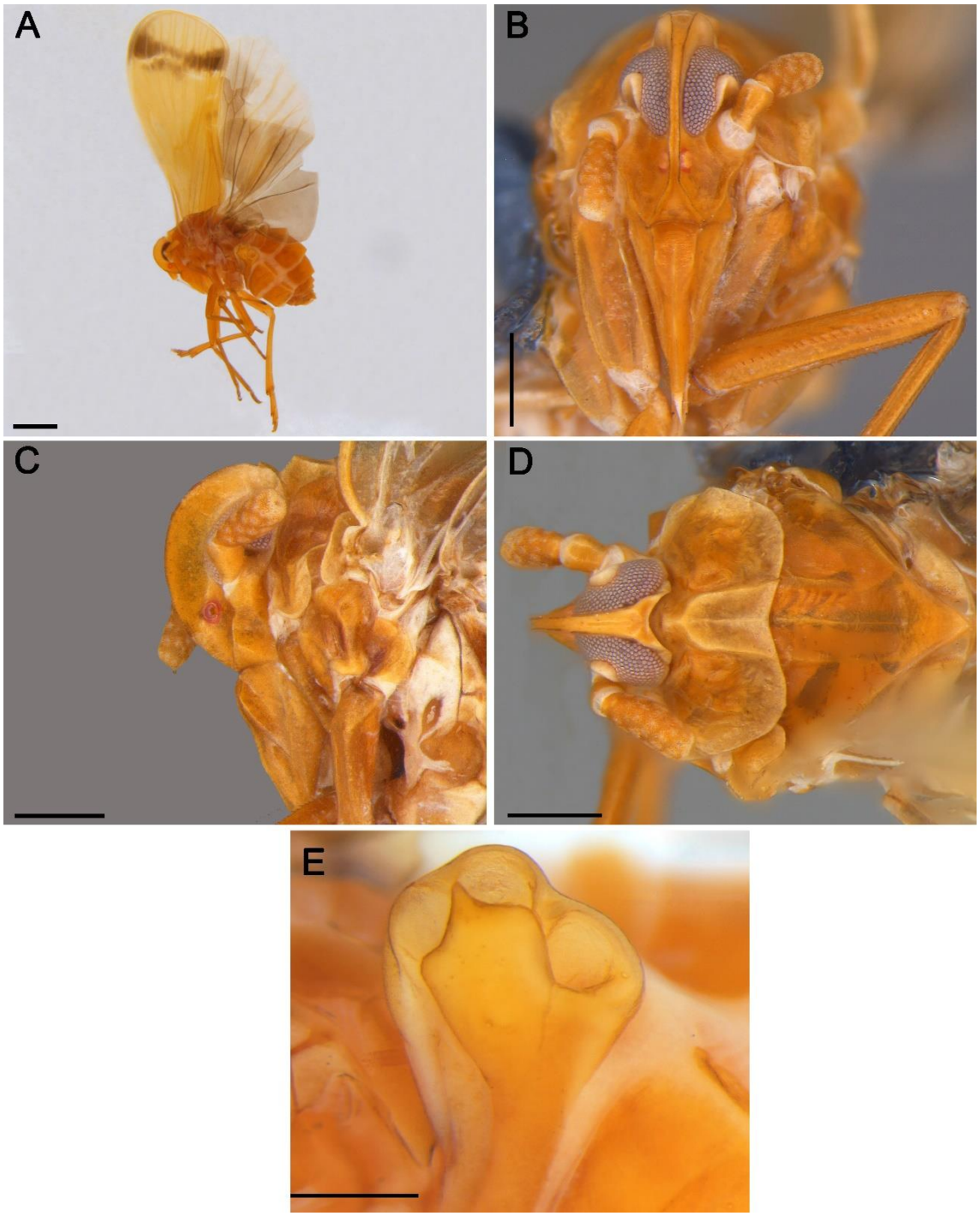

Figures 14 A–E. *Bebaiotes oliveirai* **sp. nov.**, female holotype (INPA): **A**. Male habitus, lateral view; **B**. Male head, anterior view; **C**. Male head and thorax, lateral view; **D.** Male head and thorax, dorsal view; **E**. Male abdominal process, lateral view. Scale bars: A = 1mm; B–D = 0.4 mm; E = 0.3 mm.

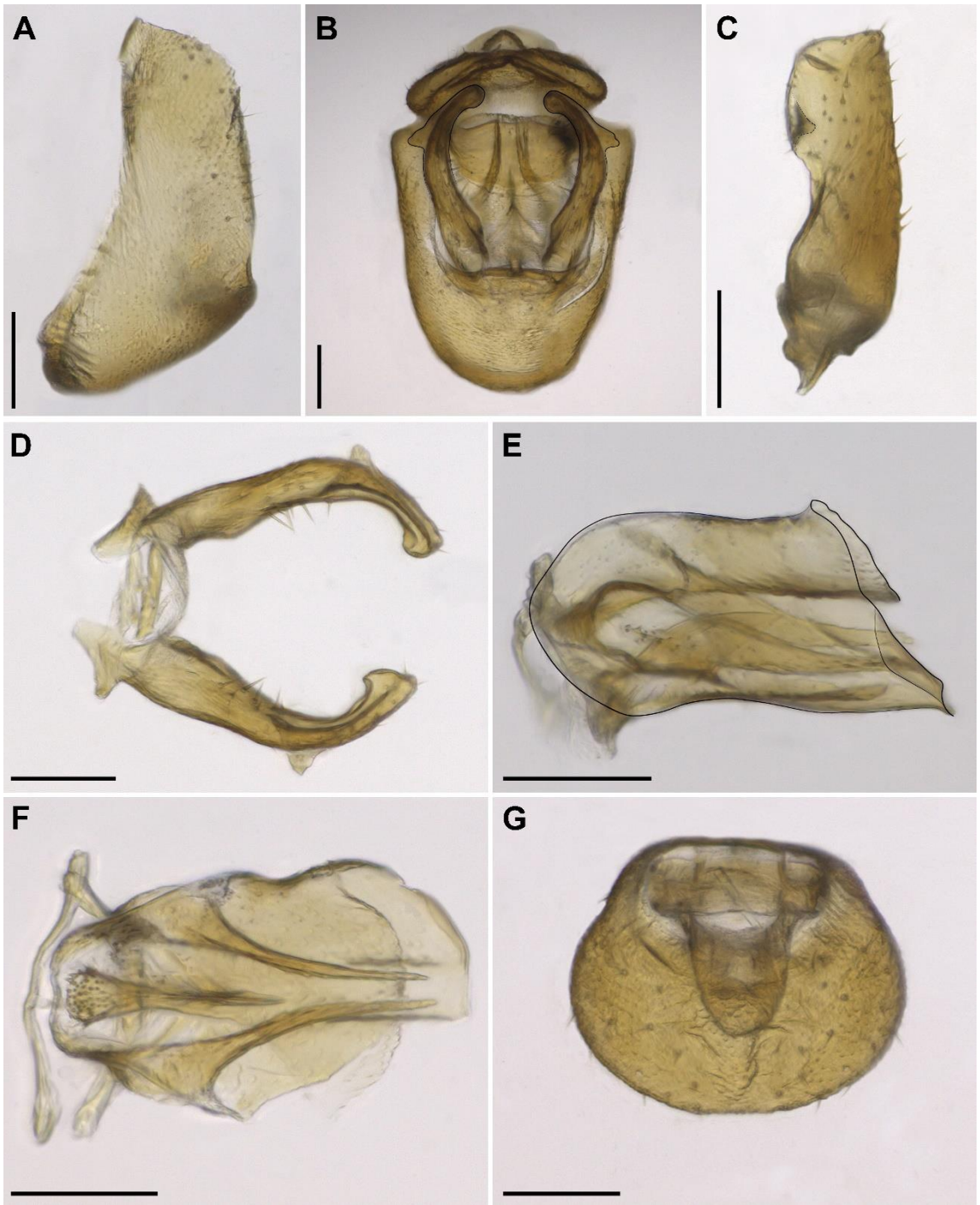

867
868 **Figures 15 A–G.** *Bebaiotes oliveirai* **sp. nov.**, male genitalia, paratype (INPA): **A.**
869 Pygofer, lateral view; **B**. Genital capsule, posterior view; **C**. Gonostyli, lateral view; **D.**
870 Gonostyli, dorsal view; **E** Periandrium and inner sclerotized plate, lateral view; **F**.
871 Periandrium and inner sclerotized plate, dorsal view; **G**. Anal tube (segment X), dorsal
872 view. Scale bars: A–G = 0.1 mm.
873

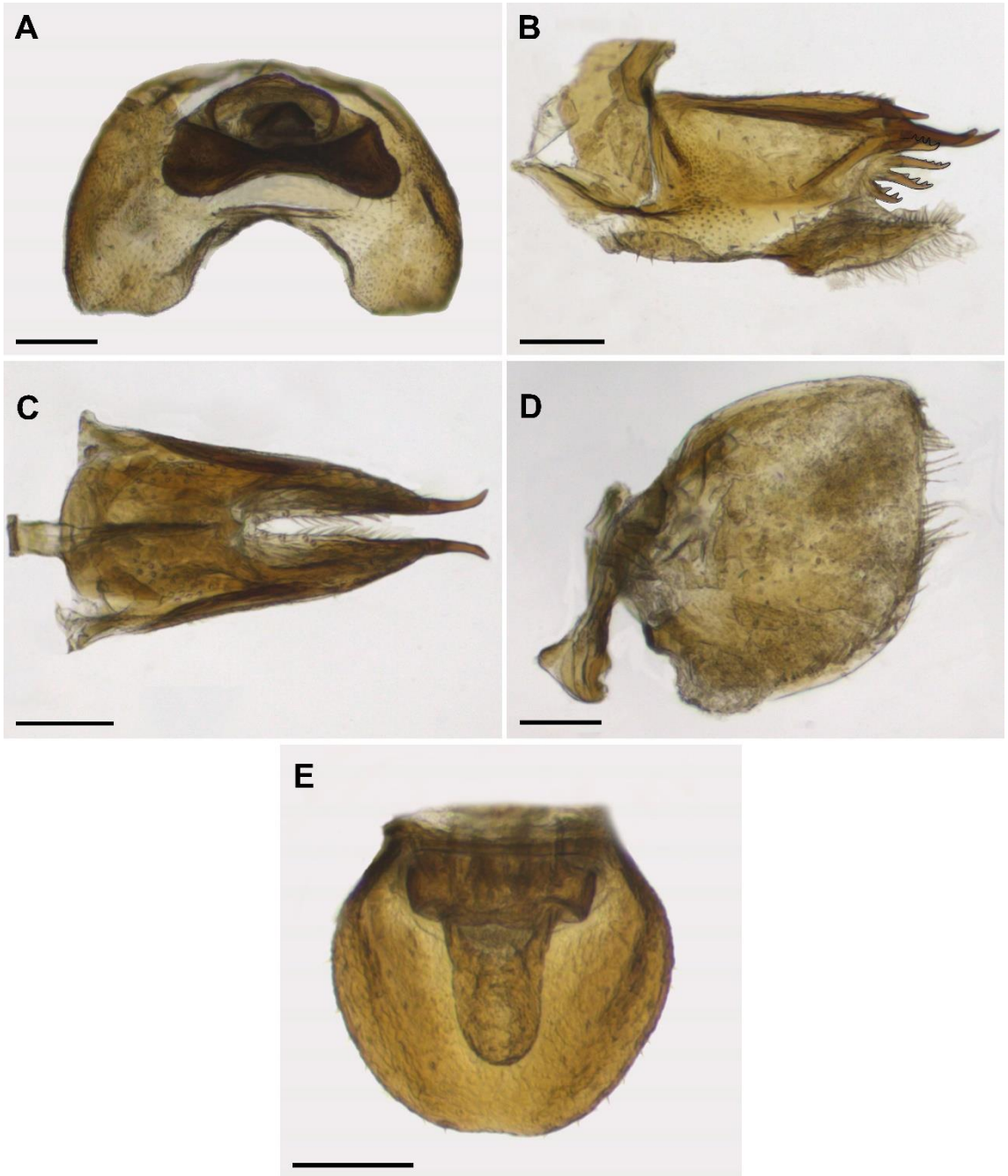

Figures 16 A–E. *Bebaiotes oliveirai* **sp. nov.**, female genitalia, holotype (INPA): **A**. Pygofer posterior view; **B**. Gonapophysis VIII, lateral view (first valvula) lateral view; **C**. Gonapophysis IX (second valvula), dorsal view; **D**. Gonoplac (third valvula), lateral view; **E**. Anal tube (segment X), dorsal view. Scale bars: A–E = 0.1 mm.

Bebaiotes pallidinervis Muir, 1934

Figs 17 A–E

Bebaiotes pallidinervis Muir, 1934: 132-134: fig.1 (genitalia); Metcalf, 1945: 217 (world catalogue); Fennah, 1947: 188 (key); Wilson, 1989: 491 (citation).

Diagnosis. Median region of frons without lozenge-shaped spots (Fig. 17 C). Pronotum with lateral carinae subparallel to each other towards posterior margin in dorsal view (Fig. 17 B). Forewing without m-cu1 cross-vein (Fig. 17 B).

Type material

Holotype

ECUADOR • ♂; Napo, Pano River, 1800 feet elevation, 7.iv.1923, F.X. Williams, nº1250; BPBM

Paratype

ECUADOR • ♂; Napo, Pano River, 1800 feet elevation, 7.iv.1923, F.X. Williams, 013585589; NHM (Paratype condition: glued on paper triangle; right antenna broken and lost, left flagellum broken and lost; left proleg broken and lost).

Redescription. Coloration. General body color dark brown (Figs 17 A, B). Lateral regions of frons, gena, clypeus, scape, median and lateral longitudinal carinae of pronotum and mesonotum, pustules, posterior margin of pronotum, long narrow stripe at lateral region of mesonotum yellowish brown. Forewing light brown, semihyaline, with yellow veins with white regions: narrow stripe covering c-sc cross-vein, ir cross-vein, RA vein, and RP vein; medial region of CA vein red; small white spot at middle region of the postcostal cell; white radial, median and cubital cells; large white stripe extending from apex of RP vein and extending through the MP vein to CuA2 vein; white rounded spot at C3a, C3', C3b cells and apex of medial cell; white rectangular spot at apical portion of

CuA2 vein. Abdomen yellowish brown, except, sternite II, sensory pits of the sternite III, posterior half of sternite III light yellow.

Head: Frons large (Fig. 17 C); median carina of clypeus strongly marked, present on distal three-fourths, not extending to epistomal suture (Fig. 3 C). Pedicel oblong (Fig. 3 C). Thorax: Pronotum anterior margin tapering; median longitudinal carina present, strongly marked; lateral carinae subparallel to each other towards posterior margin in dorsal view; posterior margin concave with shallow median notch in dorsal view; with pustules on posterior margin; Mesonotum with median longitudinal carina present, strongly marked (Fig. 17 B). Forewing: RA vein with apex gently curved anteriorly; RP vein with strongly curved anteriorly; ir cross-vein distant from r-m2 cross-vein; MP vein with four branches with gently curved anteriorly; MP1, MP2, MP3 MP4 veins unbranched; MP1+2 and MP3+4 branching distad to r-m cross-vein; m-cu1 cross-vein absent; m-cu2 cross-vein aligned with icua cross-vein; CuA vein bifurcation before to r-m cross-vein; apex of clavus forming acute angle (Fig. 17 A).

Male terminalia not examined.

Distribution. Ecuador (Napo).

Taxonomic notes. *Bebaiotes pallidinervis* Muir, 1934 differs from *B. bucayensis* Muir, 1924 as previously discussed in the description of the latter.

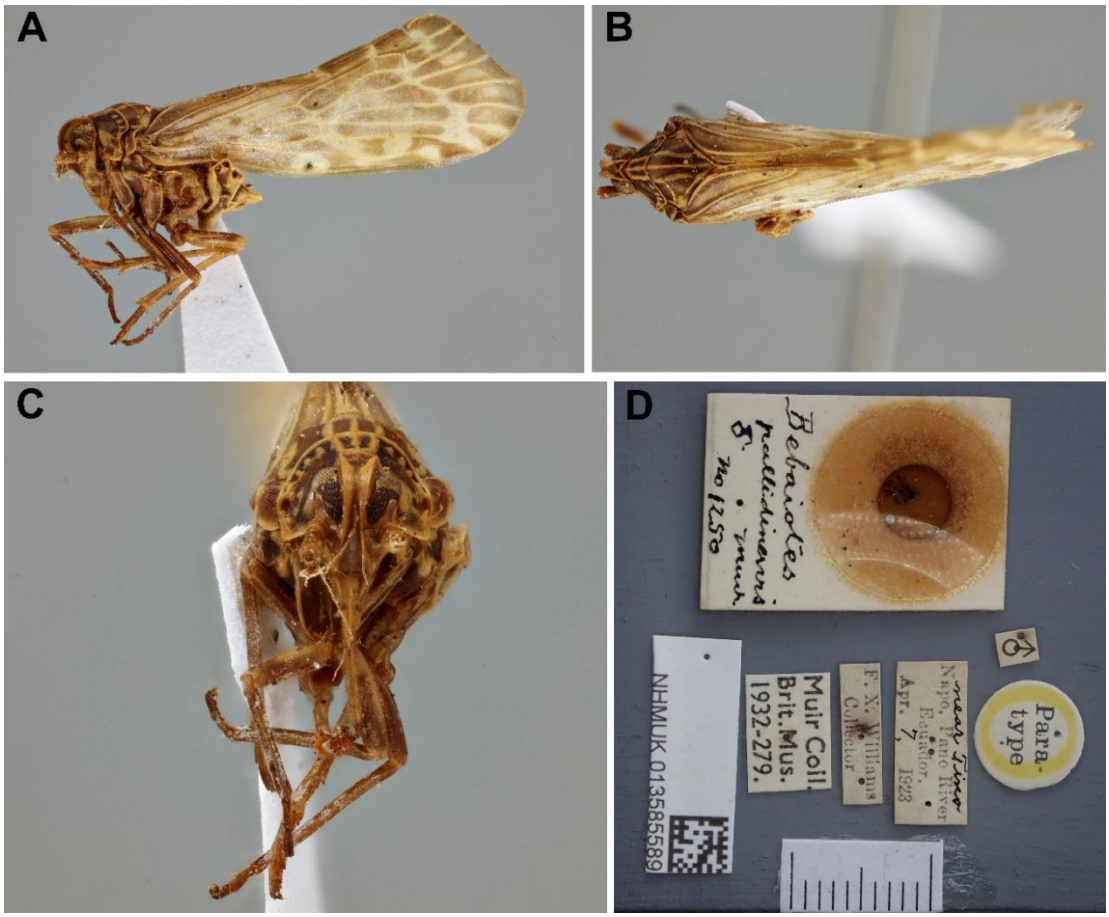

Figures 17 A–D. *Bebaiotes pallidinervis* Muir, 1934, male paratype (NHM): **A.** Male habitus, lateral view; **B**. Male head, anterior view; **C**. Male head, thorax, wings, dorsal view; **D.** Information tags. Fotos: Webb (2019).

***Bebaiotes specialis* Viegas, Takiya & Ale-Rocha sp. nov.**

Figs 18 A–E, 19 A–E, 21 E, F, 23

Diagnosis. Anterior margin of the pronotum rounded (Fig. 18 D). Median and lateral longitudinal carinae of mesonotum absent (Fig. 18 D). Scutellum yellow (Fig. 18 D). Gonapophysis VIII (first valvula) with one lateroapical projection (Fig. 19 E).

Type material

Holotype

BRASIL • ♀; **Bahia**, Una, Reserva Biológica de Una, Sede Piedade, Riacho; 15˚09'37" S, 39˚10'32"W; 91 m; 07–08.viii.2016; A.P. Pinto, A.P.M. Santos, D.M. Takiya & P.M.

Souto leg; DZRJ (ENT6127). (Holotype condition: right forewing mounted between coverslips; left forewing and hind wing mounted between coverslips; right and left prothoracic lost; right mesotarsus lost; abdomen removed and stored in a microtube; genitalia dissected and stored in a microtube).

Paratypes

BRASIL • 1 ♀; **Alagoas**, Quebrangulo, Reserva Biológica de Pedra Talhada, trilha para Riacho Cafuringa; 9˚15'15.2"S, 36˚25'7.9"W; 20.vi.2014; sweep; D.M. Takiya & A.C. Domahovski leg.; DZRJ.

Measurements. Body length: female: 3.6 mm (5.7 mm including wings) (N=1).

Description. Coloration. General body color yellowish brown (Figs 18 A–D). Apical article of rostrum dark brown. Pronotum and mesonotum with paired lateral longitudinal wide brown bands. Forewing semihyaline, light brown with white regions: narrow stripe covering RA vein; stripe covering ir cross-vein; narrow stripe extending from apex of RP vein to median region of MP4 vein; X-shaped region covering m-cu2 cross-vein; middle region of CuA1 vein and icua cross-vein; narrow stripe covering icu cross-vein; and apex of clavus (Fig. 21 E). Hind wing hyaline, light brown (Fig. 21 F). Legs light brown, except metatarsi light yellow.

Head: frons large, distance between lateral carinae of frons, at median portion, approximately 1.5 times shorter than maximum width of vertex (Fig. 18 B). Clypeus approximately 2.5 times longer than maximum width; median carina strongly marked, present on distal three-fourths; not extending to epistomal suture, (Fig. 18 B). Scape longer than wide (Fig. 18 B). Pedicel oblong, approximately 3 times longer than the scape (Figs 18 B, C).

Thorax: pronotum anterior margin rounded; median longitudinal carina present, strongly marked; lateral carinae gently diverging towards tegulae in dorsal view; posterior

961 margin concave with shallow median notch in dorsal view; without pustules on posterior
962 margin. Mesonotum with median and lateral longitudinal carinae absent (Fig. 18 D).
963 Forewing: RA and RP veins with apex gently curved anteriorly; r-m cross-vein
964 approximately subequal to length of r-m2 cross-vein; ir cross-vein distant from r-m2
965 cross-vein; MP vein with four branches with uncurved apex; MP1, MP2, MP3, and MP4
966 vein unbranched; MP1+2 and MP3+4 branching arising near r-m cross-vein; m-cu cross-
967 vein present; m-cu cross-vein approximately subequal m-cu2 cross-vein; m-cu2 cross-
968 vein aligned with icua cross-vein; CuA vein bifurcation basad to r-m cross-vein; CuP vein
969 approximately three times longer than Pcu + A1 vein; apex of clavus forming acute angle
970 (Fig. 21 E). Hind wing: first bifurcation of MP vein arising basad to m-cu cross-vein (Fig.
971 21 F). Legs: metatibia with 7 apical spines; metatarsus with 7+5 apical spines. Male
972 unknown.

973 Female terminalia (Figs 19 A–E): Gonapophysis VIII (first valvula) broad; with
974 sparse setae at basal and median regions; with small spiniform projections; single
975 lateroapical projection with irregular teeth on dorsal margin in lateral view (Fig. 19 B).
976 Bursa copulatrix densely filamentous apically, with obtuse apex; surface with small
977 spiniform projections (Fig. 19 B). Gonapophysis IX (second valvula) robust; bifid at
978 apical half; lobes with a pointed, strongly curved latero-ventrally apex, hook-like in dorsal
979 view (Fig. 19 D). Gonoplac (third valvula) subtrapezoidal; apex rounded with many
980 sparse laterally setae (Fig. 19 D). Anal tube (segment X) short and rounded in dorsal
981 view; apex rounded in dorsal view (Fig. 19 E).

982 **Variations.** Forewing with wide white stripe covering ir cross-vein and wide white stripe
983 extending from apex of RP vein to median region of MP4 vein; wide white stripe
984 extending from C2a cell to C5a cell; narrow white stripe covering Cup vein.

985 **Etymology.** From the Latin *specialis*, special. The species name alludes to its unique
986 character of the gonapophysis VIII (first valvula) with only one single projection on
987 lateroapical margin. This is also the only *Bebaiotes* species known to occur in Atlantic
988 Rainforest areas, as others species occur in areas of Amazonian Rainforest in South
989 America or Panamá.

990 **Distribution**. Brazil (Bahia and Alagoas) (Fig. 23).

991 **Taxonomic notes**. *B. specialis* **sp. nov**. can be promptly distinguished from other species
992 of *Bebaiotes* by its general yellowish brown coloration; frons wide; median and lateral
993 longitudinal carinae of mesonotum absent; and gonapophysis VIII (first valvula) with a
994 single lateroapical projection.

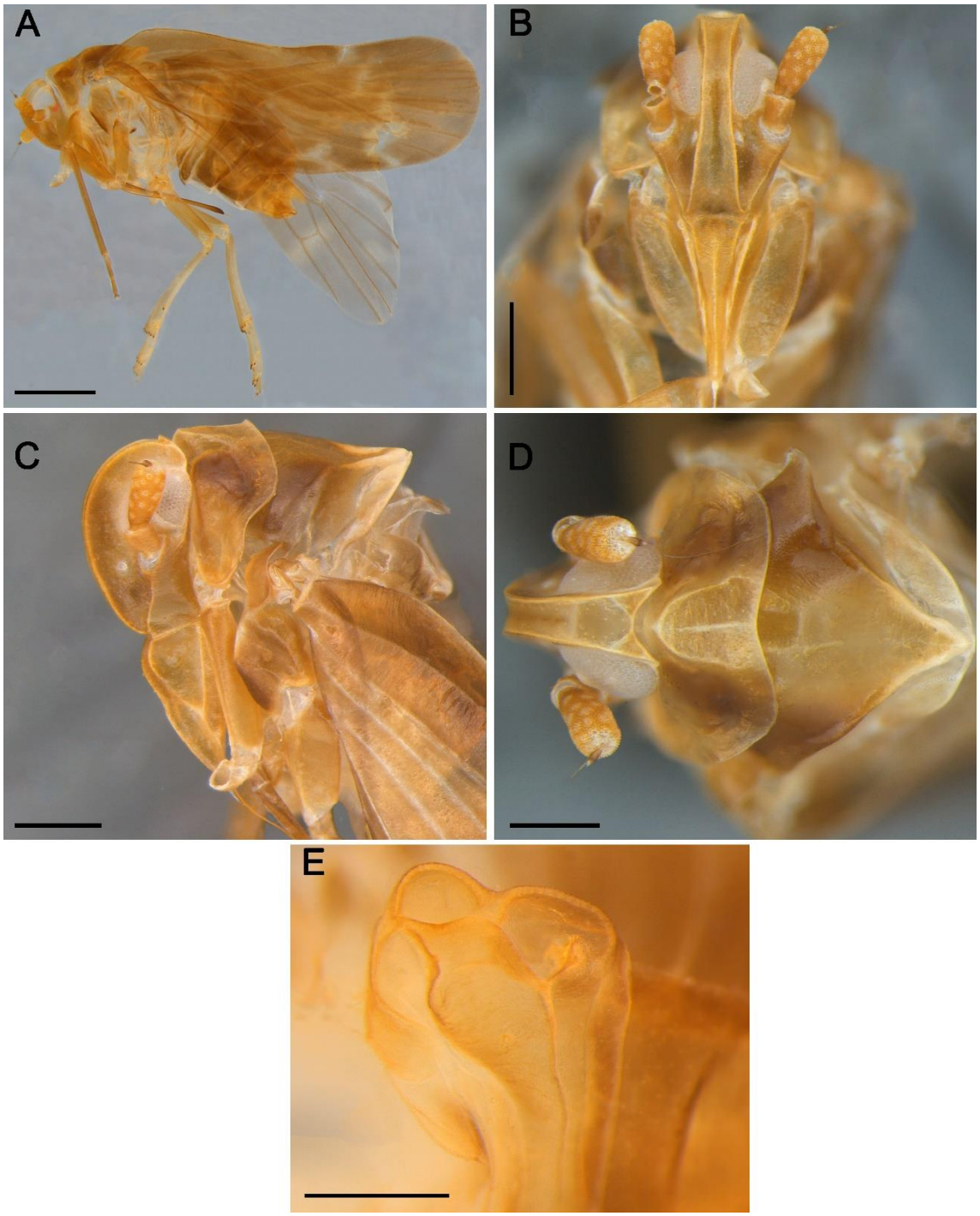

Figures 18 A–E. *Bebaiotes specialis* **sp. nov.**, female holotype (DZRJ): **A**. Female habitus, lateral view; **B**. Female head, anterior view; **C**. Female head and thorax, lateral view **D.** Female head and thorax, dorsal view; **E**. Male abdominal process, lateral view. Scale bars: A = 1 mm; B, C = 0.4 mm; D, E = 0.3 mm.

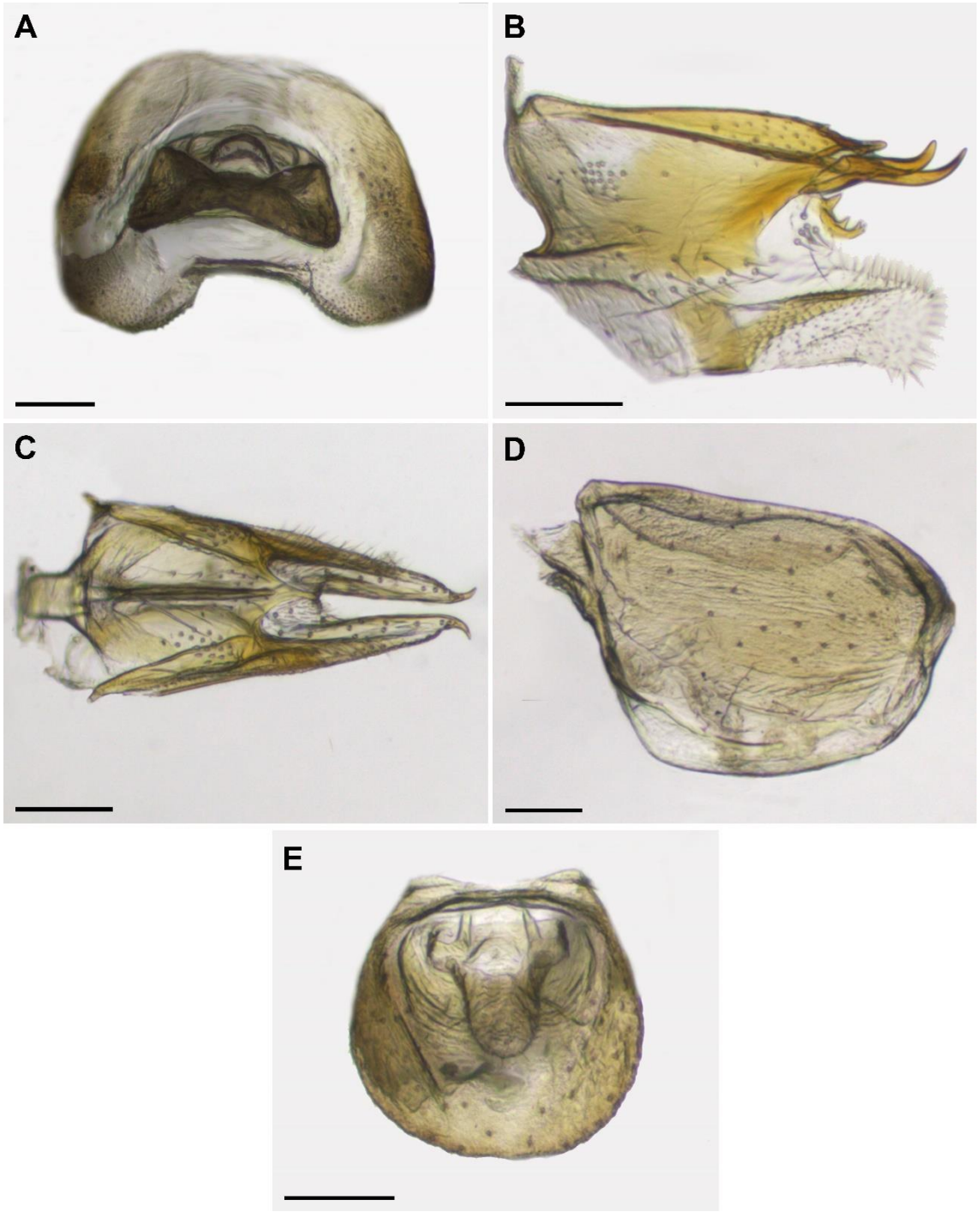

Figures 19 A–E. *Bebaiotes specialis* **sp. nov.**, female genitalia, paratype (DZRJ): **A**. Pygofer posterior view; **B**. Gonapophysis VIII, lateral view (first valvula) lateral view; **C**. Gonapophysis IX (second valvula), dorsal view; **D**. Gonoplac (third valvula), lateral view; **E**. Anal tube (segment X), dorsal view. Scale bars: A-E = 0.1 mm.

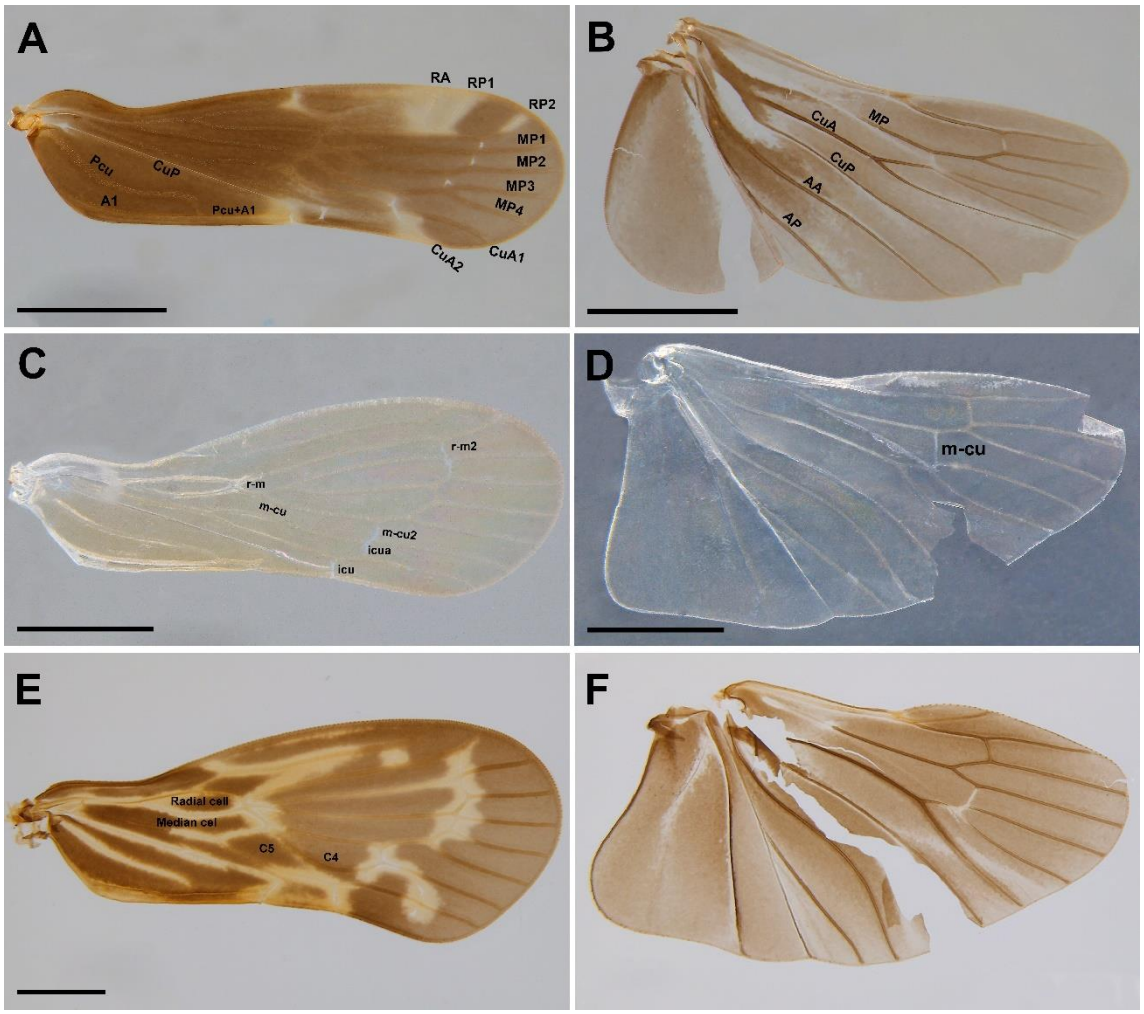

Figures 20 A–F. Wings of *Achilixius* and *Bebaiotes* species. **A.** *Achilixius dietrichi* **sp. nov.**, forewing; **B.** *Achilixius dietrichi* **sp. nov.**, hind wing, **C.** *Bebaiotes cavichiolii* **sp. nov.**, female forewing; **D.** *Bebaiotes cavichiolii* **sp. nov.**, female hind wing; **E.** *Bebaiotes clarice* **sp. nov.**, forewing; **F.** *Bebaiotes clarice* **sp. nov.**, hind wing; Abbreviations: Forewing: A1, first anal vein; C4, cell C4; C5, cell C5; CuA1, first cubitus anterior branch; CuA2, second cubitus anterior branch; CuP, cubitus posterior; icu cross-vein, cubital area; icua cross-vein, anterior cubital area; m-cu, m-cu2 cross-vein; median cell; MP1, first media posterior branch; MP2, second media posterior branch; MP3, third media posterior branch; MP4, fourth media posterior branch; Pcu, postcubitus; Pcu+A1, postcubitus+first anal vein; radial cell; r-m1, r-m2 cross-vein; RA, radius anterior branch; RP, radius posterior branch. Hind wing: AA, anterior Anal; AP, posterior Anal; CuA, anterior cubitus; CuP, posterior cubitus; m-cu, cross-vein MP, posterior media. Scale bars: A–F = 1 mm.

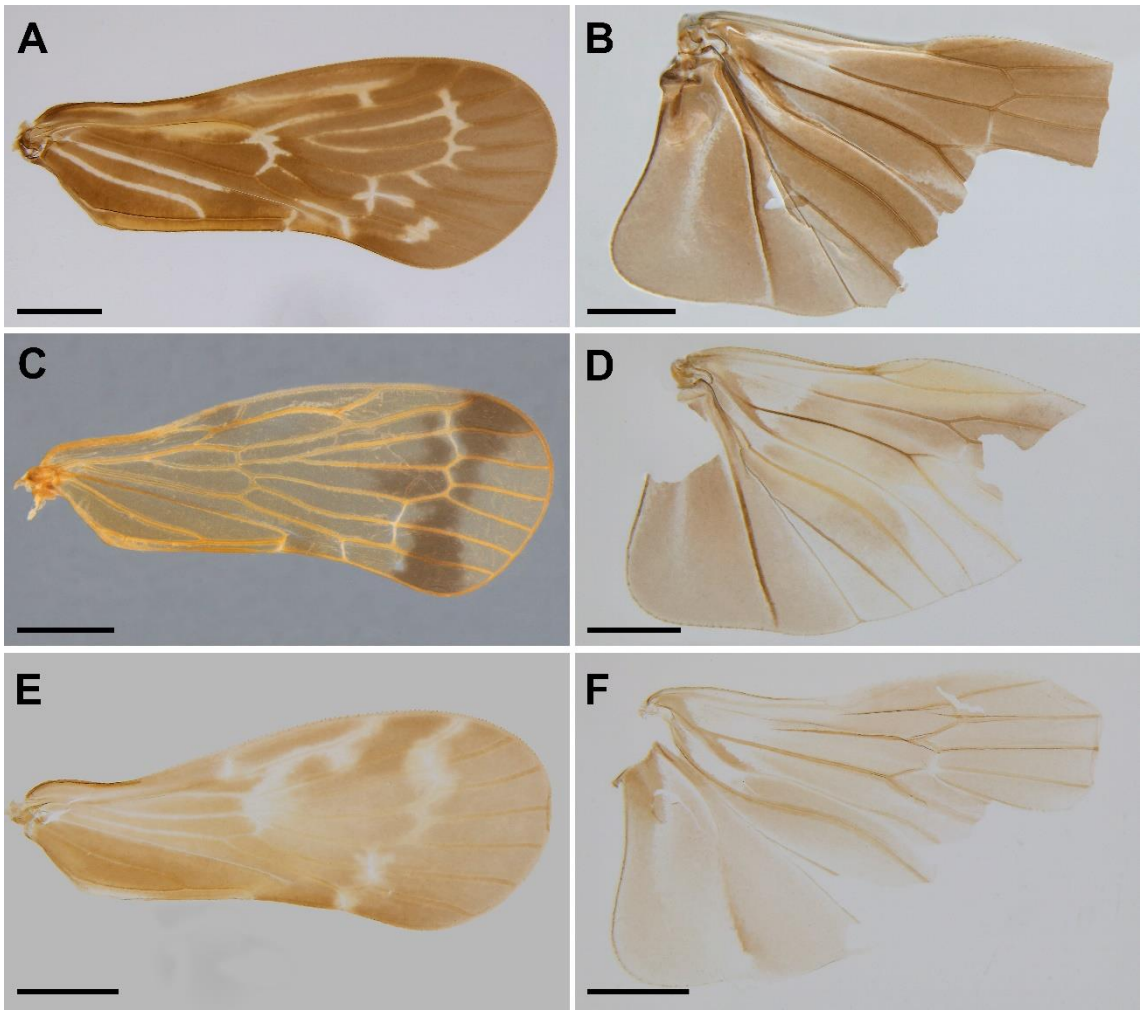

Figures 21 A–F. Wings of *Bebaiotes* species. **A.** *Bebaiotes oiapoquensis* **sp. nov.**, **B.** *Bebaiotes oiapoquenis* **sp. nov.**; **C.** *Bebaiotes oliveirai* **sp. nov.**, forewing; **D.** *Bebaiotes oliveirai* **sp. nov.**, hind wing; **E**. *Bebaiotes specialis* **sp. nov.**, female forewing; **F**. *Bebaiotes specialis* **sp. nov.**, female hind wing. Scale bars: A–F = 1 mm.

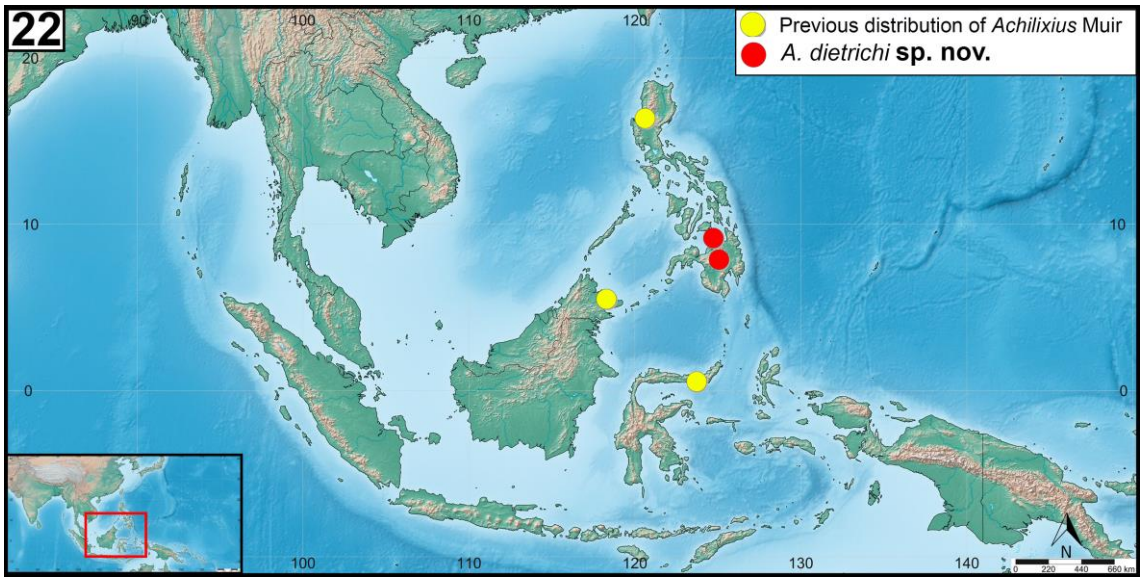

Figure 22. Geographical distribution of *Achilixius*. Previous known distribution of *Achilixius* Muir in yellow circles and of *Achilixius dietrichi* **sp. nov.** in red circles.

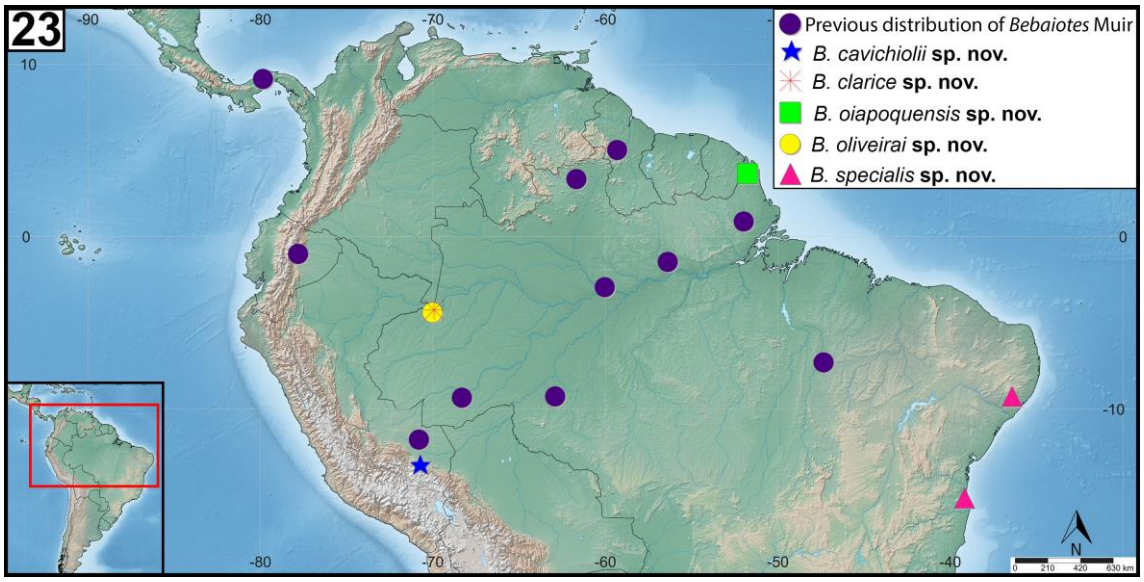

Figure 23. Geographical distribution of *Bebaiotes*. Previous known distribution of *Bebaiotes* Muir in purple circles. See legend for symbols referring to the distribution of the new species: *Bebaiotes cavichiolii* **sp. nov.**; *Bebaiotes clarice* **sp. nov.**; *Bebaiotes oiapoquensis* **sp. nov.**; *Bebaiotes oliveirai* **sp. nov.** and *Bebaiotes specialis* **sp. nov.**

4.5. Discussion

Knowledge about Achilixiidae has been growing in recent years (Viegas & Ale-Rocha, 2023), such as, for example, the increase in the number of species, expansion of their distributional records, and availability of illustrations of male and female genitalia, an important addition to this group. It is worth mentioning that there is a gap in the knowledge on the distribution of the group and this is probably due to the lack of collecting efforts and specialists directed to the study of the family, which reinforces the importance of research focused on Achilixiidae, aiming to generate more knowledge for the scientific community.

The herein presented results points to an increase of 58% in the number of known species of the family, emphasizing the importance of studying neglected taxonomic groups in order to better quantify our biodiversity.

4.6. Acknowledgements

We thank curators Dr. Marcio Luiz de Oliveira (INPA) and Dr. Christopher H. Dietrich (INHS) for loaning specimens studied. We also thank the curator Mr Michael D. Webb (NHM) for photographs of *Bebaiotes* and *Achilixius* types. Collecting permit for Peruvian specimens was obtained with the help of A. Asenjo and G. Melo (Universidade Federal do Paraná). Coordenação de Aperfeiçoamento de Pessoal de Nível Superior (CAPES) provided EFGV with a doctoral scholarship. RAR and DMT are research productivity fellows from Conselho Nacional de Desenvolvimento Científico e Tecnológico (CNPq, Procs. 304313/2018-1 and 314557/2021-0) and DMT is also a Cientista do Nosso Estado fellow from Fundação Carlos Chagas Filho de Amparo à Pesquisa do Estado do Rio de Janeiro (FAPERJ, Proc. E- 26/200.503/2023). This study was also financed in part by the Fundação de Amparo à Pesquisa do Estado do Amazonas (FAPEAM) –POSGRAD.

1059

1060 **4.7. References**

1061 Bourgoin, T. & Huang, J. 1990. Morphologie comparée des genitalia mâles des
1062 Trypetimorphini et remarques phylogénétiques (Hemiptera: Fulgoromorpha:
1063 Tropiduchidae). *Annales de la Société entomologique de France*, New Series, 26
1064 (4), 555–564.
1065 Bourgoin, T. 1988. A new interpretation of the homologies of the Hemiptera male
1066 genitalia, illustrated by the Tettigometridae (Hemiptera, Fulgoromorpha). *In*:
1067 Vidano, C. & Arzone, A (Eds.), *Proccedings of the 6th Auchenorrhyncha Meeting,*
1068 *Turin, Italy, 7–11 September 1987*. Consiglio Nazionale delle Ricerche-Special
1069 Project IPRA, Turin, 113–120.
1070 Bourgoin, T. 1993. Female genitalia in Hemiptera Fulgoromorpha, morphological and
1071 phylogenetic data. *Annales de la Société Entomologique de France*, New Series, 29
1072 (3), 225–244.
1073 Bourgoin, T., Wang, R.-R., Asche, M., Hoch, H., Soulier-Perkins, A., Stroinski, A., Yap,
1074 S. & Szwedo, J. 2015. From micropterism to hyperpterism: recognition strategy and
1075 standardized homology-driven terminology of the forewing venation patterns in
1076 planthoppers (Hemiptera: Fulgoromorpha). *Zoomorphology*, 134, 63–77.
1077 Dworakowska, I.D. 1988. Main veins of the wings of Auchenorrhyncha (Insecta,
1078 Rhynchota: Hemelytrata). *Entomol. Abh. Staatl. Mus. Tierkd. Dresden*, 52, 63–108.
1079 Fennah, R.G. 1946. A synopsis of the Achilixiidae of the New World (Homoptera:
1080 Fulgoroidea). *Annals and Magazine of Natural History*, 11 (13), 183–191.
1081 Emeljanov A.F. 1991. To the problem of the limits and subdivisions of the family
1082 Achilidae (Homoptera, Cicadina). *Entomologicheskoe Obozrenie*, 70(2): 373–393.

1083 Hoch, H., Wessel, A., Asche, M., Baum, D., Beckmann, F., Bräunig, P., Ehrig, K.,
1084 Mühlethaler, R., Riesemeier, H., Staude, A., Stelbrink, B., Wachmann, E.,
1085 Weintraub, P., Wipfler, B., Wolff, C. & Zilch, M. 2014. Non-sexual abdominal
1086 appendages in adult insects challenge a 300 million year old Bauplan. *Current*
1087 *Biology*, 24 (1), 16–17.
1088 https://doi.org/10.1016/j.cub.2013.11.040
1089 Liang A. P. 2001. Morphology of antennal sensilla in *Achilixius sandakanensis* Muir
1090 (Hemiptera: Fulgoromorpha: Achilixiidae) with comments on the phylogenetic
1091 position of the Achilixiidae. *The Raffles Bulletin of Zoology*, 49 (2), 221–225.
1092 Metcalf, Z.P. 1945. Derbidae, Achilixiidae, Meenoplidae, Kinnaridae. General catalogue
1093 of the Hemiptera, *Fascicle IV Fulgoroidea*, Parts 4–7. Smith College, Northampton,
1094 MA.
1095 Muir, F. 1923. *Achilixius*, a new genus constituting a new family of the Fulgoroidea
1096 (Homoptera). *Philippine Journal of Science*, 22, 483–487.
1097 Muir, F. 1924. A new genus of the family Achilixiidae (Homoptera). *Canadian*
1098 *Entomologist*, 56, 33–34.
1099 O'Brien, L.B. & Wilson, S.W. 1985. Planthopper systematics and external morphology.
1100 In: Nault, L.R., Rodriguez, J.G. (Eds.), *The Leafhoppers and Planthoppers*. Wiley,
1101 New York, 61–102.
1102 Santos, J.C. do C.V.; Bento, D. de M. & Ferreira, R.L. 2022. Hemiptera: Auchenorryncha.
1103 In: Zampulo, R. de A. & Procus, X. *Fauna de Cavernícola do Brasil*. Belo
1104 Horizonte. *Rupestre* Editora.317–339.
1105 Shorthouse, D.P. 2010. SimpleMappr, an online tool to produce publication-quality point
1106 maps. Available from: http:// www. simplemappr.net (accessed 12 December
1107 2022).

1108 Viegas E.F.G. & Ale-Rocha R. 2022. Study of the Neotropical genus *Bennarella* Muir,
1109 1930 with description of six new species (Hemiptera: Fulgoromorpha: Cixiidae).
1110 *Zootaxa*, 5124 (2), 155–187.
1111 Viegas, E.F.G. & Ale-Rocha, R. (Submitted) A century of Achilixiidae Muir, 1923
1112 (Hemiptera: Auchenorrhyncha: Fulgoroidea): taxonomic study of the genus
1113 *Bebaiotes* Muir, 1924 and description of eight new species from Brazil. Zootaxa, in
1114 review.
1115 Wilson, M.R. 1989. The planthopper family Achilixiidae (Homoptera, Fulgoroidea): a
1116 synopsis with a revision of the genus *Achilixius. Systematic Entomology*, 14, 487–
1117 50.

5. CAPÍTULO II

Viegas, E. F.G.; Ale-Rocha, R; Dietrich & Takiya, D. M. Evolution of the disjunct Neotropical and Oriental Achilixiidae (Hemiptera: Fulgoromorpha) during the gondwanan breakup

Manuscrito formatado para *Molecular Phylogenetics and Evolution*[1].

[1]Fator de impacto:4.1; Qualis biodiversidade: A1

Title

Evolution of the disjunct Neotropical and Oriental planthopper family Achilixiidae (Hemiptera: Fulgoromorpha)

Authors

Eduarda Fernanda Gomes Viegas[a,*], Rosaly Ale-Rocha[b], Christopher H Dietrich[c] & Daniela Maeda Takiya[d]

Affiliations

[a]Graduate Program in Entomology, Instituto Nacional de Pesquisas da Amazônia, Av. André Araújo, Petrópolis, 2936, Manaus, 69067- 375, Amazonas, Brazil.

[b]Coordenação de Biodiversidade, Instituto Nacional de Pesquisas da Amazônia, Caixa Postal 2223, Manaus, 69080-971, Amazonas, Brazil. Fellowship PQ/CNPq.

[c]Illinois Natural History Survey, Prairie Research Institute, University of Illinois, 1816 South Oak Street, Champaign, IL 61820, USA

[d]Laboratório de Entomologia, Departamento de Zoologia, Instituto de Biologia, Universidade Federal do Rio de Janeiro, Caixa Postal 68044, Rio de Janeiro, 21941-971, Rio de Janeiro, Brazil.

**Corresponding author*.

E-mail addresses: edwviegasgomes@gmail.com (E.F.G. Viegas), rosalyale@gmail.com (R. Ale-Rocha), chdietri@illinois.edu (C.H. Dietrich), takiya@gmail.com (D.M. Takiya)

5.1. Abstract

Achilixiidae is a rare planthopper family with 32 described species, which includes two genera that are morphologically quite distinct and have a disjunct distribution. Although the presence of lateral abdominal processes is a striking characteristic of the family (though similar ones are also found in Cixiidae), processes found in *Achilixius* Muir and *Bebaiotes* Muir differ substantially morphologically from the other and had raised questions about the family's monophyly. Furthermore, *Achilixius*' distribution is currently restricted to some islands of the Malay archipelago, while *Bebaiotes* is distributed on northern South America and Panama. For this study, two nuclear ribosomal (18S rDNA and 28S rDNA), one nuclear protein-coding (H3), and one mitochondrial (16S rRNA) markers were sequenced and analyzed with available sequences in GenBank building a concatenated data matrix of 67 taxa and 4,379 base pairs. The taxon sampling is constituted by representatives of all Fulgoromorpha families, including newly generated sequences of seven outgroup taxa and 15 species of both genera of Achilixiidae. Phylogenetic analyses based on maximum likelihood and Bayesian inference recovered Achilixiidae nested within Achilidae representatives, as sister to a clade containing the Plectoderine genera *Catonia*, *Synecdoche*, and *Spino*. This placement agrees with results of a few previous molecular hypotheses. Herein, the monophyly of Achilixiidae was recovered for the first time, with strong support (SH-aLRT = 99, UFBoot = 100, and PP = 1.00). Thus, the results support that at least paired processes derived from the third

abdominal segment are homologous and a synapomorphy of Achilixiidae, while they are convergent with processes found in Bennarellini (Cixiidae), for which sequences were also generated for the first time. Furthermore, a relaxed-clock divergence time analysis suggests that the initial divergence of Achilixiidae occurred **s**ometime during the Triassic through the Jurassic (median age of 240.20 Mya), a period marked by the Gondwana breakup, which is postulated to be the main vicariant event separating ancestors of *Achilixius* and *Bebaiotes*. Additionally, initial divergences of *Bebaiotes* species in the Neotropical Region occurred in the Early Jurassic at around 176 Mya, while *Achilixius* species lineage started to diverge in the Malay archipelago much later in the Early Cretaceous at around 83 Mya. While there are many more interesting questions concerning this enigmatic family, the present study contributes to a deeper understanding of the evolution and phylogenetic relationships within the family Achilixiidae.

Keywords: *Achilixius*; *Bebaiotes*; Biogeography; Divergence date; Molecular phylogeny;

5.2. Introduction

The planthopper (Fulgoromorpha) family Achilixiidae Muir, 1923 is divided into two genera and 32 described and species. The distribution of the family is completely disjunct. *Achilixius* Muir currently comprises 16 species and is restricted to the southern Oriental Region, more specifically restricted to the Malay archipelago, with distributional records on Malaysia (Sabbah), Indonesia (Sulawesi), and Philippines (Wilson, 1989). On the other hand, *Bebaiotes* Muir comprises 16 species distributed on the northern Neotropical

region with records on Brazil, Ecuador, Guyana, and Panama (Wilson, 1989, Viegas & Ale-Rocha, 2023).

Historically, the family was erected by Muir (1923), who proposed the type genus *Achilixius* (type species: *A. singularis* Muir, 1923) to include three described species from the Philippines and Malaysia and *Achilixius tubulifer* (Melichar, 1914) from the Philippines, previously in Derbidae. The proposal of the new family was based on the forewing claval vein running into the apex of the clavus which is roundly closed, similarly to Achilidae, and abdominal processes similar to those found in Bennini and Bennarellini of the Cixiidae. However, Muir (1923) added that they had distinct male genitalia from other fulgoromorphs, but it was most similar to Meenoplidae. Muir (1924) included in the family a second genus, *Bebaiotes* (type species: *B. bucayensis* Muir, 1924), described based on two new species from Ecuador, recording the family for the first time for the Neotropical region. A third monotypic genus from Panama, *Muirilixius* Metcalf, 1938, was proposed by Metcalf (1938), but it was posteriorly synonymized with *Bebaiotes* by Wilson (1989), in his revision of the family. Wilson (op. cit.) provided a systematic account of the family, with redescriptions and key to genera, new family geographical records, species redescriptions and descriptions of twelve new species of *Achilixius*. Only two other taxonomic works on the family were conducted: Fennah (1947) who described three neotropical *Bebaiotes* from Ecuador and Viegas & Ale-Rocha (submitted) who described eight species of *Bebaiotes* from the Brazilian Amazon, highlighting how understudied the family is in the Neotropical Region.

Until now, there are no studies focusing on the phylogenetic relationships within Achilixiidae, especially in regards to testing their monophyletic status given such disjunct distribution. In addition, their phylogenetic position within Fulgoromorpha is also dubious. The family was rarely included in more comprehensive phylogenetic

studies of the Fulgoromorpha based on morphological data (Asche, 1987; Emeljanov, 1990; Bourgoin, 1993; Chen & Yang, 1995). Most phylogenetic proposals either treated Achilixiidae tentatively within Achilidae (Emeljanov, 1990), within the Cixiidae-clade (Chen & Yang, 1995), or did not mention them at all, except of Asche (1987) who clearly considered the family monophyletic because of the lateral abdominal processes with sensory pits and related to Achilidae because of characters of the female ovipositor modified into an "excavating-apparatus". Other authors, based on morphological studies, further proposed that Achilixiidae were related to Achilidae (Emeljanov, 1991) or to Cixiidae (Liang, 2001) or that most characters mentioned of relevance to positioning Achilixiidae were plesiomorphic, thus not usable to infer relationships (Wilson, 1989).

The use of multiple DNA sequence markers in phylogenetic studies has played an important role in hypothesizing the evolutionary history of species, due to, for example, different selection pressures and rates of evolution (Huelsenbeck et al., 1996). The use of molecular data has been extremely important for Fulgoromorpha phylogenetics, taking into account that this method has increased the knowledge of family-relationships and internal relationships of many families (Yeh et al., 2005; Urban & Cryan, 2007, 2009; Urban et al., 2010; Ceotto & Bourgoin, 2008; Song & Liang, 2013; Bucher et al., 2023). As far as DNA-sequence data, all more recently proposed planthopper phylogenies (Song & Liang, 2013; Boucher et al., 2023) included only 18S and 28S rDNA, histone H3, and wingless sequences generated by Urban & Cryan (2007) from a single unidentified female *Bebaiotes* specimen voucher. Thus, resulting phylogenies are also incongruent in relation to placing Achilixiidae, sometimes recovered in a clade with non-monophyletic "Achilidae" + Derbidae (Urban & Cryan, 2007), as sister to part of "Achilidae" + several other planthopper families (Urban &

Cryan, 2007), as sister to part of "Nogodinidae" + Derbidae (Song & Liang, 2013), as sister to Achilidae (Song & Liang, 2013), and more recently nested within "Achilidae" (Bucher et al., 2023).

Given the enigmatic position of this poorly studied planthopper family, the present study analyzed sequences of one mitochondrial (16S rDNA) and three nuclear (histone H3, 18S rDNA, and 28S rDNA) markers of 15 achilixiid terminal species (and seven outgroup species) to sequences of other Fulgoromorpha families available at GenBank. Our main goals were to test the monophyly of Achilixiidae, provide the first backbone of internal relationships, and estimate the divergence date for the initial divergence of Achilixiidae, in order to postulate a time-congruent biogeographical hypothesis.

5.3. Material and Methods

5.3.1. Taxon sampling

Material studied belong to Coleção de Invertebrados do Instituto Nacional de Pesquisas da Amazônia, Manaus (INPA); Coleção Zoológica do Maranhão, Universidade Estadual do Maranhão, Caxias (CZMA); Centro de Estudos em Biologia Subterrânea, Universidade Federal de Lavras, Lavras (UFLA); Coleção Entomológica Professor José Alfredo Pinheiro Dutra, Rio de Janeiro, Universidade Federal do Rio de Janeiro (DZRJ), and Illinois Natural History Survey, University of Illinois, Urbana-Champaign (INHS).

Genomic DNA was extracted from 22 representatives of 15 species of Achilixiidae that we had at hand, but amplification and sequencing had a low rate of success given the preservation of old specimens. We have generated sequence data for a total of two *Achilixius* and 13 *Bebaiotes* species at the end, as well as one Achilidae, two Derbidae, and four Cixiidae, including two Benarellini (Table 1). These sequences were complemented with sequences of all Fulgoromorpha families available in GenBank,

147 resulting in a data matrix with a total of 16 species of Achilixiidae comprising the ingroup
148 and 49 species of 18 Fulgoromorpha families and two Cercopoidea terminals for rooting,
149 comprising the outgroup (Table 1). This expanded outgroup sampling was included to
150 test Achilixiidae monophyly and its phylogenetic position in Fulgoromorpha.
151

Table 1. Taxa included in the present molecular phylogenetic analysis of Achilixiidae, with respective DNA specimen voucher(s) code(s) and its(their) geographical information. GenBank accession numbers for sequences of 16S, 18S, and 28S rDNA and histone H3 used are provided. References are given for published sequences and those in bold were herein generated.

Taxon	Voucher code	Geographical source	GenBank Accession Number			
			16S	18S	28S	H3
Acanaloniidae						
Acanalonia bivitatta		USA: New York	–	DQ532504[a]	DQ532583[a]	DQ532661[a]
Acanalonia depressa		St. John	–	DQ532503[a]	DQ532582[a]	DQ532660[a]
Achilidae						
Catonia sp. 1		St. John	–	DQ532506[a]	DQ532585[a]	DQ532663[a]
Deferunda acuminata			JX556696[b]	JX556746[b]	JX556785[b]	–
Magadha flavisigna			JX556716[b]	JX556763[b]	JX556803[b]	–
Spino sp. 1		Costa Rica	–	DQ532508[a]	DQ532587[a]	DQ532665[a]
Synecdoche sp. 2	ENT6244	Brazil: MG, Carmo do Riacho	**OP555332**	**OP554220**	**OP555349**	**OP549688**
Achilixiidae						
Achilixius sp. 1	ENT6099	Philippines	**OP555333**	**OP554221**	**OP555362**	–
Achilixius dietrichi	ENT6102	Philippines	**OP555334**	**OP554222**	**OP555350**	**OP549689**
Bebaiotes amazonica	ENT6101	Brazil: Amazonas, Manaus	**OP555335**	**OP554223**	**OP555351**	**OP549690**
Bebaiotes banksi	ENT6321	Brazil: Pará, Parauapebas	**OP555336**	–	–	**OP549691**
Bebaiotes bia	ENT6269	Brazil: Acre, Bujari	–	**OP554236**	–	**OP549693**
Bebaiotes dorsivittata	ENT6320 / 6242*	Brazil: Pará, Parauapebas	**OP555337**	**OP554224**	**OP555352**	**OP549694***
Bebaiotes guianesus	ENT6274 / 6268#	Brazil: Amazonas, Tefé	–	**OP554237**	–	**OP549695#**
Bebaiotes macroptera	ENT6232	Brazil: Amazonas, Atalaia do Norte	**OP555338**	**OP554225**	**OP555353**	**OP549696**
Bebaiotes pennyi	ENT6238	Brazil: Amazonas, Manaus	–	**OP554226**	**OP555354**	**OP549697**
Bebaiotes pulla	ENT6237	Brazil: Acre, Senador Guiomard	**OP555339**	**OP554227**	**OP555355**	**OP549698**
Bebaiotes sp. 1	ENT6098	Brazil: Maranhão, Caxias	**OP555340**	–	–	**OP549692**
Bebaiotes clarice	ENT6123	Brazil: Amazonas, Tabatinga	**OP555341**	**OP554238**	–	**OP549700**
Bebaiotes specialis	ENT6127	Brazil: Bahia	**OP555342**	**OP554228**	**OP555356**	**OP549701**
Bebaiotes sp. C	ENT6317	Brazil: Tocantins, Xambioá	–	**OP554239**	**OP555363**	**OP549699**
Bebaiotes tigrina	ENT6097	Brazil: Amazonas, Atalaia do Norte	–	**OP554229**	**OP555364**	–
Bebaiotes sp. 1		Ecuador	–	DQ532509[a]	DQ532588[a]	DQ532666[a]
Caliscelidae						
Aphelonema sp. 1		USA: Delaware	–	DQ53254[a]	DQ532625[a]	DQ532698[a]
Bruchomorpha sp. 1		USA (MD)	–	DQ53254[a]	DQ532624[a]	DQ532697[a]

Table 1 (*continued*)

Species	Voucher code	Geographical source	GenBank Accession Number			
			16S	18S	28S	H3
Cercopoidea						
Neophilaenus lineatus		USA: Vermont	–	DQ53249[a]	DQ532579[a]	DQ532658[a]
Philaenus spumarius			NC_005944[f]	UU06480[d]	AY744813[e]	AY744851[e]
Cixiidae						
Andes simplex		Cambodia	–	EU183568[c]	EU183729[c]	–
Bennarella bicoloripennis	ENT6157	Brazil: Amazonas, Manaus	**OP555343**	**OP554230**	**OP555357**	**OP549702**
Bennarella fusca	ENT6171	Brazil: Amazonas, Manaus	**OP555344**	**OP554231**	**OP555358**	**OP549703**
Bothriocera eborea		St. John	–	DQ53251[a]	DQ532591[a]	DQ532667[a]
Bothriocera sp. 2	ENT6173	Brazil: Roraima, Alto Alegre	**OP555345**	**OP554232**	**OP555359**	**OP549704**
Cixius similis		France	–	EU183588[c]	EU183740[c]	–
Haplaxius deleter		Costa Rica	–	EU183552[c]	EU183720[c]	–
Haplaxius sp. 1	ENT 6236	Brazil: Minas Gerais, Jaboticatubas	**OP555346**	**OP554233**	**OP555365**	**OP549705**
Oliarus sp. 2			JX556720[b]	JX556767[b]	JX556807[b]	–
Ozoliarus sp.			–	EU183563[c]	EU183702[c]	–
Pintalia alta		St. John	–	AY74480[e]	DQ532589[a]	AY744876[e]
Delphacidae						
Conomelus anceps			–	EU183548[c]	EU183701[c]	–
Harmalia ostorius		Australia	–	DQ53251[a]	DQ532596[a]	DQ532670[a]
Nilaparvata lugens			JX556717[b]	JX556764[b]	JX556804[b]	–
Derbidae						
Anotia sp. 1	ENT6124	Brazil: Maranhão, Caxias	**OP555347**	**OP554234**	**OP555360**	**OP549706**
Derbe sp. 1		French Guiana	–	DQ53252[a]	DQ532600[a]	DQ532674[a]
Persis (*Anapersis*) sp. 2	ENT6163	Brazil: Maranhão, Caxias	**OP555348**	**OP554235**	**OP555361**	**OP549707**
Dictyopharidae						
Dictyophara sinica			JX556698[b]	JX556748[b]	JX556787[b]	–
Rhaphiophora sp. 1		Ghana	–	DQ532527[a]	DQ532607[a]	DQ532680[a]
Eurybrachidae						
Loxocephala sp. 1			JX556713[b]	JX556761[b]	JX556800[b]	–
Olonia sp. 1		Australia	–	DQ532531[a]	DQ532611[a]	DQ532684[a]

158 **Table 1** (*continued*)

Species	Voucher code	Geographical source	GenBank Accession Number			
			16S	18S	28S	H3
Flatidae						
Geisha sp. 1			JX556702[b]	JX556751[b]	–	–
Ormenis saucia		USA: Arizona	–	DQ532536[a]	DQ532616[a]	DQ532689[a]
Fulgoridae						
Lycorma delicatula			JX556715[b]	JX556762[b]	JX556802[b]	–
Scaralis semillimpida		French Guiana	–	DQ532542[a]	DQ532622[a]	DQ532695[a]
Issidae						
Thionia argo		St. John	–	DQ532543[a]	DQ532623[a]	DQ532696[a]
Sivaloka damnosus			JX556732[b]	JX556777[b]	JX556819[b]	–
Kinnaridae						
Kinnara ochracea			JX556711[b]	JX556759[b]	JX556798[b]	–
Lophopidae						
Lophops sp. 1		Papua New Guinea	–	DQ532553[a]	DQ532633[a]	DQ532705[a]
Serida sp. 1			JX556731[b]	JX556743[b]	JX556818[b]	–
Meenoplidae						
Nisia sp. 1		Papua New Guinea	–	DQ532557[a]	DQ532637[a]	DQ532709[a]
Nisia sp. 2			JX556718[b]	JX556765[b]	JX556805[b]	–
Nogodinidae						
Biolleyana costalis		Costa Rica	–	DQ532558[a]	DQ532638[a]	DQ532710[a]
Pisacha naga		Belize	JX556722[b]	JX556770[b]	JX556809[b]	–
Ricaniidae						
Euricania sp. 1		Papua New Guinea	–	DQ532562[a]	DQ532642[a]	DQ532714[a]
Ricania marginalis			JX556727[b]	JX556741[b]	JX556814[b]	–
Tettigometridae						
Hilda sp. 1		Ghana	–	DQ532568[a]	DQ532648[a]	DQ532720[a]
Hilda undata		Ghana	–	DQ532567[a]	DQ532647[a]	DQ532719[a]
Tropiduchidae						
Neotangia caribea		Dominica	–	DQ532572[a]	DQ532652[a]	–
Sogana longiceps			JX556733[b]	JX556778[b]	JX556820[b]	–

159 [a]Urban & Cryan (2007); [b]Song & Liang (2013); [c]Ceotto et al., (2008); [d]Campbell et al., (1995); [e]Cryan (2005); [f]Stewart & Beckenbach (2005)

5.3.2. DNA extraction and polymerase chain reaction amplification (PCR)

Genomic DNA extraction from the whole specimen (ethanol preserved or pinned) was performed with the DNeasy Blood & Tissue Kit (Qiagen, Valencia, USA) following the protocol provided by the manufacturer with the following modifications: increase in digestion time to 24 hours to increase DNA yield and without maceration of the specimen in order to preserve their morphology. After extraction, specimens were returned to ethanol and deposited in their original collection, labeled as DNA vouchers.

One mitochondrial (16S rDNA) and three nuclear (histone H3, 18S rDNA, and 28S rDNA) markers were selected in order to be able to combine our generated sequences with available data at GenBank®, mostly those from Urban & Cryan (2007). These markers have been effective in recovering evolutionary relationships within Auchenorrhyncha at different levels of divergence (Cryan, 2005; Zahniser & Dietrich, 2010; Cryan & Urban, 2012; Song & Liang, 2013). A 25 µl solution for PCR (polymerase chain reaction) reaction was prepared with the following reagents: 13.0 µl DEPC water; 5.0 µl of 5x Green GoTaq® G2 buffer (Promega); 3.4 µl of $MgCl_2$ (25 mM, Promega); 1.0 µl of each forward and reverse primers (10 mM, Invitrogen); 0.5 µl of a dNTP mix (10mM, Promega=);1.0 µl of extracted DNA; and 0.1 µl of GoTaq® G2DNA polymerase (Promega). After some unsuccessful attempts, we made modifications, doubling the amount of DNA (2.0 µl), decreasing the amount of $MgCl_2$ (2.5 µl), or adding 1.0 µl of bovine serum albumin (10 mg/ml, Promega). Amplifications of the above-cited markers were done by PCR reactions in a VeritiPro 96-Well Thermal cycler (Applied Biosystems) under 35 cycles of initial temperature of 95˚C for 3 min, denaturation of 95˚C for 1 min, annealing varying from 45-54˚C for 1 min, extension of 72˚C for 2 min, and a final extension of 72˚C for 7 min. PCR primers

used are listed in Table 2. Resulting 18S rDNA sequences were amplified and sequenced in two contiguous overlapping regions (using primer pairs a0.7–bi and a2.0–9R), as well as 28S rDNA, also amplified and sequenced in two contiguous regions (using primer pairs EE–MM and Lalt–Galt).

PCR products were stained with GelRed™ (Biotium) and underwent agarose gel electrophoresis in 1.0% TBE and visualized under UV light. Amplicons were then purified using ExoSAP-IT® (USB Affymetrix) and sent to Macrogen Inc. (Seoul) for capillary sequencing of both strands using the same PCR primers.

Table 2. Primers used for PCR and sequencing of histone H3, 16S, 18S, and 28S from Achilixiidae and outgroups, with respective sequence and reference of the primers.

Primer	Sequence 5'-3'	Reference
HexAF	ATGGCTCGTACCAAGCAGACGGC	Ogden & Whiting 2003
HexAR	ATATCCTTGGGCATGATGGTGAC	Ogden & Whiting 2003
16S (F)	CCGGTYTGAACTCARATCA	Takiya et al. 2006
16S (R)	CRMCTGTTTAWCAAAAACAT	Takiya et al. 2006
18S 9R	GAT CCT TCC GCA GGT TCA CCT AC	Cryan et al. 2004
18S a2.0	ATG GTT GCA AAG CTG AAA C	Cryan et al. 2004
18S a0.7	ATT AAA GTT GTT GCG GTT	Cryan et al. 2004
18S bi	GAG TCT CGT TCG TTA TCG GA	Cryan et al. 2004
28S EE	CCG CTA AGG AGT GTG TAA	Cryan et al. 2000
28S MM	GAA GTT ACG GATCTARTTTG	Cryan et al. 2000
28S Lalt (F)	CCTCGGACCTTGAAAATCC	Dietrich et al. 2001
28S Galt (R)	TGTCTCCTTACAGTGCAAGA	Dietrich et al. 2001

5.3.3. Assemblies and Multiple Sequence Alignment

Consensus sequences were generated from assemblies of forward and reverse electropherograms in Geneious 6.0.6 (Kearse et al., 2012). After obtaining consensus sequences, they were checked for non-contamination and correct marker with BLAST® available at NCBI. A total of 74 sequences (20 of H3, 17 of 16S rDNA, 20 of 18S rDNA, and 17 of 28S rDNA) from four markers were generated in the present study and all were deposited in GenBank (Table 1).

Multiple sequence alignment of H3 sequences was conducted using Clustal W (Thompson et al., 1997) implemented in MEGA11 software (Tamura et al., 2021). This alignment was checked based on amino acid sequences. Ribosomal markers (16S, 18S, and 28S) were aligned using the Q-INS-i algorithm of alignment of MAFFT (Kuraku et al., 2013; Katoh et al., 2019).

5.3.4. Phylogenetic analyses

Phylogenetic analyses were conducted under two optimality criteria: maximum likelihood (ML) and Bayesian inference (BI). The concatenated marker dataset was combined in Sequence Matrix (Vaidya et al., 2011) and initially partitioned by marker and codon (for histone H3).

Appropriate partitioning and substitution models of the dataset were selected by BIC with ModelFinder (Kalyaanamoorthy et al., 2017) using IQ-TREE 2.2.0 (Minh et al., 2020). For probabilistic analyses conducted, partitions histone H3 codon 2 and codon 3 were merged, resulting in a total of five final partitions, each independently modeled by GTR+I+G.

Maximum likelihood analysis with 1000 ultrafast bootstrap replicates (UFBoot) (Hoang et al., 2017) and 1000 replicates for the SH-like approximate likelihood ratio test (SH-aLRT) (Guindon et al., 2010) was performed in IQ-TREE 2.2.0 (Minh et al., 2020).

Bayesian Inference (BI) analysis was conducted using the MrBayes v. 3.2.7a (Ronquist et al., 2012) in CIPRES Science Gateway online web server (Miller et al., 2010). To estimate the posterior probability of the clades, the [$(MC)^3$] (Metropolis Coupled Markov Chain Monte Carlo) algorithm was used. Data were analyzed in two simultaneous runs (Nruns=2) for 100 million generations (Ngen=100,000,000). For each generation, four MCMC chains were executed (Nchains=4), and 25% of the trees generated by the first cold chain were ignored (burnin=0.25). Independent runs convergence was assessed by the average standard deviation of split frequencies (<0.05) and parameter mixing by effective sample size (>200) for each free parameter in TRACER version 1.7.2 (Rambaut et al., 2018).

Resulting trees of the Bayesian inference and maximum likelihood analyses were visualized in the FigTree v1.4.4 program (Rambaut, 2018) and edited in Adobe Illustrator CS6. To indicate the high branch support of each node, the following were considered: PP > 0.90, SH-aLRT ≥ 80, and UFBoot ≥ 95.

5.3.5. Divergence times estimates

The dating analysis was carried out with BEAST2 (Bouckaert et al., 2019) on the CIPRES Science Gateway 3.3. (Miller et al., 2010) with 11 independent runs of 300M generations sampling every 30,000 generations and 12 independent runs of 500M generations sampling every 50,000 generations. After evaluating individual and

combinations of the sampled results in Tracer 1.7.2 (Rambaut et al., 2018), we selected to combine results of three independent runs (mean -lnL = 39610.681) of the 300M generation runs, because it was the combination that had the highest ESS values for the 91 sampled free parameters. Results (sampled parameters and trees) from independent runs were merged with LogCombiner 2.7.4 (Bouckaert et al., 2019) and the maximum credibility tree was calculated based on all 27,003 sampled trees excluding 10% of initial samples as burnin in TreeAnnotator 2.7.4 (Bouckaert et al., 2019). The tree was visualized in FigTree v1.4.4 (Rambaut, 2018) and edited in Adobe Illustrator CS6.

Divergence times were calculated with an optimized relaxed clock (Douglas et al., 2021) and tree prior following the birth–death model (Gernhard, 2008). All molecular markers had site and clock models unlinked, but linked trees. Each molecular partition was modeled by GTR+I+G4, as in previous analyses.

For node calibrations, we have selected five fossils from the more extensive analysis of Bucher et al., (2023), which follows Parham et al., (2012) about the best practices for justifying fossil calibrations. Ages of four fossils were used to calibrate the stem of their respective family using a log-normal distribution: (1) *Acixiites immodesta* Hamilton, 1990 (Achilidae) with estimated age of 125–113 Mya (log(mean)=2.5, log(Stdev)=1.1, and offset=113); (2) *Quizqueiplana alexbrowni* Bourgoin & Gnezdilov, 2015 (Caliscelidae) with estimated age of 20.44–15.97 Mya (log(mean)=1, log(Stdev)=1.0, and offset=16); (3) *Netutela annunciator* Emeljanov, 1983 (Dictyopharidae) with estimated age of 86.8–83.4 Mya (log(mean)=1, log(Stdev)=1.0, and offset=83.4); and (4) *Abraracourcix curvivenatus* Stroiński & Szwedo, 2011 (Ricaniidae) with estimated age of 56.8–54.4 Mya (log(mean)=1, log(Stdev)=0.2, and offset=55.4). In addition, the Fulgoromorpha node was calibrated with a normal distribution (log(mean)=412, log (Stdev)=20) with minimum age as the age of the fossil

†*Fulgoridiella raetica* Becker-Migdisova, 1962 dated from the Early Jurassic (199.6 Mya) and maximum age to 406 Mya as the median estimate the age of Insecta according to Misof et al., (2014).

Considering we were interested in the initial divergence of Achilixiidae, we have also constrained *Bebaiotes* to be monophyletic. Although the maximum likelihood tree of the present molecular data did not recover *Bebaiotes* as monophyletic, there was no contradicting strong statistical support. In another analysis, combining morphological data, *Bebaiotes* is supported as monophyletic with good statistical support (Viegas et al., in prep).

5.4. Results

5.4.1. Molecular analyses

Seventy-four sequences (17 sequences of 16S, twenty sequences of 18S, 17 sequences of 28S, and twenty sequences of H3) were newly generated from 15 Achilixiidae species and seven outgroup taxa and deposited in Genbank (Table 1). Maximum likelihood trees resulting of the analyses of individual markers are shown in Supplementary Figs. S1-S4). The concatenated data matrix was composed of 67 taxa and a final alignment of 4379 base pairs. Topologies recovered by the maximum likelihood analysis (Fig. 1, -lnL= 40210.5464) and Bayesian analysis (Supplementary Fig. S5) were mostly similar. The resulting phylogeny of Fulgoromorpha showed three main clades (Fig. 1, clades A-C).

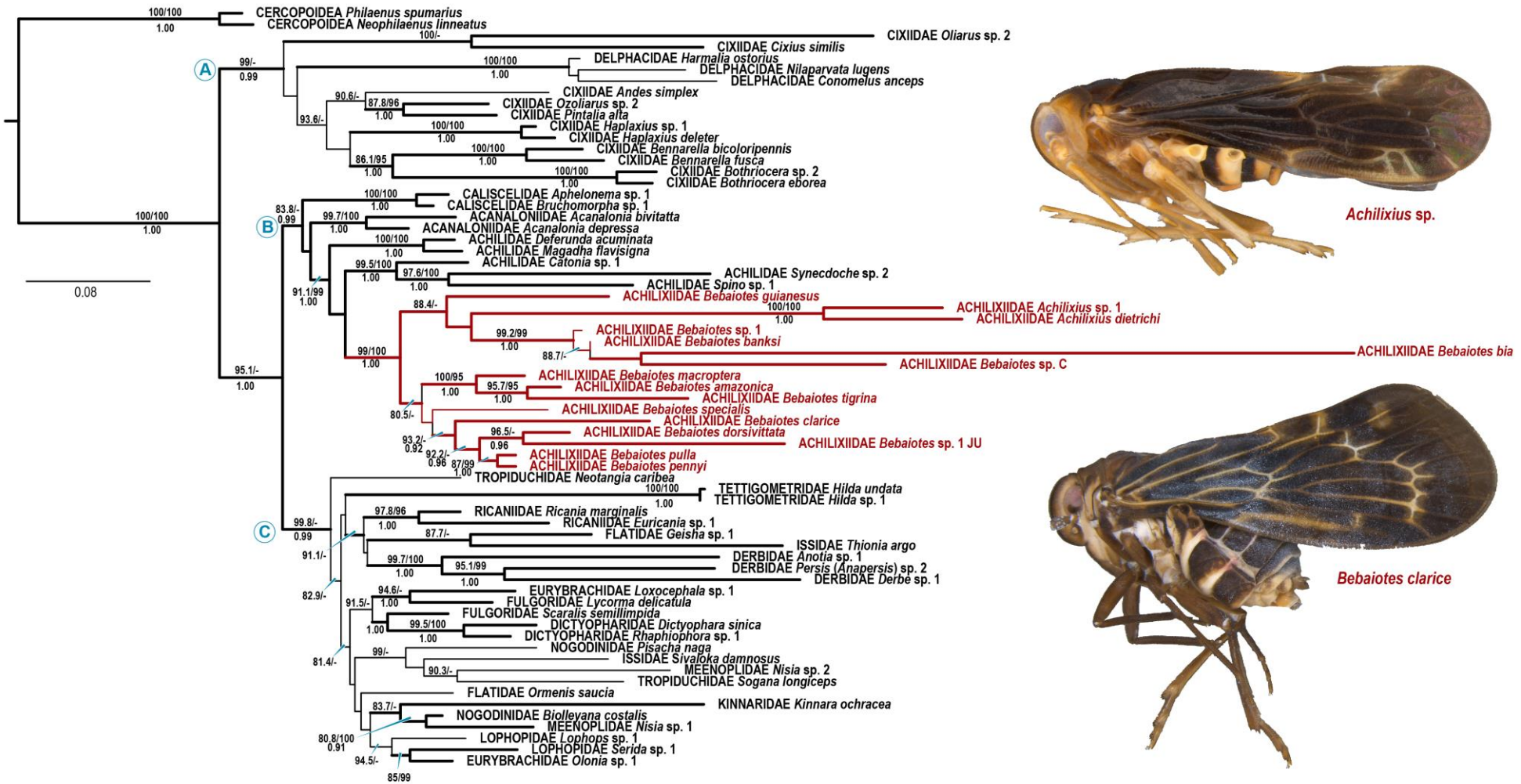

Fig. 1. Maximum likelihood tree of Achilixiidae and outgroups based on 4,379 bp of 16S, 18S, 28S, and H3 (-lnL= 40210.5464). Thickened branches are those also recovered in the Bayesian inference analysis. Values above branches are likelihood SH-aLRT / ultrafast bootstrap and below are Bayesian posterior probabilities (in percentages). We only show support values PP > 0.90, SH-aLRT ≥ 80 and UFBoot ≥ 95.

298 The first clade (Fig. 1 clade A) was recovered with high support (SH-aLRT = 99
299 and PP = 0.99) in both analyses as the sister clade to remaining families of Fulgoromorpha
300 and was formed only by representatives of "Cixiidae" and Delphacidae.
301 The second clade (Fig. 1 clade B) was recovered with high support (SH-aLRT =
302 83.8 and PP = 0.99) in both analyses and included the following relationships:
303 (((Caliscelidae + (Acanaloniidae + ("Achilidae" + ("Achilidae" + Achilixiidae))). It is
304 noteworthy that "Achilidae" was recovered as paraphyletic in relation to Achilixiidae,
305 which was recovered as sister to a clade containing the genera *Catonia*, *Synecdoche*, and
306 *Spino*, but this relationship had low support (PP < 0.90). However, "Achilidae" in part +
307 Achilixiidae was recovered with high support (SH-aLRT = 91.1, UFBoot = 99 and PP =
308 1.00). Our analyses confirmed the monophyly of Achilixiidae with high support (SH-
309 aLRT = 99, UFBoot = 100 and PP = 1.00), however, surprisingly, *Bebaiotes* was
310 recovered as paraphyletic with respect to *Achilixius*, but this relationship had low support
311 (PP < 0.90).
312 The third clade (Fig. 1 clade C) was also recovered with high support (SH-aLRT =
313 99.8 and PP = 0.99) in both analyses and included the following families:
314 "Tropiduchidae", Tettigometridae, Ricaniidae, "Flatidae", "Issidae", Derbidae,
315 "Eurybrachidae", "Fulgoridae", Dictyopharidae, "Nogodinidae", "Meenoplidae",
316 Kinnaridae, and "Lophopidae". However, most relationships among terminals of this
317 clade were not congruent between MV and IB analyses and had low clade support.
318

319 **5.4.2. Dating analysis**

320

321 We estimated for the first time the time scale of the evolution of Achilixiidae (Fig.
322 2). According to our analysis, the Achilixiidae ancestor diverged from the ancestor of

Achilidae at around 240.20 Mya (95% of high posterior density (HPD): 180.65-302.53 Mya) and the initial divergence of the lineages that constitute the former family today occurred during the Triassic, around 209.62 Mya (95% of high posterior density (HPD): 158.29-267.61 Mya) (Fig. 2, Supplementary Table S1). The initial divergence of *Bebaiotes* current species into two main lineages occurred during the Jurassic around 176.52 Mya (95% of high posterior density (HPD): 131.68-224.72 Mya) while the initial divergence of *Achilixius* current species occurred much more recently during the Cretaceous around 82.74 Mya (95% of high posterior density (HPD): 42.90-132.02 Mya) (Fig. 3, Supplementary Table S1).

Divergence time estimates for the whole Fulgoromorpha are shown in Fig. 2, and age estimates of most relevant clades are summarized in Supplementary Table S1.

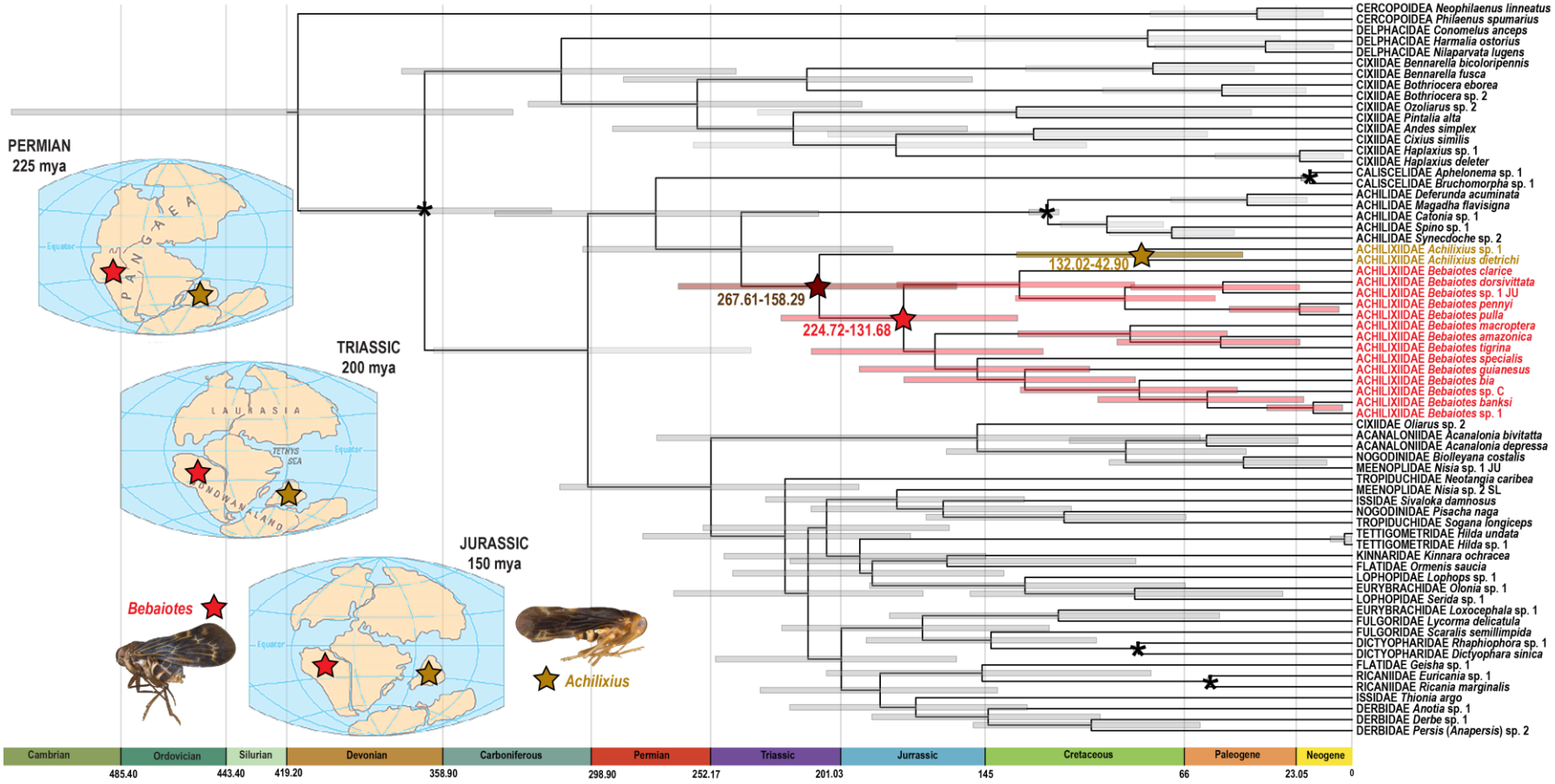

Fig. 2. Dated phylogenetic tree of Achilixiidae (yellow *Achilixius* and red *Bebaiotes*) and other planthoppers. Chronogram based on the same concatenated dataset (67 taxa; 4 gene regions: 16S, 18S, 28S, and H3), using unlinked substitution models (GTR+I+G), uncorrelated lognormal relaxed clock, and five fossil calibration points (black asterisks at nodes). Horizontal bars correspond to the 95% highest posterior density (HPD) of each node age.

5.5. Discussion

5.5.1. Position of Achilixiidae in Fulgoromorpha

The closer relationship of Achilixiidae to representatives of Achilidae found herein and in Bucher et al. (2023), was not consistently recovered in previous molecular phylogenetic hypotheses (Urban & Cryan, 2007, Song & Liang, 2013). However, this close relationship was previously suggested by Fennah (1947), Asche (1987) and Wilson (1989) based mainly on morphological characteristics of the clavus and female genitalia. The paraphyly of Achilidae in relation to Achilixiidae thoroughly corroborates Emeljanov's (1991) classification in treating the two achilixiid genera within Achilidae. It is also important to emphasize that few other authors suggested a close relationship of Achilixiidae to Cixiidae, based on the morphology of the antennal sensilla (Liang, 2001) or because of the presence of abdominal processes, such as those found in cixiid tribes Bennini and Bennarellini (Metcalf, 1945). This position was never corroborated in previous robustly sampled phylogenetic analyses of whole Fulgoromorpha (Urban & Cryan, 2007; Bucher et al., 2023) or herein, where Cixiidae is usually found strongly related to Delphacidae (Fig. 2, Clade A) forming a clade that is sister to the remaining planthoppers. Nonetheless, the tribes Bennini and Benarellini were not included in published molecular phylogenies, except for an unidentified Bennini terminal in Bucher et al., (2023) and the two *Bennarella* species sampled here for the first time.

5.5.2. Paraphyly of Achilidae and the sister group of Achilixiidae

All previous molecular phylogenetic studies that recovered the close relationship of Achilixiidae and Achilidae, recovered the former as related to representatives of the Plectoderini (Song & Liang, 2013; Bucher et al., 2023), a diverse tribe with 353 species in 99 genera worldwide distributed (Bourgoin, 2023). Song & Liang's (2013) Fulgoromorpha phylogeny based on markers 16S rDNA, 18S rDNA, 28S rDNA, and cytb recovered *Bebaiotes* in the Bayesian inference analysis as a sister of a clade composed by *Defuranda* Distant, 1912 and *Magadha* Distant, 1906, the only Achilidae sampled, without statistical support. It is important to highlight that none of these genera have records for the Neotropical region to date. *Defuranda* has a distribution that covers the Oriental, Palearctic and Australian regions (Long et al., 2013), while the genus *Magadha* has records only from China, India, and Sri Lanka (Bourgoin, 2023).

However, in the phylogenetic proposal of Bucher et al., (2023) *Bebaiotes* was recovered as sister to *Spino* Fennah, 1950, with high clade support value (UFBS = 100), and, furthermore, *Catonia* Uhler, 1895 was recovered as the sister group of this clade. It is interesting to note that sequences of *Catonia* and *Spino,* as well as of *Bebaiotes*, used by Bucher et al., (2023) were generated by Urban & Cryan (2007), but analyses by the latter authors did not find the close relationship of Achilixiidae and Achilidae, showing an increase in robustness of the phylogenetic hypothesis because of the increase in taxon sampling.

In the present study, Achilixiidae was recovered as a sister group of a clade containing *Catonia*, *Spino*, and an unidentified *Synecdoche*. The unidentified *Synecdoche* was included here and collected in Minas Gerais State, Southeastern Brazil, although the 22 species of the genus so far are known only from North America. Present results highlight the inadequate taxonomic knowledge of South American fulgoromorphs, which

certainly need to be studied to fill in the evolutionary gaps of the Fulgoromorpha phylogeny.

5.5.3. Monophyly of Achilixiidae and evolution of abdominal processes

There are few studies with sequence data that report the position of Achilixiidae in the Fulgoromorpha in a comprehensive way (Urban & Cryan, 2007; Song & Liang, 2013; Bucher et al., 2023). However, all these studies used the same sequences from a single unidentified female *Bebaiotes* specimen voucher generated by Urban & Cryan (2007). Thus, the family's monophyly was never tested.

Emeljanov (1991) questioned the family's monophyly and proposed that the two achilixiid genera should represent distinct subfamilies of Achilidae, mainly because he envisioned them as not related due to distinct wing venation and convergent origin of abdominal processes. Although the presence of lateral abdominal processes is a striking characteristic of the family, they differ substantially morphologically between the two genera, while both genera have paired processes deriving from the third abdominal segment, in *Bebaiotes* each process shows three sensory pits, while in *Achilixius* it shows two, in addition to *Achilixius* having an additional pair of processes deriving from the fifth abdominal segment (Wilson, 1989).

Similarly occurred with cixiid representatives with abdominal processes. Bennarellini was erected by Emeljanov (1989) based on genera previously included in Bennini and currently includes South and Central American cixiids with abdominal processes (Holzinger & Kunz, 2006, Holzinger et al., 2013, Viegas et al., 2021). This separation was primarily based on the morphology of the abdominal processes, which Hoch (1987) did not consider homologous. Neotropical cixiids (Bennarellini) have

411 plate-shaped paired processes derived from the fourth and fifth abdominal segments,
412 while Oriental cixiids (Bennini) have paired elongate, rod-like, articulated appendages
413 derived from the third and fourth abdominal segments. The Bennini abdominal articulated
414 appendages (called LASSO) are unique in insects and are remarkable complex sensory
415 and secretory structures (Hoch et al., 2104).

416 So far, no phylogenetic proposal tested either Achilixiidae or Bennini+Bennarellini
417 are monophyletic to understand the evolution of these abdominal processes. Herein we
418 have sampled for the first time a total of 15 achilixiid terminal species from both genera,
419 and under both reconstruction methods (maximum likelihood and Bayesian inference) the
420 monophyly of Achilixiidae is well supported. The monophyly of Achilixiidae supports
421 that at least the paired processes derived from the third abdominal segment are a
422 synapomorphy of Achilixiidae. Furthermore, this is the first study that sampled
423 Bennarellini species, and our results places them well nested within Cixiidae (as sister to
424 Bothriocerini), showing that, at least, Bennarellini processes do not seem to be
425 homologous to Achilixiidae ones.

426 Present results, however, recovered *Bebaiotes* as paraphyletic in relation to
427 *Achilixius*, although internal relationships supporting this paraphyly are not statistically
428 sound. We believe that the molecular marker sampling was not adequate to resolve most
429 internal relationships of Achilixiidae and that taxon sampling was unequal, thus biased,
430 as we only had available two specimens of *Achilixius*. Furthermore, a combined
431 morphological and molecular phylogenetic study is currently being conducted, and
432 preliminary results strongly support monophyly of both genera (Viegas et al., in prep.).
433 Nevertheless, strong morphological and geographical evidence supports these two genera
434 as distinct. *Achilixius* can be distinguished from *Bebaiotes* by the following set of
435 characters: frons with median longitudinal carina (absent in *Bebaiotes*); gena without

subantennal carina (present in *Bebaiotes*); lateral carinae of pronotum strongly diverging towards the tegula (gently diverging or subparallel in *Bebaiotes*); sternite III with pair of abdominal processes, each with two sensory pits (three pits in *Bebaiotes*); sternite V with pair of abdominal processes (absent in *Bebaiotes*); RP vein of the forewing branched (unbranched in *Bebaiotes*); icua crossvein of the forewing absent (present in *Bebaiotes*); and phallic complex without internal sclerotized plates (present in *Bebaiotes*). Until now, there have only been records of *Achilixius* in the Oriental region, including the Philippines, Sulawesi, and Sabah (Wilson, 1989, Viegas & Ale-Rocha, 2023), while *Bebaiotes* is limited to Central America and northern South America. Given the morphological distinctiveness and disjunct geographical distribution, we refrain at the moment to propose any nomenclatural changes at genus-level or contest *Bebaiotes* monophyly.

5.5.4. Historical processes associated with the divergence of the Achilixiidae

Present divergence time estimates suggest that the initial divergence of Achilixiidae () occurred sometime during the Triassic through the Jurassic, a period in which the Gondwana breakup started (Reeves & de Wit, 2000; Muir et al., 2020).

The fragmentation of Gondwana began approximately at the end of the Neoproterozoic period, around 600 million years ago (Stampfli et al., 2013). Events such as the closure of the Mozambique Ocean, resulted in the separation of East Gondwana (Australia, Antarctica, India, Madagascar, and Arabia) from West Gondwana (Africa and South America), mark the final separation of Gondwana (Cawood & Buchan, 2007). This separation had a significant impact on the history of life on Earth, as it allowed different groups of organisms to evolve in isolation in

different regions over time (McLoughlin, 2001; Brown & Lomolino, 2006). Thus, vicariance by continental drift may have played a major role in the separation of ancestral lineages of the Oriental *Achilixius* and Neotropical *Bebaiotes*.

Regarding the age of diversification of the genera of Achilixiidae, we recovered that it happened in two distinct periods, *Bebaiotes* diversifying in the Early Jurassic at 176.36 Mya, while *Achilixius* started diversifying much later in the Early Cretaceous at 82.57 Mya. These distinct periods of time present intriguing biogeographical implications and the later diversification of *Achilixius* in the Malay archipelago is consistent with its geological history considering that *Achilixius* is currently restricted to Sabah, Sulawesi, and the Philippines, and its ancestor diverged from the *Bebaiotes* ancestor due to the breakup of Gondwana, most likely this ancestor was restricted to the Argo and/or Banda (and inner Banda) fragments that started to drift off from Gondwana at 155 Mya and docked at Sundaland (core of Southeast Asia) at around 90-85 Mya (Hall, 2012, 2014). Subsequent major tectonic events during the Cenozoic (Hall, 2002), especially the formation of the Luzon arc system, certainly played a role in *Achilixius* diversification in the Malay archipelago. Nevertheless, we should be cautious with these results, provided that present taxon sampling was very limited in *Achilixius*.

5.6. Conclusions

In conclusion, although the two genera of Achilixiidae have disjunct distributions and show many morphological differences, they share an exclusive common ancestor and form a unique branch within the infraorder Fulgoromorpha. The molecular data gathered allowed a deeper understanding of

the evolutionary history of these insects for the first time, highlighting their genetic and evolutionary connections.

Furthermore, the investigation of the temporal origins of the Achilixiidae revealed remarkable patterns. The main split of the Achilixiidae ancestor that led to the generic lineages occurred sometime during the Triassic through the Jurassic, probably through a vicariant event related to the Gondwana breakup. Furthermore, initial divergences of *Bebaiotes* in South America occurred in the Early Jurassic at around 176 Mya, while *Achilixius* started diversifying much later in the Early Cretaceous at around 83 Mya. This later diversification of *Achilixius* in the Malay Archipelago is consistent with its geological history. These discoveries highlight the gradual diversification of this family over geological time and provide valuable insights into the evolutionary processes that shaped this family's history.

However, it is essential to recognize that knowledge is constantly evolving, and new studies can bring even more details and changes to the understanding of the history of Achilixiidae. We emphasize that the combination of molecular data with information from fossils and morphological analyses will open new horizons in the investigation of the evolutionary secrets not only of this group but may also contribute to a broader understanding of the diversity and adaptation of different forms of life over the geological ages.

5.7. Acknowledgments

We thank curators Dr. M. L. Oliveira (INPA), Dr. R. R. Cavichioli (DZUP), and R. L. Ferreira (UFLA) for loaning part of specimens studied. The first author would like to thank André Antunes, Clayton Gonçalves, Nathalia Pecly, Jádila Prando, Luana Barros,

Sandra Duque, Maria Rozo, and all friends of Laboratório de Diptera (INPA) and Laboratório de Entomologia (UFRJ) for all the help provided. Coordenação de Aperfeiçoamento de Pessoal de Nível Superior (CAPES) provided EFGV with a doctoral scholarship. RAR and DMT are research productivity fellows from Conselho Nacional de Desenvolvimento Científico e Tecnológico (CNPq, Procs. 312351/2021-6 and 314557/2021-0) and DMT is also a Cientista do Nosso Estado fellow from Fundação Carlos Chagas Filho de Amparo à Pesquisa do Estado do Rio de Janeiro (FAPERJ, Proc. E-26/200.503/2023). This study was also in part financed by Fundação de Amparo à Pesquisa do Estado do Amazonas (FAPEAM, POSGRAD).

5.8. References

Asche, M. 1987. Preliminary thoughts on the phylogeny of Fulgoromorpha (Homoptera: Auchenorrhyncha). In: Proceedings of the 6th Auchenorrhyncha Meeting, Turin, Italy, 7th–11th September, 47–53.

Becker-Migdisova, E.E., 1962. Some new Hemiptera and Psocoptera. Paleontol. Zh. 1, 89–104.

Bouckaert, R., Vaughan, T.G., Barido-Sottani, J., Duchêne, S., Fourment, M., Gavryushkina, A., Heled, J., Jones, G, Kuhnert, D., Maio, N.de, Matschiner, M., Mendes, F.K., Muller, N.F., Ogilvie, H.A., Plessis, L.du, Popinga, A., Rambaut, A., Rasmussen, D., Siveroni, I., Suchard, M.A., Wu, C., Xie, D., Zhang, C., Stadler, T., Drummond. A.J., 2019. BEAST 2.5: An advanced software platform for Bayesian evolutionary analysis. PLoS Comput. Biol. 154: e1006650. https://doi.org/10.1371/journal.pcbi.1006650.

Bourgoin, T., 1993. Female genitalia in Hemiptera Fulgoromorpha, morphological and phylogenetic data. Ann. Soc. Entomol. Fr. 29 (3), 225–244. https://doi.org/10.1080/21686351.1993.12277686.

Bourgoin, T. 2023. FLOW (Fulgoromorpha Lists on The Web): a world knowledge base dedicated to Fulgoromorpha. Version 8, updated [10-06-2023] accessed 13 October 2003). https://flow. hemiptera-databases.org/flow/.

Bourgoin, T., Wang, R.R., Gnezdilov, V.M., 2015. First fossil record of Caliscelidae (Hemiptera: Fulgoroidea): a new Early Miocene Dominican amber genus extends the distribution of Augilini to the Neotropics. J. Syst. Palaeontol. 14 (3), 211–218. https://doi.org/10.1080/14772019.2015.1032376.

Brown, J.H., Lomolino, M.V., 2006. Biogeografia. FUNPEC – editora, 2ºed, p. 692.

Bucher, M., Condamine, F.L., Luo, Y., Wang, M., Bourgoin, T., 2023. Phylogeny and diversification of planthoppers Hemiptera Fulgoromorpha based on a comprehensive molecular dataset and large taxon sampling. Mol. Phylogenet. Evol. 186, 107862. https://doi.org/10.1016/j.ympev.2023.107862.

Cawood, P.A., Buchan, C., 2007. Linking accretionary orogenesis with supercontinent assembly. Earth-Schi.Rev.82, 217e256.https://doi.org/10.1016/j.earscirev.2007.03 .003.

Ceotto, P., Bourgoin, T., 2008. Insights into the phylogenetic relationships within Cixiidae Hemiptera: Fulgoromorpha: cladistic analysis of a morphological dataset. Syst. Entomol. 333, 484–500. https://doi.org/10.1016 /j.ympev.2008.04.026.

Chen, S., Yang, C.T., 1995. The metatarsi of the Fulgoroidea Homoptera: Auchenorrhyncha. Chinese J. Entomol. 15, 257–269. https://doi.org/10.6660/TES FE.1995023.

559 Cryan, J.R., 2005. Molecular phylogeny of Cicadomorpha Insecta: Hemiptera:
560 Cicadoidea, Cercopoidea, and Membracoidea: adding evidence to the controversy.
561 Syst. Entomol. 30 (1), 563–574.
562 Cryan, J.R., Urban, J.M., 2012. Higher-level phylogeny of the insect order Hemiptera: is
563 Auchenorrhyncha really paraphyletic? Syst. Entomol. 37 (1), 7–21.
564 https://doi.org/10.1111/j.1365-3113.2011.00611.x.
565 Douglas J., Zhang R., Bouckaert, R., 2021. Adaptive dating and fast proposals: Revisiting
566 the phylogenetic relaxed clock model. PLoS Comput. Biol. 172: e1008322.
567 https://doi.org/10.1371/journal.pcbi.1008322.
568 Emeljanov, A.F., 1983. Nosatka iz mela Taïmyra Insecta, Homoptera. Paleontol. Zh. 3,
569 79–85.
570 Emeljanov, A.F., 1989. To the problem of division of the family Cixiidae (Homoptera,
571 Cicadina). Entomol. Obozr. 68 (1), 93–106. [in Russian. English translation:
572 Entomol. Rev. 68 (4), 54–67.]
573 Emeljanov, A.F., 1990. An attempt of construction of the phylogenetic tree of the
574 planthoppers (Homoptera, Cicadina). Entomol. Rev. 69 (2), 353–356.
575 Emeljanov, A.F., 1991. Toward the problem of the limits and subdivisions of Achilidae
576 Homoptera, Cicadina*. Entomol. Obozr. 70, 373–393.
577 Fennah, R.G., 1947. A synopsis of the Achilixiidae of the New World Homoptera:
578 Fulgoroidea. Ann. Mag. Nat. Hist. 11 (13): 183–191.
579 Gernhard, T., 2008. The conditioned reconstructed process. J. Theor. Biol. 253 (4), 769-
580 778. https://doi.org/10.1016/j.jtbi.2008.04.005.
581 Guindon, S., Dufayard, J. F., Lefort, V., Anisimova, M., Hordijk, W., Gascuel, O., 2010.
582 New algorithms and methods to estimate maximum-likelihood phylogenies:

583 assessing the performance of PhyML 3.0. Syst. Biol. 59 (3), 307–321.
584 https://doi.org/10.1093/sysbio/syq010.
585 Hamilton, K.G.A., 1990. Chapter 6. Homoptera. In: Grimaldi, D.A. (ed). Insecta from the
586 Santana formation, lower Cretaceous, of Brazil. Bull. Am. Mus. Nat. Hist. 195, pp.
587 82–122.
588 Hall, R. 2002. Cenozoic geological and plate tectonic evolution of SE Asia and the SW
589 Pacific: computer-based reconstructions, model and animations. J. Asian Earth Sci.
590 20 (4), 353–431. https://doi.org/10.1016/S1367-9120(01)00069-4.
591 Hall, R., 2012. Late Jurassic-Cenozoic reconstructions of the Indonesian region and the
592 Indian Ocean. Tectonophysics. 570–571, 1–41. http://dx.doi.org/10.1016/j.tecto.
593 2012.04.021.
594 Hall, R., 2014. The origin of Sundaland. In: Proceedings Of Sundaland Resources
595 Annual Convention. pp. 17–18.
596 Hoang, D.T., Chernomor, O., Von Haeseler, A., Minh, B.Q., Vinh, L.S., 2017. UFBoot2:
597 improving the ultrafast bootstrap approximation. Mol. Biol. Evol. 35 (2), 518–522.
598 https://doi.org/10.1093/molbev/msx281.
599 Hoch, H. 1987. The tribe Bennini - a monophyletic group within the Cixiidae
600 (Homoptera, Fulgoroidea). In: Proceedings of the 6th Auchenorrhyncha Meeting,
601 Turin, Italy, 7–11, 55–57.
602 Hoch, H., Wessel, A., Asche, M., Baum, D., Beckmann, F., Bräunig, P., Ehrig, K.,
603 Mühlethaler, R., Riesemeier, H., Staude, A., Stelbrink, B., Wachmann, E.,
604 Weintraub, P., Wipfler, B., Wolff, C., Zilch, M., 2014. Non-sexual abdominal
605 appendages in adult insects challenge a 300 million year old Bauplan. Curr. Biol.
606 24 (1), 16–17. https://doi.org/10.1016/j.cub.2013.11.040.

607 Holzinger, W.E. & Kunz, G. (2006) A new genus and species of Bennarellini form Costa
608 Rica (Hemiptera: Fulgoromorpha: Cixiidae). Zootaxa. 1353 (1), 53–61.
609 https://doi.org/10.11646/zootaxa.1353.1.3
610 Holzinger, W.E., Holzinger, I., Egger, J., 2013. A new genus, Loisirella, and two new
611 species of Bennarellini from Ecuador (Hemiptera: Auchenorrhyncha:
612 Fulgoromorpha: Cixiidae). Acta Musei Moraviae, Sci. Biol. 98 (2), 143–153.
613 Huelsenbeck, J. P., Bull, J. J., Cunningham, C. W., 1996. Combining data in phylogenetic
614 analysis. Trends Ecol. Evol. 11 (4), 152–158. https://doi.org/10.1016/0169-
615 5347(96)10006-9
616 Kalyaanamoorthy, S., Minh, B. Q., Wong, T. K., Von Haeseler, A., Jermiin, L. S., 2017.
617 ModelFinder: fast model selection for accurate phylogenetic estimates. Nat.
618 Methods. 14 (6), 587–589. https://doi.org/10.1038/nmeth.4285.
619 Katoh, K., Rozewicki, J. Yamada, K.D., 2019. MAFFT online service: multiple sequence
620 alignment, interactive sequence choice and visualization. Brief. Bioinform. 20 (4),
621 1160–1166. https://doi.org/10.1093/bib/bbx108.
622 Kearse, M., Moir, R., Wilson, A., Stones-Havas, S., Cheung, M., Sturrock, S.,
623 Drummond, A., 2012. Geneious Basic: An integrated and extendable desktop
624 software platform for the organization and analysis of sequence data.
625 Bioinformatics. 28 (12), 1647–1649. https://doi.org/10.1093/bioinformatics/bts
626 199.
627 Kuraku, S., Zmasek, C.M., Nishimura, O., Katoh, K., 2013. aLeaves facilitates on-
628 demand exploration of metazoan gene family trees on MAFFT sequence alignment
629 server with enhanced interactivity. Nucleic Acids Res. 41 (W1), W22–W28.
630 https://doi.org/10.1093/nar/gkt389.

631 Liang A.P., 2001. Morphology of antennal sensilla in *Achilixius sandakanensis* Muir
632 Hemiptera: Fulgoromorpha: Achilixiidae with comments on the phylogenetic
633 position of the Achilixiidae. Raff. Bull. Zool. 49 (2), 221–225.
634 Long, J. k., Yang, L., Xiang-Sheng, C., 2013. Review of the Chinese species of Deferunda
635 (Hemiptera: Fulgoromorpha: Achilidae) with descriptions of two new species. Fla.
636 Entomol. 96 (4), 1263–1273. http://dx.doi.org/10.1653/024.096
637 .0404.
638 McLoughlin, S., 2001. The breakup history of Gondwana and its impact on pre-Cenozoic
639 floristic provincialism. Aust. J. Bot. 49 (3), 271–300.
640 Melichar, L., 1914. Neue Fulgoriden von den Philippinen: I. Theil. Philipp. J. Sci. 9 (3),
641 269–285.
642 Metcalf, Z. P., 1938. The Fulgorina of Barro Colorado and other parts of Panama. Bull.
643 Mus. Comp. Zool. Harv. 82, 275–423.
644 Metcalf Z. P., 1945. Part 5. Achilixiidae. In: Metcalf Z. P. 1954 - General Catalogue of
645 the Homoptera. Fascicule IV, North Carolina State College, Raleigh (United States
646 of America). p. 213–218.
647 Miller, M.A., Pfeiffer, W., Schwartz, T., 2010. Creating the CIPRES Science Gateway
648 for inference of large phylogenetic trees. In: Proceedings of the Gateway
649 Computing Environments Workshop (GCE). New Orleans, LA. p. 1–8.
650 https://doi.org/10.1109/GCE.2010.5676129.
651 Minh, B.Q., Schmidt, H.A., Chernomor, O., Schrempf, D., Woodhams, M.D., Von
652 Haeseler, A., Lanfear, R., 2020. IQ-TREE 2: new models and efficient methods for
653 phylogenetic inference in the genomic era. Mol. Biol. Evol. 37 (5), 1530–1534.
654 https://doi.org/10.1093/molbev/msaa015.
655 Misof, B., Liu, S., Meusemann, K., Peters, R.S., Donath, A., Mayer, C., Frandsen, P.B.,

Ware, J., Flouri, T., Beutel, R.G., Niehuis, O., Petersen, M., Izquierdo-Carrasco, F., Wappler, T., Rust, J., Aberer, A.J., Aspöck, U., Aspöck, H., Bartel, D., Zhou, X., 2014. Phylogenomics resolves the timing and pattern of insect evolution. Science. 346 (6210), 763–767. https://doi.org/10.1126/science.1257570.

Muir, F., 1923. *Achilixius*, a new genus. Constituting a new family of the Fulgoroidea Homoptera. Philipp. J. Sci. 22, 483–487.

Muir, F., 1924. A new genus of the family Achilixiidae (Homoptera). Can. Entomol. 56, 33–34.

Muir, R.A., Bordy, E.M., Mundil, R., Frei, D., 2020. Recalibrating the breakup history of SW Gondwana: U–Pb radioisotopic age constraints from the southern Cape of South Africa. Gondwana Res. 84, 177–193.

Parham, J.F., Donoghue, P.C.J., Bell, C.J., Calway, T.D., Head, J.J., Holroyd, P.A., Inoue, J.G., Irmis, R.B., Joyce, W.G., Ksepka, D.T., Patané, J.S.L., Smith, N.D., Tarver, J.E., van Tuinen, M., Yang, Z., Angielczyk, K.D., Greenwood, J.M., Hipsley, C.A., Jacobs, L., Benton, M.J., 2012. Best practices for justifying fossil calibrations. Syst. Biol. 61 (2), 346–359. https://doi.org/10.1093/sysbio/syr107.

Rambaut, A., 2018. FigTree v.1.4.4. [accessed 20 August 2022]. Available em: http://tree.bio.ed.ac.uk/software/figtree

Rambaut, A., Drummond, A. J., Xie, D., Baele, G., Suchard, M.A., 2018. Posterior summarization in Bayesian phylogenetics using Tracer 1.7. Syst. Bio. 675, 901–904. https://doi.org/10.1093/sysbio/syy032.

Reeves, C., De Wit, M., 2000. Making ends meet in Gondwana: retracing the transforms of the Indian Ocean and reconnecting continental shear zones. Terra Nova. 12 (6), 272–280. https://doi.org/10.1046/j.1365-3121.2000.00309.x.

Ronquist, F., Teslenko, M., var der Mark, P., Ayres, D.L., Darling, A., Höhna, S.,

Larget, B., Liu, L., Suchard, M.A., Huelsenbeck, J.P., 2012. MrBayes 3.2: Efficient Bayesian phylogenetic inference and model choice across a large model space. Syst. Bio. 61 (3), 539–542. https://doi.org/10.1093/sysbio/sys029.

Song, N., Liang, A.P., 2013. A preliminary molecular phylogeny of planthoppers (Hemiptera: Fulgoroidea) based on nuclear and mitochondrial DNA sequences. PLoS One. 8 (3), e58400. https://doi.org/10.1371/journal.pone.0058400.

Stampfli, G. M., Hochard, C., Vérard, C., Wilhem, C., 2013. The formation of Pangea. Tectonophysics. 593, 1–19. https://doi.org/10.1016/j.tecto.2013.02.037.

Stroiński, A., Szwedo, J., 2011. Abraracourcix curvivenatus n. gen. n. sp. from the Lowermost Eocene Oise amber Hemiptera: Fulgoromorpha: Ricaniidae. In: Ann. Soc. Entomol. Fr. 47 (3–4), 480–486. https://doi.org/10.1080/00379271. 2011.10697739.

Tamura, K., Stecher, G., Kumar, S., 2021. MEGA11: Molecular Evolutionary Genetics Analysis Version 11. Mol. Biol. Evol. 38 (7), 3022–3027. https://doi.org/10.1093/ molbev/msab120.

Thompson, J.D., Gibson, T.J., Plewniak, F., Jeanmougin, F., Higgins, D.G., 1997. The ClustalX windows interface: flexible strategies for multiple sequence alignment aided by quality analysis tools. Nucleic Acids Res. 25 (24), 4876–4882.

Urban, J.M., Cryan, J.R., 2007. Evolution of the planthoppers (Insecta: hemiptera: Fulgoroidea). Mol. Phylogenet. Evol. 42 (2), 556–572. https://doi.org/ 10.1016/j.ympev.2006.08.009.

Urban, J.M., Cryan, J.R., 2009. Entomologically famous, evolutionarily unexplored: the first phylogeny of the lanternfly family Fulgoridae (Insecta: Hemiptera: Fulgoroidea). Mol. Phylogenet. Evol. 50 (3), 471–484. https://doi.org/10.1016/j. ympev.2008.12.004.

706 Urban, J.M., Bartlett, C.R., Cryan, J.R., 2010. Evolution of Delphacidae (Hemiptera:
707 Fulgoroidea): combined-evidence phylogenetics reveals importance of grass host
708 shifts. Syst. Entomol. 35 (4), 678–691. https://doi.org/10.1111/j.1365-
709 3113.2010.00539.x.
710 Vaidya, G., Lohman, D.J., Meier, R., 2011. SequenceMatrix: concatenation software for
711 the fast assembly of multi-gene datasets with character set and codon information.
712 Cladistics. 27 (2), 171–180.https://doi.org/10.1111/j.1096-0031.2010.00329.x.
713 Viegas E.F.G., Ale-Rocha, R., Takiya, D.M., 2021. First record of Loisirella Holzinger,
714 Holzinger & Egger, 2013 and description of a new species from Brazil (Hemiptera:
715 Fulgoromorpha: Cixiidae). Zootaxa, 5072 (1), 88–94. https://doi.
716 org/10.11646/zootaxa.5072.1.10.
717 Viegas, E.F.G., Ale-Rocha, R. (Submitted). A century of Achilixiidae Muir, 1923
718 Hemiptera: Auchenorrhyncha: Fulgoroidea: taxonomic study of the genus
719 Bebaiotes Muir, 1924 and description of eight new species from Brazil. *Zootaxa*, in
720 review.
721 Viegas, E.F.G.,Takiya, D.M., Ale-Rocha, R. (in prep) Morphology-based phylogeny of
722 Achilixiidae (Hemiptera: Fulgoromorpha) with emphasis on the internal
723 relationships of Bebaiotes Muir, 1924.
724 Wilson, M.R., 1989. The planthopper family Achilixiidae Homoptera, Fulgoroidea: a
725 synopsis with a revision of the genus Achilixius. Syst. Entomol. 14 (4), 487–506.
726 https://doi.org/10.1111/j.1365-3113.1989.tb00299.x.
727 Yeh, W.B., Yang, C.T., Hui, C.F., 2005. A Molecular phylogeny of planthoppers
728 (Hemiptera: fulgoroidea) inferred from mitochondrial 16S rDNA sequences. Zool.
729 Stud. 44 (4), 519–535.

730 Zahniser, J.N., Dietrich, C.H., 2010. Phylogeny of the leafhopper subfamily
731 Deltocephalinae Hemiptera: Cicadellidae based on molecular and morphological
732 data with a revised family-group classification. Syst. Entomol. 35 (3), 489–511.
733 https://doi.org/10.1111/j.1365-3113.2010.00522.
734

6. CAPÍTULO III

Viegas, E. F.G.; Takiya, D. M. & Ale-Rocha, R. Morphology-based phylogeny of Achilixiidae (Hemiptera: Fulgoromorpha) with emphasis on internal relationships of *Bebaiotes* Muir, 1924.

Manuscrito formatado para Zootaxa[1].

[1] JCR-2022 / Fator de impacto:1.026; Qualis biodiversidade: A4

MORPHOLOGY-BASED PHYLOGENY OF ACHILIXIIDAE (HEMIPTERA: FULGOROMORPHA) WITH EMPHASIS ON INTERNAL RELATIONSHIPS OF *BEBAIOTES* MUIR, 1924

Eduarda Fernanda Gomes Viegas[1*], Daniela Maeda Takiya[2], Rosaly Ale-Rocha[3]

[1*] Postgraduate Program in Entomology (PPG-Ent), Instituto Nacional de Pesquisas da Amazônia, Caixa Postal 2223, CEP 69080-971, Manaus, Amazonas, Brazil. Corresponding author: edwviegasgomes@gmail.com, ORCID: https://orcid.org/0000-0003-3349-5639

[2] Laboratório de Entomologia, Departamento de Zoologia, Instituto de Biologia, Universidade Federal do Rio de Janeiro, Rio de Janeiro, 21941-902, Rio de Janeiro, Brazil. Email: takiya@gmail.com, ORCID: https://orcid.org/0000-0002-6233-3615

[3] Coordenação de Biodiversidade, Instituto Nacional de Pesquisas da Amazônia, Caixa Postal 2223, CEP 69080-971, Manaus, Amazonas, Brasil. Email: alerocha@inpa.gov.br, ORCID: https://orcid.org/0000-0001-9874-9770

6.1. Abstract

Achilixiidae currently comprises 32 species and two genera, *Achilixius* and *Bebaiotes*, recorded from the Neotropical and Oriental regions, respectively. Since its elevation to family status, no specific phylogenetic studies have been carried out. Although it has been included in more comprehensive studies on the phylogenetic relationships of Fulgoromorpha, Achilixiidae has not have its monophyly tested including both genera and multiple species, in order to encompass all of its diversity. Therefore, objectives of this study were to test the monophyly of Achilixiidae, as well as of the currently accepted genera based on morphological characters. The data matrix was composed of 99

morphological characters (63 characters from general external morphology, while 16 are from female, and 20 from male terminalia) and 44 terminal species, nine being outgroups. A parsimony analysis resulted in 640 equally parsimonious trees (L=338, CI=0.42 and IR =0.71). Our result supports the monophyly of Achilixiidae with high clade support values (Bremer=7; Bootstrap=90) and eight non-homoplastic synapomorphies. Derbidae was recovered as paraphyletic, with *Anotia* sp. 2 and *Persis* (*Persis*) recovered as sister to Achilixiidae. This study represents an important advance in understanding the phylogenetic history of Achilixiidae.

Keywords. *Achilixius*; cladistic analysis**;** Fulgoroidea; Planthopper.

6.2. Introduction

Achilixiidae Muir, 1923 is one of the less diverse families within Fulgoroidea Latreille, 1807 and currently comprises 36 species distributed into two genera: *Achilixius* Muir, 1923 (16 species), recorded in the Oriental Region; and *Bebaiotes* Muir, 1924 (16 species), recorded in the Neotropical Region (Wilson, 1989; Viegas & Ale-Rocha, 2023).

Syntames tubulifer Melichar, 1914, was originally described in the family Derbidae, but Muir (1923) noticed significant differences of this species in relation to other members of Derbidae, such as the length of the apical rostrum article, which is longer than wide. When trying to relocate this species to another family, Muir (1923) observed that *S. tubulifer* shared some character states with representatives of Cixiidae and Achilidae, but had unique features that excluded it from both families. Hence, he established Achilixiidae to accommodate *S. tubulifer* and three other species with similar characteristics. Additionally, he designated *Achilixius singularis* Muir, 1923 as the type

819 species, and described another two species, *A. sandakanensis* Muir, 1923 and *A.*
820 *davaoensis* Muir, 1923.

821 The characteristics based on which the family was distinguished from other
822 planthopper families included: 1) vertex and frons curved in lateral view; 2) absence of a
823 median ocellus; 3) frons with complete median and lateral carinae; 4) forewings not
824 overlapping when at rest, maintaining a tectiform arrangement; and 5) sternites III and V
825 each with a pair of lateral processes (Muir, 1923).

826 *Bebaiotes* was the second genus of the family described by Muir (1924), who
827 described *Bebaiotes bucayensis* Muir, 1924 (type species) and *B. nigrigaster* Muir, 1924,
828 both from Ecuador, representing first records of the family in the Neotropical Region.
829 Muir (1934) subsequently included in the genus two additional species from Ecuador: *B.*
830 *pallidinervis* Muir, 1934 and *B. pulla* Muir, 1934, and Metcalf (1938) proposed the
831 monotypic genus *Muirilixius* for *Muirilixius banksi* (Metcalf, 1938) species from Panamá.

832 A taxonomic study on Achilixiidae from the New World was conducted by Fennah
833 (1947). In this study, two species were described in *Bebaiotes*: *B. dorsivittata* Fennah,
834 1947, from Ecuador, and *B. nivosa* Fennah, 1947, from Guyana. Additionally, one species
835 was included in *Muirilixius*, *M. guianesus* Fennah, 1947, collected in Guyana.
836 Furthermore, *B. nigrigaster* Muir, 1924 was transferred to *Muirilixius*.

837 After 66 years, Wilson (1989) conducted a revision of *Achilixius* and analyzed the
838 status of the genus based on morphology. As a result, he synonymized *Muirilixius* with
839 *Bebaiotes*. In this work, the following species were redescribed: *A. singularis* Muir, 1923,
840 and *A. tubulifer* (Melichar, 1914), both from the Philippines; *A. sandakanensis* Muir,
841 1923 from Malaysia; and *A. davaoensis* Muir, 1923 from the Philippines and Indonesia.
842 In addition, 12 new species were described by Wilson (1989): *A. danaumoati* Wilson,
843 1989, *A. fasciata* Wilson, 1989, *A. kolintangi* Wilson, 1989, *A. minahassae* Wilson, 1989,

844 *A. morowali* Wilson, 1989, *A. muajati* Wilson, 1989, and *A. torautensis* Wilson,
845 1989from Indonesia; *A. fennahi* Wilson, 1989 and *A. muiri* Wilson, 1989, both from
846 Malaysia; and *A. bakeri* Wilson, 1989, *A. irigae* Wilson, 1989, and *A. mayoyae* Wilson,
847 1989 from the Philippines.

848 Recently, Viegas & Ale-Rocha (2023, submitted) discovered eight species of
849 *Bebaiotes* in Brazil and revised and expanded the distribution of four previously described
850 species: *B. banksi* (Metcalf, 1938) (Brazil - Amazonas and Pará; Panama); *B. dorsivittata*
851 Fennah, 1947 (Brazil - Amapá, Amazonas, Pará, Rondônia, and Roraima; Ecuador; Peru);
852 *B. guianesus* (Fennah, 1947) (Brazil - Amazonas; Guiana); and *B. pulla* Muir, 1934
853 (Brazil - Acre and Amazonas; Ecuador).

854 There is so far no species-level phylogenetic study for Achilixiidae. The family has
855 only been included in more comprehensive studies of Fulgoroidea, in which only one
856 representative of *Bebaiotes* was used in molecular analyses, therefore, their family status
857 remains uncertain (Urban & Cryan 2007; Song & Liang 2013; Bucher et al. 2023).

858 The family status of Achilixiidae has been a subject of debate since its
859 establishment by Muir (1923). This is due to its representatives share characteristics with
860 some other families, while also possessing unique features. Among these similarities, the
861 presence of lateral abdominal processes, also found in Bennini (Cixiidae), generated
862 questions about their family status (Metcalf, 1945; Hoch, 1987), however, these doubts
863 have not been deeply investigated. Fennah (1947) also commented on these abdominal
864 processes in both families, but considered this character to have little phylogenetic
865 significance, suggesting that the emergence of these processes likely occurred
866 independently throughout the evolutionary history of the two families.

867 Asche (1987), based on morphological characters of Fulgoromorpha families and
868 male and female terminalia, recovered Achilixiidae and Achilidae in proximity due to the

similarity in the function of the female terminalia, whose function is to excavate, rather than drill. However, Asche did not delve into this result, leaving uncertainty regarding the relationship between these families.

In Wilson's work (1989), based on morphology, the author questioned the homologous nature of achilixiid abdominal processes, not considering them homologous because there are two pairs of processes in *Achilixius*, while in *Bebaiotes* there is only one pair of processes. This suggests the need for further studies to define relationships between these genera.

Based on external morphology and male terminalia, Emeljanov (1991) disagreed with the family status of Achilixiidae and proposed subfamilies Bebaiotinae and Achilixiinae as belonging to the Achilidae. In contrast, Liang (2001) studied the morphology of the antennal sensilla of *Achilixius sandakanensis* and concluded that the flagellar process was a synapomorphy of Achilixiidae and Cixiidae, suggesting the transfer of the subfamilies Bebaiotinae and Achilixiinae to Cixiidae.

On molecular data, Urban & Cryan (2007) proposed a phylogeny of Fulgoromorpha based on 18S rDNA, 28S rDNA, H3-Histone subunit 3, and Wg-Wingless sequence data, which included a single representative of Achilixiidae, an unidentified *Bebaiotes*. Their results did not support the hypothesis of a relationship between Achilixiidae and Cixiidae, but results were inconsistent and with low branch support as to the sister family of Achilixiidae. Later, Song & Liang (2013) expanded the molecular data from Urban & Cryan (2007) by including more taxa (but not of Achilixiidae) and some mitochondrial sequences (16S rDNA and cytb). They further supported the hypothesis that Achilixiidae and Cixiidae are not related, but also showed inconsistent results as to the sister group of Achilixiidae.

Finally, the most recent contribution to the phylogeny of Fulgoromorpha was by Bucher et al. (2023), also using molecular data (18S, 28S D3-D5, 28S D6-D10, Wg, COI, and Citb), where the same representative of Achilixiidae was included in the analysis. According to the results of the maximum likelihood analysis, *Bebaiotes* sp. was recovered within a clade composed of representatives of Achilidae, as the sister group to *Spino* sp.

In this way, we herein propose to carry out the first phylogenetic analysis of Achilixiidae based on morphological data, which sampled a large number of representative species from both genera, with the goal of understanding their evolutionary history.

6.3. Material and Methods

6.3.1. Taxon sampling

Taxon sampling of the morphological matrix included 44 terminal species (Table 1). The ingroup comprised 35 species of Achilixiidae (13 species of *Achilixius* and 22 species of *Bebaiotes*). This represents 89.74% of all valid species of Achilixiidae. The outgroup was composed of three species of Achilidae, two of Derbidae, and four of Cixiidae. The latter family was used for rooting the phylogenetic trees, thus the basis for character polarization (Nixon & Carpenter, 1993).

Morphological caracteres were coded from specimens studied belonging to: Coleção de Invertebrados do Instituto Nacional de Pesquisas da Amazônia, Manaus (INPA); Coleção Entomológica Professor Padre Jesus Santiago Moure, Universidade Federal do Paraná, Curitiba (DZUP); Museu Paraense Emilio Goeldi, Belém (MPEG); Coleção Zoológica do Maranhão, Universidade Estadual do Maranhão, Caxias (CZMA); Centro de Estudos em Biologia Subterrânea, Universidade Federal de Lavras, Lavras (CEBS); Coleção Entomológica José Alfredo Pinheiro Dutra, Universidade Federal do

Rio de Janeiro, Rio de Janeiro (DZRJ); and Illinois Natural History Survey, University of Illinois, Champaign (INHS).

Material was not available for study for 15 species, and those were coded in the morphological matrix based on photographs of type and paratypes specimens housed in the Bernice Pauhai Bishop Museum, Honolulu (BPBM) and Natural History Museum, London (NHM) and/or original descriptions.

6.3.2. Morphological characters

Terminology of the head characters mostly follows O'Brien & Wilson (1985), whereas forewing venation follows Bourgoin et al. (2015), hindwing venation follows Dworakowska (1988), male genitalia mostly follow Bourgoin (1988) and Bourgoin & Huang (1990), and female genitalia follows Bourgoin (1993).

For the examination of genital structures, abdomen was detached from thorax, macerated into 85% hot lactic acid, studied under a Leica M165C stereomicroscope, and illustrated immersed in glycerin jelly. Afterwards, genitalia were kept in plastic microvials filled with glycerin and pinned together with the specimen. Forewing and hind wing of a specimen were detached, cleaned by a short xylol bath, and mounted between cover glasses with Euparal. After drying, sides of cover slides were glued to a small piece of cardboard and pinned with the specimen. Digital photographs were taken with a Leica MC 170 HD camera attached to a stereomicroscope and combined into expanded focus images by Leica Application Suite software.

6.3.3. Construction of morphological characters

Characters were proposed from external and internal morphology of male and female adults. Different body parts including head, thorax, legs, wings, abdomen, and genitalia were studied. The data matrix was constructed using Mesquite software, version 3.81 (Maddison & Maddison, 2023). The list of characters was built by some characters

944 previously used in previous phylogenetic studies, duly referenced, as well as by new
945 characters.

946 Character coding was based on the four components proposed by Sereno (2007),
947 which consist of: locator (L_n) (morphological structure), variable (V) (aspect that varies),
948 variable qualifier (q) (variable modifier), and character state (V_n) (mutually exclusive
949 condition of a character). From these components, two-character patterns can be
950 identified: neomorphic (absent and present of a character) and transformational (character
951 quality) (Sereno, 2007). The symbols "?" and "–" were used for unobserved and non-
952 comparable characters, respectively.

953 In the analysis of characters, we use the system proposed by Amorin (1982) for the
954 nomenclature of precocious branches. According to this method, the taxon is referred to
955 as a group, with the addition of the name corresponding to the precocious branch of the
956 first dichotomy, followed by the symbol '+'.

957 In the cladogram, black squares represent non-homoplastic apomorphy and light
958 green squares represent homoplastic apomorphy.

959

Table 1. Species of Achilixiidae and outgroups included in the phylogenetic analyses, indicating number and gender of individuals studied (N), depository collections, and whether the terminalia was dissected. When specimens were not available, morphological characters were coded based on the literature (L) and/or habitus type photographs (P).

Families	Species	N	Collection	Dissection ♂	Dissection ♀
Cixiidae					
	Bennarella bicoloripennis	1 ♂, 1♀	INPA	**x**	**x**
	Bothriocera sp. 1	1♂, 1♀	INPA	**x**	**x**
	Melanoliarus sp. 1	1♂, 1♀	INPA	**x**	**x**
	Pintalia sp. 1	1♂, 1♀	INPA	**x**	**x**
Derbidae					
	Anotia sp. 2	1♂, 1♀	INPA	**x**	**x**
	Persis (*Persis*)	1♂, 1♀	INPA	**x**	**x**
Achilidae					
	Catonia sp. 2	1♂, 1♀	INPA	**x**	**x**
	Sevia sp. A	1♂, 1♀	INPA	**x**	**x**
	Synecdoche sp. 2	1♂, 1♀	INPA	**x**	**x**
Achilixiidae					
Achilixius					
	Achilixius davaoensis	L and P	NHM		
	Achilixius dietrichi	1♂	INHS	**x**	
	Achilixius fasciata	L and P ♂	NHM		
	Achilixius fennahi	L and P ♂	NHM		
	Achilixius irigae	L and P ♂	NHM		
	Achilixius kolintangi	L and P ♂	NHM		
	Achilixius mayoyae	L and P ♂	NHM		
	Achilixius minahassae	L and P ♂	NHM		
	Achilixius muiri	L and P ♂	NHM		
	Achilixius sandakanensis	L and P ♂	NHM		
	Achilixius singularis	L and P ♂	NHM		
	Achilixius sp. 1	1♀	INHS		**x**
	Achilixius tubulifer	L ♂	NHM		
Bebaiotes					
	Bebaiotes amazonica	1♂, 1♀	INPA	**x**	**x**
	Bebaiotes banksi	1♂, 1♀	INPA	**x**	**x**
	Bebaiotes bia	1♂, 1♀	INPA	**x**	**x**
	Bebaiotes bucayensis	L and P ♂	NHM		
	Bebaiotes cavichiolii	1♂, 1♀	MUSM	**x**	**x**
	Bebaiotes clarice	1♂, 1♀	INPA	**x**	**x**
	Bebaiotes dichromata	1♂, 1♀	INPA		
	Bebaiotes dorsivittata	1♂, 1♀	INPA	**x**	**x**
	Bebaiotes guianesus	1♂, 1♀	INPA		

Table 1. Continued.

Families	Species	N	Collection	Dissection ♂	Dissection ♀
	Bebaiotes macroptera	1♂, 1♀	INPA	**x**	**x**
	Bebaiotes nigrigaster	L and P	NHM	**x**	
	Bebaiotes nivosa	L and P ♀	NHM		
	Bebaiotes oiapoquensis	1♂	INPA	**x**	
	Bebaiotes oliveirai	1♂, 1♀	INPA	**x**	**x**
	Bebaiotes pallidinervis	1 ♂			
	Bebaiotes parallela	1♂, 1♀	INPA	**x**	**x**
	Bebaiotes pennyi	1♂, 1♀	INPA	**x**	**x**
	Bebaiotes pulla	1♂, 1♀	INPA	**x**	**x**
	Bebaiotes specialis	1♀	DZRJ		**x**
	Bebaiotes tigrina	1♂, 1♀	INPA	**x**	**x**
	Bebaiotes wilsoni	1♂, 1♀	INPA	**x**	**x**
	Bebaiotes 6317 sp. C	1♂, 1♀	CEBS	**x**	**x**

CEBS, Centro de Estudos em Biologia Subterrânea, Universidade Federal de Lavras; DZRJ, Coleção Entomológica José Alfredo Pinheiro Dutra, Universidade Federal do Rio de Janeiro, Rio de Janeiro, Brazil; INHS, Illinois Natural History Survey, University of Illinois, Champaign, USA; INPA, Coleção de Invertebrados do Instituto Nacional de Pesquisas da Amazônia, Manaus, Brazil; MUSM, Museo de Historia Natural de la Universidade Mayor de San Marcos, Lima, Peru

6.3.4. Phylogenetic analysis

The monophyly of Achilixiidae was evaluated using the criterion of parsimony. This criterion seeks to find the tree with the smallest number of evolutionary changes, using the optimization approach proposed by Fitch (1971) and characters with equal weights. To search for the most parsimonious trees, a Traditional search was adopted in TNT 1.5 (Goloboff & Catalano, 2016), as follows: 10,000 replications were performed, using the TBR (tree bisection reconnection) algorithm, with the retention of 10 trees for each replication. Resulting most parsimonious trees were visualized in the FigTree v1.4.4 program (Rambaut, 2018) and a strict consensus tree was edited in Adobe Illustrator CS6. The statistical support of tree branches was evaluated by the Bremer decay index (Bremer, 1994) calculated with the aquickie.run script and 1000 non-parametric bootstrap

replicates (Felsenstein, 1985). To indicate high branch support of each clade, the following were considered: Bootstrap ≥ 80.

Consistency (IC) and retention (IR) indices were calculated for obtained trees, using the wstats.run script, while to obtain these values for each character, the statsall.run script, both in TNT were used (Goloboff & Catalano, 2016).

Optimization of morphological characters was performed under equal weights parsimony using the Mesquite software, version 3.81 (Maddison & Maddison, 2016) over all most parsimonious trees found. Character states of unambiguous optimization for each branch were plotted manually over the strict consensus tree found in Adobe Illustrator CS6. Ambiguous characters were not plotted on the cladogram.

6.4. Results

6.4.1. Morphological characters

The morphological matrix was composed of 99 characters (65 binary and 34 multistate) (Table 2). Of these, 63 characters pertain to general morphology (male and female), while 16 are of female and 20 of male terminalia. We emphasize that sexual dimorphism is not accentuated within *Bebaiotes*, except for *Bebaiotes macroptera*, where the abdominal coloration can range from brown to yellow (Viegas & Ale-Rocha, 2023, submitted). In *Achilixius*, all described specimens are male, but in our analysis, we included an unidentified female specimen.

Characters and their respective states and comments, when necessary, are listed as follows:

Head

1. Head, transition frons to vertex, transverse carina. (0) present; (1) absent. [CI=1.0; RI=1.0]. Figures 1 A–D.

This character has already been employed in previous cladistic studies by Löcker et al. (2006) and Ceotto & Bourgoin (2008). The state 1 of this character has been recovered as a non-homoplastic synapomorphy of the Derbidae+Achilixiidae clade (Figs 1 C, D).

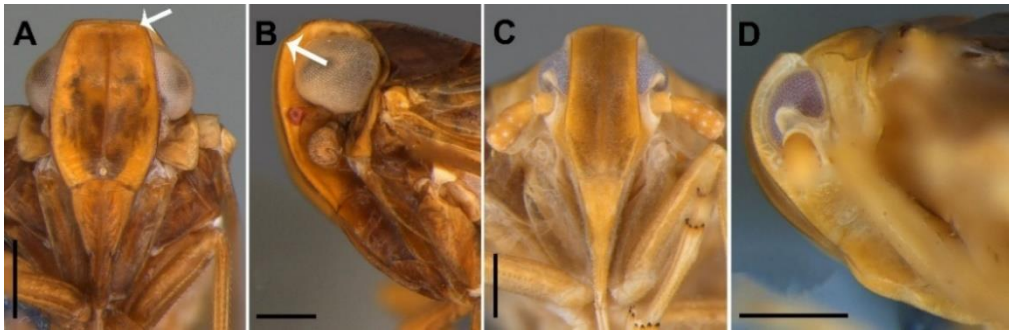

Figures 1 A–D. Head, transition frons to vertex. **A**, *Pintalia* sp. 1, anterior view. **B**, *Pintalia* sp. 1, lateral view. **C**, *Achilixius dietrichi*, anterior view. **D**, *Achilixius dietrichi*, lateral view. Scale bars: A, D = 0.4 mm; B, C = 0.3 mm. Arrow highlighting the presence of the transverse carina (char. 1, state 0).

2. Head, frons, median longitudinal carina: (0) present; (1) absent. [CI=0.5; RI=0.9]. Figures 2 A–D.

This character was previously utilized in studies of Löcker et al. (2006) and Ceotto & Bourgoin (2008). In our analysis, we observed that state 0 of the character was recovered as a homoplastic synapomorphy of *Achilixius* species (Fig 2 B).

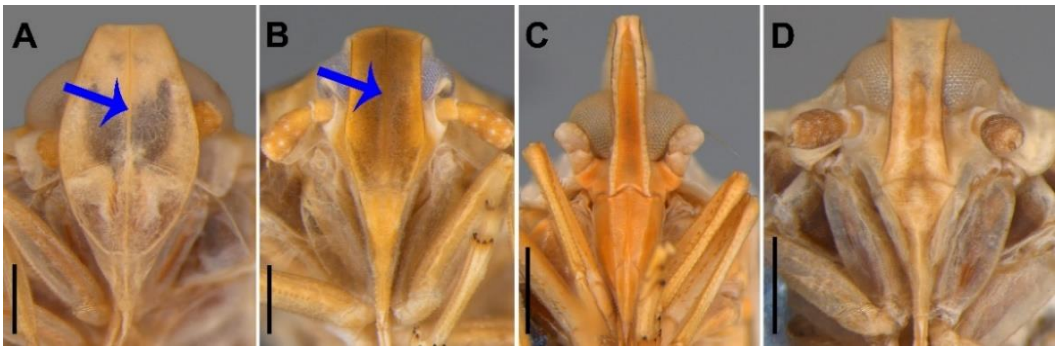

Figures 2 A–D. Head, frons, anterior view. **A**, *Synecdoche* sp. 2. **B**, *Achilixius dietrichi*. **C**, *Persis* (*Persis*). **D**, *Bebaiotes tigrina*. Scale bars: A, B = 0.3 mm; C = 0.5 mm; D = 0.4 mm. Arrow highlighting the presence of the median longitudinal carina (char. 2, state 0).

3. Head, frons, lateral longitudinal carinae, median region, direction: (0) parallel; (1) divergent. [CI=0.5; RI=0.8]. Figures 3 A–D.

The state 0 of the character was recovered as a homoplastic synapomorphy of the Derbidae+Achilixiidae clade.

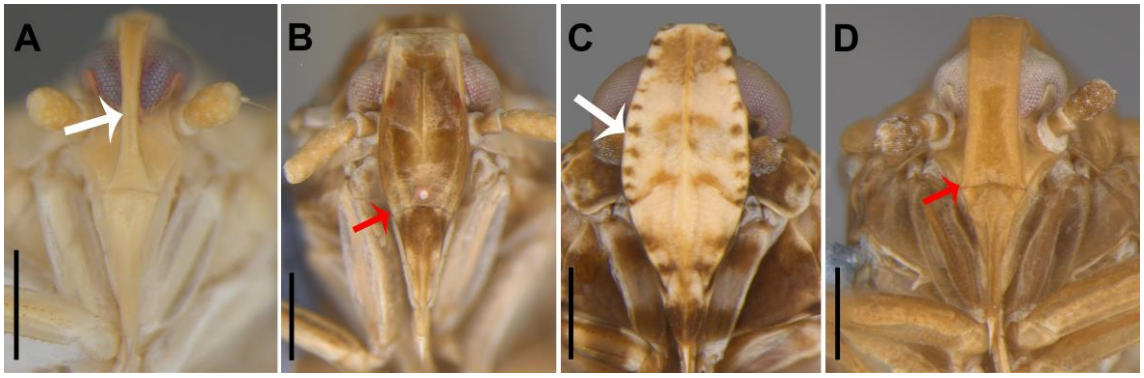

Figures 3 A–D. Head, frons, anterior view. **A**, *Bebaiotes cavichiolii*. **B**, *Bennarella bicoloripennis*. **C**, *Catonia* sp. 2. **D**, *Bebaiotes amazonica*. Scale bars: A–D= 0.4 mm. White arrows highlighting direction of lateral longitudinal carinae (char. 3): A, *Bebaiotes cavichiolii* (state 0) and C, *Catonia* sp. 2 (state 1). Red arrows highlighting the direction of the apex of lateral longitudinal carinae (char. 4): B, *Bennarella bicoloripennis* (state 0) and D, *Bebaiotes amazonica* (state 1).

4. Head, frons, lateral longitudinal carinae, apex, direction: (0) convergent; (1) divergent. [CI=0.2; RI=0.5]. Figures 3 B, D.

The state 1 of this character was recovered as a homoplastic synapomorphy of *Anotia* sp2 (Derbidae), *Bebaiotes* 6317 sp. C, *Bebaiotes pennyi*, *Bebaiotes clarice* +*Bebaiotes specialis* (Fig 3 D), and *Bebaiotes parallela*+ clade, except for *Bebaiotes nivosa*, where this character could not be visualized due to the way were mounted and it was coded as '?'

5. Head, frons, median width in relation to maximum width of the vertex: (0) subequal; (1) narrower; (2) wider. [CI=0.3; RI=0.7]. Figures 4 A–D.

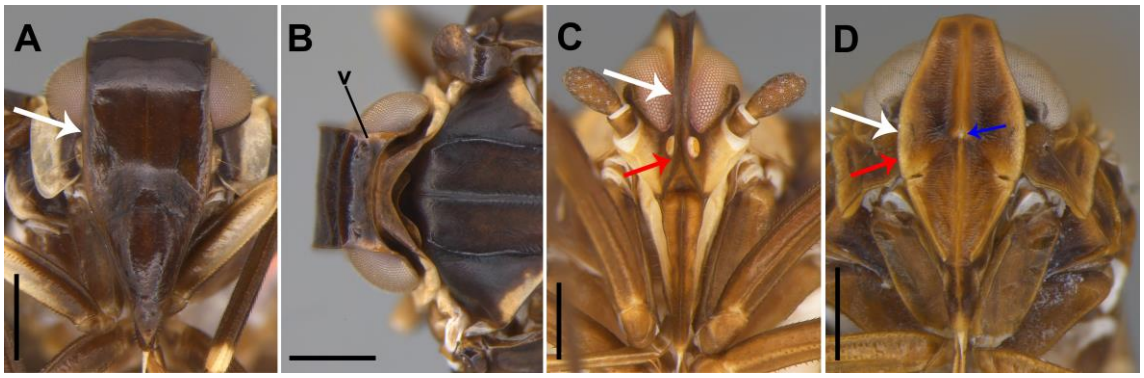

Figures 4 A–D. Head. **A**, **C**, **D**. Head, frons, anterior view. **A**, *Sevia* sp. A. **C**, *Bebaiotes clarice*. **D**, *Melanoliarius* sp. 1. **B**. Head, vertex, dorsal view. **B**, *Sevia* sp. A. Scale bars: A, B = 0.6 mm; C = 0.4 mm; D = 0.5 mm. White arrows highlighting the median width of the frons in relation to maximum width of the vertex (char. *5):* A, B *Sevia* sp. A (state 0), *C, Bebaiotes clarice* (state 1) and D, *Melanoliarius* sp. 1 (state 2). Red arrows highlighting the extension of lateral margins at median region of the frons (char. 6): C, *Bebaiotes clarice* (state 0) and D, *Melanoliarius* sp. 1 (state 1). Blue arrow highlighting the presence of the median ocellus (char. 7, state 1). Abbreviation: v, vertex.

6. Head, frons, lateral margins, median region, anterior view, lateral extension: (0) not covering lateral ocelli; (1) covering lateral ocelli. [CI=0.5; RI=0.8]. Figures 4 C, D.

The state 0 of the character was recovered as homoplastic synapomorphy of the Derbidae+Achilixiidae clade and homoplastic autapomorphy of *Bennarella bicoloripennis* (Cixiidae).

7. Head, median ocellus: (0) absent; (1) present. [CI=1.0; RI=1.0]. Figure 4 D.

Löcker et al. (2006) and Ceotto & Bourgoin (2008) used this character in their phylogenetic analyses with Cixiidae. In both analyses, this character underwent reversals and convergences throughout its evolutionary history, demonstrating its high variability within Cixiidae. The state 0 of this character was recovered as a non-homoplastic synapomorphy of the clade composed of Achilidae+ (Fig 4 D).

8. Head, lateral ocellus insertion, lateral view, position in relation to inferior margin of the compound eye: (0) aligned with; (1) below. [CI=0.2; RI=0.7]. Figures 5 A–D.

State 0 of this character is a homoplastic synapomorphy of *Bebaiotes dichromata* and *Bebaiotes cavichiolli*+ clade (Fig 5 C), except for *Bebaiotes nivosa*, where this character could not be visualized due to the way it was photographed and it was coded as '?'.

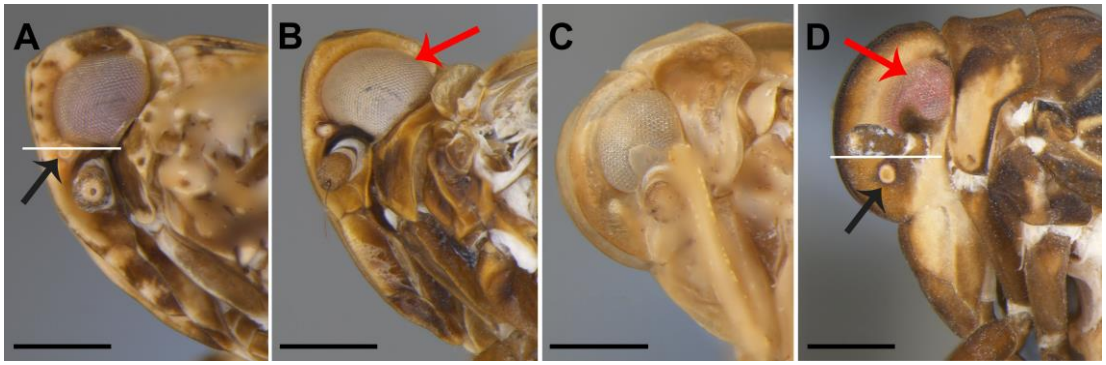

Figures 5 A–D. Head, lateral view. **A**, *Synecdoche* sp. 2. **B**, *Melanoliarius* sp. 1. **C**, *Bebaiotes tigrina*. **D**, *Bebaiotes clarice*. Scale bars: A, C = 0.4 mm; B, D = 0.5 mm. Black arrows highlighting the lateral ocellus insertion (char. 8): A, *Synecdoche* sp. 2. (state 0) and D, *Bebaiotes clarice* (state 1). Red arrows highlighting the compound eye shape (char. 9): B, *Melanoliarius* sp. 1 (state 0) and D, *Bebaiotes clarice* (state 1).

9. Head, compound eye, lateral view, shape: (0) rounded; (1) reniform. [CI=1.0; RI=1.0]. Figures 5 A–D.

The shape of the compound eye is influenced by the size of the ocular concavity, being present in all species in this analysis. The state 1 of this character was recovered as a non-homoplastic synapomorphy of the Derbidae+Achilixiidae clade (Figs 5C, D).

10. Head, antenna, pedicel, length in relation to width: 0) subequal; (1) longer. [CI=0.2; RI=0.6]. Figures 6 A–C.

This character has already been employed in previous cladistic studies by Löcker et al. (2006) and Ceotto & Bourgoin (2008). The state 1 of the character was recovered as a homoplastic apomorphies, as it arose independently in the Derbidae+Achilixiidae clade and the terminal *Bennarella bicoloripennis* (Cixiidae) (Fig 6 B), although a

reversion occurred in *Bebaiotes dichromata* and *Bebaiotes parallela* to the plesiomorphic state (Fig 6 A).

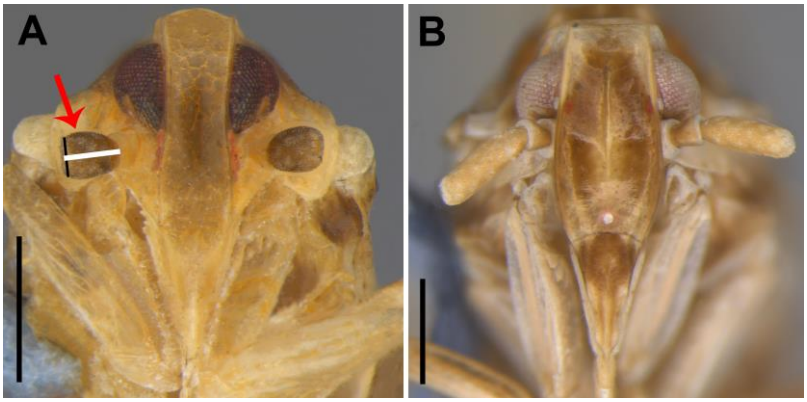

Figures 6 A–B. Head, frons, anterior view. **A**, *Bebaiotes dichromata*. **B**, *Bennarella bicoloripennis*. Scale bars: A= 0.5 mm; B= 0.4 mm. Arrow highlighting the pedicel (char. 10, state 0).

11. Head, antennal insertion, lateral view, position in relation to inferior margin of the compound eye: (0) aligned with; (1) below. [CI=0.5; RI=0.8]. Figures 7 A–C.

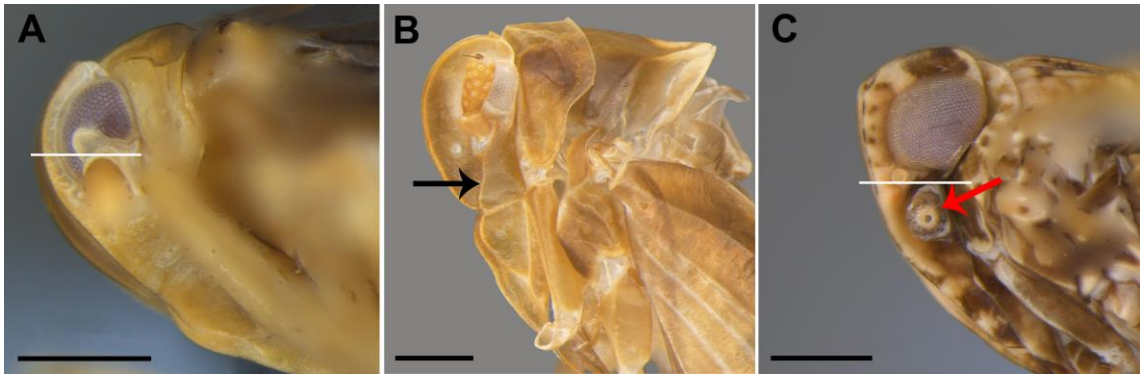

Figures 7 A–C. Head, lateral view. A, *Achilixius dietrichi*. B, *Bebaiotes specialis*. C, *Synecdoche* sp. 2. Scale bars: A–C= 0.4 mm. Red arrow highlighting antennal insertion (char. 11): *Achilixius dietrichi* (state 0) and C, *Synecdoche* sp. 2 (state 1). Black arrow highlighting the presence of the subantenal carina (char. 11, state 1).

12. Head, gena, subantennal carina: (0) absent; (1) present. [CI=0.5; RI=0.9]. Figures 7 A–C.

Ceotto & Bourgoin (2008) used this character in their phylogenetic analyses of Cixiidae. In Achilixiidae, the state 1 of this character was recovered as a homoplastic

synapomorphy of *Bebaiotes*, being one of the diagnostic characters of this genus (Fig 7 B).

13. Head, epistomal suture, shape: (0) convex; (1) almost straight; (2) concave. [CI=0.6; RI=0.8]. Figures 8 A–C.

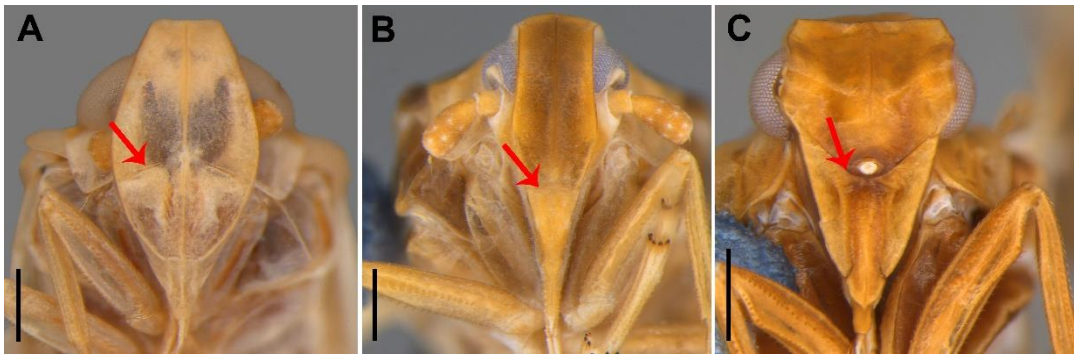

Figures 8 A–C. Head, frons, epistomal suture, anterior view. **A**, *Synecdoche* sp. 2. **B**, *Achilixius dietrichi*. **C**, *Bothriocera* sp. 1. Scale bars: A, B= 0.3 mm; C = 0.4 mm. Red arrow highlighting epistomal suture (char. 13): A, *Synecdoche* sp. 2. (state 0), B, *Achilixius dietrichi* (state 1), and C, *Bothriocera* sp. 1 (state 2).

14. Head, lora, lateral view, shape: (0) subrectangular; (1) subtriangular. [CI=1.0; RI=1.0]. Figures 9 A–B.

The lora is a head sclerite, bounded dorsally by the epistomal suture, anteriorly by the longitudinal lateral carina of the clypeus, and posteriorly by the maxillary lobe (Mejdalani, 1998). The shape of the lora is determined by the shape of the longitudinal lateral carina of the clypeus in the lower half. State 1 of this character was identified as a non-homoplastic synapomorphy of Achilixiidae (Fig 9 B). However, it was not possible to observe this trait in all species of *Achilixius* due to the way they were mounted.

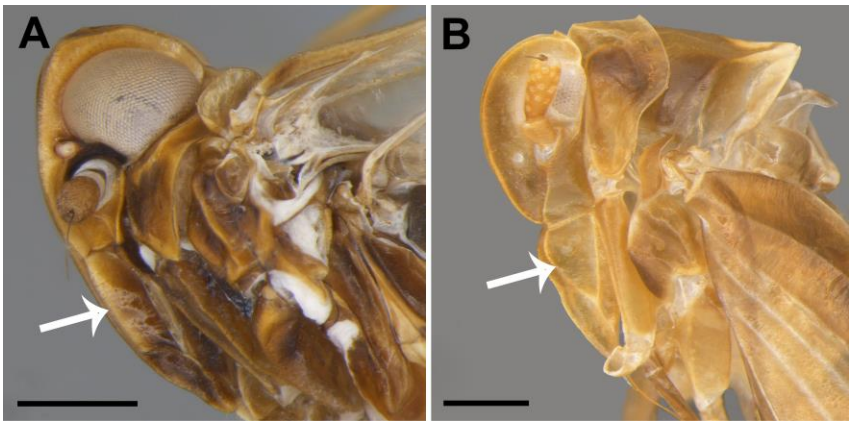

Figures 9 A–B. Head, lateral view. **A**, *Melanoliarius* sp. 1. **B**, *Bebaiotes specialis*. Scale bars: A= 0.4 mm; B= 0.5 mm. White arrows highlighting the lora (char. 14): A, *Melanoliarius* sp. 1. (state 0) and B, *Bebaiotes specialis* (state 1).

15. Head, clypeus, median longitudinal carina: (0) present; (1) absent. [CI=1.0; RI=1.0]. Figures 10 A–C.

This character has already been employed in previous cladistic studies by Löcker et al. (2006) and Ceotto & Bourgoin (2008).

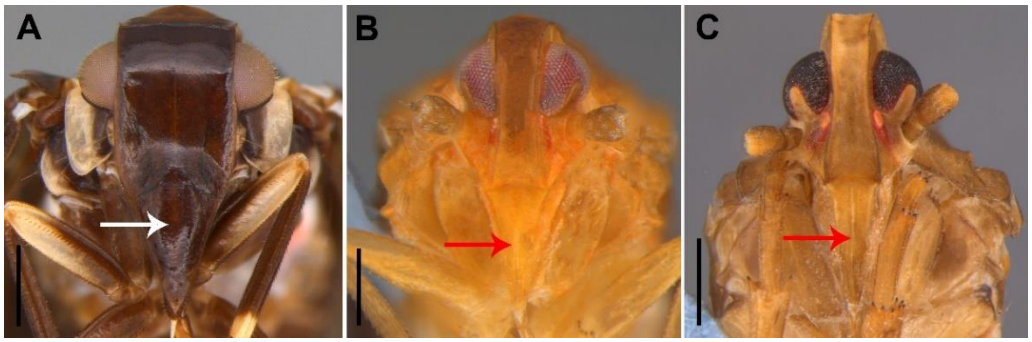

Figures 10 A–C. Head, frons, anterior view. **A**, *Sevia* sp. A. **B**, *Bebaiotes macroptera*. **C**, *Bebaiotes dorsivittata*. Scale bars: A= 0.6 mm; B= 0.3 mm; C = 0.5 mm. White arrow highlighting the absence of the median carina of the clypeus (char. 15, state 1). Red arrows highlighting the extension of the median carina of the clypeus (char. 16): B, *Bebaiotes macroptera* (state 0) and C, *Bebaiotes dorsivittata* (state 1).

16. Head, clypeus, median longitudinal carina, extension: (0) between ¼ and ½; (1) longer than ¾. [CI=0.5; RI=0.0]. Figures 10 A–C.

This character has already been employed in previous cladistic studies by Löcker et al. (2006) and Ceotto & Bourgoin (2008). State 0 of this character appears as homoplastic autapomorphies of *Bebaiotes dichromata* and *Bebaiotes macroptera.*

17. Head, clypeus, ventral view, extension in relation to protrochanter: (0) reaching anterior margin; (1) reaching half-length; (2) extending posteriorly beyond. [CI=0.2; RI=0.0]. Figures 11 A–C.

This character has already been employed in previous cladistic studies by Ceotto & Bourgoin (2008). State 1 of this character appears as homoplastic autapomorphies of *Bebaiotes macroptera*, *Bebaiotes wilsoni*, *Bebaiotes oliveirai*, *Bebaiotes clarice*, *Bebaiotes pulla*, *Bebaiotes oiapoquensis*, *Catonia* sp. 2 (Achilidae), and *Persis* (*Persis*) (Derbidae).

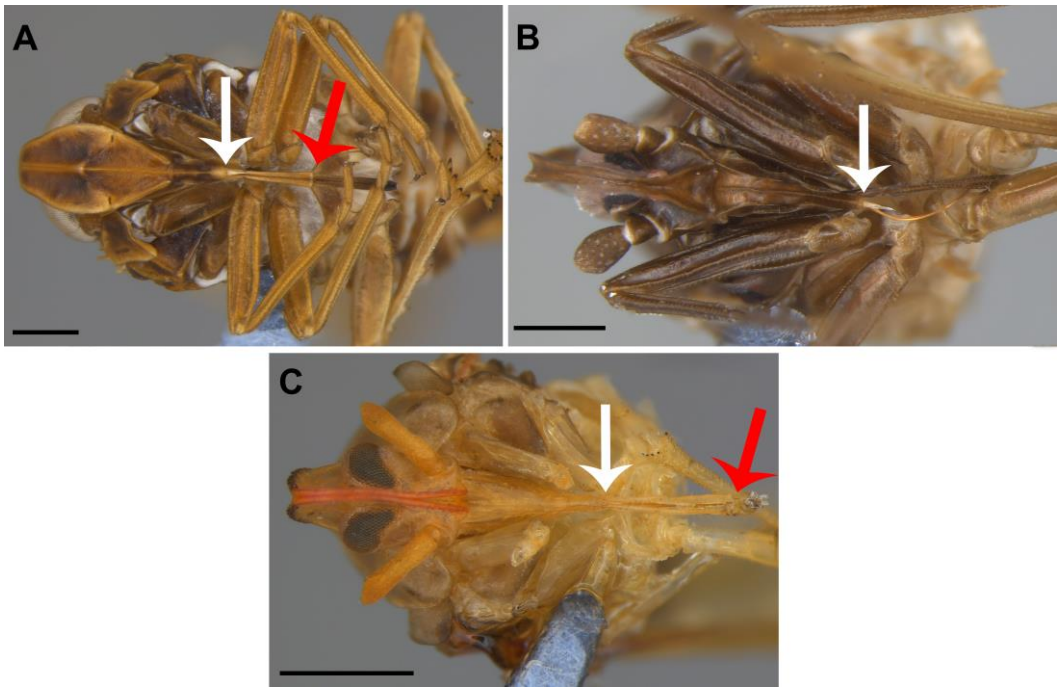

Figures 11 A–C. Clypeus and labium, ventral view. **A**, *Synecdoche* sp. 2. **B**, *Bebaiotes oiapoquensis*. **C**, *Anotia* sp. 2. Scale bars: A, B= 0.5 mm; C = 1 mm. White arrows highlighting the extension of the clypeus (char. 17): A, *Synecdoche* sp. 2 (state 0), B, *Bebaiotes oiapoquensis* (state 1), and C, *Anotia* sp. 2 (state 2). Red arrows highlighting the apex of the second labial segment (char. 18): A, *Synecdoche* sp. 2 (state 0) and C, *Anotia* sp. 2 (state 2).

18. Head, labium, ventral view, apex of the second labial segment, extension in relation to metacoxal: (0) reaching anterior margin; (1) reaching half-length; (2) extending posteriorly beyond. [CI=0.3; RI=0.7]. Figures 11 A, C.

This character has already been employed in previous cladistic studies by Ceotto & Bourgoin (2008). Within *Bebaiotes*, state 1 was recovered as homoplastic synapomorphies of *Bebaiotes banksi*+ and *Bebaiotes amazonica*+ clades, except for *Bebaiotes nivosa*, where this character could not be visualized due to the way were mounted and it was coded as '?'. However, it was not possible to observe this trait in all species of the *Achilixius* due to the way they were mounted and photographed, and it was coded as '?'.

19. Thorax, pronotum, dorsal view, median length in relation to median length of mesonotum: (0) less than ¼; (1) longer than ½. [CI=1.0; RI=1.0]. Figures 12 A–D. This character has already been employed in previous cladistic studies by Ceotto & Bourgoin (2008). The median length of the pronotum was measured in relation to the median length of the mesonotum. State 1 of this character was identified as a non-homoplastic synapomorphy of Achilixiidae (Figs 12 B–D).

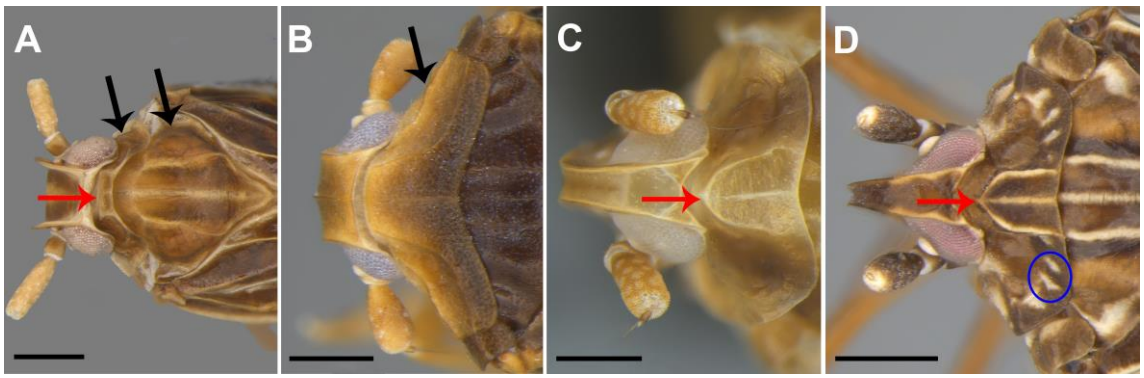

Figures 12 A–D. Thorax, dorsal view. **A**, *Bennarella bicoloripennis*. **B**, *Achilixius dietrichi*. **C**, *Bebaiotes specialis*. **D**, *Bebaiotes pulla*. Scale bars: A= 0.4 mm; ; B, C = 0.3 mm, D = 0.4 mm. Black arrows highlighting the pronotum and mesonotum (char. 19): A, *Bennarella bicoloripennis* (state 0) and B, *Achilixius dietrichi* (state 1). Red arrows highlighting the anterior pronotum pronotum (char. 20): A, *Bennarella bicoloripennis* (state 0), C, *Bebaiotes specialis* (state 2), and C, *Bebaiotes pulla* (state 1). Blue circle highlighting the presence of pustules on the posterior margin of the pronotum (char. 21, state 1).

20. Thorax, pronotum, dorsal view, anterior margin, shape: (0) truncated; (1) tapered; (2) rounded. [CI=0.2; RI=0.6]. Figures 12 A, C, D.

The state 1 of the character was recovered as a homoplastic apomorphies of the *Bebaiotes macroptera*, *Bebaiotes cavichiolii, Synecdoche* sp. 2 (Achilidae), *Anotia* sp. 2 (Derbidae) and *Bebaiotes pallidinervis*+ clade (Fig 12 D). Within *Bebaiotes pallidinervis*+ clade, state 2 of the character was recovered as homoplastic autapomorphies of the *Bebaiotes wilsoni, Bebaiotes specialis*, and *Bebaiotes bucayensis* (Fig 12 C).

21. Thorax, pronotum, posterior margin, pustules: (0) absent; (1) present. [CI=0.3; RI=0.5]. Figures 12 A–C.

Within *Bebaiotes*, state 1 of this character was found as a homoplastic autapomorphy of *Bebaiotes pallidinervis* and synapomorphy of *Bebaiotes bucayensis*+ clade, although a reversion occurred in *Bebaiotes dorsivittata* to the plesiomorphic state.

22. Thorax, pronotum, lateral longitudinal carinae: 0) present; (1) absent. [CI=1.0; RI=1.0]. Figures 13 A–C.

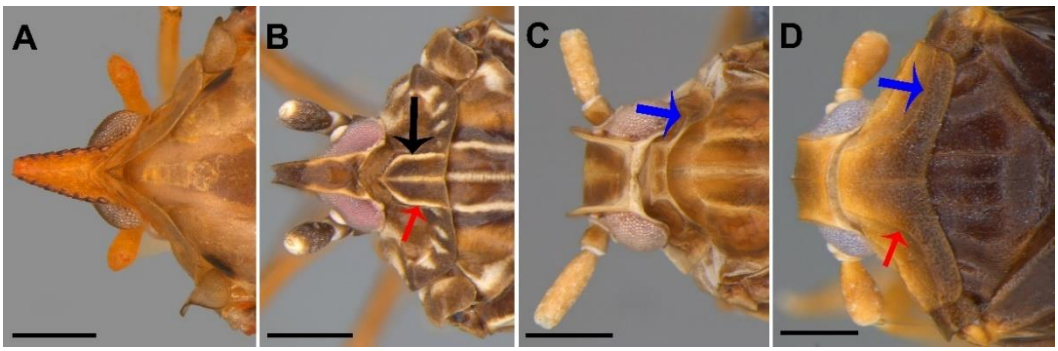

Figures 13 A–D. Thorax, pronotum, dorsal view. **A**, *Anotia* sp. 2. **B**, *Bebaiotes pulla*. **C**, *Bennarella bicoloripennis*. **D**, *Achilixius dietrichi*. Scale bars: A = 0.6 mm; B = 0.5 mm; C = 0.4 mm; D = 0.3 mm. Black arrow highlighting the lateral longitudinal carinae on the posterior margin (char. 22, state 0). Red arrows highlighting the direction of lateral longitudinal carinae on the posterior margin (char. 23): B, *Bebaiotes pulla* (state 0) and D, *Achilixius dietrichi* (state 1). Blue arrows highlighting the direction of posterior half of lateral longitudinal carinae (char. 24): C, *Bennarella bicoloripennis* (state 1) and D, *Achilixius dietrichi* (state 2).

23. Thorax, pronotum, dorsal view, lateral longitudinal carinae, anterior half, direction: (0) subparallel; (1) divergent posteriorly. [CI=0.2; RI=0.2]. Figures 13 B, D.

Within *Bebaiotes*, state 0 of this character was found as homoplastic autapomorphies of *Bebaiotes dichromata*, *Bebaiotes pallidinervis*, and *Bebaiotes guianesus* (Fig 12 B).

24. Thorax, pronotum, dorsal view, lateral longitudinal carinae, posterior half, direction: (0) continues anterior half direction; (1) directed anteriorly; (2) directed laterally. [CI=0.6; RI=0.9]. Figures 13 A–B.

25. Thorax, pronotum, posterior margin, shape: (0) roundly concave; (1) acutely concave. [CI=0.2; RI=0.2]. Figures 14 A–B.

This character has already been employed in previous cladistic studies by Ceotto & Bourgoin (2008). State 0 of this character was recovered as a homoplastic synapomorphy of Achilixiidae and a homoplastic autapomorphy of *Sevia* sp. A (Achilidae).

26. Thorax, mesonotum, scutellum, apex, shape: (0) tapered; (1) rounded or truncated. [CI=0.5; RI=0.0]. Figures 14 A–B.

This character has already been employed in previous cladistic studies by Ceotto & Bourgoin (2008).

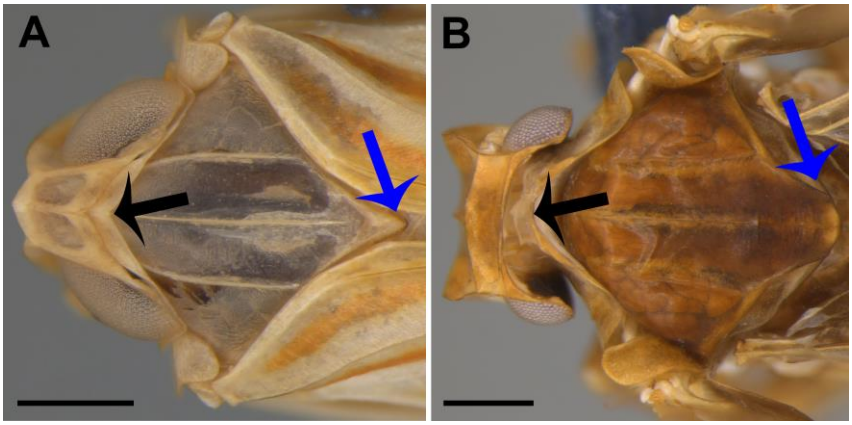

Figures 14 A–B. Thorax, dorsal view. **A**, *Synecdoche* sp. 2. **B**, *Bothriocera* sp. 1. Scale bars: A–B= 0.4 mm. Black arrows highlighting the posterior margin of the pronotum (char. 25): A, *Synecdoche* sp. 2 (state 1) and B, *Bothriocera* sp. 1. (state 0). Blue arrows highlighting the apex of the scutellum (char. 26): A, *Synecdoche* sp. 2 (state 0) and B, *Bothriocera* sp. 1. (state 1).

27. Thorax, forewing, position of ScP+R branching in relation total length of CuP vein: (0) aligned at basal half of CuP; (1) aligned at apical half of CuP. [CI=0.2; RI=0.0]. Figures 15 A–C.

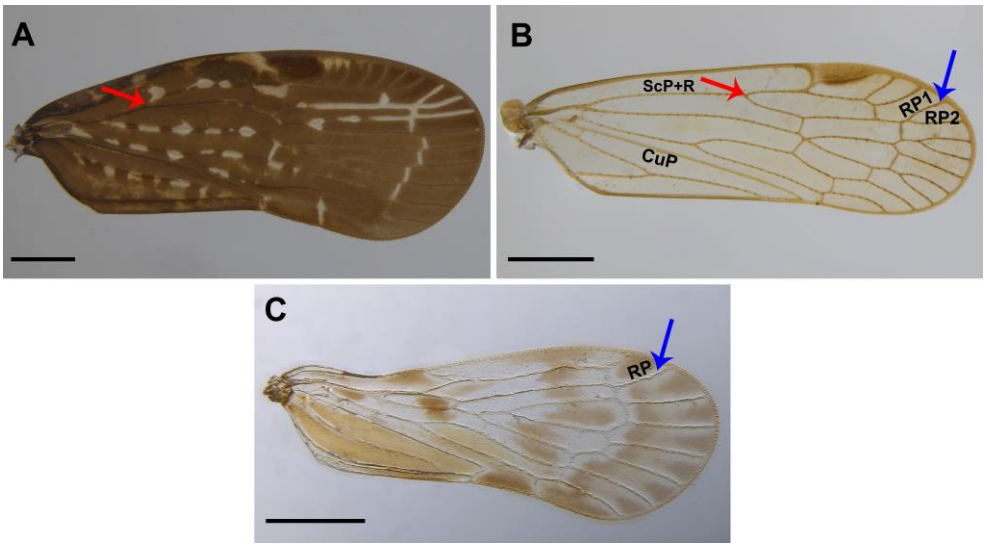

Figures 15 A–C. Forewing. **A**, *Sevia* sp. A. **B**, *Melanoliarus* sp. 1. **C**, *Bebaiotes dichromata*. Scale bars: A–C= 1 mm. Red arrows highlighting the position of the ScP+RP branching (char. 27): A, *Sevia* sp. A (state 0) and B, *Melanoliarus* sp. 1 (state 1). Blue arrow highlighting the RP vein (char. 28): B, *Melanoliarus* sp. 1and C (state 0), *Bebaiotes dichromata* (state 1). Abbreviations: CuA, anterior cubitus; RP, radial posterior; ScP, posterior subcosta.

28. Thorax, forewing, RP vein, branching: (0) branched; (1) unbranched. [CI=1.0; RI=1.0]. Figures 15 A–B.

State 1 of this character was recovered as a non-homoplastic synapomorphy of *Bebaiotes* (Fig 15 C).

29. Thorax, forewing, MP1 vein, branching: (0) branched; (1) unbranched. [CI=0.5; RI=0.7]. Figures 16 A–C.

State 1 of this character was recovered as a non-homoplastic synapomorphy of the Achilidae+ clade, except for some species of *Achilixius*, where this character could not be visualized due to the forewings not being mounted, and it was coded as '?'. In addition, within the Achilidae+ clade, a reversion occurred in *Anotia* sp. 2 (Derbidae) to the plesiomorphic state (Fig 16 A).

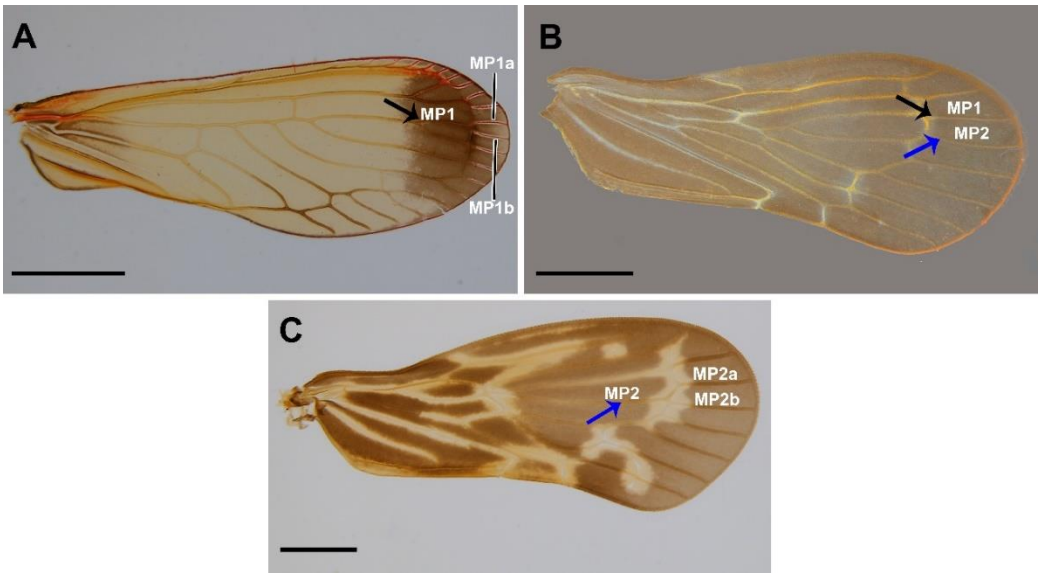

1228

Figures 16 A–C. Forewing. **A**, *Anotia* sp. 2. **B**, *Bebaiotes parallela*. **C**, *Bebaiotes clarice*. Scale bars: A–C= 1 mm. Black arrow highlighting the MP1 vein (char. 29): A, *Anotia* sp. 2 (state 0) and B, *Bebaiotes parallela* (state 1). Blue arrows highlighting the MP2 vein (char. 30): C, *Bebaiotes clarice* (state 0) and B, *Bebaiotes parallela* (state 1). Abbreviations: MP1, first media posterior branch; MP2, second media posterior branch.

1229

1230 30. Thorax, forewing, MP2 vein, branching: (0) branched; (1) unbranched. [CI=1.0;

1231 RI=0.0]. Figures 16 A–C.

1232 State 0 of this character was recovered as an autapomorphy of *Bebaiotes clarice*

1233 (Fig 16 C).

1234 31. Thorax, forewing, fusion of MP3 in relation MP4: (0) separate; (1) fused. [CI=0.5;

1235 RI=0.0]. Figures 17 A–C.

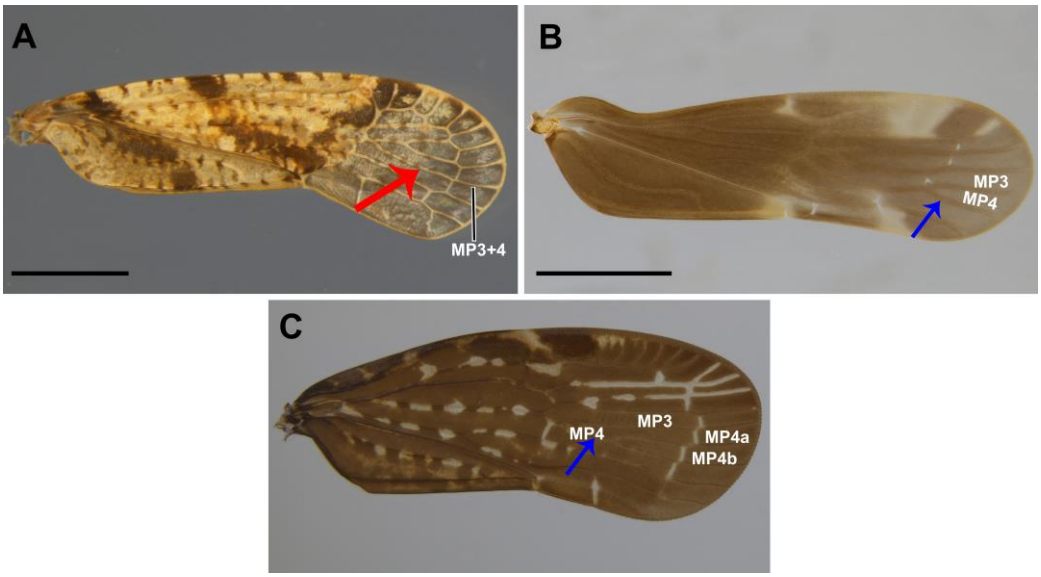

1236

Figures 17 A–C. Forewing. **A**, *Catonia* sp. 2. **B,** *Achilixius dietrichi*. **C,** *Sevia* sp. A. Scale bars: A–*B*= 1 mm. Red arrow highlighting MP3+MP4 vein fused (char. 31, state 0). Blue arrows highlighting MP4 vein (char. 33): B, *Achilixius dietrichi* (state 1) and C, *Sevia* sp. A (state 0). Abbreviations: MP3+4, third media + fourth media posterior branches; MP3, third media posterior branch; MP4, fourth media posterior branch. Abbreviations: MP3+4, third media + fourth media posterior branches; MP3, third media posterior branch; MP4, fourth media posterior branch.

1237

1238 32. Thorax, forewing, MP3 vein, branching: (0) branched; (1) unbranched. [CI=0.5;

1239 RI=0.8].

1240 State 0 of this character was recovered as a non-homoplastic synapomorphy of *Ano-*

1241 *tia* sp. 2 and *Bebaiotes bucayensis*+ clade. It is important to note that within the genus

1242 *Bebaiotes*, this character has arisen only once, making it one of the homoplastic synapo-

1243 morphy supporting the clade *Bebaiotes bucayensis*+.

1244 33. Thorax, forewing, MP4 vein, branching: (0) branched; (1) unbranched. [CI=1.0;

1245 RI=1.0]. Figures 17 A–C.

1246 34. Thorax, forewing, position of MP1+2 and MP3+4 branching in relation to r-m

1247 crossvein: (0) basal; (1) apical; (2) aligned with. [CI=0.3; RI=0.7]. Figures 18 A–C.

The topology obtained in this study indicates that the character is homoplastic and arose independently in two distinct clades within Achilixiidae, in *Bebaiotes dichromata*+ and *Bebaiotes clarice*+.

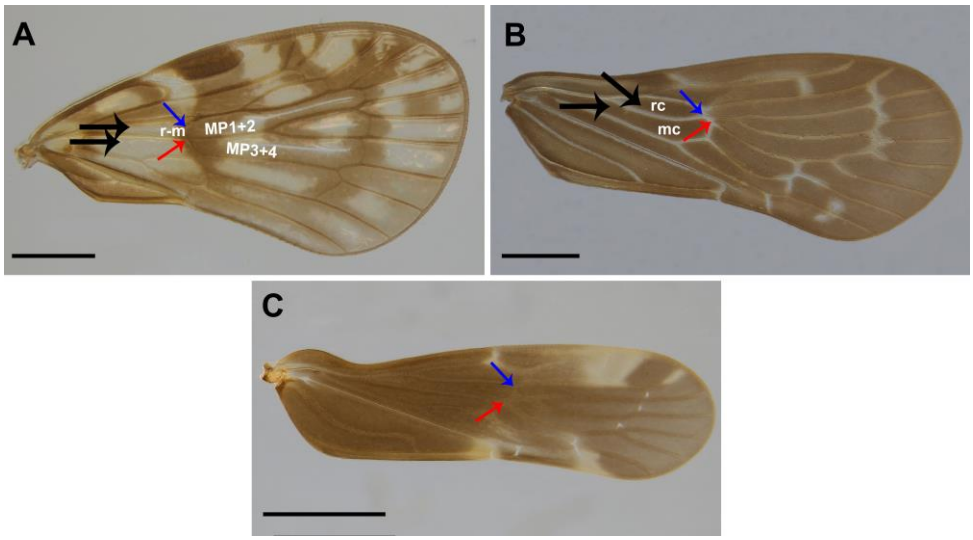

Figures 18 A–C. Forewing. **A**, *Bothriocera* sp. 1. **B**, *Bebaiotes pulla*. **C**, *Achilixius dietrichi*. Scale bars: A–C= 1 mm. Black arrows highlighting the radial cell in relation to median cell (char. 35): A, *Bothriocera* sp. 1 (state 0) and B, *Bebaiotes pulla* (state 1). Blue arrows highlighting the r-m crossvein. Red arrows highlighting the position MP1+2 and MP3+4 branching (char. 36): A, *Bothriocera* sp. 1 (state 2), B, *Bebaiotes pulla* (state 1), C, *Achilixius dietrichi* (state 0). Abbreviations: mc, median cell; MP1+2, first media + second media posterior branches MP3+4, third media + fourth media posterior branches; rc, radial cell; r-m, radio-medial crossvein.

35. Thorax, forewing, length of radial cell in relation to median cell length: (0) subequal; (1) half length; (2) twice longer. [CI=0.6; RI=0.9]. Figures 18 A–C.

State 1 was recovered as a homoplastic synapomorphy of *Bebaiotes*, being considered an important character to corroborate the diagnosis of the genus.

36. Thorax, forewing, position of r-m crossvein in relation to apex of clavus: (0) basal; (1) apical; (2) aligned with. [CI=0.4; RI=0.6]. Figures 18 A–C.

Within the Achilixiidae+ clade, the state 0 of the character was recovered as a homoplastic synapomorphy of the *Bebaiotes*+ clade.

37. Thorax, forewing, m-cu1 crossvein: (0) present; (1) absent. [CI=0.5; RI=0.0]. Figures 19 A–C.

State 1 of this character was recovered as homoplastic autapomorphies of *Bebaiotes pallidinervis* and *Bennarella bicoloripennis* (Cixiidae).

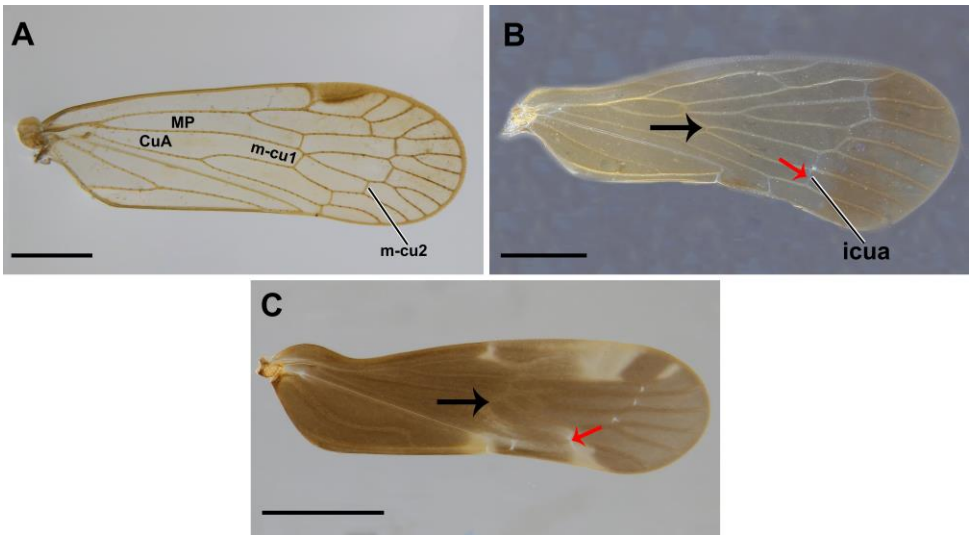

Figures 19 A–C. Forewing. **A**, *Melanoliarus* sp. 1. **B**, *Bebaiotes wilsoni*. **C**, *Achilixius dietrichi*. Scale bars: A–C= 1 mm. Black arrows highlighting the position m-cua crossvein (char. 38): A, *Melanoliarus* sp. 1 (state 0), B, *Bebaiotes wilsoni* (state 1) and C, *Achilixius dietrichi* (state 2). Red arrows highlighting the presence and absence of the m-cua2 crossvein (char. 39): B, *Bebaiotes wilsoni* (state 0) and C, *Achilixius dietrichi* (state 1). Abbreviations: CuA, cubitus anterior; MP, posterior media; m-cua1, first mediocubital crossvein; m-cua2, second mediocubital crossvein; icua, intercubital crossvein.

38. Thorax, forewing, length of m-cu1 crossvein in relation to m-cu2 crossvein length: (0) subequal; (1) shorter; (2) longer. [CI=0.2; RI=0.5]. Figures 19 A–C.

State 1 of this character was recovered as homoplastic autapomorphies of *Synecdoche* sp. 2 (Achilidae) and *Bebaiotes parallela* and homoplastic synapomorphy of *Bebaiotes tigrina*+*Bebaiotes nivosa* clade. State 2 was recovered as homoplastic autapomorphies of *Pintalia* sp. 1 (Cixiidae), *Anotia* sp. 2 (Derbidae), and *Bebaiotes pulla*.

39. Thorax, forewing, icua crossvein: (0) present; (1) absent. [CI=0.5; RI=0.8]. Figures 19 A–C.

State 1 was recovered as a homoplastic synapomorphy of *Achilixius*, despite missing data for some species, being considered an important character in the diagnosis of genus.

40. Thorax, forewing, position of m-cu2 crossvein in relation to icua crossvein: (0) not aligned; (1) aligned. [CI=0.1; RI=0.4]. Figures 20 A–C.

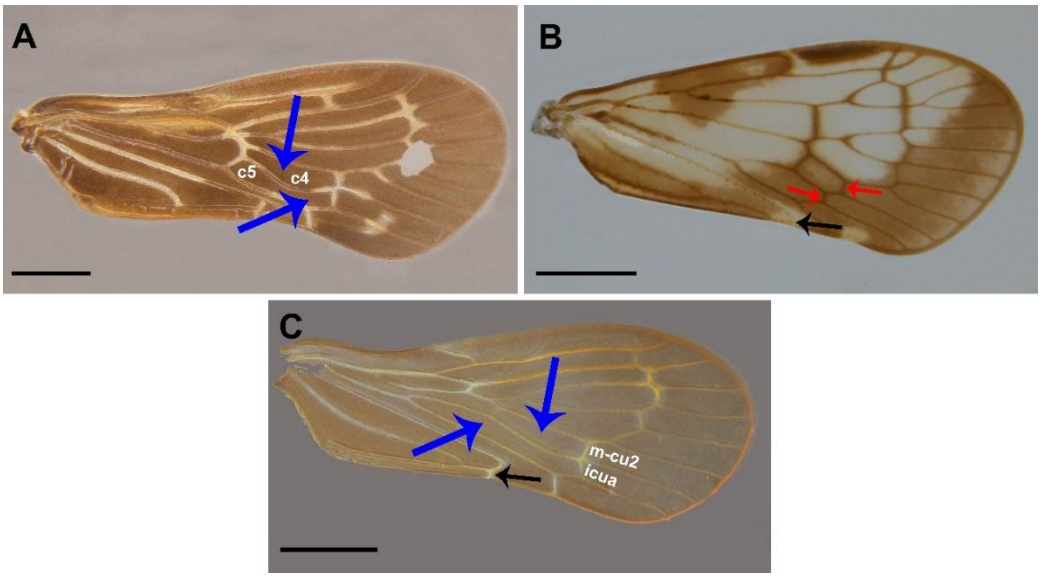

Figures 20 A–C. Forewing. **A**, *Bebaiotes oiapoquensis*. **B**, *Pintalia* sp. 2. **C**, *Bebaiotes parallela*. Scale bars: A–C= 1 mm. Red arrows highlighting the position of the m-cu2 crossvein in relation to icua crossvein (char. 40, state 0). Blue arrows highlighting the length of C4 cell in relation to C5 cell (char. 41): A, *Bebaiotes oiapoquensis* (state 2) and C, *Bebaiotes parallela* (state 0). Black arrows highlighting the apex of the CuP vein (char. 42): B, *Pintalia* sp. 02 (state 0), C, *Bebaiotes parallela* (state 1). Abbreviations:C4, cell C4; C5, cell C5; CuP, cubitus posterior; icua, intercubital crossvein; m-cua2, second mediocubital crossvein.

41. Thorax, forewing, length of C4 cell in relation to C5 cell: (0) less than ½; (1) between ½ and 2/3; (2) longer than ¾. [CI=0.4; RI=0.8]. Figures 20 A–C.

State 2 was recovered as a homoplastic synapomorphy of *Bebaiotes nigrigaster*+ clade and homoplastic autapomorphy of *Anotia* sp. 2 (Derbidae). State 0 of this character as homoplastic autapomorphies of *Pintalia* sp. 1 (Cixiidae) and *Bebaiotes parallela*.

42. Thorax, forewing, apex of the CuP vein, curvature: (0) straight; (1) abruptly curved forming a 90º degree angle. [CI=0.5; RI=0.8]. Figures 20 A–B.

State 1 was recovered as homoplastic synapomorphies of Achilidae and Achilixiidae. In Achilixiidae, all species have the apex of the CuP vein curved abruptly, forming a 90° angle, except for some species of *Achilixius*, where this character could not be visualized due to the forewings not being mounted, and it was coded as '?'.

43. Thorax, forewing, veins, tubercles: (0) present; (1) absent. [CI=0.5; RI=0.5].

44. Thorax, forewing, apex position: (0) overlapping the other; (1) not overlapping. [CI=1.0; RI=1.0]. Figures 21 A–C.

This character has already been employed in previous cladistic studies by Ceotto & Bourgoin (2008). The overlapping of the apex of the forewing is a non-homoplastic synapomorphy of Achilidae.

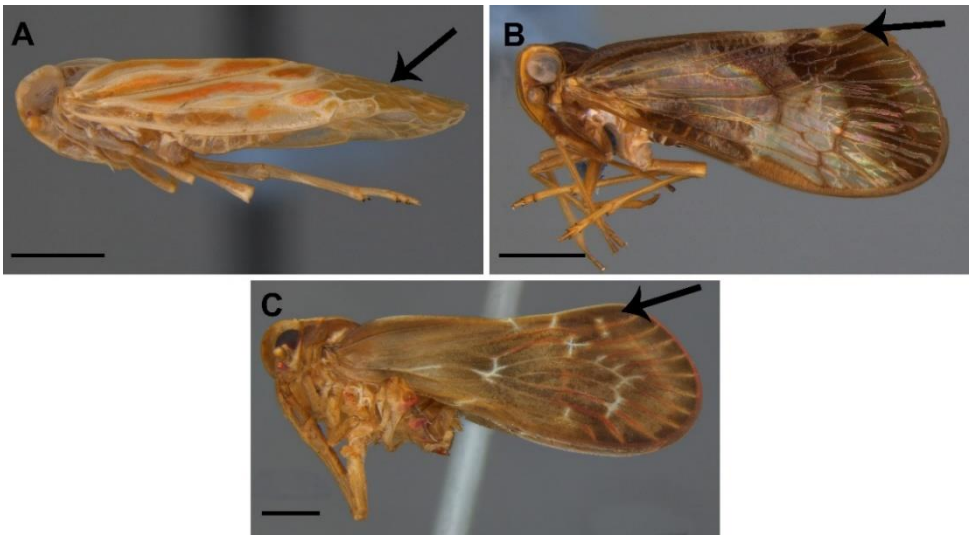

Figures 21 A–C. Forewing. **A**, *Synecdoche* sp. 2. **B**, *Pintalia* sp. 2. **C**, *Bebaiotes dorsivittata*. Scale bars: A–C= 1 mm. Black arrows highlighting the position apex position of the forewings (char. 44): A, *Synecdoche* sp. 2 (state 0), B, *Pintalia* sp. 2 (state 0), and C, *Bebaiotes dorsivittata* (state 0).

45. Thorax, forewing, Pcu vein, apex, curvature: (0) curved; (1) almost straight. [CI=0.2; RI=0.4]. Figures 22 A–B.

Within *Bebaiotes*, state 1 was recovered as homoplastic apomorphies of *Bebaiotes amazonica* + *Bebaiotes macroptera* clade, *Bebaiotes bia* + *Bebaiotes* 6317 sp. C clade, and *Bebaiotes oliveirai*.

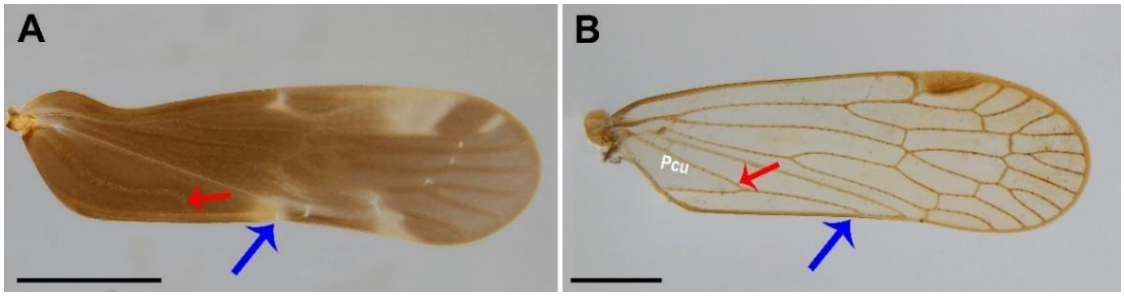

Figures 57 A–B. Forewings. **A**, *Achilixius dietrichi*. **B**, *Melanoliarus* sp. 01. Scale bars: A–B= 1 mm. Red arrows highlighting the apex of the Pcu vein (char. 45): A, *Achilixius dietrich*i (state 0) and B, *Melanoliarus* sp. 01 (state 1). Blue arrows highlighting the post-claval margin (char. 46): A, *Achilixius dietrichi* (state 1) and B, *Melanoliarus* sp. 01 (state 0). Abbreviations: Pcu, postcubitus.

46. Thorax, forewing, postclaval margin, curvature: (0) almost straight; (1) concave. [CI=0.5; RI=0.8]. Figures 22 A–B.

Within *Bebaiotes*, state 1 was recovered as a homoplastic synapomorphy of the *Bebaiotes amazonica*+ clade.

47. Thorax, hind wing, position of MP1+2 and MP3+4 branch in relation to m-cu crossvein: (0) basal; (1) apical; (2) aligned with. [CI=0.2; RI=0.4]. Figures 23 A–C.

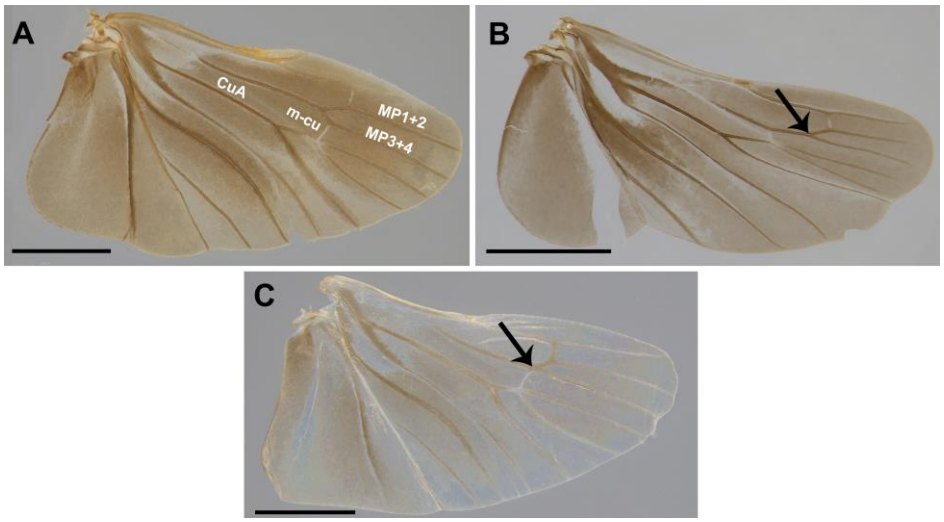

Figures 23 A–C. Hindwings **A**, *Bebaiotes wilsoni*. **B**, *Achilixius dietrichi*. **C**, *Bebaiotes tigrina*. Scale bars: A–C= 1 mm. Black arrows highlighting the MP1+2 and MP3+4 branch (char. 47): B, *Achilixius dietrichi* (state 1) and C, *Bebaiotes tigrina* (state 2). Abbreviations: MP1+2, first media + second media posterior branches MP3+4, third media + fourth media posterior branches; m-cu, mediocubital crossvein.

48. Thorax, profemur, anterior face, seta, thickness: (0) thick; (1) slender. [CI=0.5; RI=0.9]. Figures 24 A–B.

State 1 of this character was recovered as a non-homoplastic synapomorphy of *Bebaiotes*, although a reversion occurred in *Bebaiotes cavichiolii* to the plesiomorphic state.

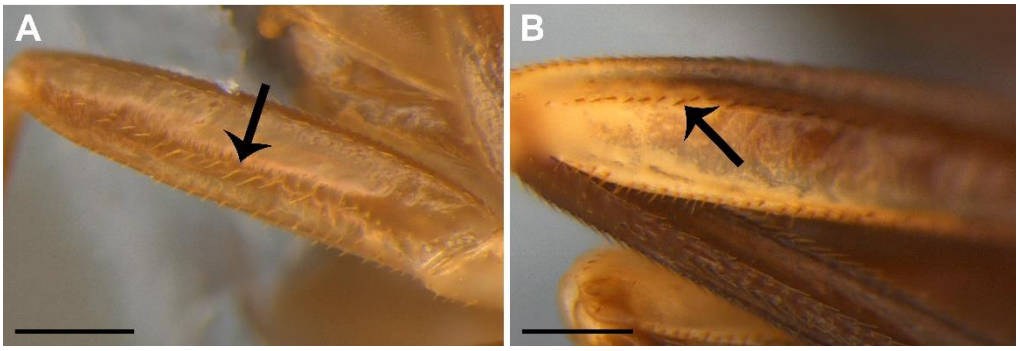

Figures 24 A–B. Profemur, anterior face. **A**, *Bebaiotes amazonica*. 1. **B**, *Sevia* sp. A. Scale bars: A, B= 0.2 mm. Black arrows highlighting the seta (char. 48): A, *Bebaiotes amazonica* (state 1) and B, *Sevia* sp. A (state 0).

49. Thorax, metatibia, lateral spines: (0) present; (1) absent. [CI=0.5; RI=0.5].

This character has already been employed in previous cladistic studies by Löcker et al. (2006) and Ceotto & Bourgoin (2008). State 1 of this character was recovered homoplastic autapomorphies of *Bennarella bicoloripennis*, *Bothriocera* sp. 1, and *Persis* (*Persis*).

50. Thorax, metatibia, number of lateral spines: (0) 1; (1) 2; (2) 3. [CI=1.0; RI=1.0].

This character has already been employed in previous cladistic studies by Löcker et al. (2006) and Ceotto & Bourgoin (2008).

51. Thorax, metatarsus, number of apical teeth on 1st tarsomere: 0) 5; (1) 6; (2) 7; (3) 8. [CI=0.4; RI=0.6].

This character has already been employed in previous cladistic studies by Löcker et al. (2006).

52. Thorax, metatarsus, number of apical teeth on 2nd tarsomere: (0) 4; (1) 5; (2) 6; (3) 7; (4) 8 ; (5) 9; (6) 10. [CI=0.6; RI=0.2].

This character has already been employed in previous cladistic studies by Löcker et al. (2006). Within *Bebaiotes*, state 1 of this character was recoveres as homoplastic apomorphies of *Bebaiotes dichromata*, *Bebaiotes specialis*, and *Bebaiotes dorsivittata* + *Bebaiotes oiapoquensis* clade.

Abdomen

53. Abdomen, shape: 0) laterally compressed; (1) dorsoventrally depressed. [CI=0.3; RI=0.7]. Figures 25 A–C.

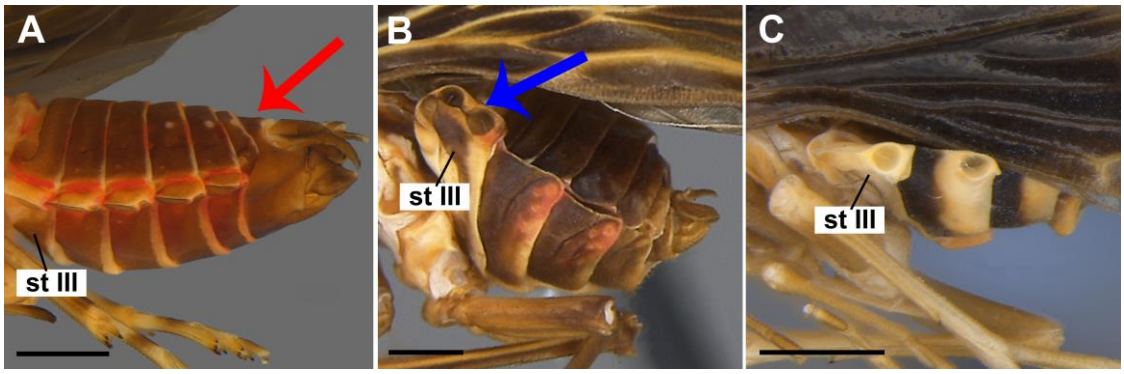

Figures 25 A–C. Abdomen, sternite III. **A**, *Catonia* sp. 2. **B**, *Bebaiotes clarice*. **C**, *Achilixius dietrichi.* Scale bars: A, C= 0.5 mm; B = 1 mm. Red arrow highlighting the shape of the abdomen (char. 53, state 1). Blue arrow highlighting the sternite III (char. 54, state 1). Abbreviations: st III, sternite III.

54. Abdomen, sternite III, lateral abdominal processes: (0) absent; (1) present. [CI=1.0; RI=1.0]. Figures 25 A–C.

Some Cixiidae have abdominal processes in some sternites, but they differ in the location, shape, and number of pits. In this analysis, state 1 of this character was recovered as a non-homoplastic synapomorphy of Achilixiidae (Figs 25 B, C).

55. Abdomen, sternite III, lateral abdominal processes, number of pits: (0) two; (1) three. [CI=1.0; RI=1.0]. Figures 26 A–B.

Within Achilixiidae the number of pits is different within its genera. In *Achilixius* sternite III processes have two pits each (Fig 26 A), while in *Bebaiotes*, sternite III processes have three pits each (Fig 26 B).

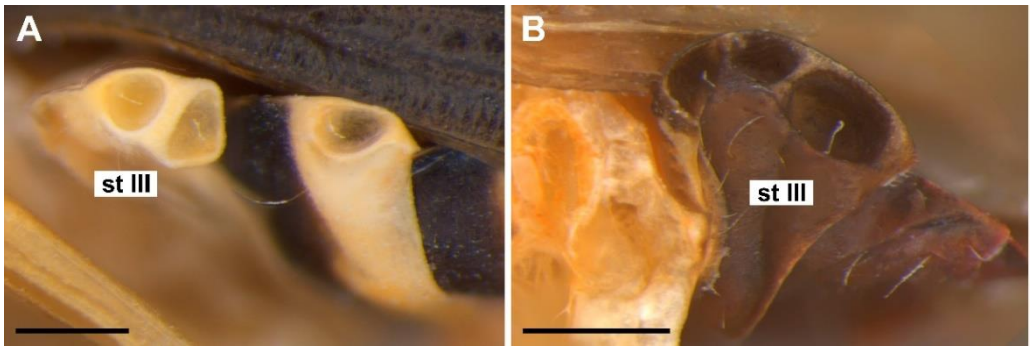

Figures 26 A–B. Abdomen, sternite III. **A**, *Achilixius dietrichi*. **B**, *Bebaiotes macroptera*. Scale bars: A = 0.2 mm; B = 0.3 mm. Abbreviations: st III, sternite III.

56. Abdomen, sternite III, median longitudinal region, ventral view, sclerotization: (0) as sclerotized as lateral regions; (1) membranous. [CI=1.0; RI=1.0]. Figures 27 A–B.

The membranous median longitudinal region of sternite III was recovered as a non-homoplastic synapomorphy of Achilixiidae.

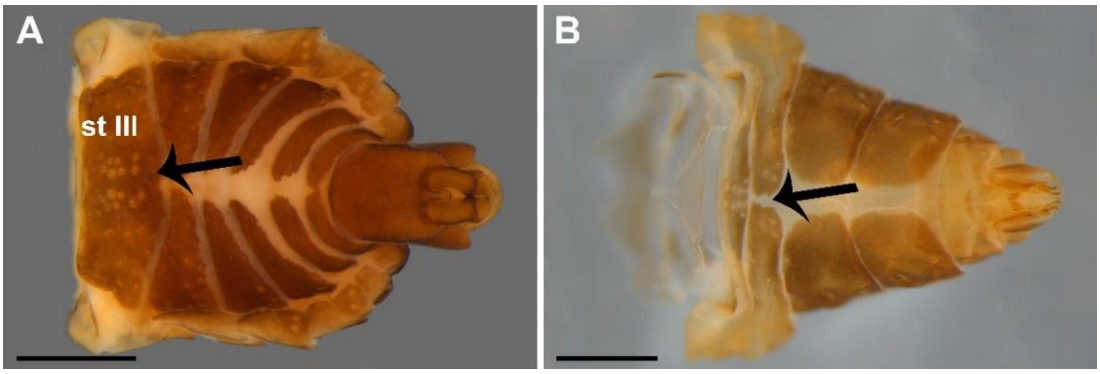

Figures 27 A–B. Abdomen, sternite III, ventral view. **A**, *Pintalia* sp. 2. **B**, *Bebaiotes specialis*. Scale bars: A–B = 0.5 mm. Black arrows highlighting the median longitudinal region of the sternite III (char. 56): A, *Pintalia* sp. 2 (state 0) and B, *Bebaiotes specialis* (state 1). Abbreviations: st III, sternite III.

57. Abdomen, sternite IV, lateral abdominal processes: (0) absent; (1) present. [CI=1.0; RI=1.0]. Figures 28 A–B.

This character has already been employed in previous cladistic studies by Ceotto & Bourgoin (2008). State 1 of this character was recovered as an autapomorphy of *Bennarella bicoloripennis* (Cixiidae).

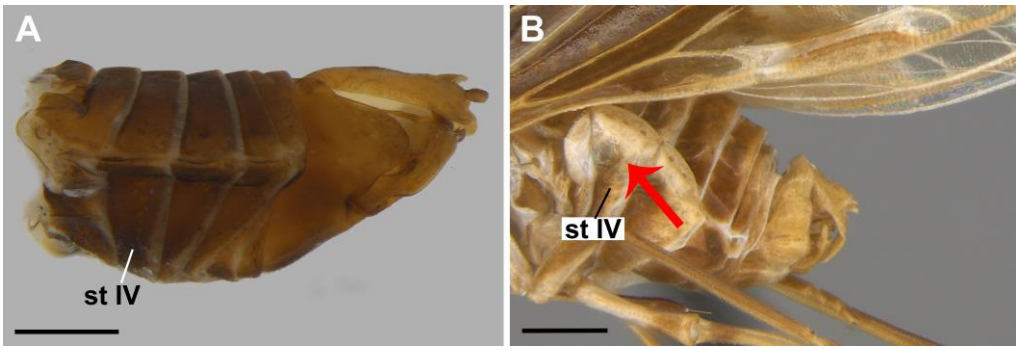

Figures 28 A–B. Abdomen, sternite IV, lateral view. **A**, *Melanoliarus* sp. 2. **B**, *Bennarella bicoloripennis*. Scale bars: A, B = 0.5 mm. Red arrow highlighting the sternite IV (char. 57, state 1). Abbreviations: st IV, sternite IV.

58. Abdomen, sternite IV, connection to sternite V: (0) connected by membrane; (1) fused. [CI=1.0; RI=1.0]. Figures 29 A–C.

In the basic plan of Fulgoroidea, the abdomen has 3-7 subrectangular sternites (O'Brien & Wilson, 1985). State 1 of this character was recovered as a non-homoplastic synapomorphy of Achilixiidae.

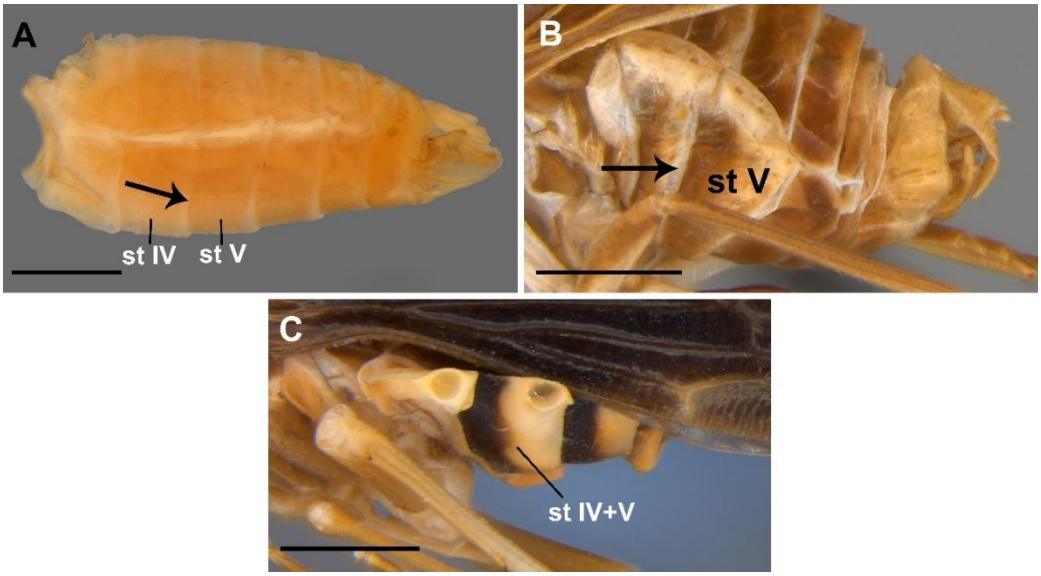

Figures 29 A–C. Abdomen, sternites IV and V, lateral view. **A**, *Synecdoche* sp. 2. **B**, *Bennarella bicoloripennis*. **C**, *Achilixius dietrichi.* Scale bars: A–C = 0.5 mm. Black arrow highlighting the connection of sternites IV (char. 58, state 0). Abbreviations: st IV, sternite IV; st V, sternite V.

59. Abdomen, sternite IV, median longitudinal region, ventral view, sclerotization: (0) as sclerotized as lateral regions; (1) membranous. [CI=0.5; RI=0.7]. Figures 30 A–C.

State 1 was recovered as homoplastic synapomorphies of Achilixiidae and Cixiidae.

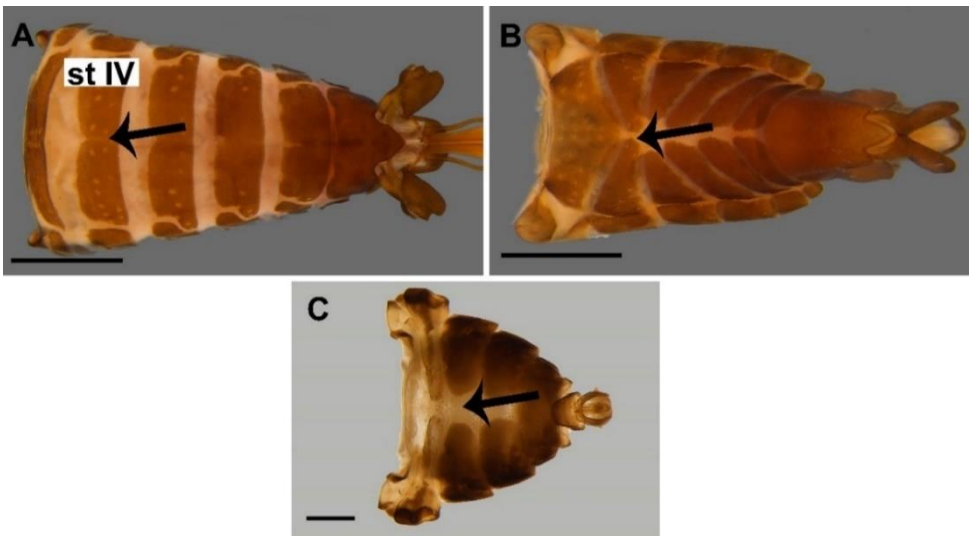

Figures 30 A–C. Abdomen, sternite IV, ventral view. **A**, *Sevia* sp. A. **B**, *Pintalia* sp. 2. **C**, *Bebaiotes clarice*. Scale bars: A= 1 mm; B, C = 0.5 mm. Black arrows highlighting the median longitudinal region of the sternite IV (char. 59): A, *Sevia* sp. A (state 0), B, *Pintalia* sp. 2 (state 1) and C, *Bebaiotes clarice* (state 1). Abbreviations: st IV, sternite IV.

60. Abdomen, sternite V, lateral abdominal processes: (0) absent; (1) present. [CI=0.5; RI=0.9]. Figures 31 A–C.

This character has already been employed in previous cladistic studies by Ceotto & Bourgoin (2008). In Achilixiidae, the number of abdominal processes in sternites differ between their genera. In *Bebaiotes*, it is present only in sternite III, while in *Achilixius*, it is present in sternites III and V. Within Cixiidae, two tribes (Bennini and Bennarellini) also have abdominal processes, which also vary in the shape and quantity of these

abdominal processes. In our study, we used a representative of Bennarelini that has abdominal processes in sternites IV and V.

State 1 arose independently in *Achilixius* and in *Bennarella bicoloripennis* (Cixiidae), the Bennarellini representative. Although homoplastic, the presence of the abdominal processes of sternite V in *Achilixius* was important to support the monophyly and diagnosis of this genus.

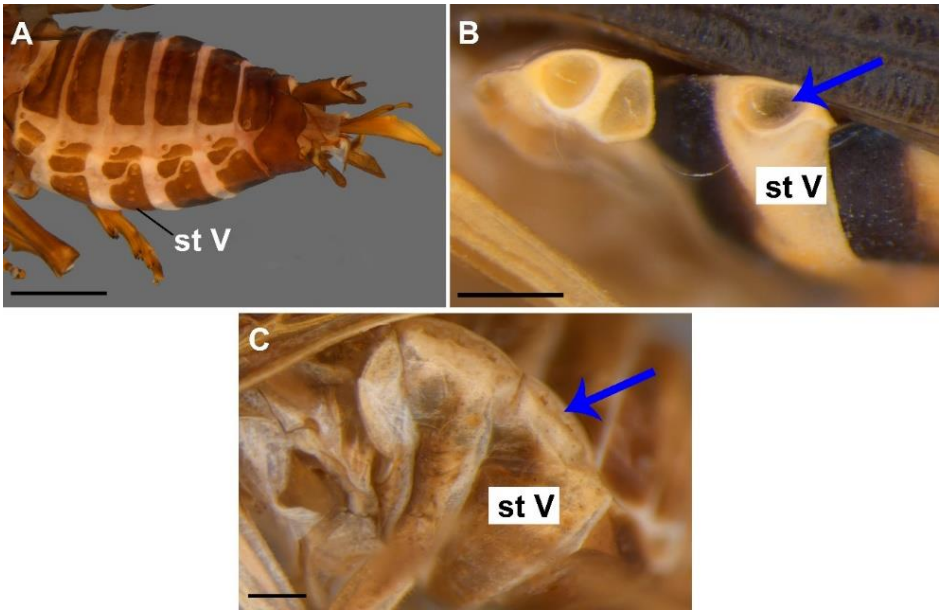

Figures 31 A–C. Abdomen, sternite IV, ventral view. **A**, *Sevia* sp. A. **B**, *Achilixius dietrichi*. **C**, *Bennarella bicoloripennis*. Scale bars: A= 1 mm; B, C = 0.2 mm. Blue arrows highlighting the number of pits in sternite V (char. 61): B, *Achilixius dietrichi* (state 0), C, *Bennarella bicoloripennis* (state 1). Abbreviations: st V, sternite V.

61. Abdomen, sternite V, lateral abdominal processes, number of pits: (0) one; (1) two. [CI=1.0; RI=1.0]. Figures 31 A–B.

62. Abdomen, sternite V, lateral abdominal processes, pits depth: (0) shallow: (1) deep. [CI=1.0; RI=1.0]. Figures 31 B–C.

63. Abdomen, sternite VIII, connection to pygofer: (0) connected by membrane; (1) fused. [CI=0.5; RI=0.8]. Figures 32 A–B.

In the general structure of Fulgoroidea, sternite VIII can be distinct from or fused with the pygofer (O'Brien & Wilson, 1985). State 1 of this character was recovered as a homoplastic synapomorphies for Achilidae and Achilixiidae.

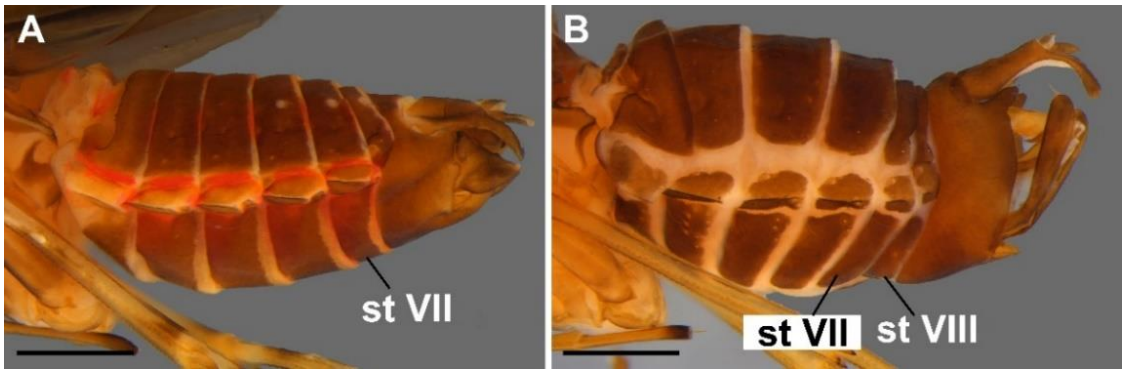

Figures 32 A–B. Abdomen, sternites VII and VIII, ventral view. **A**, *Catonia* sp. 2. **B**, *Pintalia* sp. 2. Scale bars: A= 1 mm; A, B = 0.5 mm. Abbreviations: st VII, sternite VII; st VIII, sternite VIII.

Male abdomen

64. Male abdomen, pygofer, medioventral process: (0) present; (1) absent. [CI=0.3; RI=0.6]. Figures 33 A–C.

This character has already been employed in previous cladistic studies by Ceotto & Bourgoin (2008). The state 1 of the character was recovered within Achilixiidae clade, although reversions occurred in *Achilixius fasciata*, *Achilixius kolintangi*, *Achilixius minahassae*, *Achilixius muiri*, and *Bebaiotes clarice* to the plesiomorphic state. The males of *Achilixius* sp. 1, *Bebaiotes nivosa*, and *Bebaiotes specialis* are unknown, and it was coded as '?'.

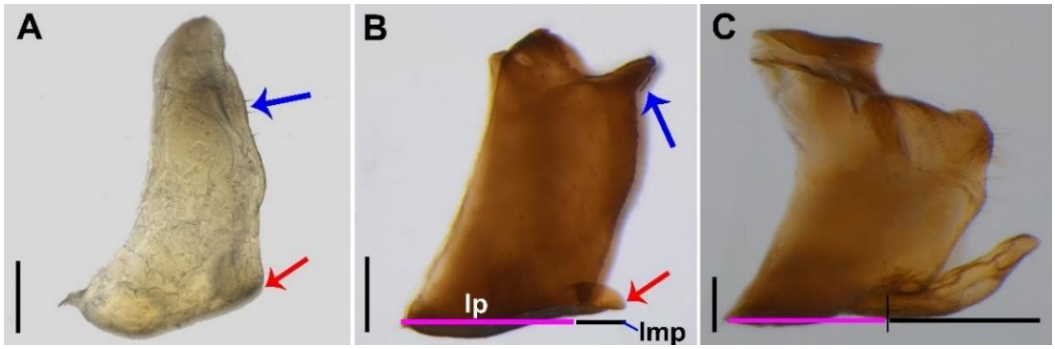

Figures 33 A–C. Pygofer, lateral view. **A**, *Achilixius dietrichi.* **B**, *Pintalia* sp. 2. **C**, *Catonia* sp. 2. Scale bars: A, C= 0.1 mm; B= 0.2 mm. Red arrow*s* highlighting the absence (A) or presence (B) of the medioventral process. Blue arrow*s* highlighting the posterior margin of pygofer (char. 65): A, *Achilixius dietrichi* (state 0) and B, *Pintalia* sp. 2 (state 1). Abbreviations: lmp, length medioventral process; lp, length pygofer.

65. Male abdomen, pygofer, lateral view, posterior margin, dorsal half, dorsal projection: (0) absent; (1) present. [CI=0.3; RI=0.0]. Figures 33 A–C.

The state 1 of this character was identified as homoplastic autapomorphies, having independently arisen in *Pintalia* sp. 1, *Bebaiotes macroptera,* and *Bebaiotes clarice*. Due to the absence of the male of *Bebaiotes specialis* for coding in the analysis, there is ambiguity at the base of the node for *Bebaiotes clarice* + *Bebaiotes specialis*.

66. Male abdomen, pygofer, medioventral process, lateral view, length in relation to length pygofer up to base of process: (0) subequal; (1) less than 1/4; (2) between 1/4 and 1/2. [CI=0.6; RI=0.8]. Figures 33 B–C.

The character was only coded for the taxa that possess a medioventral process of the pygofer.

67. Gonostylus, lateral view, apex, shape: 0) rounded; (1) truncated. [CI=0.2; RI=0.4]. Figures 34 A–C.

The state 0 of this character was recovered as homoplastic autapomorphies of *Achilixius fennahi*, *Achilixius irigae*, *Achilixius singularis*, *Achilixius tubulifer*, *Bebaiotes dichromata*, *Bebaiotes amazonica*, and *Bebaiotes guianesus*.

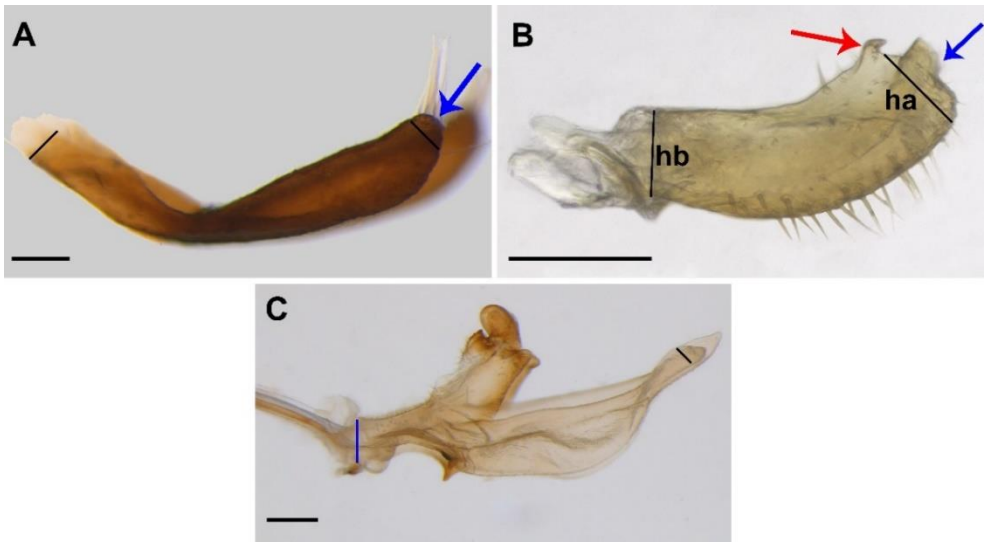

Figures 34 A–C. Gonostylus, lateral view. **A**, *Pintalia* sp. 02. **B**, *Achilixius dietrichi.* **C**, *Persis* (*Persis*). Scale bars: A, B= 0.1 mm; C= 0.2 mm. Blue arrows highlighting the apex of gonostylus (char. 67): A, *Pintalia* sp. 2 (state 0) and B, *Achilixius dietrichi* (state 1). Red arrow highlighting the projection on the outer margin (char. 69, state 1). Abbreviations: ha, length apex; hb, length base.

68. Gonostylus, lateral view, height basal in relation to height apical: (0) shorter; (1) subequal; (2) higher. [CI=0.2; RI=0.5]. Figures 34 A–C.

State 1 of this character was recovered as homoplastic apomorphies of *Synecdoche* sp. 2 (Achilidae) and *Bebaiotes*, although a reversion occurred in *Bebaiotes bia* to the plesiomorphic state.

State 2 of this character was recovered as homoplastic autapomorphies of *Achilixius singularis*, *Pintalia* sp. 1 (Cixiidae), *Sevia* sp. A (Achilidae), and *Persis* (*Persis*) (Derbidae).

69. Gonostylus, projection, lateral view, outer margin, apical half: (0) absent; (1) present. [CI=0.3; RI=0.7]. Figures 34 A–C.

The absence of the projection on the outer margin of the gonostylus is observed only in a single species of Achilixiidae, in *Achilixius singularis*.

70. Phallic complex, symmetry: (0) asymmetrical; (1) symmetrical. [CI=0.5; RI=0.8]. Figures 35 A–F.

This character has already been employed in previous cladistic studies by Ceotto & Bourgoin (2008). Some Fulgoroidea families may exhibit processes on the periandrium and aedeagus, which can vary in quantity and location (Bourgoin & Huang, 1990). In Achilixiidae, the phallic process is quite simple, lacking any processes. The state 1 of the character was recovered as a homoplastic synapomorphy of the Achilixiidae clade and homoplastic autapomorphy of *Anotia* sp. 2 (Derbidae).

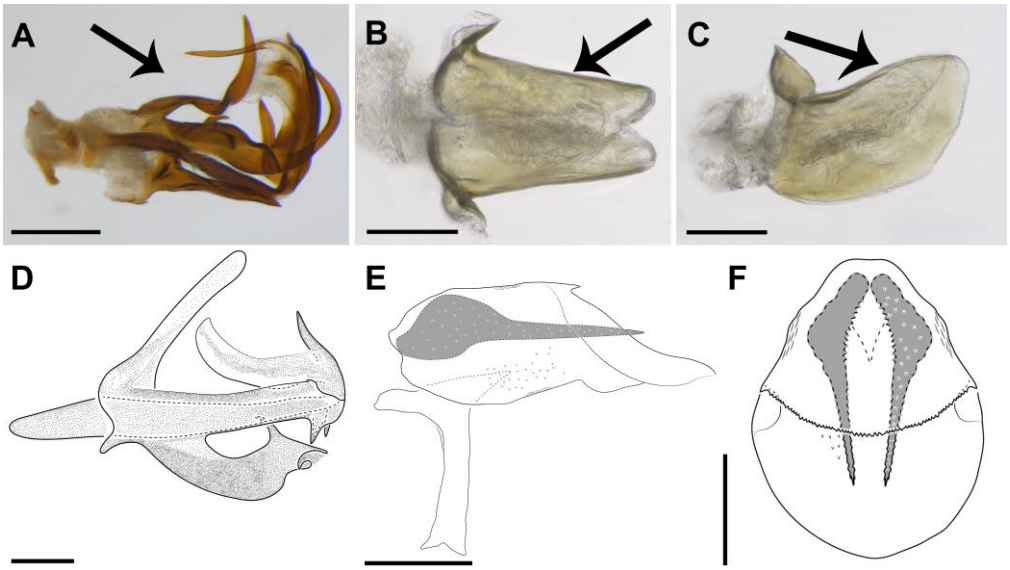

Figures 35 A–F. Phallic complex. **A**, *Melanoliarus* sp. 1, left lateral view, lateral view. 02. **B**, *Achilixius dietrichi,* dorsal view. **C**, *Achilixius dietrichi*, left lateral view, lateral view. **D**, *Bennarella bicoloripennis,* left lateral view, lateral view. **E**, *Bebaiotes bia*, left lateral view, lateral view. **F**, *Bebaiotes bia*, dorsal view. Scale bars: A= 0.3 mm; B–F = 0.1 mm; C= 0.2 mm. Black arrow*s* highlighting the phallic complex (char. 70): A, *Melanoliarus* sp. 1 (state 0) and B, C *Achilixius dietrichi* (state 1).

71. Periandrium, dorsal margin apex, dorsal view, shape: (0) concave; (1) straight; (2) roundly convex; (3) tapered. [CI=0.3; RI=0.1]. Figures 36 A–D.

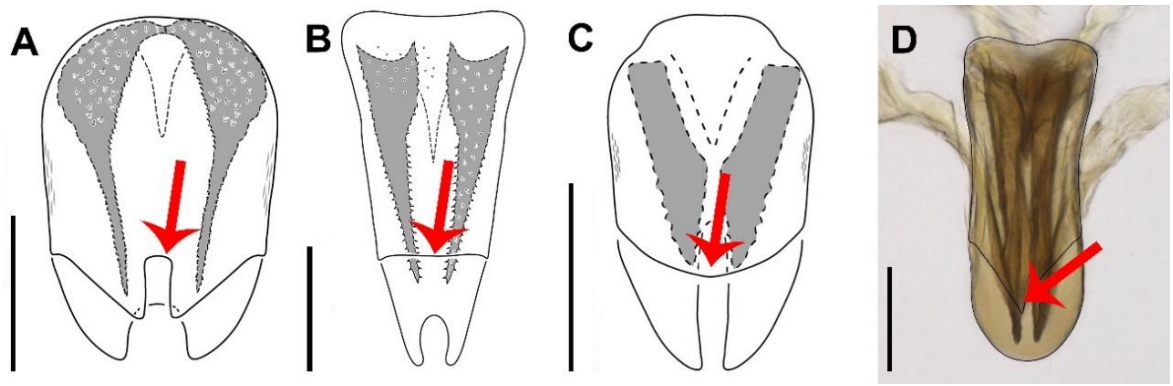

Figures 36 A–D. Periandrium, dorsal margin apex, dorsal view. **A**, *Bebaiotes amazonica*. **B**, *Bebaiotes dorsivittata*. **C**, *Bebaiotes macroptera*. **D**, *Bebaiotes clarice*. Scale bars: A–D = 0.1 mm. Red arrows highlighting the dorsal margin apex (char. 71): A, *Bebaiotes amazonica* (state 0), B, *Bebaiotes dorsivittata* (state 1), C, *Bebaiotes macroptera* (state 2), and D, *Bebaiotes clarice* (state 3).

72. Phallic complex, shape: (0) laterally compressed: (1) dorsoventrally depressed. [CI=0.5; RI=0.9]. Figures 37 A–D.

State 1 of this character independently arose in *Synecdoche* sp. 2 and in the *Bebaiotes* clade. Despite being a homoplastic synapomorphy, state 1 arose only once within Achilixiidae, supporting the clade composed exclusively of *Bebaiotes* species.

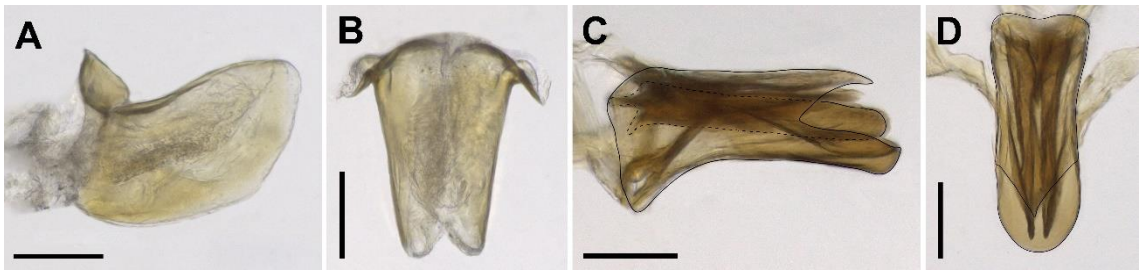

Figures 37 A–D. Phallic complex, shape. **A**, *Achilixius dietrichi*, left lateral view, lateral view. **B**, *Achilixius dietrichi*, dorsal view. **C**, *Bebaiotes clarice*, left lateral view, lateral view. **D**, *Bebaiotes clarice*, dorsal view. Scale bars: A–D = 0.1 mm.

73. Phallic complex, articulation: (0) articulated; (1) unarticulated. [CI=0.5; RI=0.8]. Figures 38 A–B.

State 1 was recovered as a homoplastic synapomorphies of Achilixiidae and Achilidae.

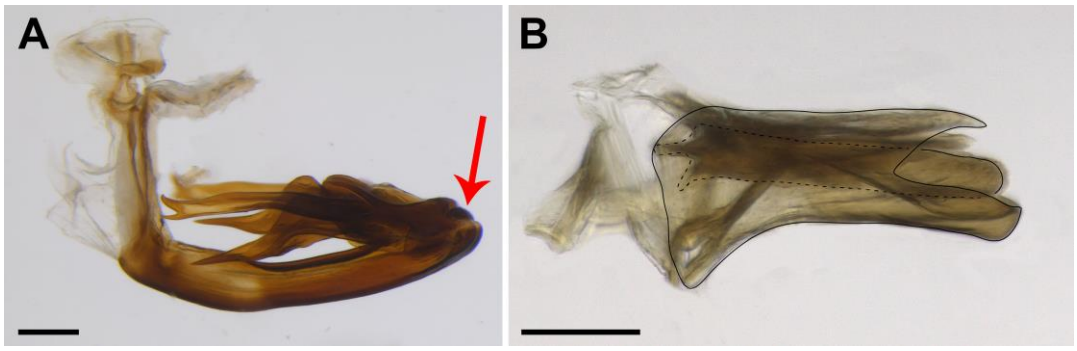

Figures 38 A–B. Phallic complex, articulation. **A**, *Persis* (*Persis*), left lateral view, lateral view. **B**, *Bebaiotes clarice*, left lateral view, lateral view. Scale bars: A= 0.2 mm; B= 0.1 mm. Red arrow highlighting the articulation of the phallic complex (char. 73, state 0).

74. Phallic complex, inner sclerotized plates: (0) absent; (1) present. [CI=1.0; RI=1.0]. Figures 39 A–C.

The origin of these inner sclerotized plates remains unknown, with only suppositions that they might be periandrium processes. State 1 of this character has been recovered as a non-homoplastic synapomorphy of *Bebaiotes*, furthermore, has been considered important for the diagnosis of this genus.

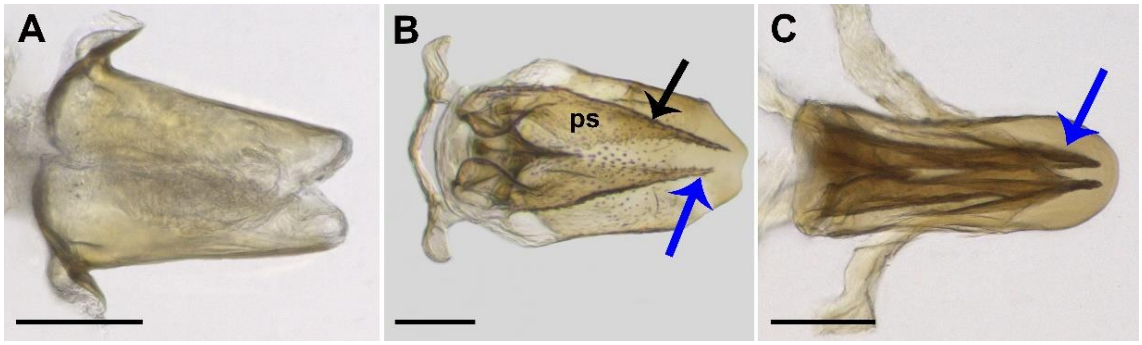

Figures 39 A–C. Inner sclerotized plates, dorsal view. **A**, *Achilixius dietrichi*, dorsal view. **B**, *Bebaiotes oiapoquensis*. **C**, *Bebaiotes clarice*. Scale bars: A–C = 0.1 mm. Black arrow highlighting the inner sclerotized plates (char. 74, state 1). Blue arrows highlighting the direction of the inner sclerotized plates (char. 75): B, *Bebaiotes oiapoquensis* (state 0) and C, *Bebaiotes clarice* (state 1). Abbreviation: ps, inner sclerotized plates.

75. Phallic complex, inner sclerotized plates, dorsal view, direction towards apex: (0) converging; (1) parallel. [CI=0.2; RI=0.3]. Figures 39 B–C.

This character was only coded for taxa that have inner sclerotized plates. Within *Bebaiotes*, the converging apex of the inner sclerotized plates was recovered as apomorphies of *Bebaiotes amazonica, Bebaiotes wilsoni, Bebaiotes guianesus*, *Bebaiotes bia* + *Bebaiotes* 6317 sp. C clade, and *Bebaiotes dorsivittata* + *Bebaiotes oiapoquensis* clade.

76. Phallic complex, inner sclerotized plate, dorsal view, basal width in relation to apical width: (0) subequal; (1) wider. [CI=0.5; RI=0.0]. Figures 39 B–C.

This character was only coded for taxa that have inner sclerotized plates. Within *Bebaiotes*, the state 0 of this character was recovered as homoplastic autapomorphies of *Bebaiotes macroptera* and *Bebaiotes pulla*.

77. Periandrium concave, dorsal margin, apex, dorsal view, length of concavity in relation to length of whole dorsal margin: (0) less than 1/5; (1) between 1/5 and 1/3; (2) longer than 1/2. [CI=1.0; RI=1.0]. Figures 40 A–C.

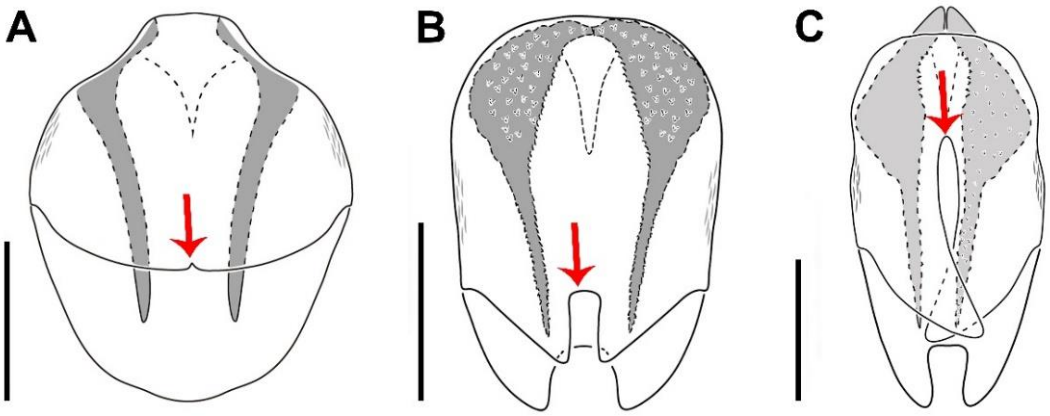

Figures 40 A–C. Periandrium, dorsal margin apex, dorsal view. **A**, *Bebaiotes banksi*. **B**, *Bebaiotes amazonica*. **C**, *Bebaiotes parallela*. Scale bars: A–C = 0.1 mm. Red arrows highlighting the concavity of the apex of the dorsal margin (char. 77): A, *Bebaiotes banksi* (state 0), B, *Bebaiotes amazonica* (state 1) and C, *Bebaiotes parallela* (state 2).

78. Periandrium, dorsal margin, apex, dorsal view, aspect: (0) smooth; (1) serrate. [CI=0.5; RI=0.5]. Figures 41 A–B.

Within *Bebaiotes*, state 1 of this character was recovered as homoplastic apomorphies of *Bebaiotes guianesus* + *Bebaiotes oliveirai* clade and *Bebaiotes bia*.

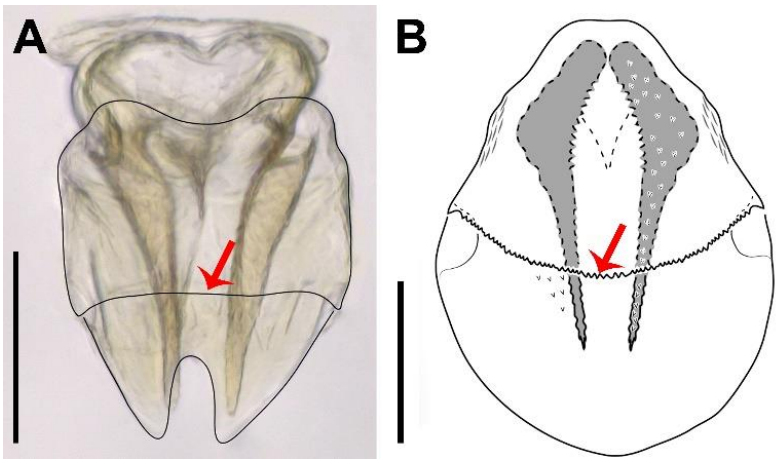

Figures 41 A–B. Periandrium, dorsal margin apex, dorsal view. **A**, *Bebaiotes cavichiolii*. **B**, *Bebaiotes bia*. Scale bars: A, B= 0.1 mm. Red arrows highlighting the aspect of the apex of the dorsal margin (char. 78): A, *Bebaiotes cavichiolii* (state 0) and B, *Bebaiotes bia* (state 1).

79. Periandrium concave, ventral margin, apex, dorsal view, shape: (0) concave: (1) roundly convex; (2) tapered; (3) straight. [CI=0.7; RI=0.7]. Figures 42 A–D.

Within *Bebaiotes*+ clade, the state 1 of this character was recovered as homoplastic apomorphies of *Bebaiotes banksi*+ clade and *Bebaiotes clarice*. To date, there are no illustrations of the periandrium in the dorsal view of *Bebaiotes bucayensis*, *Bebaiotes pallidinervis*, and *Bebaiotes nigrigaster* and the males of *Bebaiotes nivosa* and *Bebaiotes specialis* is unknown, and they were all coded as '?'.

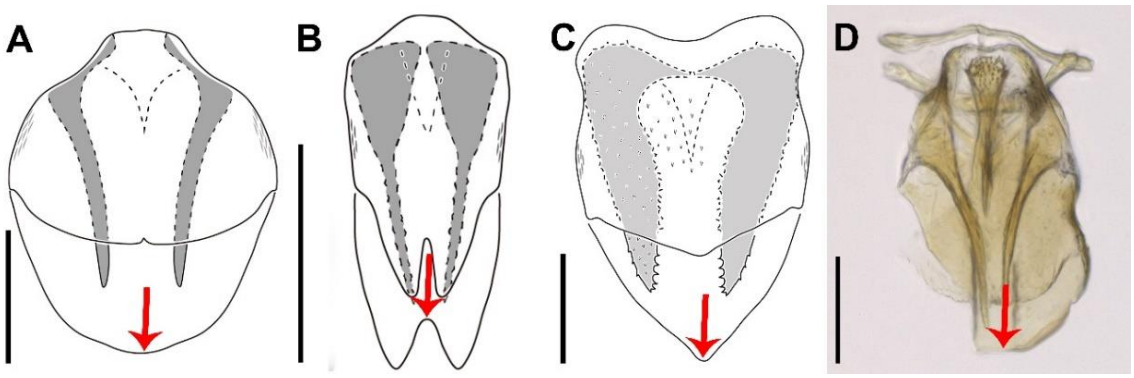

Figures 42 A–D. Periandrium, ventral margin apex, dorsal view. **A**, *Bebaiotes banksi*. **B**, *Bebaiotes tigrina*. **C**, *Bebaiotes pulla*. **D**, *Bebaiotes oliveirai*. Scale bars: A–D = 0.1 mm. Red arrows highlighting the ventral margin apex (char. 79): A, *Bebaiotes banksi* (state 1),

B, *Bebaiotes tigrina* (state 0), C, *Bebaiotes pulla* (state 2) and D, *Bebaiotes oliveirai* (state 3).

80. Periandrium, dorsal view, ventral margin, apex, dorsal view, length of concavity in relation to length of whole dorsal margin: (0) smoothly (less than 1/4): (1) short: (2) long. [CI=1.0; RI=1.0]. Figures 43 A–C.

State 2 of this character was recovered within *Bebaiotes* as an autapomorphy of *Bebaiotes macroptera*.

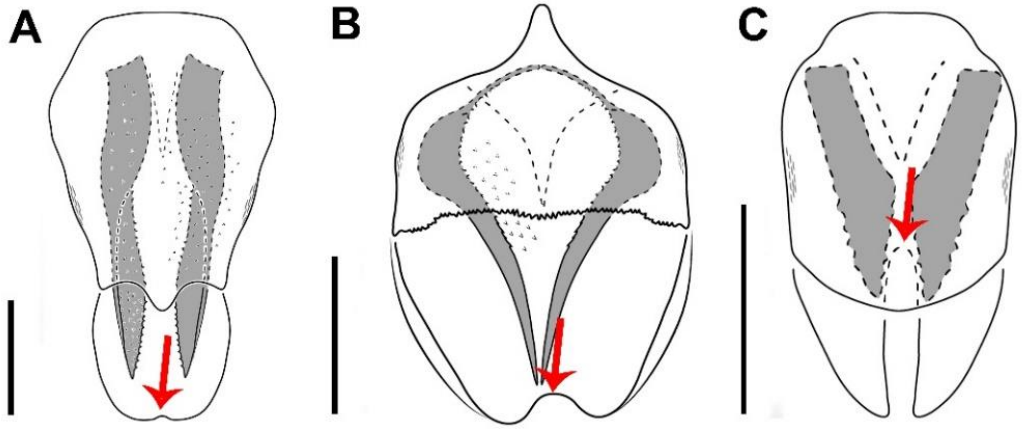

Figures 43 A–C. Periandrium, ventral margin apex, dorsal view. **A**, *Bebaiotes pennyi*. **B**, *Bebaiotes guianesus*. **C**, *Bebaiotes macroptera*. Scale bars: A–C = 0.1 mm. Red arrows highlighting the concavity of the apex of the ventral margin (char. 80): A, *Bebaiotes pennyi* (state 0), B, *Bebaiotes guianesus* (state 1) and C, *Bebaiotes macroptera* (state 2).

81. Male abdomen, Anal tube (segment X), dorsal view, apex, shape: (0) rounded: (1) triangular: (2) truncated: (3) concave. [CI=0.2; RI=0.5]. Figures 44 A–D.

This character has already been employed in previous cladistic studies by Ceotto & Bourgoin (2008). State 0 of this character was recovered as homoplastic apomorphies of *Sevia* sp. A (Achilidae), *Achilixius fennahi*, *Achilixius irigae*, *Bebaiotes amazonica*, *Bebaiotes cavichiolii*, and *Bebaiotes guianesus*+ clade and within *Bebaiotes guianesus*+ clade, a change occurred in *Bebaiotes oiapoquensis* to state 3.

State 2 of this character was recovered as homoplastic apomorphies of *Bebaiotes dichromata*, *Bebaiotes pulla*, *and Bebaiotes bia* + *Bebaiotes* 6317 sp. C clade.

Figures 44 A–D. Anal tube (segment X), apex, shape, dorsal view. **A**, *Bebaiotes clarice*. **B**, *Bennarella bicoloripennis*. **C**, *Achilixius dietrichi*. **D**, *Persis* (*Persis*). Scale bars: A–C = 0.1 mm; D= 0.2 mm.

82. Male abdomen, Anal tube (segment X), dorsal view, shape: (0) rounded; (1) subpentagonal; (2) subretangular; (3) subtrapezoidal; (4) subtriangular; (5) suboval. [CI=0.6; RI=0.7]. Figures 45 A–D.

Figures 45 A–D. Anal tube (segment X), shape, dorsal view. **A**, *Bebaiotes clarice*. **B**, *Bothriocera* sp. 1. **C**, *Persis* (*Persis*). ***D***, *Synecdoche* sp. 2. Scale bars: A, B, D = 0.1 mm; C= 0.2 mm.

83. Male abdomen, Anal tube (segment X), lateral view, length of dorsal margin in relation to ventral margin: (0) less than 1/4 of ventral margin; (1) between 1/4 and 1/2; (2) longer than 3/4. [CI=0.5; RI=0.8]. Figures 46 A–C.

State 0 was recovered as a non-homoplastic synapomorphy of *Bebaiotes*.

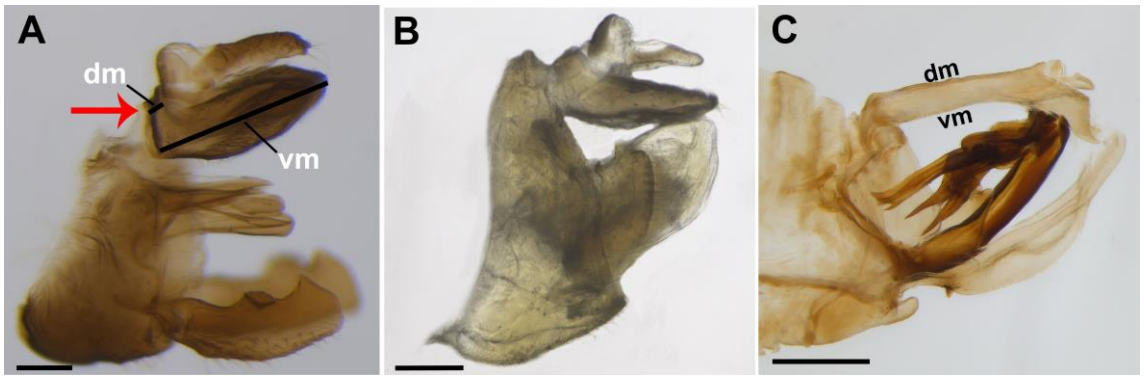

Figures 46 A–C. Anal tube (segment X), lateral view. **A**, *Bebaiotes clarice*. **B**, *Achilixius dietrichi* **C**, *Persis* (*Persis*). Scale bars: A, B = 0.1 mm; C= 0.2 mm. Red arrow highlighting the length of dorsal margin in relation to ventral margin of Anal tube (segment X) (char. 83, state 0). Abbreviations: md, dorsal margin; mv, ventral margin.

Female abdomen

84. Ovipositor, degree of development: (0) well developed; (1) reduced. [CI=1.0; RI=1.0].

Figures 47 A–D.

This character has already been employed in previous cladistic studies by Ceotto & Bourgoin (2008). This character was previously utilized by Ceotto & Bourgoin (2008). In Fulgoromorpha, ovipositors can be classified into two types, depending on the size of their gonapophyses (Bourgoin, 1993), each with its distinct function. When gonapophyses are elongated, it characterizes the orthopteroid-type ovipositor, whose main function is piercing and excavating, likely used for inserting eggs into plant tissue (Bourgoin, 1993; Wilson et al., 1994; Holzinger et al., 2002) (Figs 47 A, B). Families such as Cixiidae and Delphacidae have this type of ovipositor. On the other hand, there is the derived ovipositor, fulgoroid-type, which is associated with egg deposition in plant tissue and covering the eggs with wax (Bourgoin, 1993; Wilson et al., 1994) (Figs 47 C, D), the state 1 was recovered as a non-homoplastic synapomorphy of Achilidae+ clade.

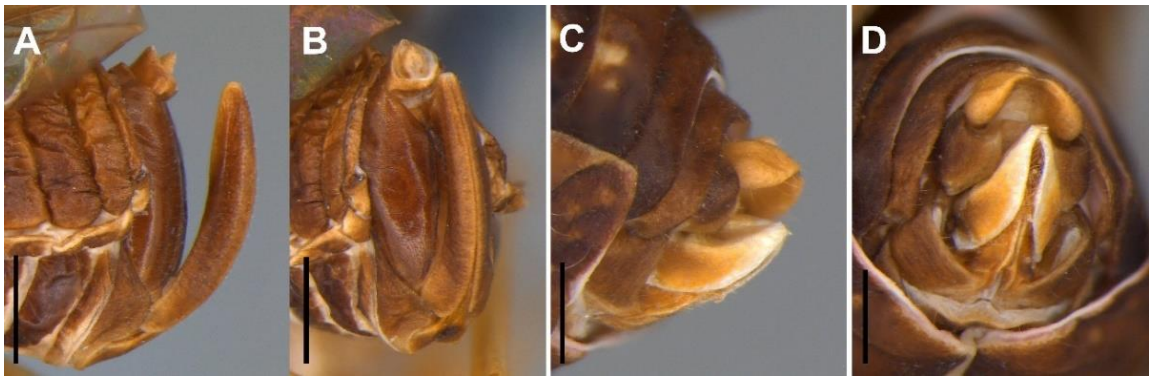

Figures 47 A–D. Ovipositor. **A**, *Bothriocera* sp. 1, lateral view. 1. **B**, *Bothriocera* sp. 1, posterior view. **C**, *Bebaiotes pulla*, lateral view. **D**, *Bebaiotes pulla*, posterior view. Scale bars: A, B = 0.4 mm; C, D= 0.3 mm.

85. Gonapophysis VIII (first valvula), dorsoapical margin, projection: (0) absent; (1) present. [CI=1.0; RI=1.0]. Figures 48 A–C.

The fulgoroid-type ovipositor has some modifications that may be related to the fact that one of its functions is likely to cover these eggs. Achilidae, Achilixiidae, and Derbidae have this type of ovipositor. State 0 was recovered as a non-homoplastic synapomorphy of Achilidae+ clade.

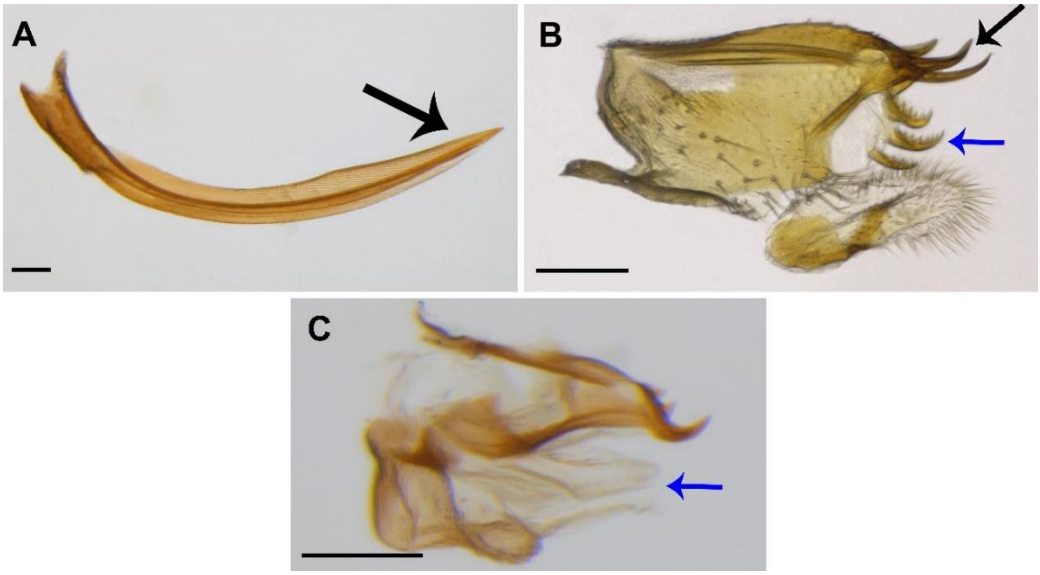

Figures 48 A–C. Gonapophysis VIII (first valvula), lateral view. **A**, *Bennarella bicoloripennis*. 1. **B**, *Bebaiotes clarice.* **C**, *Synecdoche* sp. 2. Scale bars: A–C = 0.1 mm. Black arrows highlighting the dorsoapical margin (char. 85): A, *Bennarella bicoloripennis* (state 0) and B, *Bebaiotes clarice* (state 1). Blue arrows highlighting the lateroapical margin (char. 86): B, *Bebaiotes clarice* (state 1) and C, *Synecdoche* sp. 2 (state 0).86. Gonapophysis VIII (first valvula), lateroapical margin, projection: (0) absent; (1) present. [CI=1.0; RI=1.0]. Figures 48 A–D.

87. Gonapophysis VIII (first valvula), projections on lateroapical margin, number: (0) one; (1) two; (2) three; (3) four. [CI=0.5; RI=0.6]. Figures 49 A–D.

Within *Bebaiotes*, the state 0 of this character was recovered as homoplastic autapomorphies of *Bebaiotes cavichiolii* and *Bebaiotes specialis*. State 1 of this character was recovered as homoplastic autapomorphies of *Bebaiotes macroptera* and *Bebaiotes pulla*. State 3 of this character was recovered as a non-homoplastic synapomorphy of the *Bebaiotes guianesus*+ clade.

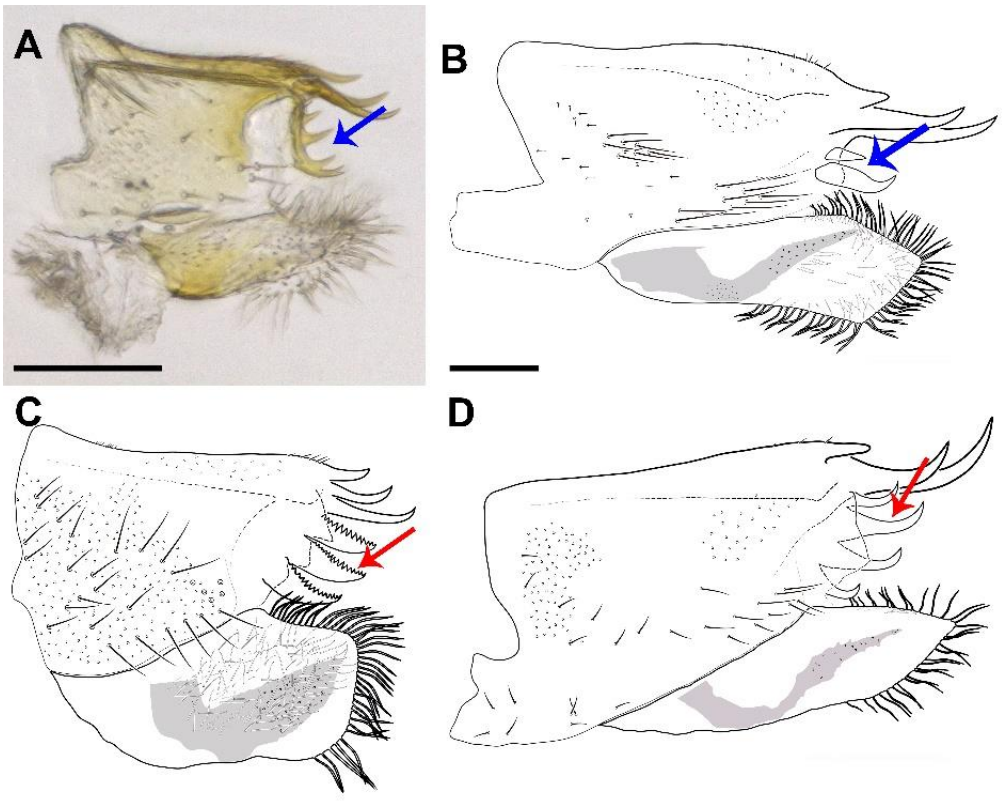

Figures 58 A–D. Gonapophysis VIII (first valvula), lateral view. **A**, *Bebaiotes cavichiolii*. **B**, *Bebaiotes pulla*. **C**, *Bebaiotes amazonica*. **D**, *Bebaiotes banksi*. Scale bars: A–D = 0.1 mm. Blue arrows highlighting the number of projections on the apical side margin (char. 87): A, *Bebaiotes cavichiolii* (state 0), B, *Bebaiotes pulla* (state 1), C, *Bebaiotes amazonica* (state 2) and D, *Bebaiotes banksi* (state 3). Red arrows highlighting the aspect of the latero-apical margin (char. 88): C, *Bebaiotes amazonica* (state 1), D, *Bebaiotes banksi* (state 0).

88. Gonapophysis VIII (first valvula), projections on lateroapical margin, dorsal margin, aspect: (0) smooth; (1) with projections. [CI=0.2; RI=0.2]. Figures 50 A–D.

Within *Bebaiotes*, the state 0 of this character was recovered as homoplastic apomorphies of *Bebaiotes nivosa* and *Bebaiotes pennyi* + *Bebaiotes pulla* clade.

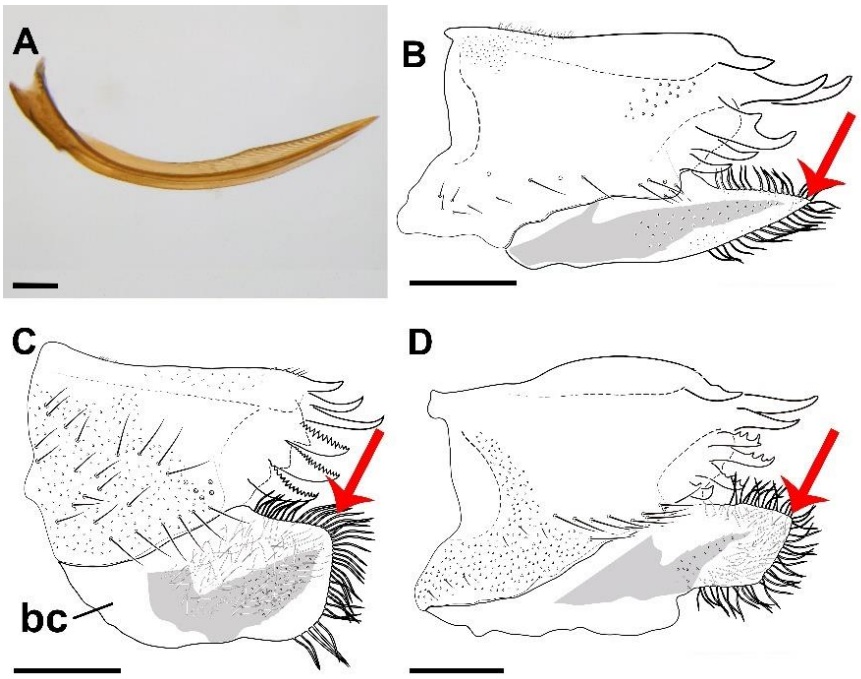

Figures 50 A–D. Gonapophysis VIII (first valvula), lateral view. **A**, *Bennarella bicoloripennis*. 1. **B**, *Bebaiotes wilsoni*. **C**, *Bebaiotes amazonica*. **D**, *Bebaiotes guianesus*. Scale bars: A–D = 0.1 mm. Red arrows highlighting the apex of the bursa copulatrix (char. 90): B, *Bebaiotes wilsoni* (state 0), C, *Bebaiotes amazonica* (state 1) and D, *Bebaiotes guianesus* (state 2).

89. Gonapophysis VIII (first valvula), bursa copulatrix: (0) absent; (1) present. [CI=1.0; RI=1.0]. Figures 50 A–D.

The bursa copulatrix is located postero-dorsally to the vagina, also known as the posterior vagina, and may have small ornamentations (Bourgoin, 1993). The presence of the bursa copulatrix is a non-homoplastic synapomorphy of the Achilidae+ clade.

90. Gonapophysis VIII (first valvula), bursa copulatrix, lateral view, angle of apex: (0) acute (<90°); (1) obtuse (>90°); (2) straight (=90°). [CI=0.2; RI=0.4]. Figures 51 A–D.

State 1 of this character was recovered as homoplastic apomorphies of *Sevia* sp. A (Achilidae), *Anotia* sp. 2 (Derbidae), and *Bebaiotes dichromata*+ clade, except for *Bebaiotes nivosa*, where this character could not be visualized due to limited detail of the illustration of the bursa copulatrix and it was coded as '?'.

State 2 of this character was recovered as homoplastic apomorphies of *Catonia* sp. 2 (Achilidae), *Bebaiotes parallela*, *Bebaiotes guianesus*, and *Bebaiotes specialis*+ clade, although a reversion occurred in *Bebaiotes pennyi* to the plesiomorphic state, and state 1 of this character was recovered as a homoplastic autapomorphy of *Bebaiotes clarice*.

91. Gonapophysis IX (second valvula), dorsal view, maximum width in relation to total length: (0) less than 1/4; (1) between 1/4 and 1/2; (2) longer than 3/4. [CI=1.0; RI=1.0]. Figures 51 A–D.

State 1 of this character was recovered as an autapomorphy of *Bebaiotes pennyi*.

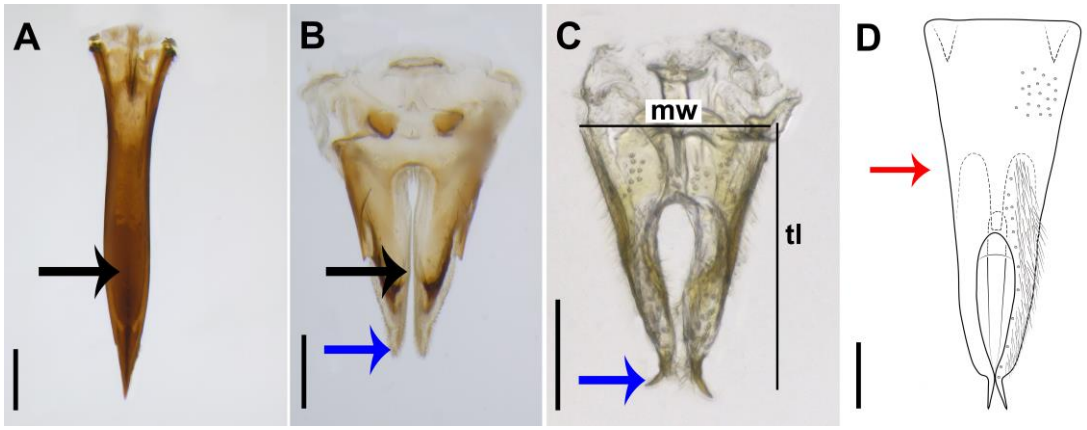

Figures 51 A–D. Gonapophysis IX (second valvula), dorsal view. **A**, *Bothriocera* sp. 1. **B**, *Anotia* sp. 2. **C**, *Bebaiotes cavichiolii***. D**, *Bebaiotes pennyi*. Scale bars: A–D = 0.1 mm. Red arrow highlighting maximum width in relation to total length of Gonapophysis IX (second valvula) (char. 91, state 1). Black arrows highlighting central region (char. 92): A, *Bothriocera* sp. 1 (sate 0) and B, *Anotia* sp. 2 (state 1). Blue arrows highlighting the apexes of lobes (char. 93): B, *Anotia* sp. 2 (state 0) and C, *Bebaiotes cavichiolii* (state 1). Abbreviations: mv, maximum width; tl, total length.

92. Gonapophysis IX (second valvula), division: (0) entire; (1) bifid. [CI=1.0; RI=1.0]. Figures 51 A–D.

The bifid Gonapophysis IX (second valvula) was recovered as a non-homoplastic synapomorphy of the Achilidae+ clade (Figs 51 B–D).

93. Gonapophysis IX (second valvula) bifid, apexes of lobes, sclerotization: (0) sclerotized; (1) membranous. [CI=1.0; RI=1.0]. Figures 51 B–D.

This character was coded only for taxa that possess the bifid Gonapophysis IX (second valvula). The state 0 of this character was recovered as a non-homoplastic synapomorphy of the Achilixiidae (Fig 51 C).

94. Gonapophysis IX (second valvula) bifid, dorsal view, apexes of lobes, direction: (0) parallel; (1) divergent; (2) convergent. [CI=1.0; RI=1.0]. Figures 52 A–D.

The state 1 of this character was recovered as a non-homoplastic synapomorphy of the Achilixiidae (Figs 52 C, D).

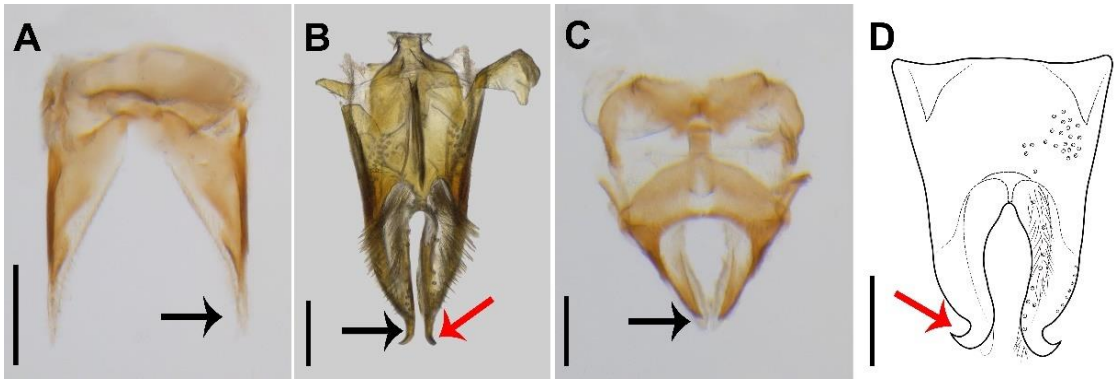

Figures 52 A–D. Gonapophysis IX (second valvula), dorsal view. **A**, *Persis* (*Persis*). **B**, *Bebaiotes clarice*. **C**, *Synecdoche* sp. 2. **D**, *Bebaiotes amazonica*. Scale bars: A–D = 0.1 mm. Black arrows highlighting the direction of the apexes of lobes (char. 94): A, *Persis* (*Persis*) (state 0), B, *Bebaiotes clarice* (state 1), C, *Synecdoche* sp. 2 (state 2). Red arrows highlighting the curvature of the apexes of lobes (char. 96): B, *Bebaiotes clarice* (state 0) and D, *Bebaiotes amazonica* (state 1).

95. Gonapophysis IX (second valvula) bifid, dorsal view, apexes of lobes, curvature: (0) not curved:(1) curved. [CI=0.5; RI=0.8]. Figures 52 A–D.

The state 1 of this character was recovered as a non-homoplastic synapomorphy of the Achilixiidae, although a reversion occurred in *Bebaiotes pennyi* to the plesiomorphic state.

96. Gonapophysis IX (second valvula) bifid, dorsal view, apexes of curved lobes, degree of curvature: (0) strongly curved, hook shaped; (1) lightly curved. [CI=0.5; RI=0.5]. Figures 52 B, D.

97. Gonapophysis IX (second valvula) bifid, dorsal view, lobes, inner margin, shape: (0) concave; (1) almost straight; (2) convex. [CI=0.5; RI=0.7]. Figures 53 A–D.

State 2 of this character was recovered as an autapomorphy of *Bebaiotes macroptera* (Fig 53 D).

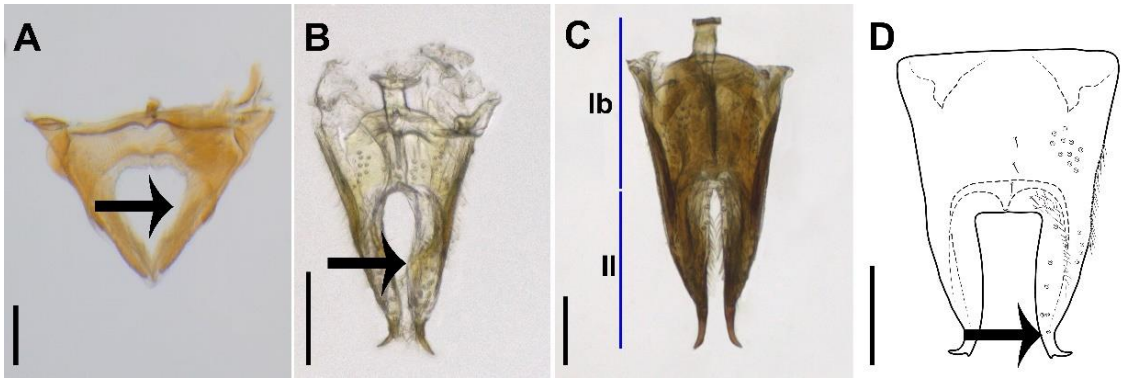

Figures 53 A–D. Gonapophysis IX (second valvula), dorsal view. **A**, *Catonia* sp. 2. **B**, *Bebaiotes cavichiolii*. **C**, *Bebaiotes oliveirai*. **D**, *Bebaiotes macroptera*. Scale bars: A–D = 0.1 mm. Black arrows highlighting the inner margin of the apexes of lobes (char. 97): A, *Catonia* sp. 2 (state 1), B, *Bebaiotes cavichiolii* (state 0), and D, *Bebaiotes macroptera* (state 2). Abbreviations: lb, length of base; ll, length of lobes.

98. Gonapophysis IX (second valvula) bifid, dorsal view, length of base in relation to length of lobes: (0) subequal; (1) shorter than lobes; (2) longer than lobes. [CI=0.3; RI=0.5]. Figures 53 A–D.

99. Gonoplac (third valvula), division: (0) entire; (1) divided longitudinally at apical portion. [CI=0.3; RI=0.3]. Figures 54 A–C.

State 0 of this character was recovered as a non-homoplastic synapomorphy of Achilixiidae found independently also in *Synecdoche* sp. 2 (Achilidae) (Fig 54 C).

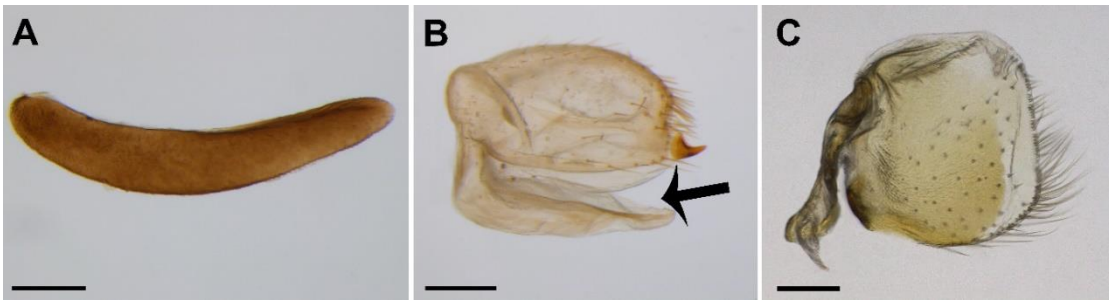

1738

Figures 54 A–C. Gonoplac, lateral view. **A**, *Bothriocera* sp. 1. **B**, *Anotia* sp. 2. **C**, *Bebaiotes clarice*. Scale bars: A–C = 0.1 mm. Black arrow highlighting gonoplac division (char. 99, state 1).

1739

1740

Table 2. Morphological data matrix used for the phylogeny of Achilixiidae.

	1	2	3	4	5	6	7	8	9	10	11	12	13	14	15	16	17	18	19	20	21	22	23	24	25	26	27	28	29	30	31	32	33	34	35	36	37	38	39	40	41	42	43	44	45	46	47	48	49	50
Cixiidae *Bennarella bicoloripennis*	0	0	1	0	2	0	1	0	0	1	0	0	0	0	0	1	0	2	0	0	0	0	1	1	0	0	1	0	0	1	0	1	1	1	0	0	1	-	0	-	-	0	1	1	0	1	1	0	1	-
Cixiidae *Bothriocera* sp. 1	0	0	1	0	0	1	1	0	0	0	0	0	2	0	0	1	0	0	0	0	0	0	1	1	0	1	0	0	0	1	0	1	1	2	0	2	0	1	0	0	2	0	1	1	1	1	1	0	1	-
Cixiidae *Melanoliarus* sp. 1	0	0	1	0	2	1	1	0	0	0	1	0	0	0	0	1	0	0	0	0	0	0	1	1	1	0	1	0	0	1	0	1	1	1	0	0	?	0	0	0	1	0	0	1	1	0	0	0	0	2
Cixiidae *Pintalia* sp. 1	0	0	1	0	2	1	1	0	0	0	1	0	0	0	0	1	0	0	0	0	0	0	1	1	0	0	0	0	0	1	0	1	1	0	0	2	0	2	0	0	0	0	0	1	1	0	1	0	0	0
Derbidae *Anotia* sp. 2	1	1	0	1	1	0	0	1	1	1	1	0	1	0	0	1	2	2	0	1	0	1	-	-	1	1	0	0	0	1	0	0	1	0	2	1	0	2	1	-	2	0	1	1	1	1	0	0	0	1
Derbidae *Persis* (*Persis*)	1	1	0	0	1	0	0	0	1	1	0	1	0	0	0	1	1	0	0	0	0	0	1	2	1	0	1	0	1	1	0	1	1	0	0	1	0	0	0	0	1	0	0	1	0	1	-	0	1	-
Achilidae *Catonia* sp. 2	0	0	1	0	2	1	0	0	0	0	1	0	0	0	0	1	1	0	0	0	0	0	1	0	1	0	1	0	1	1	1	-	-	1	0	1	0	0	0	0	1	1	1	0	0	1	1	0	0	0
Achilidae *Sevia* sp. A	0	0	0	0	0	1	0	0	0	0	1	0	0	0	1	-	2	0	0	0	0	0	1	0	0	0	0	0	1	1	0	1	0	0	0	2	0	0	0	1	1	1	1	0	0	1	0	0	0	0
Achilidae *Synecdoche* sp. 2	0	0	1	0	2	1	0	0	0	0	1	0	0	0	0	1	0	0	0	1	0	0	1	0	1	0	1	0	1	1	1	-	-	1	1	1	0	1	0	0	1	1	1	0	0	1	1	0	0	0
Achilixius davaoensis	1	0	0	?	0	?	0	?	1	1	?	0	?	?	?	?	?	?	1	0	0	0	1	2	0	0	?	?	?	?	?	?	?	?	?	?	?	?	?	?	?	?	?	?	?	?	?	?	?	?	?	?
Achilixius fasciata	1	0	0	0	0	?	0	?	1	1	?	0	1	?	?	?	?	?	1	0	0	0	1	2	0	0	?	?	?	?	?	?	?	?	?	?	?	?	?	?	?	?	?	?	?	?	?	0	?	0	1
Achilixius fennahi	1	0	0	?	0	?	0	?	1	1	?	?	?	?	?	?	?	?	1	0	0	0	1	2	0	0	?	?	?	?	?	?	?	?	?	?	?	?	?	?	?	?	?	?	?	?	?	0	?	0	?
Achilixius kolintangi	1	0	0	0	0	0	0	?	1	1	?	0	1	?	?	?	?	?	1	0	0	0	1	2	0	0	?	?	?	?	?	?	?	?	?	?	?	?	?	?	?	?	?	?	?	?	?	0	?	0	?
Achilixius irigae	1	0	0	0	0	?	0	?	1	?	?	?	?	?	?	?	?	?	1	0	0	0	1	2	0	0	?	?	?	?	?	?	?	?	?	?	?	?	?	?	?	?	?	?	?	?	?	0	?	0	?
Achilixius mayoyae	1	0	0	?	0	?	0	?	1	1	?	?	?	?	?	?	?	?	1	?	?	?	?	?	?	0	?	?	?	?	?	?	?	?	?	?	?	?	?	?	?	?	?	?	?	?	?	?	?	?	?	?
Achilixius minahassae	1	0	0	0	0	0	0	?	1	1	?	0	1	?	?	?	?	?	1	0	0	0	1	2	0	0	?	?	?	?	?	?	?	?	?	?	?	?	?	?	?	?	?	?	?	?	?	0	?	?	?
Achilixius muiri	1	0	0	0	0	?	0	?	1	1	?	?	?	?	?	?	?	?	1	?	0	0	1	2	0	0	?	?	?	?	?	?	?	?	?	?	?	1	-	?	?	1	?	?	?	?	?	?	?	?	?
Achilixius sandakanensis	1	0	0	?	0	?	0	?	1	?	?	0	?	?	?	?	?	?	1	0	0	0	1	2	0	0	?	?	?	?	?	?	?	?	?	?	?	1	-	?	?	1	1	?	?	?	?	?	?	?	?
Achilixius singularis	1	0	0	0	0	?	0	?	1	1	?	?	?	?	?	?	?	?	1	?	0	0	1	2	0	0	?	?	?	?	?	?	?	?	?	?	?	1	-	?	?	1	1	0	?	?	?	?	?	?	?
Achilixius dietrichi	1	0	0	0	0	0	0	0	1	1	1	0	0	1	1	0	1	0	1	1	0	0	0	1	2	0	0	1	0	1	1	0	1	1	0	0	1	?	2	1	-	1	1	1	1	0	1	1	0	0	1
Achilixius sp. 1	1	0	0	0	0	0	0	0	1	1	1	0	0	1	1	0	1	0	1	1	0	0	0	1	2	0	0	1	0	1	1	0	1	1	0	0	1	?	2	1	-	1	1	1	1	0	1	1	0	0	1
Achilixius tubulifer	1	0	0	0	0	0	0	0	1	1	1	0	0	1	1	0	1	?	?	1	0	0	0	?	2	0	0	1	0	1	1	0	1	1	0	0	1	?	0	1	-	1	1	1	?	0	1	1	?	?	?
Bebaiotes amazonica	1	1	0	1	0	0	0	1	1	1	0	1	0	1	0	1	0	1	1	0	0	0	1	0	0	0	1	1	1	1	0	1	1	1	1	0	0	0	0	0	1	1	1	1	1	1	0	2	1	0	1
Bebaiotes dichromata	1	1	0	0	0	0	0	0	0	1	0	0	1	0	1	0	0	0	0	1	0	0	0	0	0	0	0	1	1	1	1	0	1	1	1	1	0	0	0	0	1	1	1	1	1	0	1	2	1	0	1
Bebaiotes macroptera	1	1	0	1	0	0	0	1	1	1	0	1	0	1	0	0	1	1	1	1	0	0	1	0	0	0	1	1	1	1	0	1	1	1	1	0	0	0	0	0	1	1	1	1	1	1	0	1	1	0	1
Bebaiotes parallela	1	1	0	1	0	0	0	1	1	0	0	1	0	1	0	1	0	0	1	0	0	0	1	0	0	0	1	1	1	1	0	1	1	1	1	0	0	1	0	1	0	1	1	1	0	1	0	1	0	1
Bebaiotes tigrina	1	1	0	1	0	0	0	0	0	1	1	0	1	0	1	0	1	0	1	1	0	0	0	1	0	0	0	1	1	1	1	0	1	1	1	1	0	0	1	0	1	1	1	1	1	0	0	2	1	0	1
Bebaiotes nivosa	1	1	0	?	0	0	0	?	1	?	?	1	?	1	?	?	?	?	1	0	0	0	1	0	0	0	1	1	1	1	0	1	1	1	1	0	0	1	0	1	1	1	1	1	1	0	0	?	?	0	1
Bebaiotes bucayensis	1	1	0	0	?	0	0	1	1	1	0	1	0	1	0	1	?	?	1	2	1	0	1	0	0	0	1	1	1	1	0	0	1	1	1	0	0	1	0	1	2	1	1	1	0	1	0	?	0	1
Bebaiotes dorsivittata	1	1	0	0	0	0	0	0	1	1	1	0	1	0	1	0	1	0	0	1	1	0	0	0	0	0	0	1	1	1	1	0	0	1	1	1	0	0	0	0	1	2	1	1	1	0	1	0	1	0	1
Bebaiotes nigrigaster	1	1	0	?	1	0	0	1	1	1	0	1	?	?	0	1	?	0	1	1	0	0	1	0	0	0	1	1	1	1	0	1	1	0	1	0	0	1	0	1	2	1	1	1	0	1	?	?	0	1
Bebaiotes banksi	1	1	0	0	1	0	0	1	1	1	0	1	0	1	0	1	0	1	1	1	0	0	1	0	0	0	1	1	1	1	0	1	1	0	1	0	0	1	0	0	2	1	1	1	0	1	0	1	0	1
Bebaiotes bia	1	1	0	0	1	0	0	1	1	1	0	1	0	1	0	1	0	1	1	1	0	0	1	0	0	0	1	1	1	1	0	1	1	0	1	0	0	1	0	0	2	1	1	1	1	1	0	1	0	1
Bebaiotes guianesus	1	1	0	0	1	0	0	1	1	1	0	1	0	1	0	1	0	2	1	1	0	0	0	0	0	0	1	1	1	1	0	1	1	0	1	0	0	1	0	1	2	1	1	1	0	1	0	1	0	1
Bebaiotes pallidinervis	1	1	0	0	?	0	0	?	1	1	?	1	0	1	0	1	?	0	1	1	1	0	0	0	0	0	1	1	1	1	0	1	1	0	1	0	1	-	0	1	1	1	1	1	0	1	?	?	0	1
Bebaiotes pennyi	1	1	0	1	1	0	0	1	1	1	0	1	0	1	0	1	0	2	1	1	1	0	0	0	0	0	1	1	1	1	0	0	1	1	1	0	0	0	0	1	2	1	1	1	0	1	0	1	0	1
Bebaiotes pulla	1	1	0	0	1	0	0	1	1	1	0	1	0	1	0	1	1	2	1	1	1	0	0	0	0	0	1	1	1	1	0	0	1	1	1	0	0	2	0	0	2	1	1	1	0	1	0	1	0	1
Bebaiotes wilsoni	1	1	0	0	1	0	0	1	1	1	0	1	0	1	0	1	1	2	1	2	0	0	1	0	0	0	1	1	1	1	0	1	1	0	1	0	0	1	0	1	2	1	1	1	0	1	0	1	0	1
Bebaiotes cavichiolii	1	1	0	1	1	0	0	0	1	1	0	1	0	1	0	1	0	1	1	1	0	0	1	0	0	0	1	1	1	1	0	1	1	1	1	0	0	0	0	0	1	1	1	1	0	0	1	0	0	1
Bebaiotes clarice	1	1	0	1	1	0	0	1	1	1	0	1	0	1	0	1	1	2	1	1	0	0	1	0	0	0	1	1	1	0	0	1	1	1	1	0	0	1	0	0	2	1	1	1	0	1	0	1	0	1
Bebaiotes oiapoquensis	1	1	0	0	1	0	0	1	1	1	0	1	0	1	0	1	1	2	1	1	1	0	1	0	0	0	1	1	1	1	0	0	1	1	1	0	0	0	0	1	2	1	1	1	0	1	2	1	0	1
Bebaiotes oliverai	1	1	0	0	1	0	0	1	1	1	0	1	0	1	0	1	1	2	1	1	0	0	1	0	0	0	1	1	1	1	0	1	1	0	1	0	0	1	0	1	2	1	1	1	1	1	0	1	0	1
Bebaiotes specialis	1	1	0	1	1	0	0	1	1	1	0	1	0	1	0	1	0	2	1	2	0	0	1	0	0	0	1	1	1	1	0	1	1	1	1	0	0	1	0	1	2	1	1	1	0	1	0	1	0	1
Bebaiotes 6317 sp. C	1	1	0	1	1	0	0	1	1	1	0	1	0	1	0	1	0	1	1	1	0	0	1	0	0	0	1	1	1	1	0	1	1	0	1	0	0	1	0	1	2	1	1	1	1	1	0	1	0	1

741

Table 2. Continued.

	51	52	53	54	55	56	57	58	59	60	61	62	63	64	65	66	67	68	69	70	71	72	73	74	75	76	77	78	79	80	81	82	83	84	85	86	87	88	89	90	91	92	93	94	95	96	97	98	99
Cixiidae *Bennarella bicoloripennis*	2	3	0	0	-	0	1	0	1	1	1	0	0	0	0	2	1	0	0	0	-	0	0	0	-	-	-	-	-	-	1	1	1	0	0	0	-	-	0	-	0	0	-	-	-	-	-	-	0
Cixiidae *Bothriocera* sp. 1	3	4	0	0	-	0	0	0	1	0	-	-	0	0	0	2	1	0	0	0	-	0	0	0	-	-	-	-	-	-	2	2	1	0	0	0	-	-	0	-	0	0	-	-	-	-	-	-	0
Cixiidae *Melanoliarus* sp. 1	2	2	1	0	-	0	0	0	1	0	-	-	0	0	0	2	0	0	0	0	-	0	0	0	-	-	-	-	-	-	2	5	2	0	0	0	-	-	0	-	0	0	-	-	-	-	-	-	0
Cixiidae *Pintalia* sp. 1	2	1	0	0	-	0	0	0	1	0	-	-	0	0	1	1	0	2	0	0	-	0	0	0	-	-	-	-	-	-	2	2	1	0	0	0	-	-	0	-	0	0	-	-	-	-	-	-	0
Derbidae *Anotia* sp. 2	0	0	0	0	-	0	0	0	0	0	-	-	0	1	0	-	1	0	1	0	-	0	0	0	-	-	-	-	-	-	3	3	1	1	1	0	-	-	1	1	2	1	1	0	0	-	1	1	1
Derbidae *Persis* (*Persis*)	3	6	0	0	-	0	0	0	0	0	-	-	0	0	0	2	0	2	1	1	-	0	0	0	-	-	-	-	-	-	3	3	2	1	1	1	0	1	1	0	2	1	1	0	0	-	1	1	1
Achilidae *Catonia* sp. 2	1	2	1	0	-	0	0	0	0	0	-	-	1	0	0	0	1	0	0	0	-	0	1	0	-	-	-	-	-	-	2	2	1	1	1	0	-	-	1	2	2	1	1	2	0	-	1	1	1
Achilidae *Sevia* sp. A	3	2	1	0	-	0	0	0	0	0	-	-	1	0	0	0	0	2	1	1	-	0	1	0	-	-	-	-	-	-	0	5	1	1	1	0	-	-	1	1	2	1	1	2	0	-	1	1	1
Achilidae *Synecdoche* sp. 2	1	2	1	0	-	0	0	0	0	0	-	-	1	0	0	0	0	1	0	1	-	1	1	0	-	-	-	-	-	-	2	5	2	1	1	0	-	-	1	0	2	1	1	2	0	-	1	1	0
Achilixius davaoensis	?	?	1	1	0	?	0	1	?	1	0	1	1	1	0	-	1	0	1	?	?	?	?	?	?	?	?	?	?	?	2	2	1	?	?	?	?	?	?	?	?	?	?	?	?	?	?	?	?
Achilixius fasciata	1	?	?	1	0	?	0	1	?	1	0	1	1	0	0	1	1	0	1	?	?	?	?	?	?	?	?	?	?	?	3	2	?	?	?	?	?	?	?	?	?	?	?	?	?	?	?	?
Achilixius fennahi	?	?	?	1	0	?	0	1	?	1	0	1	1	1	0	-	0	0	1	?	?	?	?	?	?	?	?	?	?	?	0	0	?	?	?	?	?	?	?	?	?	?	?	?	?	?	?	?
Achilixius kolintangi	?	?	1	1	0	1	0	1	1	1	0	1	1	0	0	1	1	0	1	?	?	?	?	?	?	?	?	?	?	?	1	4	?	?	?	?	?	?	?	?	?	?	?	?	?	?	?	?
Achilixius irigae	?	?	?	1	0	?	0	1	?	1	0	1	1	1	0	-	0	0	1	?	?	?	?	?	?	?	?	?	?	?	0	2	?	?	?	?	?	?	?	?	?	?	?	?	?	?	?	?
Achilixius mayoyae	?	?	?	1	0	?	0	1	?	1	0	1	1	1	0	-	1	0	1	?	?	?	?	?	?	?	?	?	?	?	1	4	1	?	?	?	?	?	?	?	?	?	?	?	?	?	?	?	?
Achilixius minahassae	1	?	1	1	0	1	0	1	?	1	0	1	1	0	0	1	1	0	1	?	?	?	?	?	?	?	?	?	?	?	2	2	?	?	?	?	?	?	?	?	?	?	?	?	?	?	?	?
Achilixius muiri	1	2	?	1	0	?	0	1	?	1	0	1	1	0	0	1	1	0	1	?	?	?	?	?	?	?	?	?	?	?	1	4	?	?	?	?	?	?	?	?	?	?	?	?	?	?	?	?
Achilixius sandakanensis	?	?	?	1	0	?	0	1	?	1	0	1	1	1	0	-	1	0	1	?	?	?	?	?	?	?	?	?	?	?	?	0	?	?	?	?	?	?	?	?	?	?	?	?	?	?	?	?	?
Achilixius singularis	?	?	?	1	0	?	0	1	?	1	0	1	1	1	0	-	0	2	0	?	?	?	?	?	?	?	?	?	?	?	?	?	?	?	?	?	?	?	?	?	?	?	?	?	?	?	?	?	?
Achilixius dietrichi	1	2	1	1	0	1	0	1	1	1	0	1	1	1	0	-	1	0	1	1	0	0	1	0	?	?	0	0	0	?	2	2	1	?	?	?	?	?	?	?	?	?	?	?	?	?	?	?	?
Achilixius sp. 1	1	2	1	1	0	1	0	1	1	1	0	1	1	?	?	?	?	?	?	?	?	?	?	?	?	?	?	?	?	?	?	?	?	1	1	1	2	1	1	0	2	1	0	1	1	1	1	2	0
Achilixius tubulifer	?	?	?	1	0	?	0	1	?	1	0	1	1	1	0	-	0	0	1	?	?	?	?	?	?	?	?	?	?	?	3	0	?	?	?	?	?	?	?	?	?	?	?	?	?	?	?	?	?
Bebaiotes amazonica	1	2	0	1	1	1	0	1	1	0	-	-	1	1	0	-	0	1	1	1	0	1	1	1	0	1	1	0	0	1	0	0	0	1	1	1	2	1	1	1	2	1	0	1	1	0	0	0	0
Bebaiotes dichromata	1	1	0	1	1	1	0	1	1	0	-	-	1	1	0	-	0	1	1	1	0	1	1	1	1	1	2	0	0	1	2	0	0	1	1	1	2	1	1	1	2	1	0	1	1	1	1	1	0
Bebaiotes macroptera	1	2	0	1	1	1	0	1	1	0	-	-	1	1	1	-	1	1	1	1	2	1	1	1	1	0	-	0	0	2	3	0	0	1	1	1	1	1	1	1	2	1	0	1	1	0	2	2	0
Bebaiotes parallela	1	2	0	1	1	1	0	1	1	0	-	-	1	1	0	-	1	1	1	1	0	1	1	1	1	1	2	0	0	1	3	0	0	1	1	1	2	1	1	2	2	1	0	1	1	0	0	2	0
Bebaiotes tigrina	1	2	0	1	1	1	0	1	1	0	-	-	1	1	0	-	1	1	1	1	0	1	1	1	0	1	1	0	0	1	3	0	0	1	1	1	2	1	1	1	2	1	0	1	1	1	0	1	0
Bebaiotes nivosa	?	?	0	1	1	1	0	1	1	0	-	-	1	?	?	?	?	?	?	?	?	1	?	?	?	?	?	?	?	?	?	?	?	1	1	1	2	0	1	?	?	1	0	1	1	?	?	?	0
Bebaiotes bucayensis	?	2	0	1	1	1	0	1	1	0	-	-	1	1	0	-	1	1	?	1	?	1	1	1	?	?	?	?	?	?	?	?	?	?	1	?	?	?	?	?	?	?	?	?	?	?	?	?	?	?
Bebaiotes dorsivittata	1	1	0	1	1	1	0	1	1	0	-	-	1	1	0	-	1	1	1	1	1	1	1	1	0	1	-	0	0	1	0	0	0	0	1	1	1	2	1	1	2	2	1	0	1	1	1	0	1	0
Bebaiotes nigrigaster	?	?	0	1	1	1	0	1	1	0	-	-	1	1	?	-	?	?	?	?	?	1	?	?	?	?	?	?	?	?	?	?	?	?	?	?	?	?	?	?	?	?	?	?	?	?	?	?	?
Bebaiotes banksi	2	2	0	1	1	1	0	1	1	0	-	-	1	1	0	-	1	1	1	1	0	1	1	1	1	1	0	0	1	-	0	0	0	0	1	1	1	3	0	1	0	2	1	0	1	1	1	1	0	0
Bebaiotes bia	2	2	0	1	1	1	0	1	1	0	-	-	1	1	0	-	1	0	1	1	2	1	1	1	0	1	-	1	1	-	2	0	0	0	1	1	1	3	1	1	0	2	1	0	1	1	1	1	2	0
Bebaiotes guianesus	1	2	0	1	1	1	0	1	1	0	-	-	1	1	0	-	0	1	1	1	1	1	1	1	0	1	-	1	0	1	0	0	0	0	1	1	1	3	1	1	2	2	1	0	1	1	1	1	0	0
Bebaiotes pallidinervis	?	?	0	1	1	1	0	1	1	0	-	-	1	1	?	-	?	?	?	?	?	1	?	?	?	?	?	?	?	?	?	?	?	?	?	?	?	?	?	?	?	?	?	?	?	?	?	?	?
Bebaiotes pennyi	2	2	0	1	1	1	0	1	1	0	-	-	1	1	0	-	1	0	1	1	3	1	1	1	1	1	-	0	0	0	0	0	0	0	1	1	1	2	0	1	0	1	1	0	1	0	-	0	2	0
Bebaiotes pulla	2	2	0	1	1	1	0	1	1	0	-	-	1	1	0	-	1	0	1	1	3	1	1	1	1	0	-	0	2	-	2	0	0	1	1	1	1	0	1	2	2	1	0	1	1	1	0	2	0
Bebaiotes wilsoni	2	2	0	1	1	1	0	1	1	0	-	-	1	1	0	-	1	1	1	1	2	1	1	1	0	1	-	0	0	1	3	0	0	1	1	1	2	1	1	0	2	1	0	1	1	1	1	2	0
Bebaiotes cavichiolii	1	2	0	1	1	1	0	1	1	0	-	-	1	1	0	-	1	1	1	1	1	1	1	1	1	1	-	0	0	1	0	0	0	1	1	1	0	1	1	1	2	1	0	1	1	1	0	1	0
Bebaiotes clarice	2	2	0	1	1	1	0	1	1	0	-	-	1	0	1	1	1	0	1	1	3	1	1	1	1	1	-	0	1	-	0	0	0	1	1	1	2	1	1	1	2	1	0	1	1	1	1	2	0
Bebaiotes oiapoquensis	1	1	0	1	1	1	0	1	1	0	-	-	1	1	0	-	1	0	1	1	0	1	1	1	0	1	0	0	0	-	3	0	0	?	?	?	?	?	?	?	?	?	?	?	?	?	?	?	?
Bebaiotes oliverai	2	2	0	1	1	1	0	1	1	0	-	-	1	1	0	-	1	1	1	1	2	1	1	1	1	1	-	1	3	-	0	0	0	1	1	1	3	1	?	0	2	1	0	1	1	1	1	0	0
Bebaiotes specialis	2	1	0	1	1	1	0	1	1	0	-	-	1	?	?	?	?	?	?	?	?	?	?	?	?	?	?	?	?	?	?	?	?	1	1	1	0	1	1	2	2	1	0	1	1	1	1	2	0
Bebaiotes 6317 sp. C	2	2	0	1	1	1	0	1	1	0	-	-	1	1	0	-	1	1	1	1	0	1	1	1	0	1	0	0	1	-	2	0	0	1	1	1	3	0	1	0	2	1	0	1	1	1	0	2	0

6.4.2. Phylogenetic analysis

The cladistic analysis resulted in 640 most parsimonious cladograms (L=336, IC=0.42 e IR =0.70). A strict consensus tree containing support values for each branch was illustrated in Figure 55. The monophyly and internal topology of *Bebaiotes* was recovered in all most parsimonious trees. All parsimonious trees are also congruent in the monophyly of Cixiidae, Achilidae, and *Achilixius*, but internal relationships vary. Finally, "Derbidae" was not recovered as monophyletic, varying in which terminal species was found as the sister group of Achilixiidae.

Results found recognize Achilixiidae as a monophyletic group (clade D), with high support values (Bremer=7; Bootstrap=90).

The monophyly of Achilixiidae was strongly supported in our results by eight non-homoplastic synapomorphies (Figure 56 clade D): subtriangular lora (14:1), median length of pronotum half the median length of mesonotum (19:1), sternite III with lateral abdominal process (54:1), sclerotized median region of sternite III (56:1), fused IV+V sternite (58:1), apexes of lobes of Gonapophysis IX (second valvula) sclerotized (93: 0), apexes of lobes of Gonapophysis IX (second valvula) divergent (94:1), and apexes of lobes of Gonapophysis IX (second valvula) curved (95:1) and six homoplastic synapomorphies (Figure 56): posterior margin of pronotum roundly concave (25:0), apex of the CuP vein of forewing abruptly curved forming a 90º degree angle (42:1), median longitudinal region of membranous IV sternites (59:1), sternite VIII fused to pygofer (63:1), phallic complex unarticulated (73:1), and gonoplac (third valvula) entire (99:0).

The topology recovered the following relationship between the terminals: (Cixiidae + (Achilidae + ("Derbidae" + "Derbidae" + (Achilixiidae)))) (Figure 55).

The first clade (Figure 55 clade A) is composed exclusively of representatives of *Melanoliarus* sp. 1, *Pintalia* sp. 1, *Bothriocera* sp. 1, *Bennarella bicoloripennis*, both form Cixiidae, and it was recovered as the sister group to the other families.

The second clade (Figure 55 clade B) includes the following relationships: (Achilidae + ("Derbidae" + "Derbidae" + (Achilixiidae))). This clade has reasonable stability in the tree, according to the support values found (Bremer=9; Bootstrap=95). The clade containing the genera *Catonia* sp. 2, *Synecdoche* sp. 2, and *Sevia* sp. A, all from Achilidae was recovered as the sister group of the clade containing "Derbidae" (*Anotia* sp. 2 and *Persis*) and Achilixiidae. This clade is supported by six non-homoplastic synapomorphies (Figure 56): median ocellus absent (7:0), MP1 vein of forewing unbranched (29:1), reduced ovipositor (84:1), dorsoapical margin of Gonapophysis VIII with projections (85:1), bursa copulatrix present (89:1), and Gonapophysis IX bifid (92: 1).

The third clade (Figure 55 clade C) composed of representatives from *Anotia* sp. 2 and *Persis* (*Persis*), both from "Derbidae", and Achilixiidae. It was recovered only with a support value of Bremer = 4. Although its internal relationships are not resolved, it did not interfere with the monophyly of Achilixiidae. This clade is supported by three non-homoplastic synapomorphies (Figure 56): vertex and frons without transverse carina (1: 1), median longitudinal carina on the frons (2:1), and kidney-shaped compound eye (9: 1), and three homoplastic synapomorphies (Figure 56): lateral longitudinal carinae of the median region of the frons parallel (3:0); lateral margins of the median region of the frons not covering the lateral ocelli (6:0), and length of pedicel greater than width (10:1).

The fourth clade (Figure 55 clade D) formed only by representatives from Achilixiidae, includes the two monophyletic genera. *Achilixius* (Figure 55 clade E) was recovered with low branch support (Bremer=2) and found supported by three homoplastic

synapomorphies (Figure 56): frons with median longitudinal carina present (2:0), icua crossvein of forewing absent (39:1), and sternite V with lateral abdominal process (60:1). Internal relationships of the genus were unresolved.

Bebaiotes (Figure 55 clade F) was recovered with high support value (Bremer=5; Bootstrap=92) and supported by four non-homoplastic synapomorphies (Figure 56 clade F): unbranched forewing RP vein (28:1), profemur with seta slender (48:1), phallic complex with inner sclerotized plates present (74:1), and length of dorsal margin Anal tube (segment X) less than 1/4 of ventral margin (83:0) and supported by five homoplastic synapomorphies (Figure 56): subantennal carina present (12: 1), length of the radial cell of the forewing half the length of the medial cell (35: 1), r-m crossvein of the forewing positioned basal to apex of the clavus (36:0), basal width of gonostylus subequal to apical width (68:1), and phallic complex dorsoventrally depressed (72:1).

The first clade (Figure 55 clade G), *Bebaiotes dichromata*+, was supported by two homoplastic synapomorphies (Figure 56): MP1+2 and MP3+4 branching located apically to the transverse vein r-m (34:1) and bursa copulatrix with obtuse (90:1).

The second clade (Figure 55 clade H), *Bebaiotes pallidinervis*+, was supported by a single homoplastic synapomorphie (Figure 56 clade H): conical anterior margin of the pronotum (20:1).

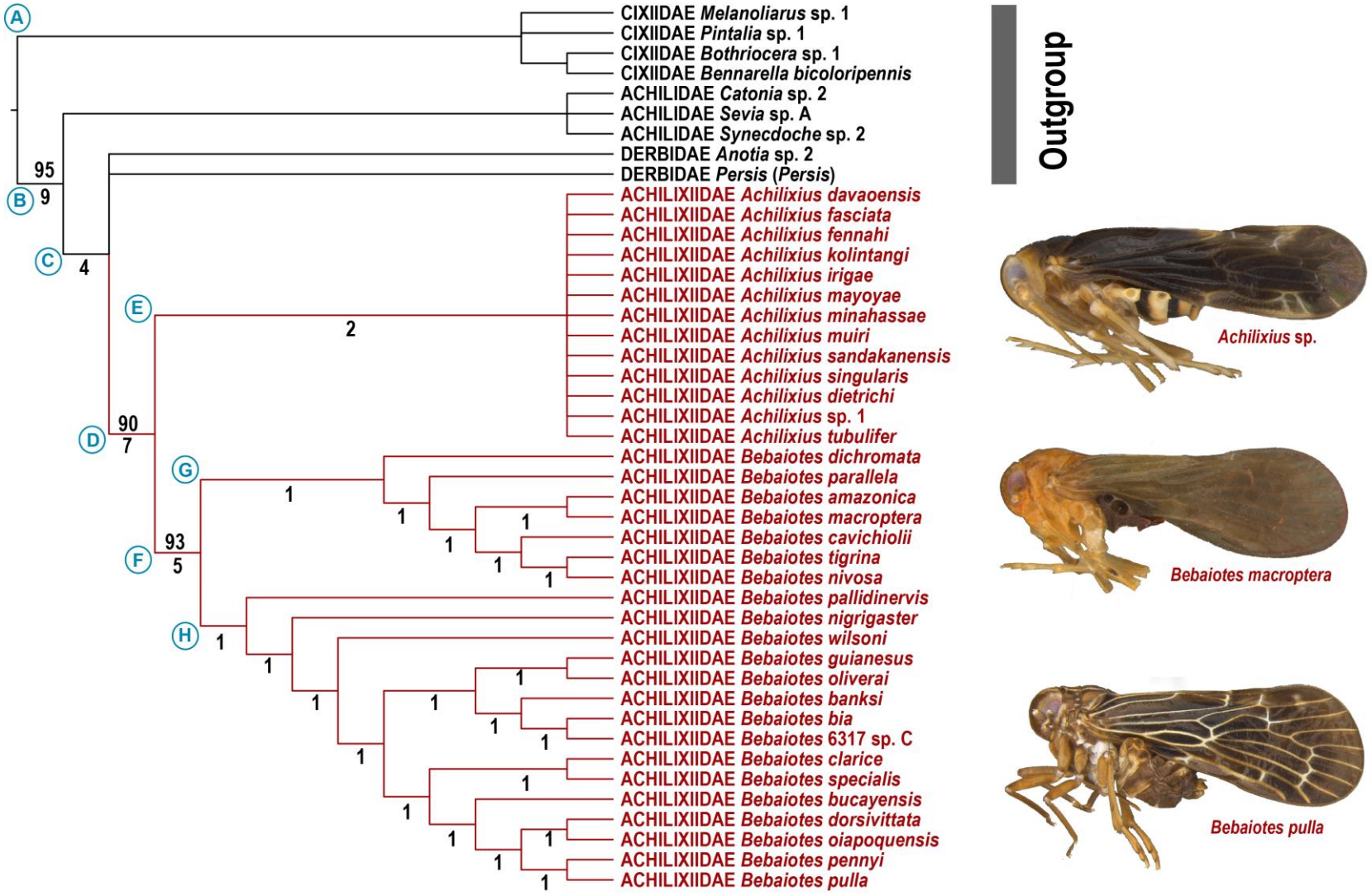

Figure 55. Strict consensus of 640 most parsimonious trees (L=338, IC=0.42 e IR =0.71) resulting from the analysis of 99 morphological characters of Achilixiidae and outgroup. Numbers above branches are bootstrap values > 80 (in percentage). Numbers below branches are Bremer support. Red clades indicate genera of Achilixiidae.

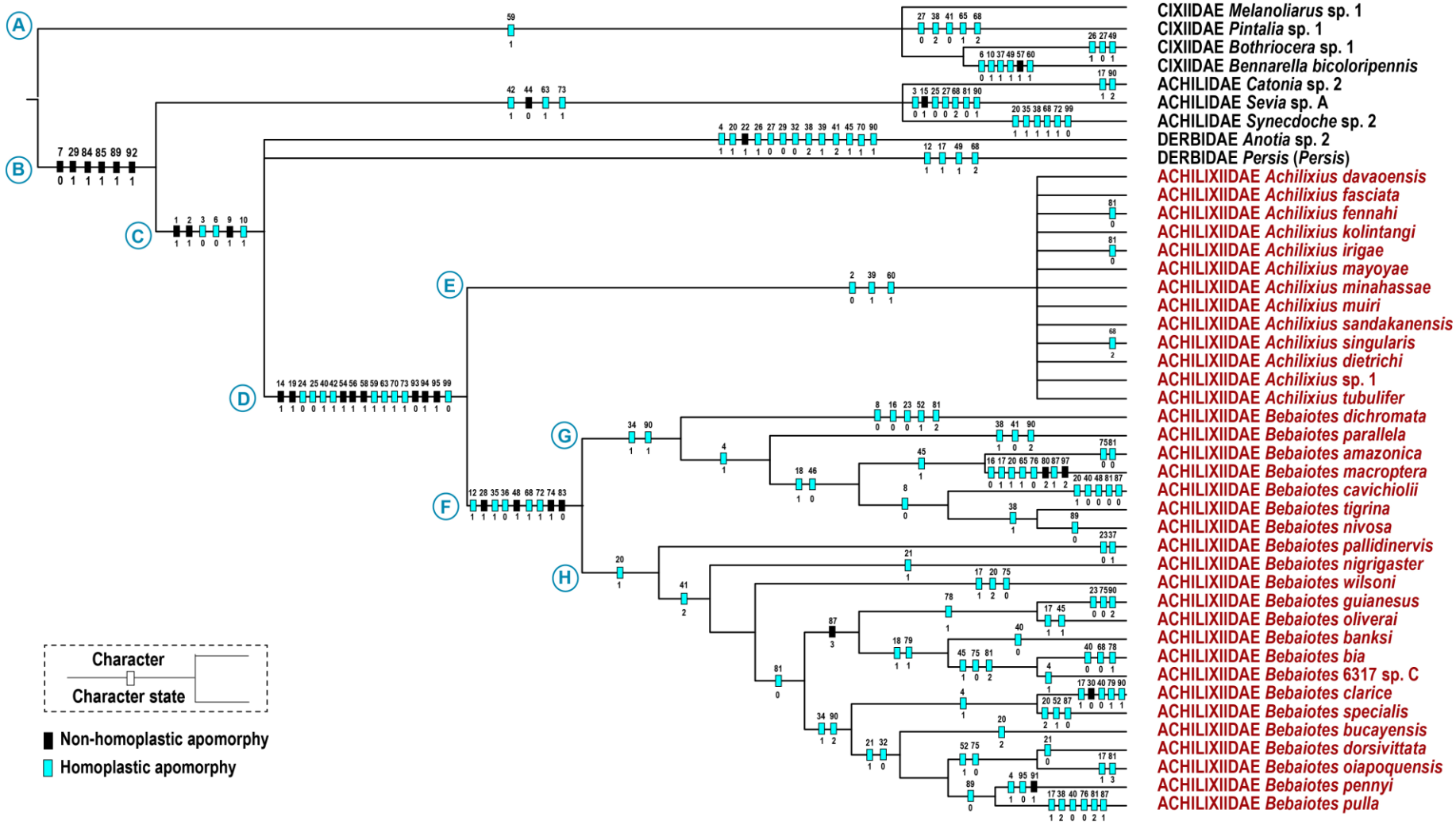

Figure 56. Strict consensus of 640 most parsimonious trees ((L=338, IC=0.42 and IR =0.71) resulting from the analysis of 99 morphological characters of Achilixiidae and outgroup. Unambiguous ancestral characters optimized with parsimony over all most parsimonious trees found are plotted over branches, with cyan squares referring to homoplastic and black to non-homoplastic synapomorphies. Numbers above rectangles refer to character number and below to state number.

6.5. Discussion

6.5.1. Phylogenetic position of Achilixiidae

All phylogenetic studies so far did not confidently place Achilixiidae among other planthopper families. Urban & Cryan (2007) found incongruent placements of Achilixiidae, placing in one clade with Derbidae + “Achilidae” and in another tree as the sister group to part of "Achilidae" and other families of Fulgoroidea. This works sampled a single representative of Achilixiidae, an unidentified female specimen of *Bebaiotes*, and sequences generated in this study were used by all subsequent molecular phylogenetic studies. In the work of Song & Liang (2013), Achilixiidae was recovered as a sister group in part of “Nogodinidae” + Derbidae and in another tree as sister to Achilidae. More recently, it has been recovered within Achilidae with better statistical support, more likely because of the wider taxon sampling (Bucher et al., 2023). These results were not corroborated by the phylogenetic analysis obtained in this study, as Achilixiidae herein was found more related to “Derbidae” species in part, without reliable bootstrap support, but relatively good decay index support (Bremer = 4). However, a molecular study is currently underway, and preliminary results indicate the support of a clade comprising *Catonia*, *Spino*, and an unidentified *Synecdoche*, all from Achilidae, as a sister group to Achilixiidae (Viegas et al., in prep. – Capítulo II desta tese).

Although abdominal processes are present in some groups of Cixiidae (Bennarellini) and in Achilixiidae, our analysis indicated that they are not homologous, and these characteristics evolved independently throughout the evolutionary history of each group. Burcher et al. (2023), based on molecular data, included a representative of Bennini and a representative of Achilixiidae. They did not observe a close relationship, placing them in distinct families (Cixiidae and Achilidae).

The clade “Derbidae” in part + Achilixiidae is supported by three non-homoplastic synapomorphies (Figure 56): vertex and frons without transverse carina (1:1), median longitudinal carina on the frons (2: 1), and kidney-shaped compound eye (9:1); and three homoplastic synapomorphies (Figure 56): lateral longitudinal carinae of the median region of the frons parallel (3:0); lateral margins of the median region of the frons not covering the lateral ocelli (6: 0), and length of pedicel greater than width (10:1).

6.5.2. Monophyly of Achilixiidae and its genera

For the first time, the monophyly od Achilixiidae and included genera were tested in a modern phylogenetic framework, by the inclusion of multiple terminals.

Emeljanov (1991) proposed transferring representatives of Achilixiidae to Achilidae, each genus representing a distinct subfamily. Both achilixiid genera do exhibit distinct characteristics that may have influenced Emeljanov's decision. For example, *Bebaiotes* has only one pair of abdominal processes located on sternite III, while *Achilixius* has two pairs of abdominal processes located on sternites III and V (Wilson, 1989). According to Emeljanov (1991), *Achilixius* and *Bebaiotes* did not share a common ancestor, leading to the creation of two distinct subfamilies.

The genera of Achilixiidae, *Achilixius*, and *Bebaiotes*, form a monophyletic group according to our results. We observed that *Bebaiotes* displayed remarkable homogeneity in external morphology. This resulted in an analysis with morphological data with limited phylogenetic signal for certain groups, due to the presence of numerous homoplastic characters. *Bebaiotes* presents reasonable stability in the tree, as indicated by the support values obtained (Bremer=5; Bootstrap=93).

The relationships between species of this *Achilixius* were not possible due to the difficulty of studying the material, with data collected through literature, photographs and four specimens (three males and one female).

The distinction between *Achilixius* and *Bebaiotes* is based on the following set of synapomorphies: frons with median longitudinal carina (absent in *Bebaiotes*); gena without subantennal carina (present in *Bebaiotes*); lateral carinae of pronotum strongly diverging towards the tegula (gently diverging or subparallel in *Bebaiotes*); sternite III with pair of abdominal processes, each with two sensory pits (three pits in *Bebaiotes*); sternite V with pair of abdominal processes (absent in *Bebaiotes*); RP vein of the forewing branched (unbranched in *Bebaiotes*); icua crossvein of the forewing absent (present in *Bebaiotes*); and phallic complex without internal sclerotized plates (present in *Bebaiotes*). Currently, *Achilixius* is recorded only in the Oriental region, including the Philippines, Sulawesi, and Sabah (Wilson, 1989; Viegas & Ale-Rocha, 2023), while *Bebaiotes* is limited to Central America and northern South America.

6.6. Conclusions

Our results recover the monophyly of Achilixiidae and included genera. Although internal relationships within *Achilixius* were not hypothesized confidently due to the lack of data, present analysis suggest that *Achilixius* form a monophyletic group. Additionally, *Bebaiotes* was also recovered as monophyletic and species relationships are proposed, opening avenues for evolutionary studies of the genus. The inclusion of *Bennarella bicoloripennis* Muir (Cixiidae), which also has abdominal processes, as an outgroup, revealed that the emergence of these abdominal processes occurred independently throughout the evolutionary history of each group.

We emphasize the importance of including female terminalia characters whenever possible in phylogenetic analyses, since we have recovered some non-homoplastic synapomorphies from these structures, such as: apexes of lobes of Gonapophysis IX (second valvula) sclerotized (93:0), apexes of lobes of Gonapophysis IX (second valvula) divergent (94:1), and apexes of lobes of Gonapophysis IX (second valvula) curved (95:1).

Finally, this is the first cladistic study that encompasses representatives from both genera of Achilixiidae. This provided a deeper understanding of the morphology and relationships of this family, identifying characters that can be used in broader studies of Fulgoromorpha, thus becoming an important contribution to direct future research.

6.7. Acknowledgments

We thank curators Dr. Marcio Luiz de Oliveira (INPA), Dr. Orlando Tobias (MPEG), Dr. Rodney R. Cavichioli (DZUP), Dr. Francisco Limeira-de-Oliveira (UEMA), Dr. Rodrigo Lopes Ferreira (UFLA), and Dr. Christopher H. Dietrich (INHS) for loaning specimens studied. We thank Dr. Mick Webb (NHMK) and Dr. Jerome Constant (RBINS) for the photographs of *Bebaiotes* and *Achilixius*. We thank Coordenação de Aperfeiçoamento de Pessoal de Nível Superior (CAPES) for providing a doctoral scholarship for the first author and Conselho Nacional de Desenvolvimento Científico e Tecnológico (CNPq) for research productivity fellowships for RAC and DMT (procs. 312351/2021-6 and 314557/2021-0). This study was financed in part by Fundação de Amparo à Pesquisa do Estado do Amazonas (FAPEAM)–POSGRAD. The first author thanks Ana Flávia Avelino, Matheus Bento, Felipe Barbosa, Clayton Gonçalves, Cristiely Oliveira, Luana Barros, Sandra Duque, for all the help provided.

6.8. References

Amorim, D.D.S. (1982) Classificação por seqüenciação: uma proposta para a denominação dos ramos retardados. *Revista brasileira de Zoologia*, 1 (1), 1-9.

Asche, M. (1987) Preliminary thoughts on the phylogeny of Fulgoromorpha (Homoptera Auchenorrhyncha). In: *Proceedings of the 6th Auchenorrhyncha Meeting*, Turin, Italy, 7–11 September: 47–53.

Bourgoin, T. & Huang, J. (1990) Morphologie comparée des genitalia mâles des Trypetimorphini et remarques phylogénétiques (Hemiptera: Fulgoromorpha: Tropiduchidae). Annales de la Société entomologique de France, New Series, 26 (4), 555–564.
https://doi.org/10.1080/21686351.1990.12277614

Bourgoin, T. (1988) A new interpretation of the homologies in the Hemiptera male genitalia, illustrated by the Tettigometridae (Hemiptera, Fulgoromorpha). Proceedings of the 6th Auchenorrhyncha Meeting, Turin, Italy, 1987 (ed. by C. Vidano and A. Arzone), pp. 113–120. Consiglio nazionale delle Ricerche, Italy.

Bourgoin, T. (1993) Female genitalia in Fulgoromorpha (Insecta, Hemiptera): morphological and phylogenetical data. *Annales de la Societe Entomologique de France*, N.S., 29, 225–244.
https://doi.org/10.1080/21686351.1993.12277686

Bourgoin, T., Wang, R.R., Asche, M., Hoch, H., Soulier-Perkins; A., Stroinski, A., Yap, S. & Szwedo, J. (2015) From micropterism to hyperpterism: recognition strategy and standardized homology-driven terminology of the forewing venation patterns in planthoppers (Hemiptera: Fulgoromorpha). *Zoomorphology*, 134, 63–77.
https://doi.org/10.1007/s00435-014-0243-6

Bremer, K. (1994) Branch support and tree stability. *Cladistics*, 10: 295–304.

https://doi.org/10.1111/j.1096-0031.1994.tb00179.x

Bucher, M., Condamine, F.L., Luo, Y., Wang, M. & Bourgoin, T. (2023) Phylogeny and diversification of planthoppers (Hemiptera Fulgoromorpha) based on a comprehensive molecular dataset and large taxon sampling. *Molecular Phylogenetics and Evolution*, 107862.

https://doi: 10.1016/j.ympev.2023.107862

Ceotto, P., & Bourgoin, T. (2008) Insights into the phylogenetic relationships within Cixiidae (Hemiptera: Fulgoromorpha): cladistic analysis of a morphological dataset. Systematic Entomology, 33(3), 484–500.

https://doi: 10.1111/j.1365-3113.2008.00426.x

Dworakowska, I.D. (1988) Main veins of the wings of Auchenorrhyncha (Insecta, Rhynchota: Hemelytrata). *Entomologische Abhandlungen*, 52 (1), 63–108.

Emeljanov, A.F. (1991) Toward the problem of the limits and subdivisions of Achilidae (Homoptera, Cicadina)*. *Entomologicheskoe Obozrenie* 70: 373–393.

Farris, J.S. (1982) Outgroups and Parsimony. *Systematic Biology*, 31(3), 328–334.

https://doi: 10.1093/sysbio/31.3.328.

Felsenstein, J. (1985) Confidence limits on phylogenies: an approach using the bootstrap. *Evolution*, 39(4): 783-791.

Fennah, R.G. (1947) A synopsis of the Achilixiidae of the New World (Homoptera: Fulgoroidea). *Annals and Magazine of Natural History*, 11 (13): 183–191.

Fitch, W.N. (1971) Toward defining the course of evolution: minimum change for a specifiedtree topology. *Systematic Zoology*, 20: 406–416.

https://doi.org/10.1093/sysbio/20.4.406

Goloboff, P.A., Farris, J.S. & Nixon, K.C. (2003) TNT: *Tree Analysis Using New Technology*. Publicado pelos autores. Tucumán, Argentina.

Hoch, H. 1987. The tribe Bennini- A monophyletic group within the Cixiidae?. In: *Proceedings of the 6th Auchenorrhyncha Meeting*, Turin, Italy, pp. 55–57.

Holzinger, W.E., Emeljanov, A.F. & Kammerlander, I. (2002) The family Cixiidae Spinola 1839 (Hemiptera: Fulgoromorpha) – a Review. *Denisia*, 4: 113-138.

Kawaguchi, W.H.; Leonart, L.P.; Fachi, M. M.; Böger, B.; Pontarolo, R. 2019. Doença de Chagas: do surgimento ao tratamento–revisão da litera-tura. *Journal of the Health Sciences Institute*, 37(2): 182-189.

Liang A.P. (2001) Morphology of antennal sensilla in *Achilixius sandakanensis* Muir (Hemiptera: Fulgoromorpha: Achilixiidae) with comments on the phylogenetic position of the Achilixiidae. *The Raffles Bulletin of Zoology*, 49 (2): 221–225.

Löcker, B., Fletcher, M. J., Larivière, M. C., Gurr, G. M., Holzinger, W.E. & Löcker, H. (2006) Taxonomic and phylogenetic revision of the Gelastocephalini (Hemiptera: Cixiidae). *Invertebrate Systematics*, 20(1), 59–160. https://doi.org/10.1071/IS05005.

Maddison, W.P. & Maddison, D.R. (2023) *Mesquite 3.81* [programa de computador]. A modular system for evolutionary analysis. Disponível em: http://mesquiteproject.org.

Mejdalani, G. (1998) Morfologia externa dos Cicadellinae (Homoptera, Cicadellidae): comparação entre *Versigonalia ruficauda* (Walker) (Cicadellini) e *Tretogonia cribrata* Melichar (Proconiini), com notas sobre outras espécies e análise da terminologia. *Revista Brasileira de Zoologia*, 15:451-544.

Melichar, L. (1914) Neue Fulgoriden von den Philippinen: I. Theil. *Philippine Journal of Science*, 9, (3), 269–285.

Metcalf, Z.P. (1938) The Fulgorina of Barro Colorado and other parts of Panama. *Bulletin* of *the Museum of Comparative Zoology, Harvard*, 82, 275–423.

Metcalf, Z.P. (1945) Derbidae, Achilixiidae, Meenoplidae, Kinnaridae. General catalogue of the Hemiptera, *Fascicle IV Fulgoroidea*, Parts 4–7. Smith College, Northampton, MA.

Muir, F. (1923) Achilixius, a new genus. Constituting a new family of the Fulgoroidea (Homoptera). *Philippine Journal of Science*, 22, 483–487.

Muir, F. (1924) A new genus of the family Achilixiidae (Homoptera). Canadian *Entomologist*, 56, 33–34.

Muir, F. (1934) Additions to our knowledge of the Achilixiidae (Fulgoroidea. Homoptera). *Entomologist's Monthly Magazine,* 70, 132–133.

Nixon, K.C. & Carpenter, J.M. (1993) On Outgroups. *Cladistics*, 9(4), 413–426. https://doi: 10.1111/j.1096-0031.1993.tb00234.x.

O'Brien, L.B. & Wilson, S.W. (1985) *Planthopper systematics and external morphology*. In: Nault, L.R., Rodriguez, J.G. (Eds.), The Leafhoppers and Planthoppers. Wiley, New York, pp. 61–102.

Rambaut A. (2018) FigTree v.1.4.4. [accessed 20 may 2023]. http://tree.bio.ed.ac.uk/software/figtree.

Sereno, P.C. (2007) Logical basis for morphological characters in phylogenetics. *Cladistics* 23: 565–587. https://doi: 10.1111/j.1096-0031.2007.00161.x

Song, N. & Liang, A.P. (2013) A Preliminary Molecular Phylogeny of Planthoppers (Hemiptera: Fulgoroidea) Based on Nuclear and Mitochondrial DNA Sequences. *PLoS ONE* 8 (3): e58400. https://doi: 10.1371/journal.pone.0058400

Urban J.M. & Cryan, J.R. (2007) Evolution of the planthoppers (Insecta: Hemiptera: Fulgoroidea). *Mol Phylogenet Evol*, 42:556-572. https://doi: 10.1016/j.ympev.2006.08.009

Viegas, E.F.G., Ale-Rocha, R. (Submitted). A century of Achilixiidae Muir, 1923 Hemiptera: Auchenorrhyncha: Fulgoroidea: taxonomic study of the genus *Bebaiotes* Muir, 1924 and description of eight new species from Brazil. *Zootaxa*, in review.

Wilson, M.R. (1989) The planthopper family Achilixiidae (Homoptera, Fulgoroidea): a synopsis with a revision of the genus *Achilixius. Systematic Entomology*, 14, 487–506. https://doi.org/10.1111/j.1365-3113.1989.tb00299.x

Wilson, S.W., Mitter, C., Denno, R.F. & Wilson, M.R. (1994) Evolutionary patterns of host plant use by delphacid planthoppers and their relatives. In: Planthoppers: their ecology and management. Boston, MA: Springer US, p. 7-11.

7. SÍNTESE

Este trabalho foi fundamental para ampliar o conhecimento sobre as relações filogenéticas dentro da família Achilixiidae, mas também dentro de Fulgoroidea. Tanto na análise morfológica quanto nas análises moleculares realizadas, os resultados recuperaram Achilixiidae como um grupo monofilético indicando que os membros desta família compartilham um ancestral comum exclusivo e formam um ramo único dentro da infraordem Fulgoromorpha.

Ampliamos o registro de espécies de *Bebaiotes* no Brasil, destacando assim a importância das coleções entomológicas brasileiras. Essas coleções são verdadeiros tesouros de informações sobre a fauna, desempenhando um papel fundamental na pesquisa científica e na documentação da biodiversidade. Além disso, projetos voltados para a coleta de material em áreas remotas desempenham um papel essencial na expansão do nosso conhecimento sobre a entomofauna brasileira. Esse esforço conjunto contribui para o avanço da ciência e a conservação da diversidade biológica em nosso país.

Após 34 anos desde a última descrição de uma espécie de *Achilixius*, tivemos o privilégio de acrescentar mais uma à lista. Essa contribuição é significativa, pois enriquece nosso conhecimento sobre a diversidade desses insetos e destaca a importância contínua da pesquisa taxonômica na atualização das informações sobre a biodiversidade entomológica.

Por fim, a divisão do ancestral de Achilixiidae que levou às linhagens genéricas ocorreu em algum momento durante o Triássico até o Jurássico, provavelmente em decorrência de um evento vicariante relacionado à fragmentação do Gondwana. Além disso, as divergências iniciais de *Bebaiotes* na América do Sul ocorreram no Jurássico Inferior por volta de 176 Mya, enquanto *Achilixius* começou a diversificar muito mais tarde no Cretáceo Inferior por volta de 83 Mya. Esta diversificação posterior de *Achilixius* no Arquipélago Malaio condiz com a sua história geológica.

8. REFERÊNCIAS BIBLIOGRÁFICAS

Almeida, P.S. de; Júnior, W.C.; Obara, M.T.; Santos, H.R.; Barata, J.M.S.; Faccenda, O. 2008. Levantamento da fauna de Triatominae (Hemiptera: Reduviidae) em ambiente domiciliar e infecção natural por Trypanosomatidae no Estado de Mato Grosso do Sul. *Revista da Sociedade Brasileira de Medicina Tropical*, 41(4):374-380. https://doi.org/10.1590/S0037-86822008000400010

Asche, M. 1987. Preliminary thoughts on the phylogeny of Fulgoromorpha (Homoptera Auchenorrhyncha). In: Proceedings of the 6th Auchenorrhyncha Meeting, Turin, Italy, 7-11 September, 1987, pp. 47-53.

Azevedo, R.L.; Lima, M.F. 2015. Cigarrinhas dos Citros, vetoras da bactéria *Xylella fastidiosa* Wells et al.: Pragas Potenciais para a Citricultura Sergipana. *Entomo Brasilis*, 8 (1): 01-07. https://doi.org/10.12741/ebrasilis.v8i1.403

Bellman. Cigarrinha-das-Pastagens: Ocorrência x Controle. Informativo direto do Campo. Janeiro/2009, ano 5, número 11.

Bourgoin, T.; Huang, J. 1990. Morphologie comparée des genitalia mâles des Trypetimorphini et remarques phylogénétiques (Hemiptera: Fulgoromorpha: Tropiduchidae). *Annales de la Société entomologique de France*, New Series, 26 (4), 555-564. https://doi.org/10.1080/21686351.1990.12277614

Bourgoin, T. 1988. A new interpretation of the homologies in the Hemiptera male genitalia, illustrated by the Tettigometridae (Hemiptera, Fulgoromorpha). Proceedings of the 6th Auchenorrhyncha Meeting, Turin, Italy, 1987 (ed. by C. Vidano and A. Arzone), pp. 113-120. Consiglio nazionale delle Ricerche, Italy.

Bourgoin, T. 1993. Female genitalia in Fulgoromorpha (Insecta, Hemiptera): morphological and phylogenetical data. *Annales de la Societe Entomologique de France*, N.S., 29, 225-244. https://doi.org/10.1080/21686351.1993.12277686

Bourgoin, T.; Wang, R.R.; Asche, M.; Hoch, H.; Soulier-Perkins, A.; Stroinski, A.; Yap, S.; Szwedo, J. 2015. From micropterism to hyperpterism: recognition strategy and standardized homology-driven terminology of the forewing venation patterns in planthoppers (Hemiptera: Fulgoromorpha). *Zoomorphology*, 134, 63-77. https://doi.org/10.1007/s00435-014-0243-6

Bourgoin T. 2023. FLOW (Fulgoromorpha Lists on The Web): a world knowledge base dedicated to Fulgoromorpha. Version 8, updated [10-06-2023]. Acessado em: 13 de junho de 2023. https://hemiptera-databases.org/flow/

Bucher, M.; Condamine, F.L.; Luo, Y.; Wang, M.; Bourgoin, T. 2023. Phylogeny and diversification of planthoppers Hemiptera Fulgoromorpha based on a comprehensive molecular dataset and large taxon sampling. Mol. Phylogenet. Evol. 186, 107862. https://doi.org/10.1016/j.ympev.2023.107862.

Campbell, B.C.; Steffen-Campbell, J.D.; Sorensen, J.T.; Raymond, J.G.;1995. Paraphyly of Homoptera and Auchenorrhyncha inferred from 18S rDNA nucleotide sequences. *Systematic Entomology*, 20, 175-194.

Chen, S.; Yang, C.T. 1995. The metatarsi of the Fulgoroidea (Homoptera: Auchenorrhyncha). *Chin. J. Entomol*. 15, 257-269.
https://doi.org/10.6660/TESFE.1995023

Cryan, J.; Urban, J.M. 2012. Higher-level phylogeny of the insect order Hemiptera: is Auchenorrhyncha really paraphyletic?. *Systematic Entomology*, 37, 7-21.
https://doi.org/10.1111/j.1365-3113.2011.00611.x

Dworakowska, I.D. 1988. Main veins of the wings of Auchenorrhyncha (Insecta, Rhynchota: Hemelytrata). *Entomol. Abh. Staatl. Mus. Tierkd. Dresden*, 52, 63-108.

Emeljanov, A.F. 1991. Toward the problem of the limits and subdivisions of Achilidae (Homoptera, Cicadina)*. *Entomol. Obozr.* 70: 373-393.

Emeljanov, A.F. 1990. An attempt of construction of the phylogenetic tree of the planthoppers (Homoptera, Cicadina). *Entomologicheskoe Obozrenie*, 69 (2), 353-356.

Fennah, R.G. 1947. A synopsis of the Achilixiidæ of the New World (Homoptera: Fulgoroidea). *Annals and Magazine of Natural History*, 11 (13): 183-191.

Gallo, D.; Nakano, O.; Silveira Neto, S.; Carvalho, R.P.L.; Batista, G.C.; Berti Filho, E.; Parra, J.R.P.; Zucchi, R.A.; Alves, S.B.; Vendramim, J.D.; Marchini, L.C.; Lopes, J.R.S.; Omoto, C. 2002. *Entomologia agrícola I.* Piracicaba - SP: FEALQ. 920 pp.

Goodchild, A.J.P. 1966. Evolution of the alimentary canal in the Hemiptera. *Biological Reviews*, 41, 97-140.

Grazia, J.; Cavichioli, R.R.; Wolf, V.R.S.; Fernandes, J.A.M.; Takiya, D.M. 2012. Hemiptera. *In*: Rafael, J.A.; Melo, G.A.R.; Carvalho, C.J.B. de; Casari, S.A.; Constantino, R. (Eds). *Insetos do Brasil*: Diversidade e Taxonomia. Ribeirão Preto. *Holos* Editora. p. 347-406.

Grimaldi, D.; Engel, M.S. 2005. *Evolution of the Insects*. Cambridge Univ. Press, New York, 755 pp.

Hamilton, K.G.A. 1981. Morphology and evolution of the rhynchotan head (Insecta: Hemiptera, Homoptera). *Canadian Entomologist*, 113 (1), 953-974. https://doi.org/10.4039/ent113953-11

Henry, T. 2009. Heteroptera, Chapter 10. *In*: Foottit, R.G.; Adler, P.H. (Eds.), *Insect Biodiversity: Science and Society*. Blackwell Publishing Ltd., Oxford, pp. 223-263.

Hoch, H. 1987. The tribe Bennini- A monophyletic group within the Cixiidae? *Proceedings of the 6th Auchenorrhyncha Meeting*, Turin, Italy, pp. 55-57.

Jiang, J.Q.; Huang, D.Y. 2017. New species of Cicadocoris (Hemiptera: Coleorrhyncha: Progonocimicidae) from mid-Jurassic deposits in northeastern China. *European Journal of Entomology*, 114, 355-364. https://doi.org/10.14411/eje.2017.045

Johnson, K.P; Dietrich; C.H.; Friedrich, F.; Beutel, R.G.; Wipfler, B.; Peters, R.S.; Allen, J.M.; Petersen, M.; Donath, A.; Walden, K.K.O.; Kozlov, A.M.; Podsiadlowski, L.; Mayer, C.; Meuseman, K.; Vasilikopoulos, A.; Waterhouse, R.M.; Cameron, S.L.; Weirauch, C.; Swanson, DR.; Percy, D.M.; Hardy, N.B.; Terry, I.; Liu, S.; Zhou, X.; Misof, B.; Robertson, H.M.; Yoshizawa, K. 2018. Phylogenomics and the evolution of hemipteroid insects. *PNAS Latest Articles*, 1-6.

Li, H.; Leavengood, J.M.J.; Chapman, E.G.; Burkhardt, D.; Song, F.; Jiang, P.L.J.; Zhou, X.; Cai W. 2017. Mitochondrial phylogenomics of Hemiptera reveals adaptive innovations driving the diversification of true bugs. *Proc Biol Sci*, 284: 1-10. https://doi.org/10.1098/rspb.2017.1223

Liang, A.P. 2001. Morphology of antennal sensilla in *Achilixius sandakanensis* Muir (Hemiptera: Fulgoromorpha: Achilixiidae) with comments on the phylogenetic position of the Achilixiidae. *The Raffles Bulletin of Zoology*, 49 (2): 221-225.

Melichar, L. 1914. Neue Fulgoriden von den Philippinen: I. Theil. *Philippine Journal* of *Science*, 9, (3). 269-285.

Metcalf, Z.P. 1938. The Fulgorina of Barro Colorado and other parts of Panama. *Bulletin* of *the Museum of Comparative Zoology, Harvard*, 82, 275-423.

Metcalf, Z.P. 1945. Derbidae, Achilixiidae, Meenoplidae, Kinnaridae. General catalogue of the Hemiptera, Fascicle IV Fulgoroidea, Parts 4-7. *Smith College*, Northampton, pp. 283.

Mifsud, D.; Cocquempot, C.; Mühlethaler, R.; Wilson, M.; Streito, J.C. 2010. Other Hemiptera Sternorrhyncha (Aleyrodidae, Phylloxeroidea, and Psylloidea) and Hemiptera Auchenorrhyncha Chapter 9.4. *BioRisk*, 4 (1): 511-552. https://doi.org/10.3897/biorisk.4.63

Muir, F. 1923. *Achilixius*, a new genus. Constituting a new family of the Fulgoroidea (Homoptera). *Philippine Journal of Science*, 22: 483-487.

Muir, F. 1924. A new genus of the family Achilixiidae (Homoptera). *Canadian Entomologist*, 56: 33-34.

Muir, F. 1934. Additions to our knowledge of the Achilixiidae (Fulgoroidea. Homoptera). *Entomologist's Monthly Magazine, 70*, 132-133.

O'Brien, L.B.; Wilson, S.W., 1985. *Planthopper systematics and external morphology*. In: Nault, L.R., Rodriguez, J.G. (Eds.), The Leafhoppers and Planthoppers. Wiley, New York, pp. 61-102.

Oliveira, C.M.; Oliveira, E.; Canuto, M.; Cruz, I. 2007. Controle químico da cigarrinha-do-milho e incidência dos enfezamentos causados por molicutes. *Pesquisa Agropecuária Brasileira*, 42 (3): 297-303.
https://doi.org/10.1590/S0100-204X2007000300001

Penny, N.O. 1980. A revision of American Bennini (Hemiptera: Fulgoroidea: Cixiidae). *Acta Amazônica*, 10 (1): 207-212.
https://doi.org/10.1590/1809-43921980101207

Pereira, R.R.; Picanço, M.C.; Jr. Santana, P.A.; Moreira, S.S.; Guedes, R.N.C.; Corrêa, A.S. 2014. Insecticide toxicity and walking response of three pirate bug predators of the tomato leaf miner Tuta absoluta. *Agricultural and Forest Entomology*, 16, 293-301.
https://doi.org/10.1111/afe.12059

Ravaneli, G.C.; Mutton, M.J.R.; Garcia, D.B.; Madaleno, L.L.; Stupiello, J.P.; Mutton, M.A. 2011. Danos promovidos pela cigarrinha-das-raízes sobre a qualidade tecnológica da cana. *Ciência &Tecnologia*, 3(1): 16-27.

Ribeiro, J.R.I.; Moreira, F.F.F.; Barbosa, J.F.; Alecrim, V.P.; Rodrigues, H.D.D. 2014. Ordem Hemiptera. *In*: Hamada, N.; Nessimian, J.L.; Querino, R.B. (Eds). *Insetos aquáticos na Amazônia brasileira: taxonomia, biologia e ecologia.* Manaus: Editora do INPA, 2014.

Song, N.; Liang, A.P. 2013. A Preliminary Molecular Phylogeny of Planthoppers (Hemiptera: Fulgoroidea) Based on Nuclear and Mitochondrial DNA Sequences. *PLoS ONE* 8 (3): e58400.
https://doi: 10.1371/journal.pone.0058400

Szwedo, J. 2011. The Coleorrhyncha (Insecta: Hemiptera) of the European Jurassic, with a description of a new genus from the Toarcian of Luxembourg. *Volumina Jurassic*, 9, 3-20.

Triplehorn, C.A.; Johnson, N.F.L. 2011. *Estudo dos insetos*: tradução da 7ª edição de Borror and Delong's introduction to the study of insects. São Paulo, Cengage Learning, 809 pp.

Urban, J.M.; Cryan, J.R. 2007. Evolution of the planthoppers (Insecta: Hemiptera: Fulgoroidea). *Mol Phylogenet Evol*, 42:556-572. https://doi: 10.1016/j.ympev.2006.08.009

Vacari, A.M.; Otuka, A.K.; De Bortoli, S.A. 2022. Desenvolvimento de Podisus nigrispinus (Dallas, 1851)(Hemiptera: Pentatomidae) alimentado com lagartas de Diatraea saccharalis (Fabricius, 1794) (lepidoptera: Crambidae). *Arquivos do Instituto Biológico*, 74: 259-265. https://doi.org/10.1590/1808-1657v74p2592007

Viegas, E.F.G.; Ale-Rocha, R. 2023. A century of Achilixiidae Muir, 1923 (Hemiptera: Auchenorrhyncha: Fulgoroidea): taxonomic study of the genus Bebaiotes Muir, 1924 and description of eight new species from Brazil. *Zootaxa* (Submetido)

Wilson, M.R. 1989. The planthopper family Achilixiidae (Homoptera, Fulgoroidea): a synopsis with a revision of the genus *Achilixius. Systematic Entomology*, 14: 487-506. https://doi.org/10.1111/j.1365-3113.1989.tb00299.x

APÊNDICE A

Estimativas de tempo das linhagens de Fulgoromorpha resultante da análise de divergência de tempo.

Supplementary Table 1. Estimated median divergence ages of Fulgoromorpha lineages with 95% credibility intervals.

Families	Estimated divergence age (Mya)	95% credibility intervals	Geological periods
Acanaloniidae	57.27	21.28-111.16	Paleogene
Achilidae	119.63	115.36-127.14	Cretaceous
Deferunda acuminata*+ *Magadha flavisigna	41.33	17.72-71.28	Paleogene
***Catonia* sp. 1+ *Spino* sp. 1 + *Synecdoch*e sp. 2**	96.44	74.21-114.65	Cretaceous
***Spino* sp. 1 + *Synecdoch*e sp. 2**	70.95	46.39-95.30	Cretaceous
Achilixiidae	209.62	158.29-267.61	Triassic
Achilixius	82.57	42.96-132.03	Cretaceous
Bebaiotes	176.36	131.60-224.48	Jurassic
B. clarice* + *B. dorsivittata* + *Bebaiotes* sp. 1 JU+ *B. pennyi* + *B. pulla	130.80	85.54-179.05	Jurassic
***B. dorsivittata* + *Bebaiotes* sp. 1 JU**	50.84	20.66-87.02	Paleogene
B. pennyi* + *B. pulla	20.68	5.21-48.24	Neogene
B. dorsivittata* + *Bebaiotes* sp. 1 JU+ *B. pennyi* + *B. pulla	89.35	53.82-132.42	Cretaceous
***B. macroptera*+ *B. amazonica* + *B. tigrina*+ *B. specialis* + *B. guianesus* + *B. bia* + *Bebaiotes* sp. C+ *B. banksi* + *Bebaiotes* sp. 1**	164.04	121.60-212.55	Jurassic
B. macroptera* + *B. amazonica* + *B. tigrina	87.31	49.19-131.35	Cretaceous
B. amazonica* + *B. tigrina	51.71	20.60-92.41	Paleogene

Supplementary Table 1 (*continued*)

***B. specialis* + *B. guianesus* + *B. bia* + *Bebaiotes* sp. C+ *B. banksi* + *Bebaiotes* sp. 1**	147.39	103.26-193.75	Jurassic
***B. guianesus* + *B. bia* + *Bebaiotes* sp. C+ *B. banksi* + *Bebaiotes* sp. 1**	128.68	85.32-176.19]	Jurassic
***B. bia* + *Bebaiotes* sp. C+ *B. banksi* + *Bebaiotes* sp. 1**	83,6788	45.20-130.36	Cretaceous
***Bebaiotes* sp. C+ *B. banksi* + *Bebaiotes* sp. 1**	56.99	19.06-99.94	Cretaceous
***B. banksi* + *Bebaiotes* sp. 1**	15.34	3.81-33.51	Neogene
Achilidae + Achilixiidae	240.20	180.65-302.53	Triassic
Caliscelidae	16.70	16.01- 20.01	Neogene
Achilidae + Achilixiidae+ Caliscelidae	273.83	209.81-337.08	Triassic
Cercopoidea	37.42	11.37-79.38	Devonian
Cixiidae	257.52	192.78-323.97	Permian
Bennarella bicoloripennis* + *Bennarella fusca	78.35	38.53-128.30	Cretaceous
***Bothriocera eborea* + *Bothriocera* sp. 2**	51.22	18.17-98.09	Paleogene
***Bennarella bicoloripennis* + *Bennarella fusca* + *Bothriocera eborea* + *Bothriocera* sp. 2**	214.42	149.36-286.53	Triassic
Ozoliarus* sp. 2 + *Pintalia alta	132.01	39.59-233.76	Cretaceous
Andes simplex* + *Cixius similis	125.29	56.92-206.17	Cretaceous
Haplaxius* sp. 1 + *Haplaxius deleter	20.61	3.45-53.93	Neogene
Andes simplex* + *Cixius similis*+ *Haplaxius* sp. 1 + *Haplaxius deleter	219.74	104.47-258.98	Jurassic
Cixiidae+ Delphacidae	257.52	192.78-323.97	Carboniferous
Delphacidae	80.41	28.24-155.68	Cretaceous
Harmalia ostorius*+*Nilaparvata lugens	34.06	7.27-77.54	Paleogene

Supplementary Table 1 (*continued*)

Cixiidae *Oliarus* sp. 2 + Acanaloniidae + Nogodinidae + Meenoplidae + Tropiduchidae + Issidae + Tettigometridae + Kinnaridae + Flatidae+ Lophopidae + Eurybrachidae + Fulgoridae + Dictyopharidae + Ricaniidae + Derbidae	252.13	193.92-311.60	Triassic
Cixiidae *Oliarus* sp. 2+ Acanaloniidae+ Nogodinidae + Meenoplidae	147.42	59.82-273.45	Jurassic
Acanaloniidae+ Nogodinidae + Meenoplidae	89.01	41.63-159.54	Cretaceaus
Nogodinidae *Biolleyana costalis* + Meenoplidae *Nisia* sp. 1 JU	42.73	9.96-95.52	Paleogene
Issidae + Tropiduchidae + Tettigometridae + Kinnaridae + Flatidae+ Lophopidae + Eurybrachidae + Fulgoridae + Dictyopharidae + Ricaniidae + Derbidae + Meenoplidae+ Tropiduchidae + Nogodinidae *Pisacha naga*	223.00	173.64-278.92	Triassic
Issidae + Tettigometridae + Kinnaridae + Flatidae+ Lophopidae + Eurybrachidae + Fulgoridae + Dictyopharidae + Ricaniidae + Derbidae + Meenoplidae+ Tropiduchidae + Nogodinidae	213.94	168.75-266.77	Triassic
Issidae + Meenoplidae + Tropiduchidae + Tettigometridae + Kinnaridae + Flatidae+ Lophopidae + Eurybrachidae + Ricaniidae + Nogodinidae	206.67	158.41-255.19	Triassic
Issidae + Meenoplida + Tropiduchidae + Nogodinidae	179.01	128.89-230.62	Jurassic
Issidae + Tropiduchidae + Nogodinidae	160.84	110.41-212.76	Jurassic
Tropiduchidae + Nogodinidae	113.27	65.39-167.58	Cretaceous
Tettigometridae + Kinnaridae + Flatidae+ Lophopidae + Eurybrachidae	193.60	144.05-246.98	Jurassic
Tettigometridae	3.00	0.35-8.62	Neogene
Kinnaridae + Flatidae + Lophopidae + Eurybrachidae	188.72	136.94-243.53	Jurassic
Kinnaridae + Flatidae *Ormenis saucia*	159.33	85.08-221.01	Jurassic
Lophopidae + Eurybrachidae + Lophopidae	128.65	65.63-189.71]	Cretaceous
Eurybrachidae + Lophopidae *Serida* sp. 1	85.48	27.26-150.22	Cretaceous

Supplementary Table 1 (*continued*)

Eurybrachidae + Fulgoridae + Dictyopharidae + Ricaniidae + Derbidae + Tropiduchidae + Flatidae + Issidae	200.86	155.55-250.34	Triassic
Eurybrachidae + Fulgoridae + Dictyopharidae	168.94	119.06-224.29	Jurassic
Eurybrachidae *Loxocephala* sp. 1 + Fulgoridae *Lycorma delicatula*	115.54	52.12-181.95	Cretaceous
Fulgoridae + Dictyopharidae	142.03	100.56-191.07	Jurassic
Flatidae+ Ricaniidae+ Issidae + Derbidae	185.60	139.40-232.76	Jurassic
Flatidae *Geisha* sp. 1 + Ricaniidae	45.48	79.08-206.71	Jurassic
Issidae + Derbidae	171.57	127.81-221.16	Cretaceous
Derbidae	143.14	99.04-188.86	Cretaceous
***Derbe* sp. 1 + *Persis* (*Anapersis*) sp. 2**	102.55	59.80-149.02	Cretaceous
Dictyopharidae	84.10	83.46, 86.01	Cretaceous
Fulgoroidea	364.73	314.77-413.57	Devonian
Ricaniidae	56.35	55.86-57.00	Paleogene

APÊNDICE B

Árvores de máxima verossimilhança de Achilixiidae e grupos externos para cada gene: 16S, 18S, 28S e H3.

.

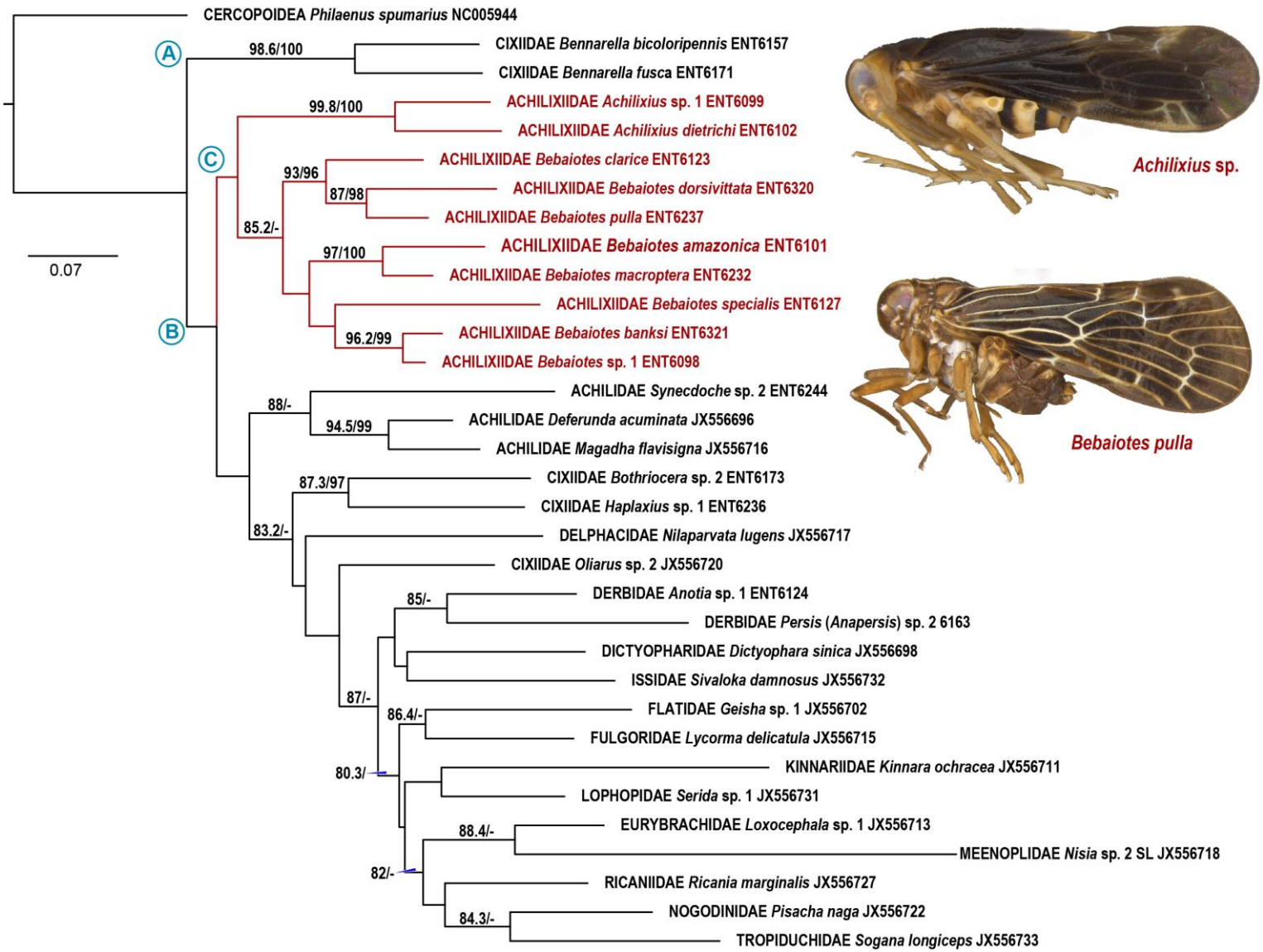

Supplementary Figure S1. Maximum likelihood tree of Achilixiidae and outgroups based on 465 bp of 16S rDNA. Values above branches are likelihood SH-aLRT ≥ 80 / ultrafast bootstrap ≥ 95.

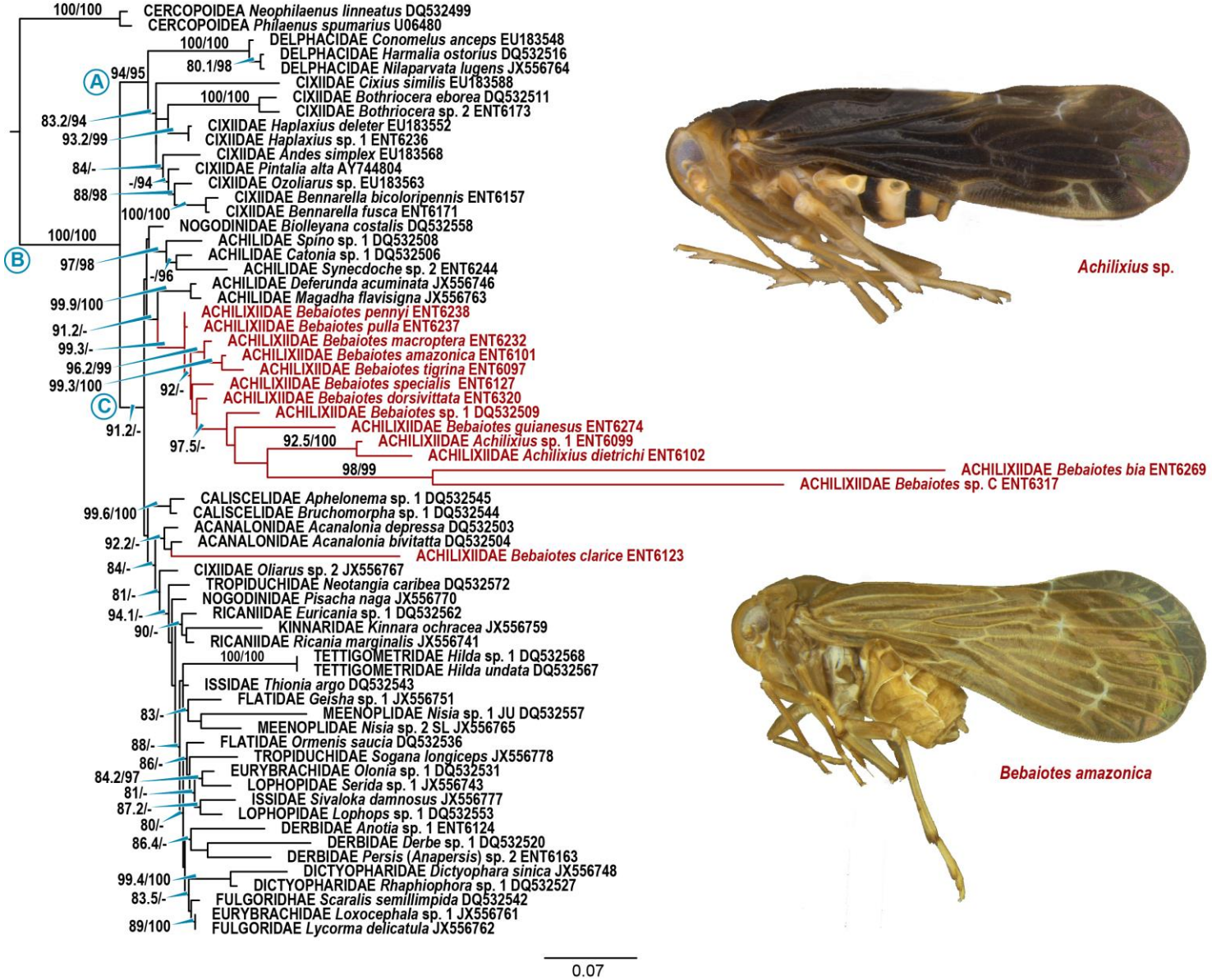

Supplementary Figure S2. Maximum likelihood tree of Achilixiidae and outgroups based on 1301 bp of 18S rDNA. Values above branches are likelihood SH-aLRT ≥ 80 / ultrafast bootstrap ≥ 95.

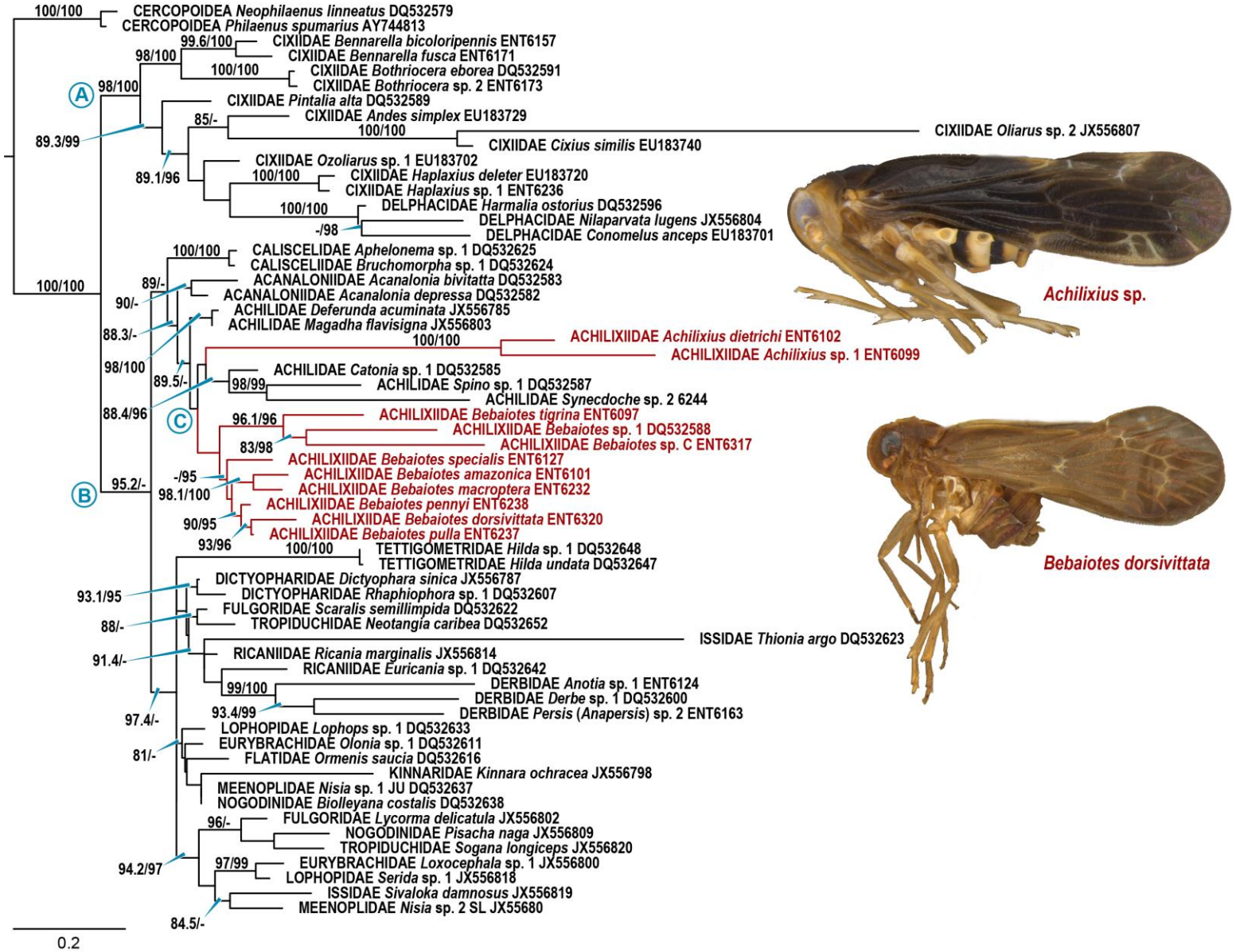

Supplementary Figure S3. Maximum likelihood tree of Achilixiidae and outgroups based on 2278 bp of 28S rDNA. Values above branches are likelihood SH-aLRT ≥ 80 / ultrafast bootstrap ≥ 95.

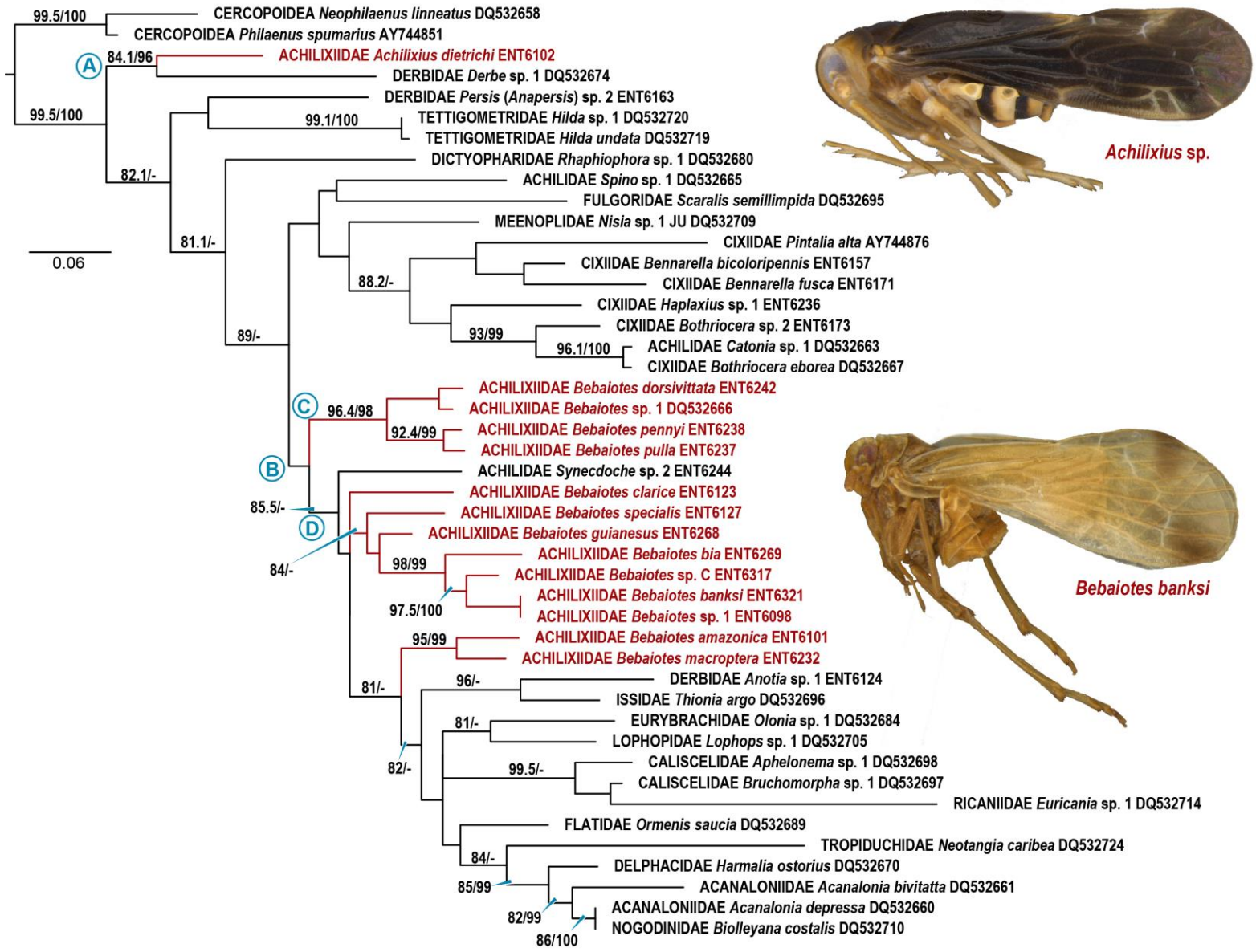

Supplementary Figure S4. Maximum likelihood tree of Achilixiidae and outgroups based on 339 bp of histone H3. Values above branches are likelihood SH-aLRT ≥ 80 / ultrafast bootstrap ≥ 95.

APÊNDICE C

Árvore de Inferência bayesiana de Achilixiidae e grupos externos resultante da concatenação dos genes 16S, 18S, 28S e H3.

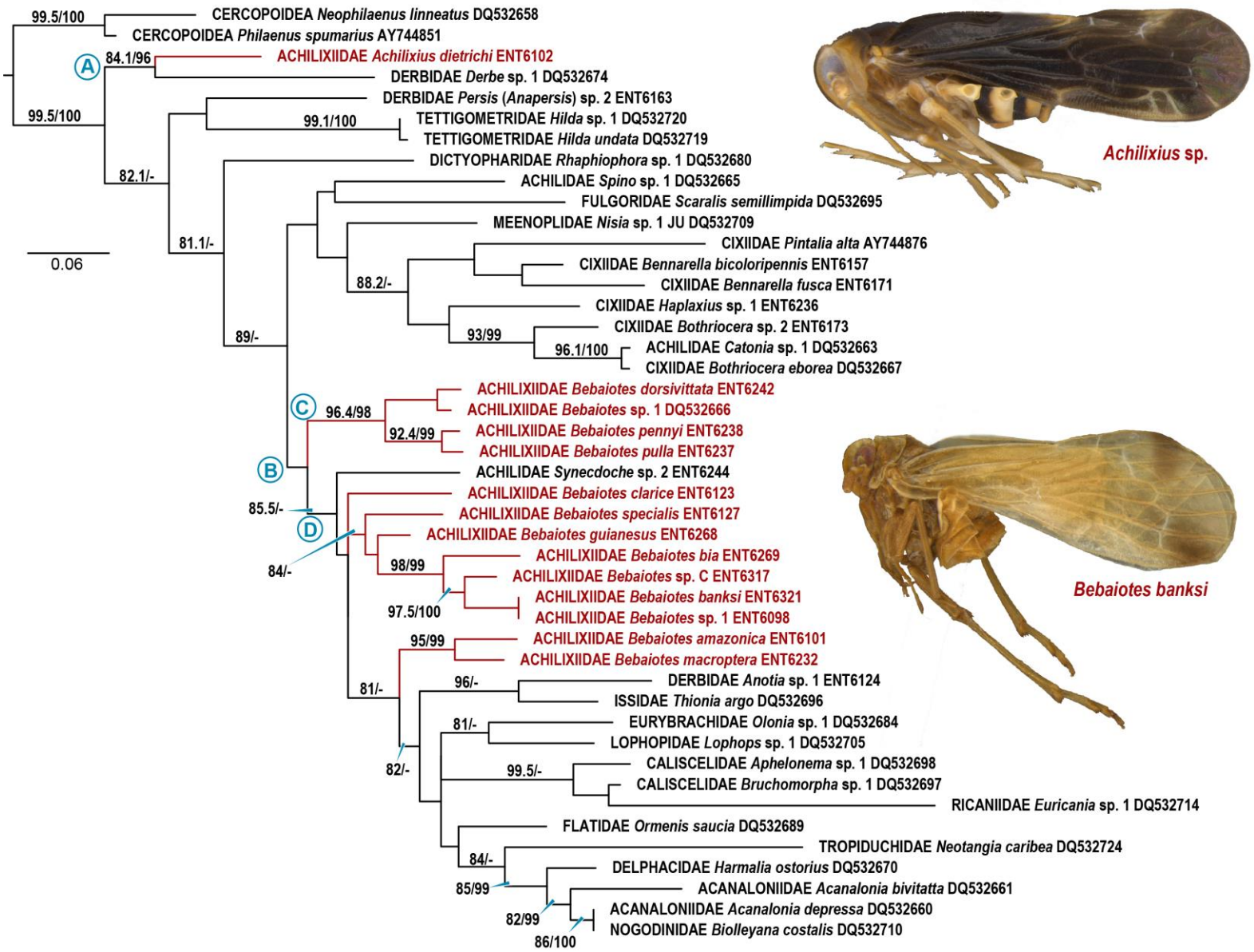

Supplementary Figure S5. Bayesian consensus of Achilixiidae and outgroups based on 4,379 bp of 16S, 18S, 28S, and H3 (-lnL= 40210.5464). Values below branches are Bayesian posterior probabilities (in percentages) > 0.90.